JAN 3 1 1990

NUREG/CR-5492
MEA-2088

Investigations of Irradiation-Anneal-Reirradiation (IAR) Properties Trends of RPV Welds

Phase 2 Final Report

Prepared by J. R. Hawthorne, A. L. Hiser

Materials Engineering Associates, Inc.

Prepared for
U.S. Nuclear Regulatory Commission

AVAILABILITY NOTICE

Availability of Reference Materials Cited in NRC Publications

Most documents cited in NRC publications will be available from one of the following sources:

1. The NRC Public Document Room, 2120 L Street, NW, Lower Level, Washington, DC 20555
2. The Superintendent of Documents, U.S. Government Printing Office, P.O. Box 37082, Washington, DC 20013-7082
3. The National Technical Information Service, Springfield, VA 22161

Although the listing that follows represents the majority of documents cited in NRC publications, it is not intended to be exhaustive.

Referenced documents available for inspection and copying for a fee from the NRC Public Document Room include NRC correspondence and internal NRC memoranda; NRC Office of Inspection and Enforcement bulletins, circulars, information notices, inspection and investigation notices; Licensee Event Reports; vendor reports and correspondence; Commission papers; and applicant and licensee documents and correspondence.

The following documents in the NUREG series are available for purchase from the GPO Sales Program: formal NRC staff and contractor reports, NRC-sponsored conference proceedings, and NRC booklets and brochures. Also available are Regulatory Guides, NRC regulations in the *Code of Federal Regulations*, and *Nuclear Regulatory Commission Issuances*.

Documents available from the National Technical Information Service include NUREG series reports and technical reports prepared by other federal agencies and reports prepared by the Atomic Energy Commission, forerunner agency to the Nuclear Regulatory Commission.

Documents available from public and special technical libraries include all open literature items, such as books, journal and periodical articles, and transactions. *Federal Register* notices, federal and state legislation, and congressional reports can usually be obtained from these libraries.

Documents such as theses, dissertations, foreign reports and translations, and non-NRC conference proceedings are available for purchase from the organization sponsoring the publication cited.

Single copies of NRC draft reports are available free, to the extent of supply, upon written request to the Office of Information Resources Management, Distribution Section, U.S. Nuclear Regulatory Commission, Washington, DC 20555.

Copies of industry codes and standards used in a substantive manner in the NRC regulatory process are maintained at the NRC Library, 7920 Norfolk Avenue, Bethesda, Maryland, and are available there for reference use by the public. Codes and standards are usually copyrighted and may be purchased from the originating organization or, if they are American National Standards, from the American National Standards Institute, 1430 Broadway, New York, NY 10018.

NUREG/CR--5492

TI90 006164

Investigations of Irradiation-Anneal-Reirradiation (IAR) Properties Trends of RPV Welds

Phase 2 Final Report

Manuscript Completed: November 1989
Date Published: January 1990

Prepared by
J. R. Hawthorne, A. L. Hiser

Materials Engineering Associates, Inc.
9700-B Martin Luther King, Jr. Highway
Lanham, MD 20706

Prepared for
Division of Engineering
Office of Nuclear Regulatory Research
U.S. Nuclear Regulatory Commission
Washington, DC 20555
NRC FIN B8900

ABSTRACT

Notch ductility, fracture toughness and tensile property trends of two high copper content, submerged arc welds with 288°C irradiation (I), 399°C postirradiation annealing (IA) and 288°C reirradiation (IAR) were investigated. Primary objectives included the determination of weld metal reembrittlement rate with fluence following an anneal and the influence of first cycle fluence level (high or low) on reembrittlement susceptibility. The welds were commercially made using a single lot of filler wire and two welding fluxes (Linde 80 and Linde 0091).

A relatively-rapid reembrittlement of both weld types was observed with initial reirradiation; however, the reembrittlement rate decreased markedly after a reirradiation fluence of ~0.3 x 10^{19} n/cm^2, E > 1 MeV. In turn, the benefit of IA procedures toward reducing total properties change with fluence was retained. The reembrittlement trend was independent of first cycle fluence level for the range investigated. Residual embrittlement after 399°C - 168 hour annealing, indexed by the 41-J temperature, appears independent of the pre-anneal condition (I or IAR); however, wide variability among welds in percent recovery is indicated. Trends in IAR behavior from Charpy-V specimen tests were found to be reinforced by tensile specimen and fracture toughness (0.5T-CT specimen) test findings.

CONTENTS

LIST OF FIGURES

LIST OF FIGURES

LIST OF FIGURES

LIST OF FIGURES

LIST OF TABLES

FOREWORD

The work reported here was performed at Materials Engineering Associates (MEA) under the program, Structural Integrity of Water Reactor Pressure Boundary Components, F. J. Loss, Program Manager. The program is sponsored by the Office of Nuclear Regulatory Research of the U. S. Nuclear Regulatory Commission (NRC). The technical monitor for the NRC is Alfred Taboada.

Prior reports under the current contract are listed below:

1. J. R. Hawthorne, "Significance of Nickel and Copper Content to Radiation Sensitivity and Postirradiation Heat Treatment Recovery of Reactor Vessel Steels," USNRC Report NUREG/CR-2948, Nov. 1982.

2. "Structural Integrity of Water Reactor Pressure Boundary Components, Annual Report for 1982," F. J. Loss, Ed., USNRC Report NUREG/CR-3228, Vol. 1, Apr. 1983.

3. J. R. Hawthorne, "Exploratory Assessment of Postirradiation Heat Treatment Variables in Notch Ductility Recovery of A 533-B Steel," USNRC Report NUREG/CR-3229, Apr. 1983.

4. W. H. Cullen, K. Torronen, and M. Kemppainen, "Effects of Temperature on Fatigue Crack Growth of A 508-2 Steel in LWR Environment," USNRC Report NUREG/CR-3230, Apr. 1983.

5. "Proceedings of the International Atomic Energy Agency Specialists' Meeting on Subcritical Crack Growth," Vols. 1 and 2, W. H. Cullen, Ed., USNRC Conference Proceeding NUREG/CP-0044, May 1983.

6. W. H. Cullen, "Fatigue Crack Growth Rates of A 508-2 Steel in Pressurized, High-Temperature Water," USNRC Report NUREG/CR-3294, June 1983.

7. J. R. Hawthorne, B. H. Menke, and A. L. Hiser, "Light Water Reactor Pressure Vessel Surveillance Dosimetry Improvement Program: Notch Ductility and Fracture Toughness Degradation of A 302-B and A 533-B Reference Plates from PSF Simulated Surveillance and Through-Wall Irradiation Capsules," USNRC Report NUREG/CR-3295, Vol. 1, Apr. 1984.

8. J. R. Hawthorne and B. H. Menke, "Light Water Reactor Pressure Vessel Surveillance Dosimetry Improvement Program: Postirradiation Notch Ductility and Tensile Strength Determinations for PSF Simulated Surveillance and Through-Wall Specimen Capsules," USNRC Report NUREG/CR-3295, Vol. 2, Apr. 1984.

9. A. L. Hiser and F. J. Loss, "Alternative Procedures for J-R Curve Determination," USNRC Report NUREG/CR-3402, July 1983.

10. A. L. Hiser, F. J. Loss, and B. H. Menke, "J-R Curve Characterization of Irradiated Low Upper Shelf Welds," USNRC Report NUREG/CR-3506, Apr. 1984.

11. W. H. Cullen, R. E. Taylor, K. Torronen, and M. Kemppainen, "The Temperature Dependence of Fatigue Crack Growth Rates of A 351 CF8A Cast Stainless Steel in LWR Environment," USNRC Report NUREG/CR-3546, Apr. 1984.

12. "Structural Integrity of Light Water Reactor Pressure Boundary Components -- Four-Year Plan 1984-1988," F. J. Loss, Ed., USNRC Report NUREG/CR-3788, Sep. 1984.

13. W. H. Cullen and A. L. Hiser, "Behavior of Subcritical and Slow-Stable Crack Growth Following a Postirradiation Thermal Anneal Cycle," USNRC Report NUREG/CR-3833, Aug. 1984.

14. "Structural Integrity of Water Reactor Pressure Boundary Components: Annual Report for 1983," F. J. Loss, Ed., USNRC Report NUREG/CR-3228, Vol. 2, Sept. 1984.

15. W. H. Cullen, "Fatigue Crack Growth Rates of Low-Carbon and Stainless Piping Steels in PWR Environment," USNRC Report NUREG/CR-3945, Feb. 1985.

16. W. H. Cullen, M. Kemppainen, H. Hanninen, and K. Torronen, "The Effects of Sulfur Chemistry and Flow Rate on Fatigue Crack Growth Rates in LWR Environments," USNRC Report NUREG/CR-4121, Feb. 1985.

17. "Structural Integrity of Water Reactor Pressure Boundary Components: Annual Report for 1984," F. J. Loss, Ed., USNRC Report NUREG/CR-3228, Vol. 3, June 1985.

18. A. L. Hiser, "Correlation of C_v and K_{Ic}/K_{Jc} Transition Temperature Increases Due to Irradiation," USNRC Report NUREG/CR-4395, Nov. 1985.

19. W. H. Cullen, G. Gabetta, and H. Hanninen, "A Review of the Models and Mechanisms For Environmentally-Assisted Crack Growth of Pressure Vessel and Piping Steels in PWR Environments," USNRC Report NUREG/CR-4422, Dec. 1985.

20. "Proceedings of the Second International Atomic Energy Agency Specialists' Meeting on Subcritical Crack Growth," W. H. Cullen, Ed., USNRC Conference Proceeding NUREG/CP-0067, Vols. 1 and 2, Apr. 1986.

21. J. R. Hawthorne, "Exploratory Studies of Element Interactions and Composition Dependencies in Radiation Sensitivity Development," USNRC Report NUREG/CR-4437, Nov. 1985.

22. R. B. Stonesifer and E. F. Rybicki, "Development of Models for Warm Prestressing," USNRC Report NUREG/CR-4491, Jan. 1987.

23. E. F. Rybicki and R. B. Stonesifer, "Computational Model for Residual Stresses in a Clad Plate and Clad Fracture Specimens," USNRC Report NUREG/CR-4635, Oct. 1986.

24. D. E. McCabe, "Plan for Experimental Characterization of Vessel Steel After Irradiation," USNRC Report NUREG/CR-4636, Oct. 1986.

25. E. F. Rybicki, J. R. Shadley, and A. S. Sandhu, "Experimental Evaluation of Residual Stresses in a Weld Clad Plate and Clad Test Specimens," USNRC Report NUREG/CR-4646, Oct. 1986.

26. "Structural Integrity of Water Reactor Pressure Boundary Components: Annual Report for 1985," F. J. Loss, Ed., USNRC Report NUREG/CR-3228, Vol. 4, June 1986.

27. G. Gabetta and W. H. Cullen, "Application of a Two-Mechanism Model for Environmentally-Assisted Crack Growth," USNRC Report NUREG/CR-4723, Oct. 1986.

28. W. H. Cullen, "Fatigue Crack Growth Rates in Pressure Vessel and Piping Steels in LWR Environments," USNRC Report NUREG/CR-4724, Mar. 1987.

29. W. H. Cullen and M. R. Jolles, "Fatigue Crack Growth of Part-Through Cracks in Pressure Vessel and Piping Steels: Air Environment Results, USNRC Report NUREG/CR-4828, Oct. 1988.

30. D. E. McCabe, "Fracture Evaluation of Surface Cracks Embedded in Reactor Vessel Cladding: Unirradiated Bend Specimen Results," USNRC Report NUREG/CR-4841, May 1987.

31. H. Hanninen, M. Vulli, and W. H. Cullen, "Surface Spectroscopy of Pressure Vessel Steel Fatigue Fracture Surface Films Formed in PWR Environments," USNRC Report NUREG/CR-4863, July 1987.

32. A. L. Hiser and G. M. Callahan, "A User's Guide to the NRC's Piping Fracture Mechanics Data Base (PIFRAC)," USNRC Report NUREG/CR-4894, May 1987.

33. "Proceedings of the Second CSNI Workshop on Ductile Fracture Test Methods (Paris, France, April 17-19, 1985)," F. J. Loss, Ed., USNRC Conference Proceeding NUREG/CP-0064, Aug, 1988.

34. W. H. Cullen and D. Broek, "The Effects of Variable Amplitude Loading on A 533-B Steel in High-Temperature Air and Reactor Water Environments," USNRC Report NUREG/CR-4929, Apr. 1989.

35. "Structural Integrity of Water Reactor Pressure Boundary Components: Annual Report for 1986," F. J. Loss, Ed., USNRC Report NUREG/CR-3228, Vol. 5, July 1987.

36. F. Ebrahimi et al., "Development of a Mechanistic Understanding of Radiation Embrittlement in Reactor Pressure Vessel Steels: Final Report," USNRC Report NUREG/CR-5063, Jan. 1988.

37. J. B. Terrell, "Fatigue Life Characterization of Smooth and Notched Piping Steel Specimens in 288°C Air Environments," USNRC Report NUREG/CR-5013, May 1988.

38. A. L. Hiser, "Tensile and J-R Curve Characterization of Thermally Aged Cast Stainless Steels," USNRC Report NUREG/CR-5024, Sept. 1988

39. J. B. Terrell, "Fatigue Strength of Smooth and Notched Specimens of ASME SA 106-B Steel in PWR Environments," USNRC Report NUREG/CR-5136, Sept. 1988.

40. D. E. McCabe, "Fracture Evaluation of Surface Cracks Embedded in Reactor Vessel Cladding: Material Property Evaluations" USNRC NUREG/CR-5207, Sept. 1988.

41. J. R. Hawthorne and A. L. Hiser, "Experimental Assessments of Gundremmingen RPV Archive Material for Fluence Rate Effects Studies," USNRC Report NUREG/CR-5201, Oct. 1988.

42. J. B. Terrell, "Fatigue Strength of ASME SA 106-B Welded Steel Pipes in 288°C Air Environments," USNRC Report NUREG/CR-5195, Dec. 1988.

43. A. L. Hiser, "Post-Irradiation Fracture Toughness Characterization of Four Lab-Melt Plates," USNRC Report NUREG/CR-5216, Rev. 1, June 1989.

44. R. B. Stonesifer, E. F. Rybicki and D. E. McCabe, "Warm Prestress Modeling: Comparison of Models and Experimental Results," USNRC Report NUREG/CR-5208, Apr. 1989.

45. A. L. Hiser and J. B. Terrell, "Size Effects on J-R Curves for A 302-B Plate," USNRC Report NUREG/CR-5265, Jan. 1989.

46. D. E. McCabe, "Fracture Evaluation of Surface Cracks Embedded in Reactor Vessel Cladding," USNRC Report NUREG/CR-5326, Mar. 1989.

47. J. R. Hawthorne, "An Exploratory Study of Element Interactions and Composition Dependencies in Radiation Sensitivity Development: Final Report," USNRC Report NUREG/CR-5357, Apr. 1989

48. J. R. Hawthorne, "Steel Impurity Element Effects on Postirradiation Properties Recovery by Annealing: Final Report," USNRC Report NUREG/CR-5388, Aug. 1989.

Prior reports dealing with the specific topic of this report are listed below:

1 J. R. Hawthorne, "Irradiation-Anneal-Reirradiation (IAR) Studies of Prototypic Reactor Vessel Weldments, USNRC Report NUREG/CR-5469, Oct. 1989.

ACKNOWLEDGMENT

The authors express their appreciation to J. W. Rogers of EG&G Idaho, Inc. for his personal efforts in neutron dosimetry determinations for the MEA irradiation assemblies.

The authors thank W. E. Hagel, L. LaMont, B. H. Menke, C. L. Miller, and K. C. Miller for their individual contributions to the irradiation and postirradiation phases of the program and E. D'Ambrosio for her contributions in preirradiation material properties determinations. The assistance of T. Ramey, in the reduction of the fracture toughness test data, E. Martinez for C_v data curve fittings and G. Carlson for the preparation of graphics for the report are also acknowledged with gratitude.

1. INTRODUCTION

Steels and weld deposits forming reactor pressure vessels are required by Title 10 of the Code of Federal Regulations (10 CFR Part 50) and the ASME Code to exhibit a certain minimum fracture resistance throughout vessel life. Specifically, the Charpy-V (C_v) upper shelf level of vessel materials must be at least 68 J (50 ft-lb) for unrestricted vessel operation. Likewise, C_v 41-J transition temperatures must be below temperature limits considered maximums for prevention of brittle fracture. For example, the Pressurized Thermal Shock Rule (10 CFR 50.61) provides a screening limit of 132°C (270°F) for axial welds and base metals. Also, the nil-ductility reference temperature (RT_{NDT}) for irradiated steel is indexed in part by the radiation-induced elevation in the C_v 41-J temperature; the RT_{NDT} in turn indexes the reference material fracture toughness (K_{IR}) curve (Ref. 1). For those cases where properties are reduced by radiation service to below minimum values, postirradiation heat treatment (i.e., annealing) for the restoration of vessel safety margins is one option available (Refs. 1 and 2). This method was applied successfully in 1967 to the Army SM-1A reactor vessel which operated at 232°C (Ref. 3). Service temperatures for commercial pressurized water reactors (PWR's) in the USA, in contrast, range from about 282°C to 302°C. Service temperature is a factor known to influence properties recovery by annealing (Ref. 4).

The practical effectiveness of any vessel annealing operation is judged not only from the vessel's properties in the irradiated plus annealed condition but also from the vessel's reirradiation properties behavior upon resumed service. Experimental definition of reembrittlement behavior following a 399°C-168 hour annealing treatment was one objective of the present investigation. A second objective was exploration of the potential for weld-to-weld variability relative to reirradiation sensitivity at 288°C. The study builds on the investigations of irradiation plus annealing (IA) and irradiation-anneal-reirradiation (IAR) vs. irradiation (I) properties changes conducted in 1980-1981 for the USNRC. The initial studies (IAR Phase 1) showed that the IAR method could reduce cumulative radiation effects appreciably depending on the annealing temperature employed (Refs. 5 and 6).

At present, high copper-high nickel content weld deposits are of particular interest to IAR studies because of their high radiation embrittlement sensitivities at typical reactor vessel service temperatures. This sensitivity has raised concerns for the resultant degradation of properties relative to pressurized thermal shock (PTS) resistance and fracture resistance in the upper shelf temperature regime. This investigation was carried forth with a set of high copper content welds produced commercially by the submerged arc process with Linde 80 and Linde 0091 welding fluxes. The former was used extensively for reactor pressure vessel (RPV) fabrication by the Babcock and Wilcox Company (B&W); the Linde 0091 welding flux along with Linde 1092 and Linde 124 are generally associated with RPV's of Combustion Engineering, Inc. (CE) manufacture. The Linde 80 flux yields relatively low as-fabricated C_v upper shelf energy (USE) levels; the Linde 0091 flux provides a relatively high USE level.

The results of the IAR Phase 1 study were very positive in terms of showing a benefit from intermediate annealing, but left important questions on the exact path of reembrittlement following annealing (see Fig. 1) and the extent of metallurgical influences on reembrittlement behavior. The IAR Phase 2 investigations reported here focus on these questions, recognizing that implementation of the annealing option and the USNRC assessment of proposed startup/shutdown pressure-temperature limits for vessel operations after an anneal would depend in great measure on resolving these uncertainties.

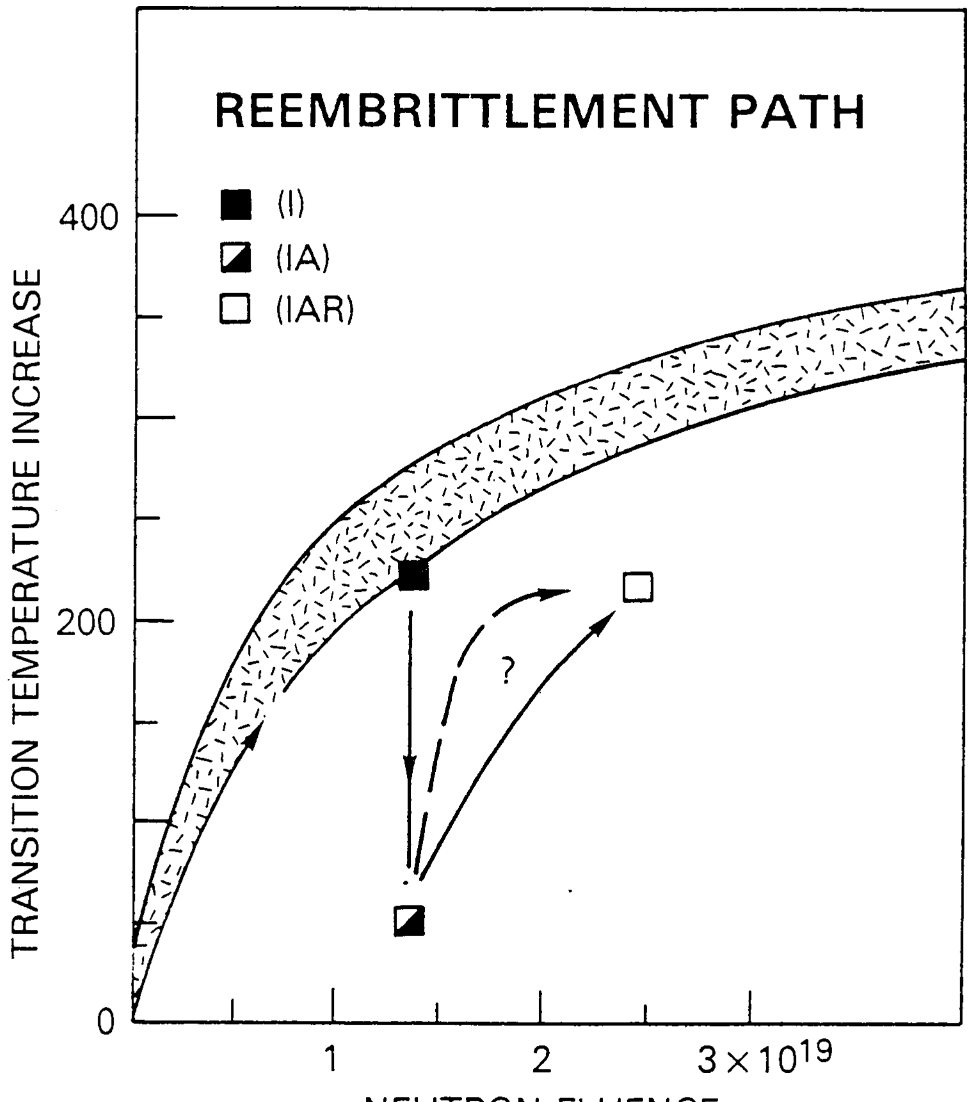

Fig. 1 Illustration showing the uncertainty over the reembrittlement path with reirradiation.

2. MATERIALS

The welds purchased for the IAR Phase 2 investigations were made with filler wire from a single steel melt. The weld made with Linde 80 welding flux was arbitrarily coded W8A; that made with Linde 0091 welding flux was coded W9A. Each flux type was from a single lot. The use of filler wire and welding flux from single lots, by design, permitted data comparisons for flux effect assessment. Weld procurement specifications and weld fabrication details are given in Appendix A. Table 1 provides key information for reference. The welds were made with copper-coated filler wire. The copper coating supplied most of the copper found in the weld deposits, comparable to RPV welds produced in the 1960's and early 1970's. The weld deposit compositions are listed in Table 2. Photomacrographs of the welds, taken after etching with a Nital solution, are shown in Figs. 2 and 3.

The welds were given a 621°C-24 hour post weld stress relief anneal; cooling rates from 621°C were less than 56°C/hour. As-fabricated notch ductility and tensile strength properties are compared in Table 3. Properties of a "sister" weld to Weld W8A (Weld W8B) produced but not used in the present study are also shown. The results indicate good weld properties reproducibility when the same flux lot is used. As expected, the Linde 80 weld (W8A) exhibited a higher C_v 41-J transition temperature and a lower C_v USE than the Linde 0091 weld (W9A). The ~79 J (58 ft-lb) C_v USE of the weld W8A permits a classification of a "low upper shelf", satisfying one objective of the procurement planning. The C_v properties of the Weld W9A are comparable to other production welds of CE (Ref. 7).

Fig. 2 Photomacrograph of submerged-arc weld deposit W8A (Linde 80). Material shown is a run-out-tab cross section.

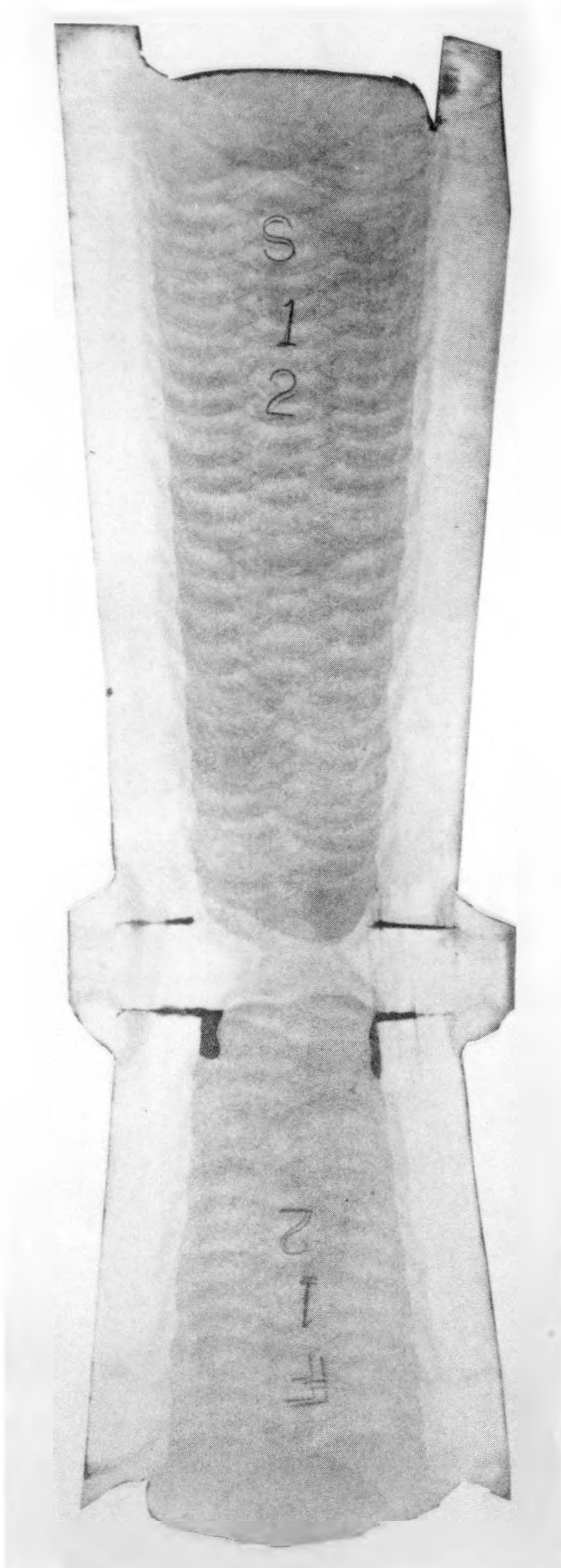

Fig. 3 Photomacrograph of submerged-arc weld deposit W9A (Linde 0091).

Table 1 Welding Specifications for IAR Phase 2 Welds

Base Plate:	210-mm thick A 533-B Class 1 Steel (0.20% Cu)
Filler Type:	High Mn-Mo-Ni
Process:	Submerged arc, single electrode
Electrode:	Heat 3P8393, 3.2-mm diameter copper coated
Flux:	Linde 80 (Lot 0418, control 8556) or Linde 0091 (Lot 0204, control 3756)
Heat Input:	80-95 kJ/inch (range)

Table 2 Compositions of Submerged-Arc Weld Deposits

Weld[a]	Chemical Composition (Wt-%)									
	C	Mn	Si	P	S	Ni	Cr	Mo	Cu	Sn
Weld W8A	0.079(min)[b]	1.27	0.71	0.010	0.012	0.55	0.10	0.42	0.37	0.002
(Linde 80 ϕ)	0.096(max)	1.36	0.79	0.017	0.019	0.68	0.13	0.50	0.42	0.004
Weld W9A	0.19(min)	1.21	0.23	0.008	0.005	0.64	0.10	0.49	0.35	0.003
(Linde 0091 ϕ)	0.19(max)	1.27	0.23	0.012	0.010	0.77	0.11	0.50	0.43	0.004

[a] Postwelding stress relief anneal 621°C ± 14°C for 24 h.

[b] Range (min/max) observed, multiple test locations in 1.83-m long weld seam.

Table 3 As-Welded Properties of IAR Phase 2 Welds

Parameter	Weld W8A	Weld W8B[a]	Weld W9A
Flux Type	Linde 80	Linde 80	Linde 0091
Heat Input	85 kJ/inch	93.5 kJ/inch	93.5 kJ/inch
Yield Strength	498 MPa	489 Pa	574 MPa
Tensile Strength	617 MPa	612 MPa	656 MPa
C_v 41 J	-23° C	-18° C	-62° C
C_v 68 J	49° C	38° C	-46° C
C_v USE (range)	79-87 J	79-84 J	153-159 J

[a] Sister weld to weld W8A; not used in present study.

3. IRRADIATION EXPERIMENT MATRIX

The general plan of materials irradiation is illustrated schematically in Fig. 4. At each indicated point, determinations of C_v and tensile properties were to be made. At the points marked by the subscript CT, fracture toughness properties were to be determined also, for correlation tests of fracture toughness vs. notch ductility change. The assemblies for fracture toughness determinations contained 12 0.5T-CT specimens each of Weld W8A and Weld W9A. This number was considered sufficient at the time for properties definition over the full temperature range (transition and upper shelf regimes). The specimen designs are illustrated in Figs. 5, 6 and 7. The 0.5T-CT specimens for upper shelf determinations were side grooved after irradiation.

As noted in Fig. 4, two sets of irradiation experiments were involved. For one set, the target first cycle fluence was 1.2 x 10^{19} n/cm^2 (E $\geq$ 1 MeV) and the reirradiation fluence intervals were ~0.3 x 10^{19} n/cm^2 to a total (reirradiation) fluence of ~1.2 x 10^{19}n/cm^2. For the second set, the target first cycle fluence was 2.4 x 10^{19}n/cm^2. Reirradiation fluence intervals were the same as for the first set. The two sets permitted an assessment of first cycle fluence level on the IAR reembrittlement trend. (Note: Unless indicated otherwise, all reported fluences are E > 1 MeV.)

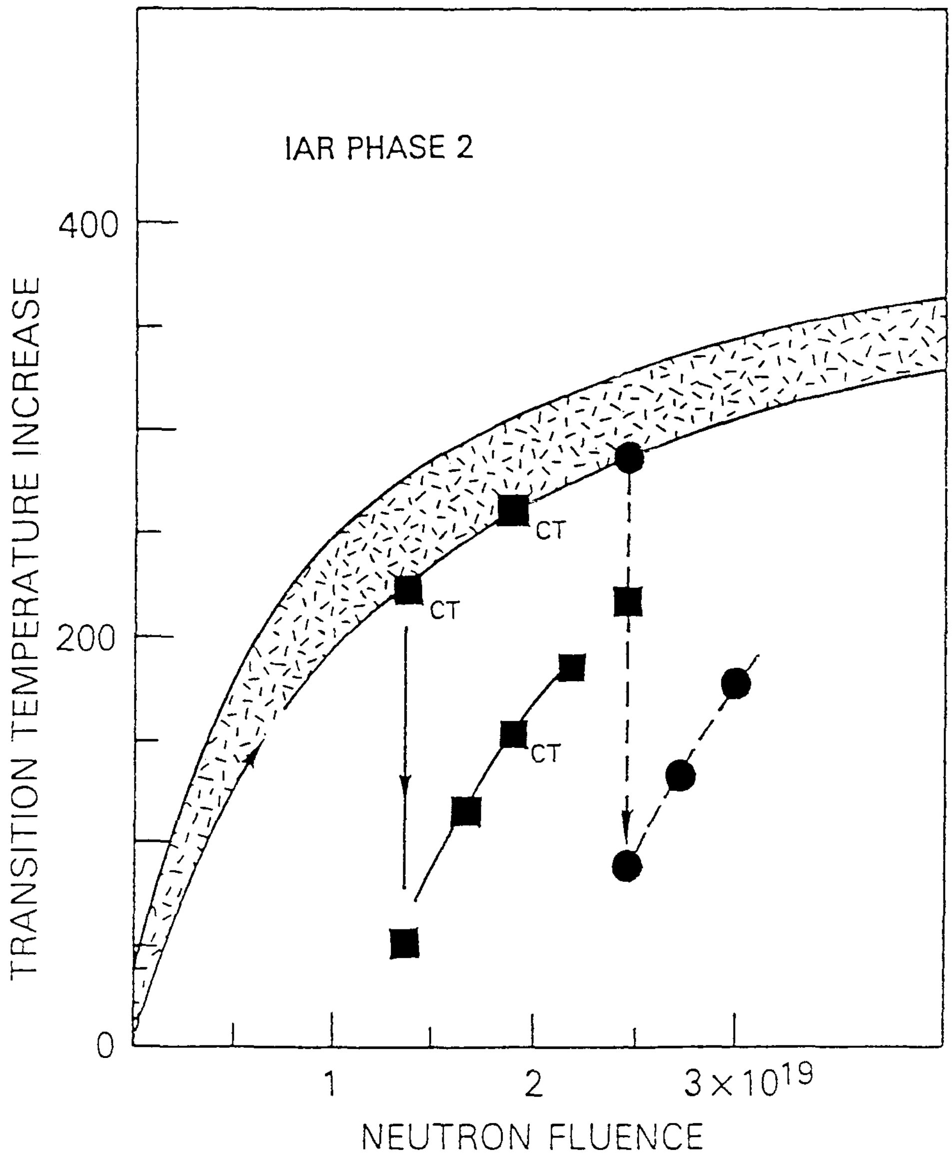

Fig. 4 Plan of IAR Phase 2 program irradiation tests. Charpy-V properties were to be developed experimentally for each point indicated. The points marked "CT" show where fracture toughness determinations were also to be developed.

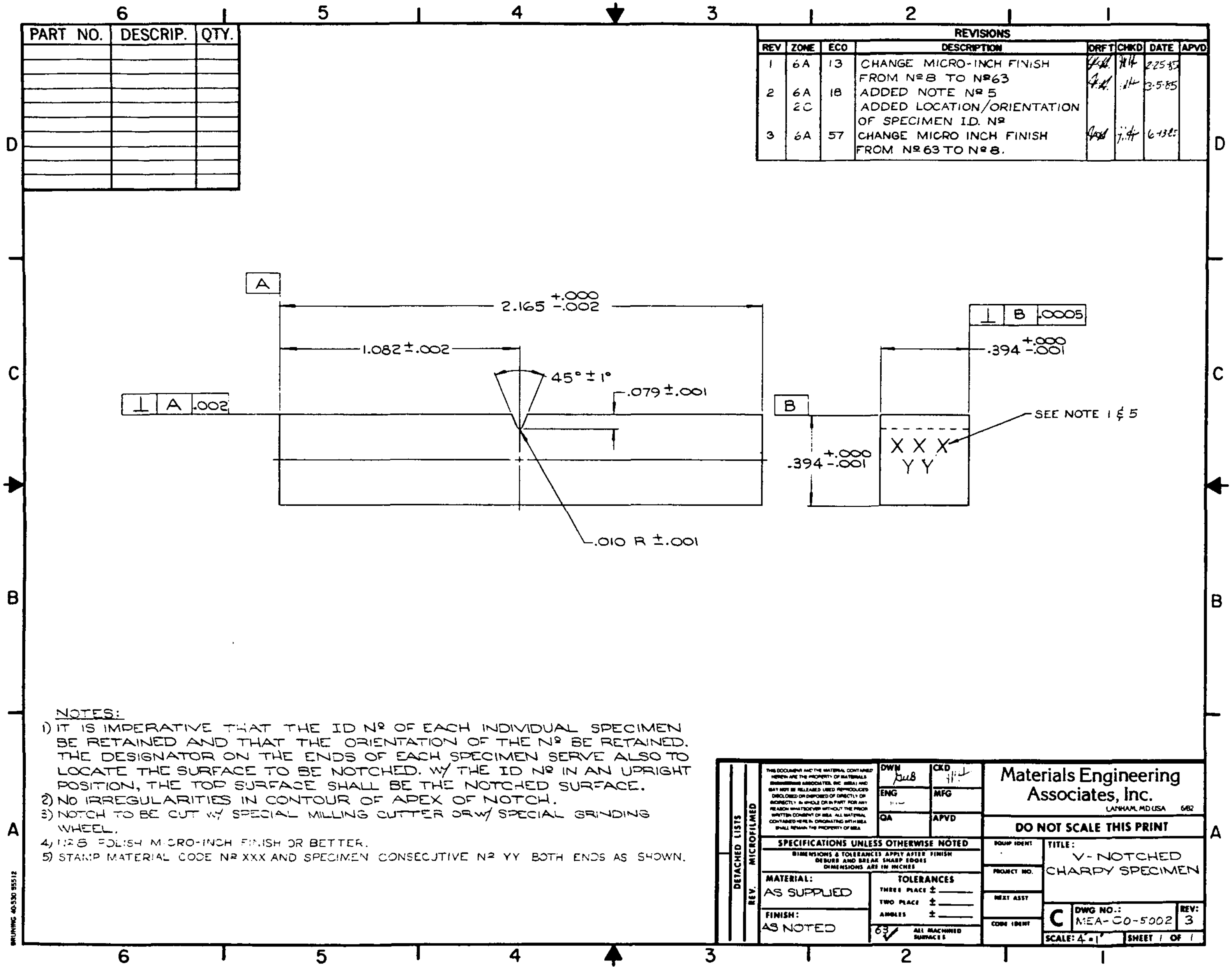

Fig. 5 Design of Charpy V-notch (C_v) test specimen.

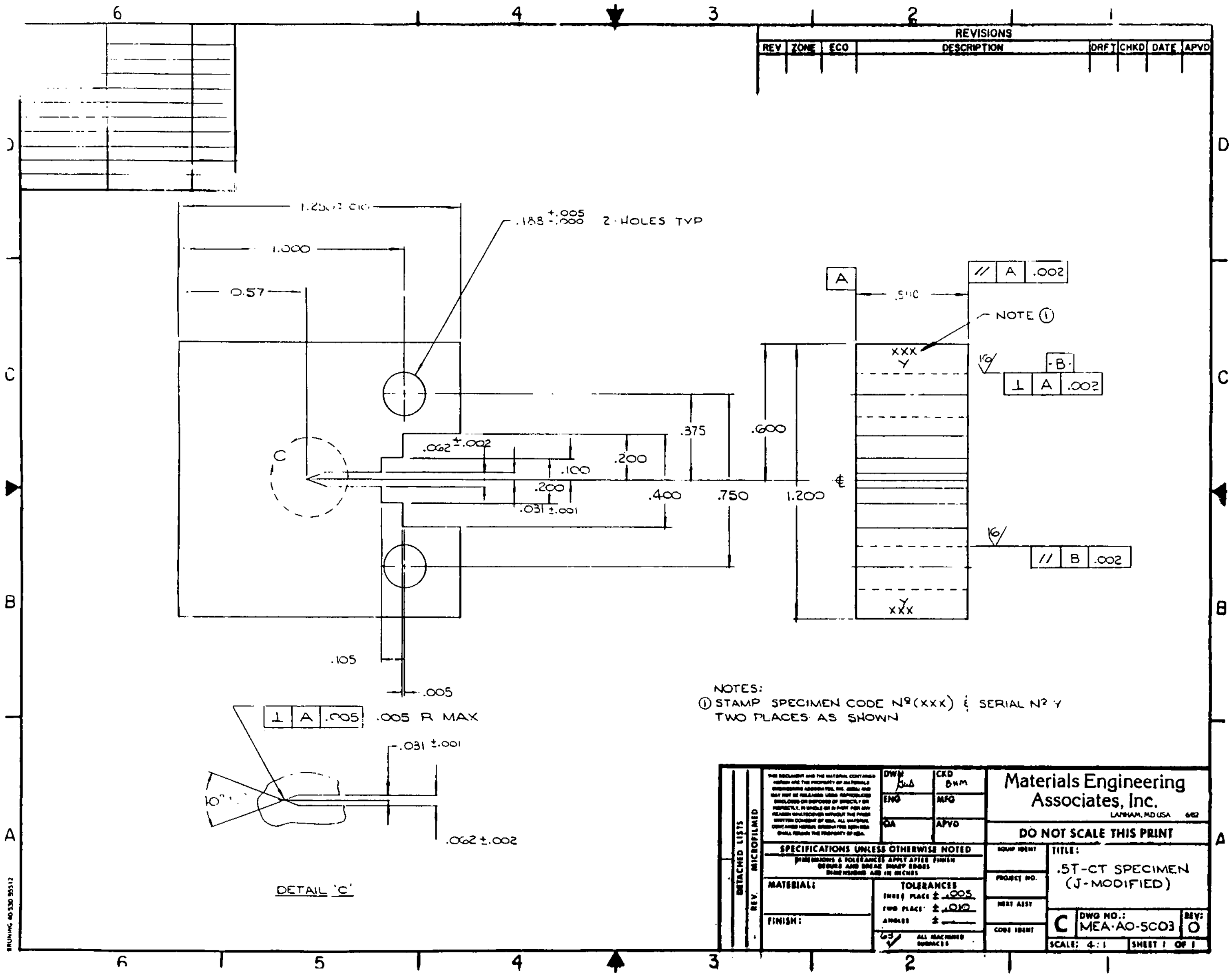

Fig. 6 Design of 0.5T-CT compact tension specimen.

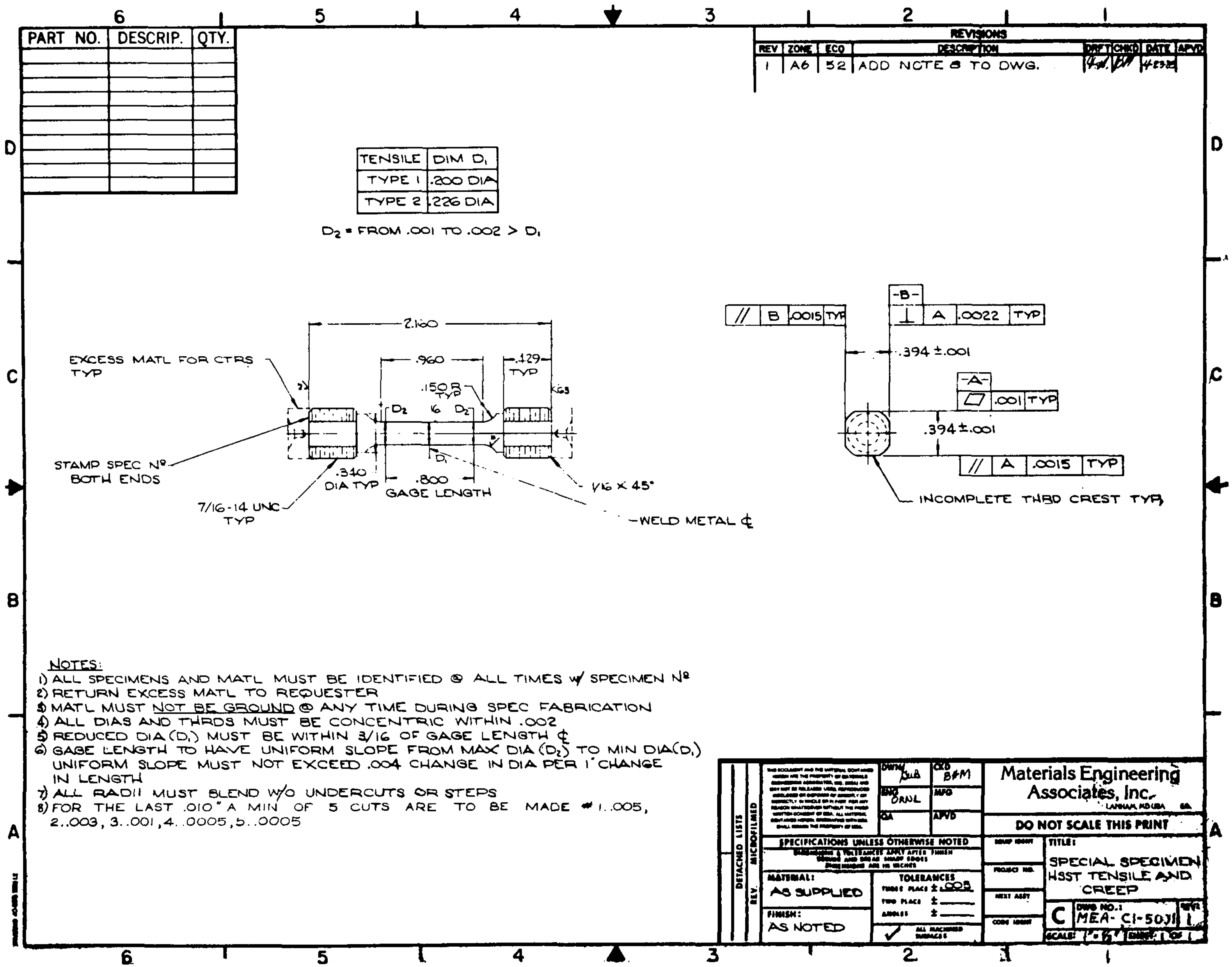

Fig. 7 Design of threaded-end, C_V-size tension test specimen. The Type 2 Design was used.

4. MATERIAL IRRADIATION

The specimens were irradiated in the light-water-cooled and moderated, 2MW pool-type test reactor known as the UBR. The UBR is located in the Buffalo Materials Research Center (BMRC) at Buffalo, New York. The experiment irradiation facilities used here are within the fuel lattice. Both B-4 and C-2 facilities were used. Fuel enrichment of the UBR is about 6 percent. Neutron spectrum conditions in the two facilities have been established (Refs. 8, 9 and 10).

The specimens were contained in temperature-controlled capsules. Thermocouples welded to specimen midsections were used for temperature monitoring and control. A total of 10 separate irradiation assemblies were required by the matrix for IAR-condition and I-condition (reference) determinations. Assembly identifications are given in Table 4. Individual specimens were placed within the specimen arrays of the irradiation assemblies as shown in Figs. 8 to 13; thermocouple placements are illustrated in Figs. 14 to 19. At full reactor power, temperature differences among C_v and tensile specimens were less than $\pm$ 8°C. Temperature differences were somewhat larger for the 0.5T-CT specimens, but generally within $\pm$12°C.

The annealing of specimens between irradiation cycles (cycles 1 and 2) was performed in a special underwater furnace. The entire assembly was inserted in the furnace. Thermocouples attached to the specimens again provided electrical signals for temperature control. Specimen temperatures typically were within $\pm$7°C of the target heat treatment temperature. Postirradiation annealing for IA-condition evaluations was accomplished in the hot cell using a recirculating air furnace. Specimen temperatures in this case were held within $\pm$3°C of the target 399°C temperature.

Dosimetry postirradiation measurements and analysis were performed by EG&G Idaho, Inc. (J.W. Rogers); Appendix B lists the average neutron fluence rate determination from the dosimeters. Neutron fluences (n/cm^2, E > 1 MeV) were determined from iron and nickel dosimeter wires placed in the notches of the C_v specimens and the 0.5T-CT specimens. (See illustrations in Appendix B.) Neutron spectrum calculations indicate that the calculated spectrum fluence, Φ^{cs} (E > 1 MeV) is 1.43 times the fission spectrum fluence, Φ^{fs}; the exposure equivalent in terms of displacements per atom (dpa, E > 1 MeV) is $1.62 \times 10^{-21} \Phi^{cs}$. The average fluence rate is on the order of 8.5×10^{12} n/cm^2-s^{-1} (E > 1 MeV). The measured fluence rate was assumed to be invariant over the total irradiation period. Thermal neutron fluences were determined from cobalt-aluminum and silver-aluminum dosimeter wires located in the C_v specimen notches.

Table 4 describes the actual I- and IAR-exposures of the various irradiation assemblies. Detailed reactor operations history for each capsule is given in Appendix C.

Neutron fluences reported herein carry uncertainties, based on counting and assumed cross section components, of $\pm$8% and $\pm$7% for the Fe and Ni dosimeters, respectively, at the 1-σ confidence level.

(text continues on pg. 29)

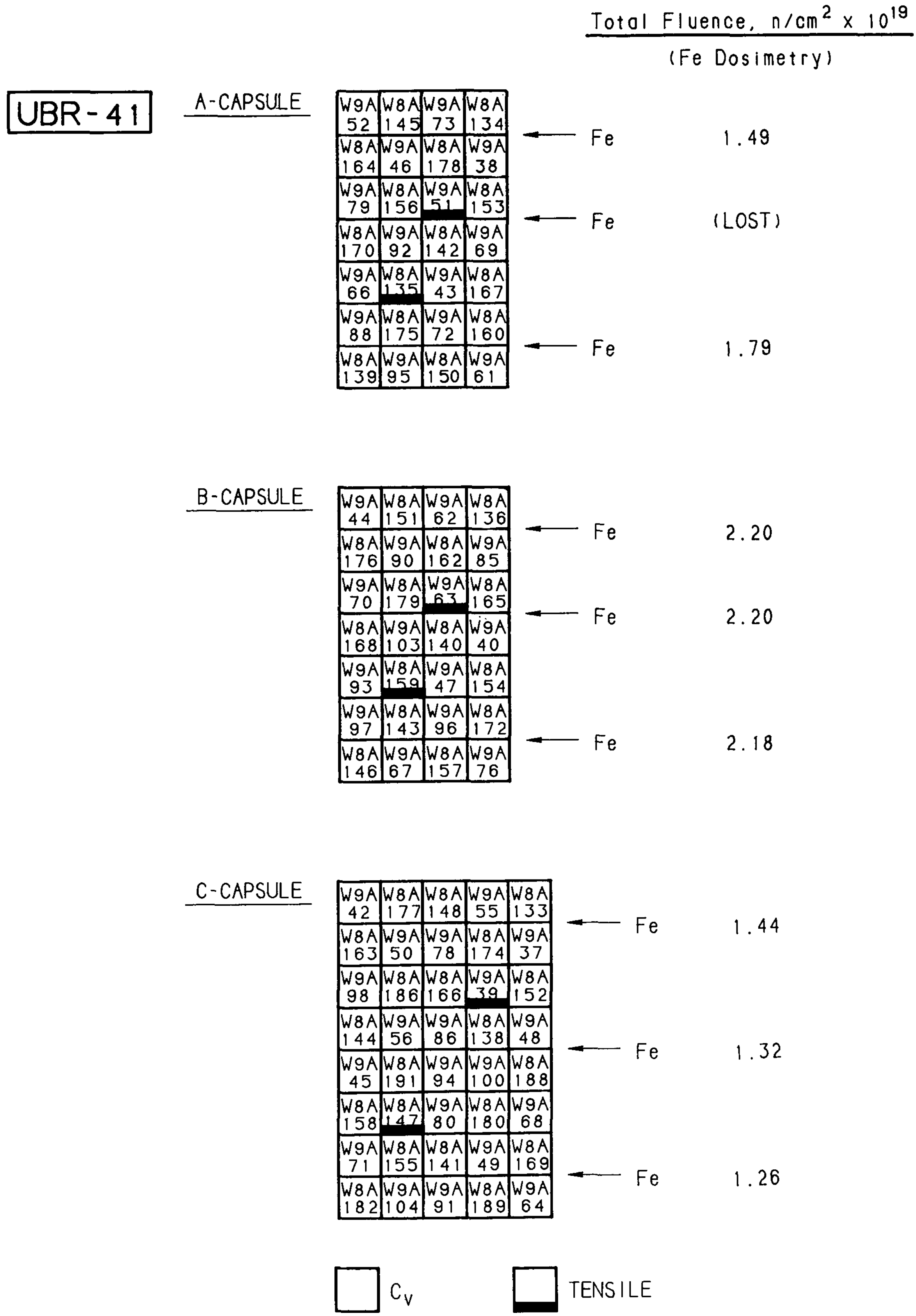

Fig. 8 Placement of C_v and tension test specimens in Irradiation Assembly UBR-41. (Capsules A, B and C; elevation view). Total neutron fluence values based on iron dosimeter wires at various locations are shown in this figure and Fig. 9 - 13.

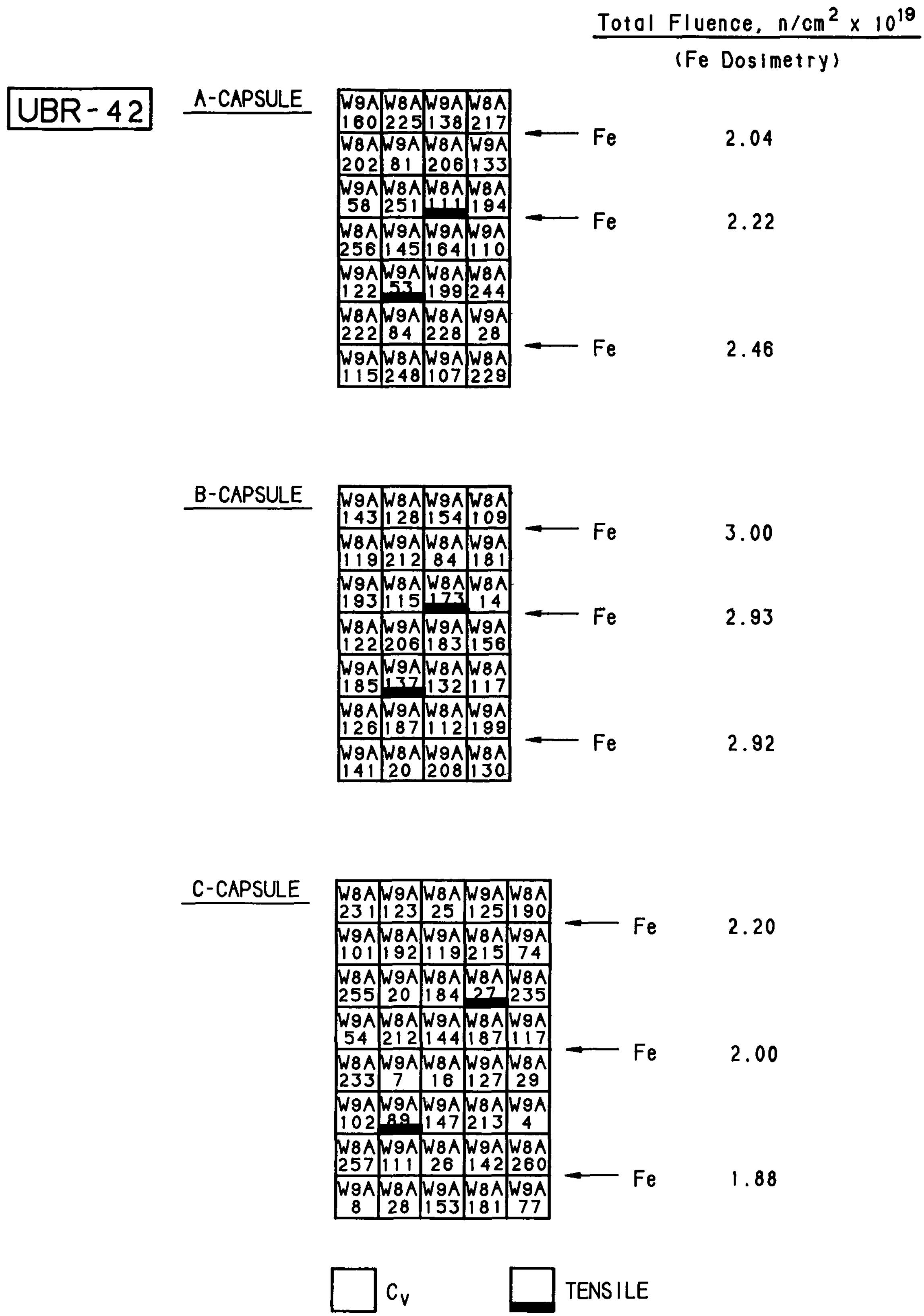

Fig. 9 Placement of C_v and tension test specimens in Irradiation Assembly UBR-42. (Capsules A, B and C; elevation view).

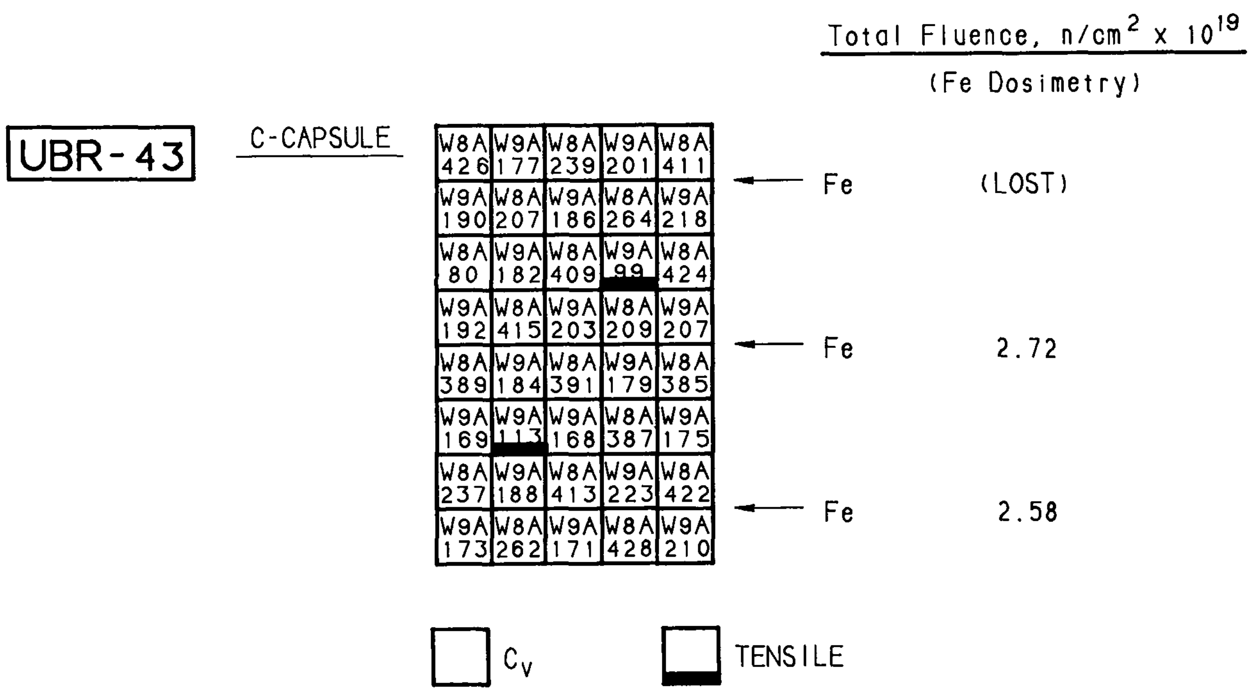

Fig. 10 Placement of C_v and tension test specimens in Irradiation Assembly UBR-43. (Capsule C; elevation view).

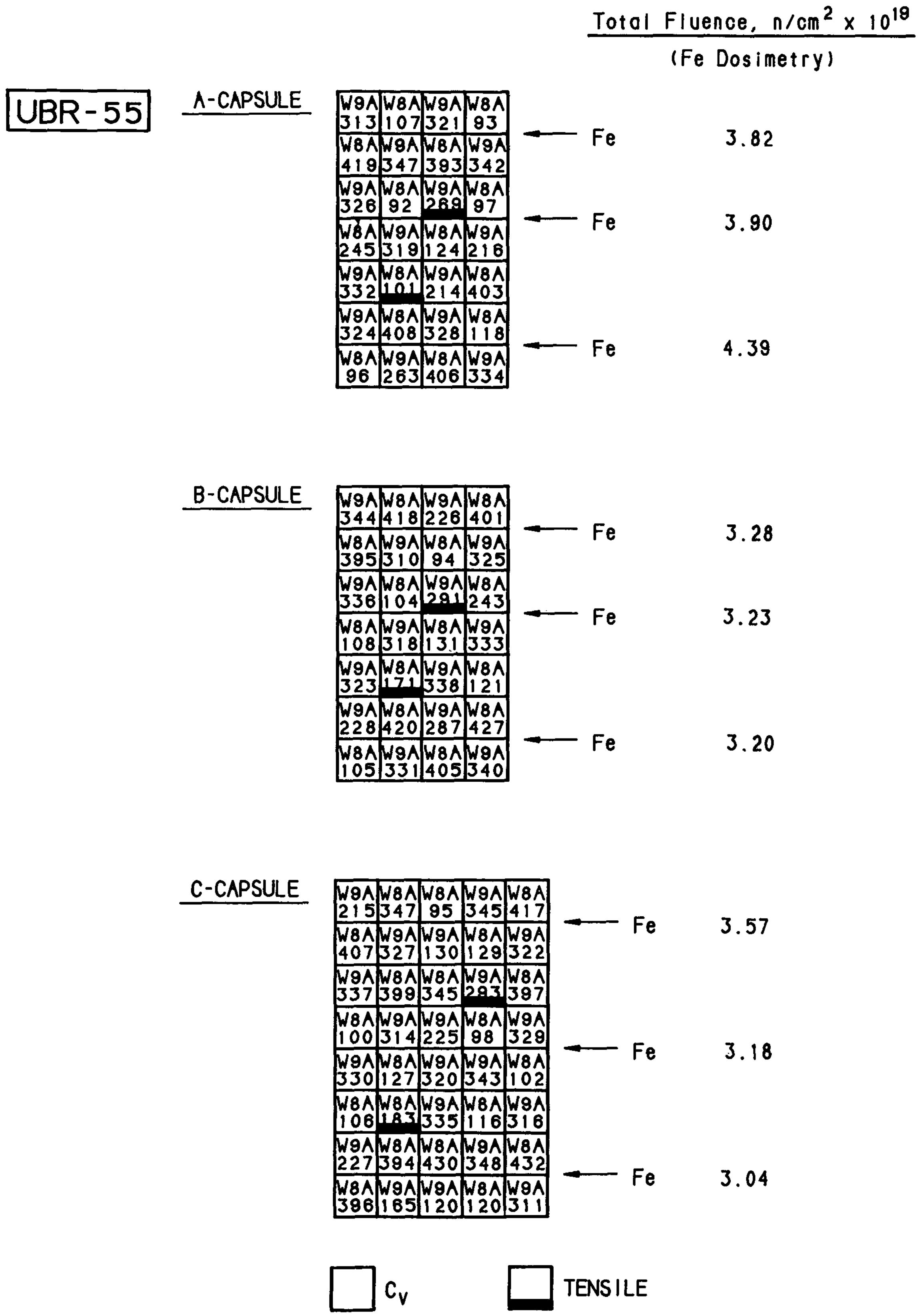

Fig. 11 Placement of C_v and tension test specimens in Irradiation Assembly UBR-55. (Capsules A, B and C; elevation view).

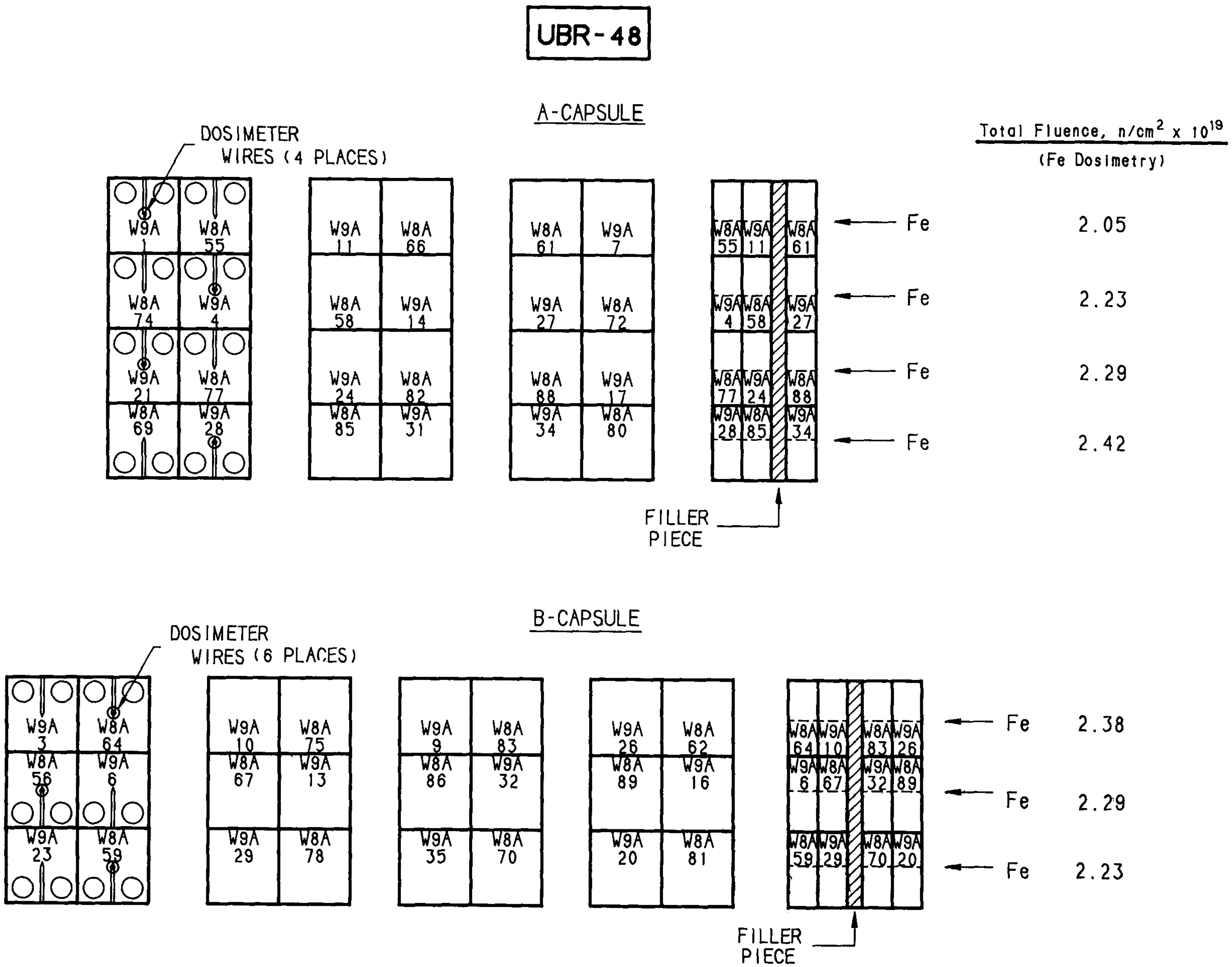

Fig. 12 Placement of 0.5T-CT specimens in Experiment UBR-48. (Capsules A and B; elevation view).

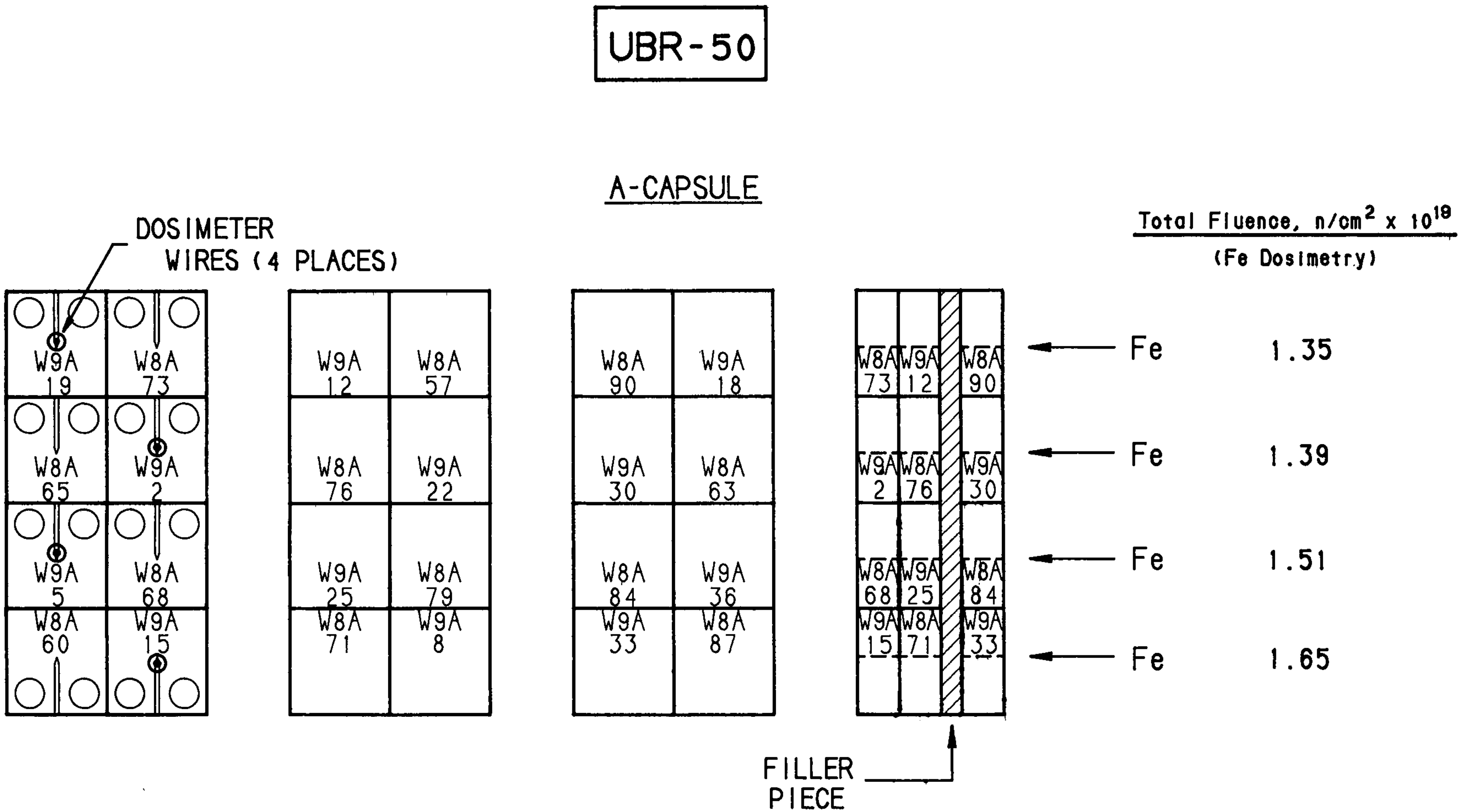

Fig. 13 Placement of 0.5T-CT specimens in Experiment UBR-50. (Capsule A; elevation view).

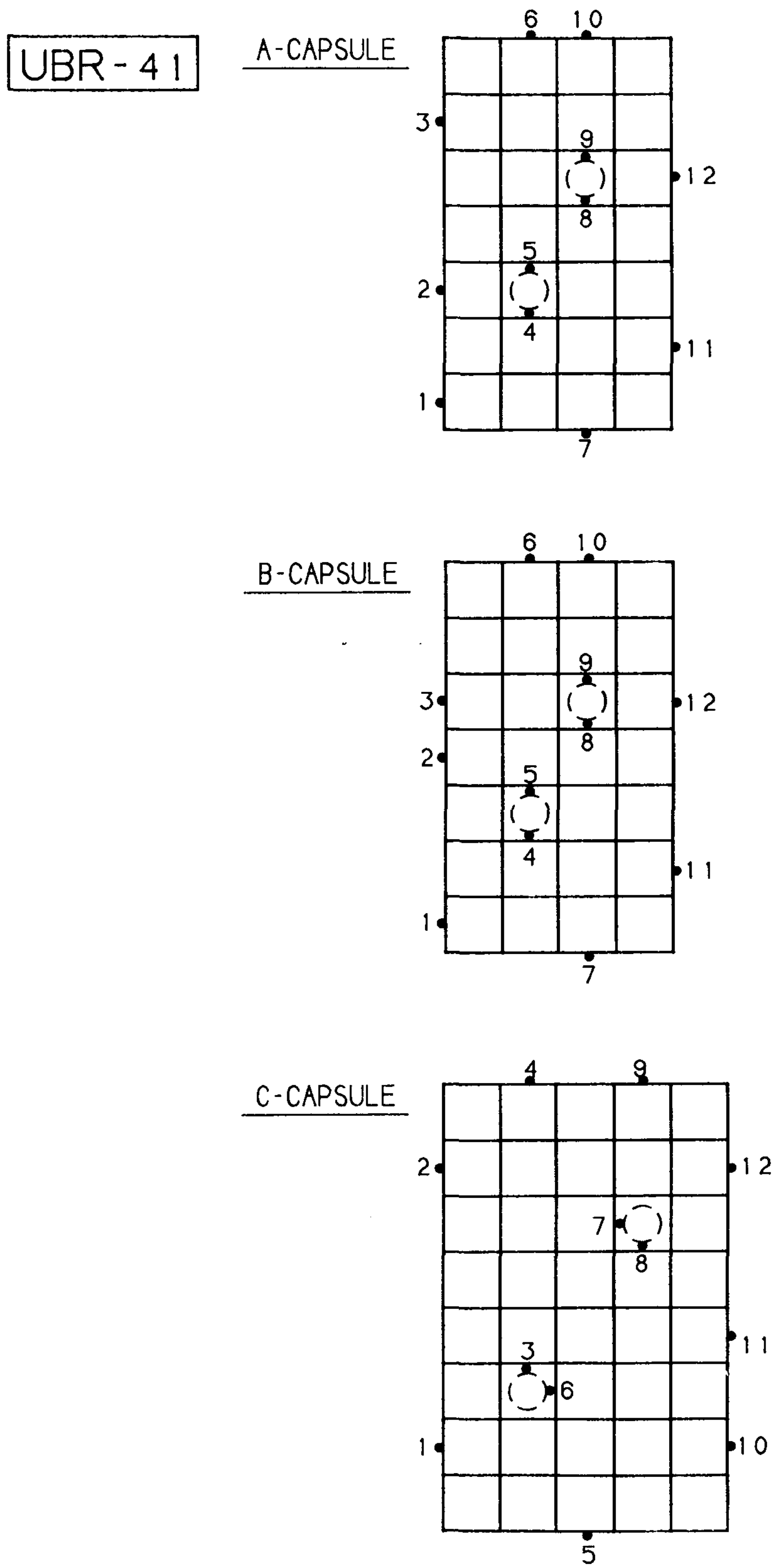

Fig. 14 Irradiation Assembly UBR-41 showing thermocouple placements in the specimen arrays.

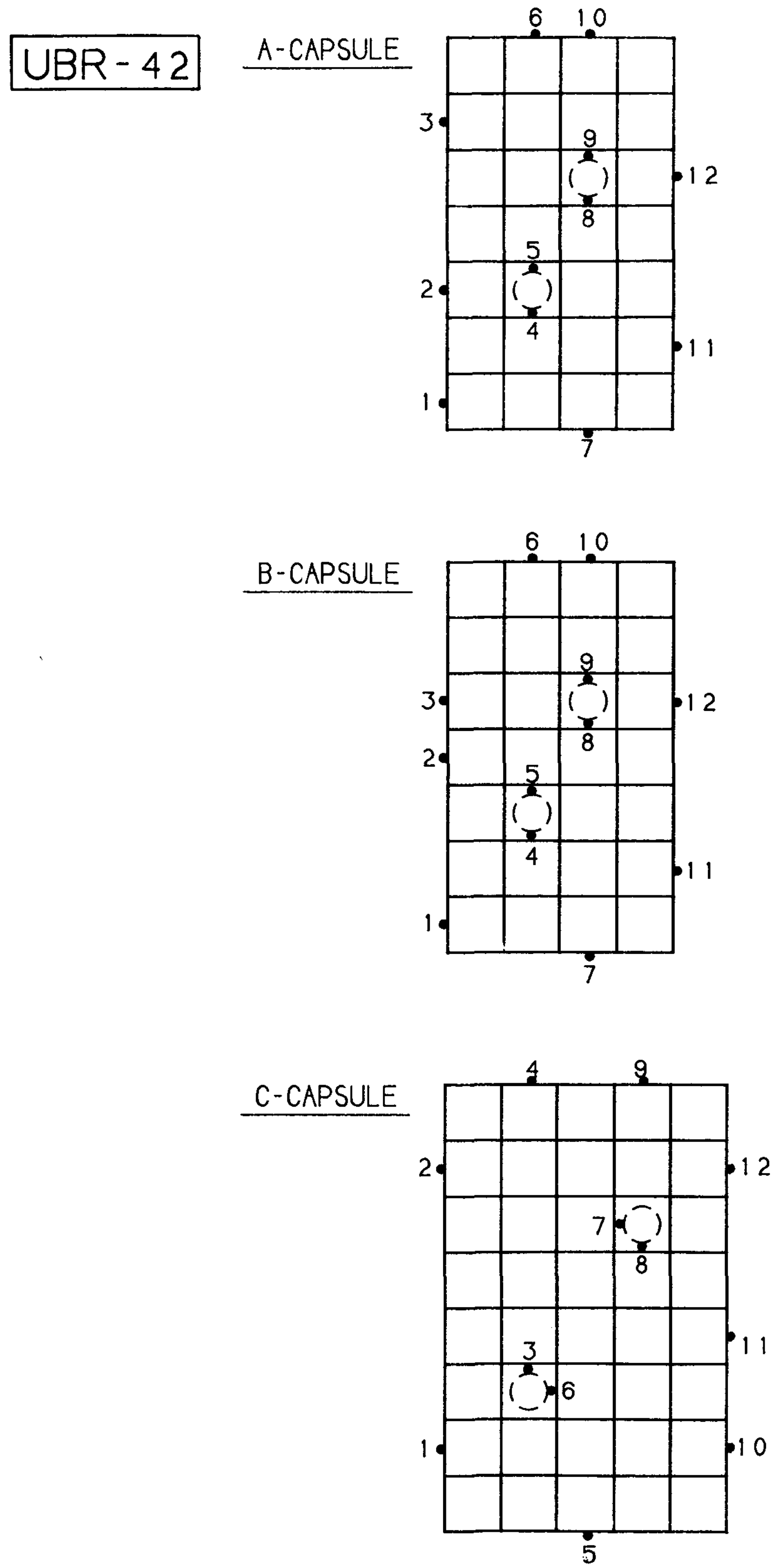

Fig. 15 Irradiation Assembly UBR-42 showing thermocouple placements in the specimen arrays.

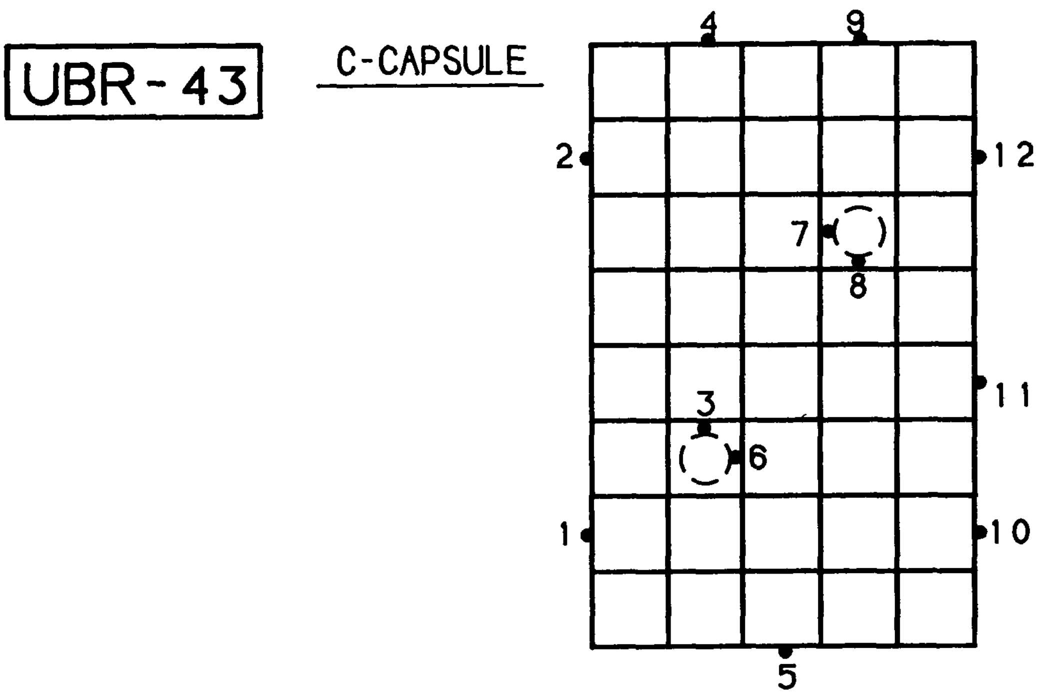

Fig. 16 Irradiation Assembly UBR-43 showing thermocouple placements in the specimen arrays.

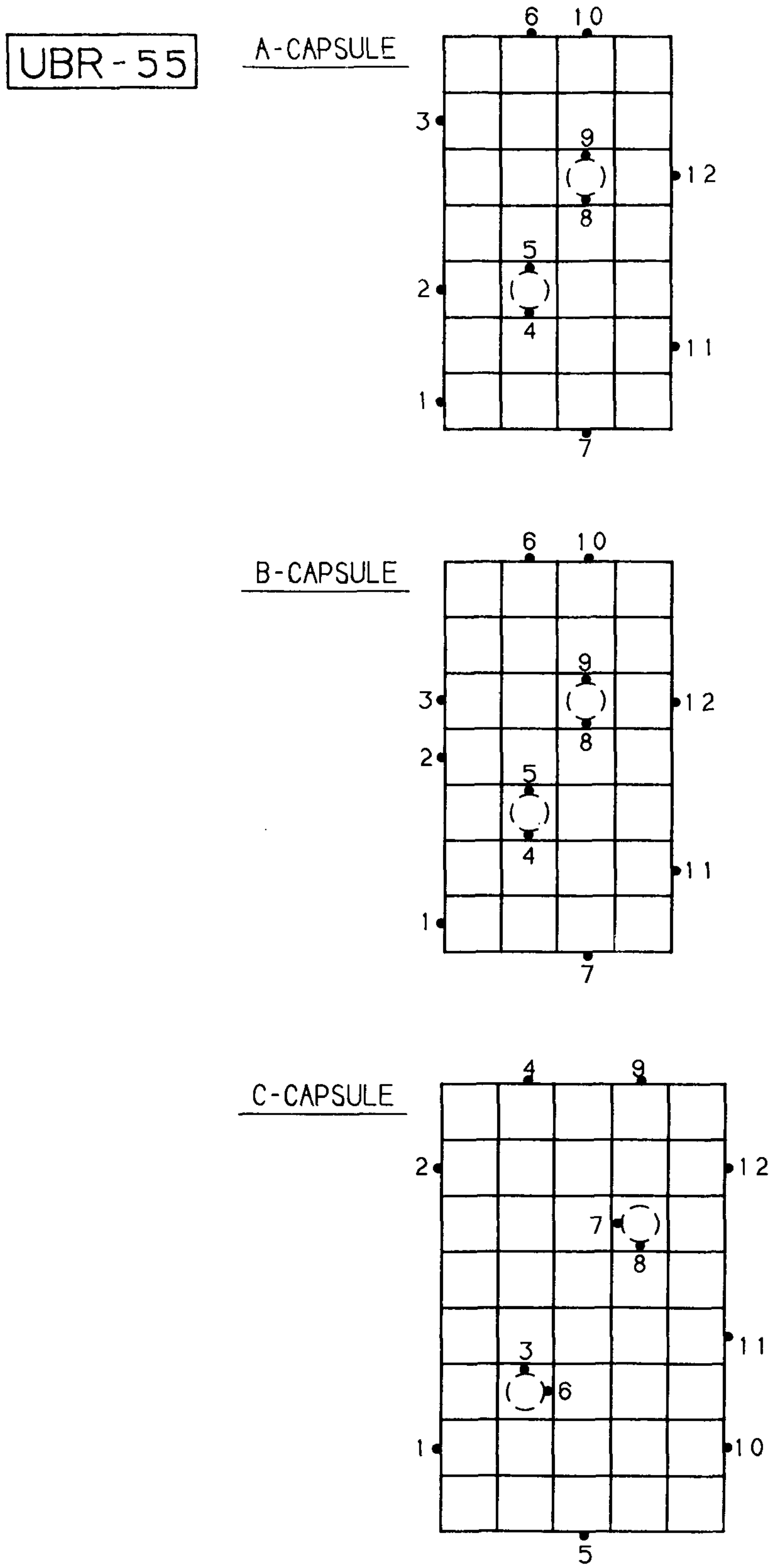

Fig. 17 Irradiation Assembly UBR-55 showing thermocouple placements in the specimen arrays.

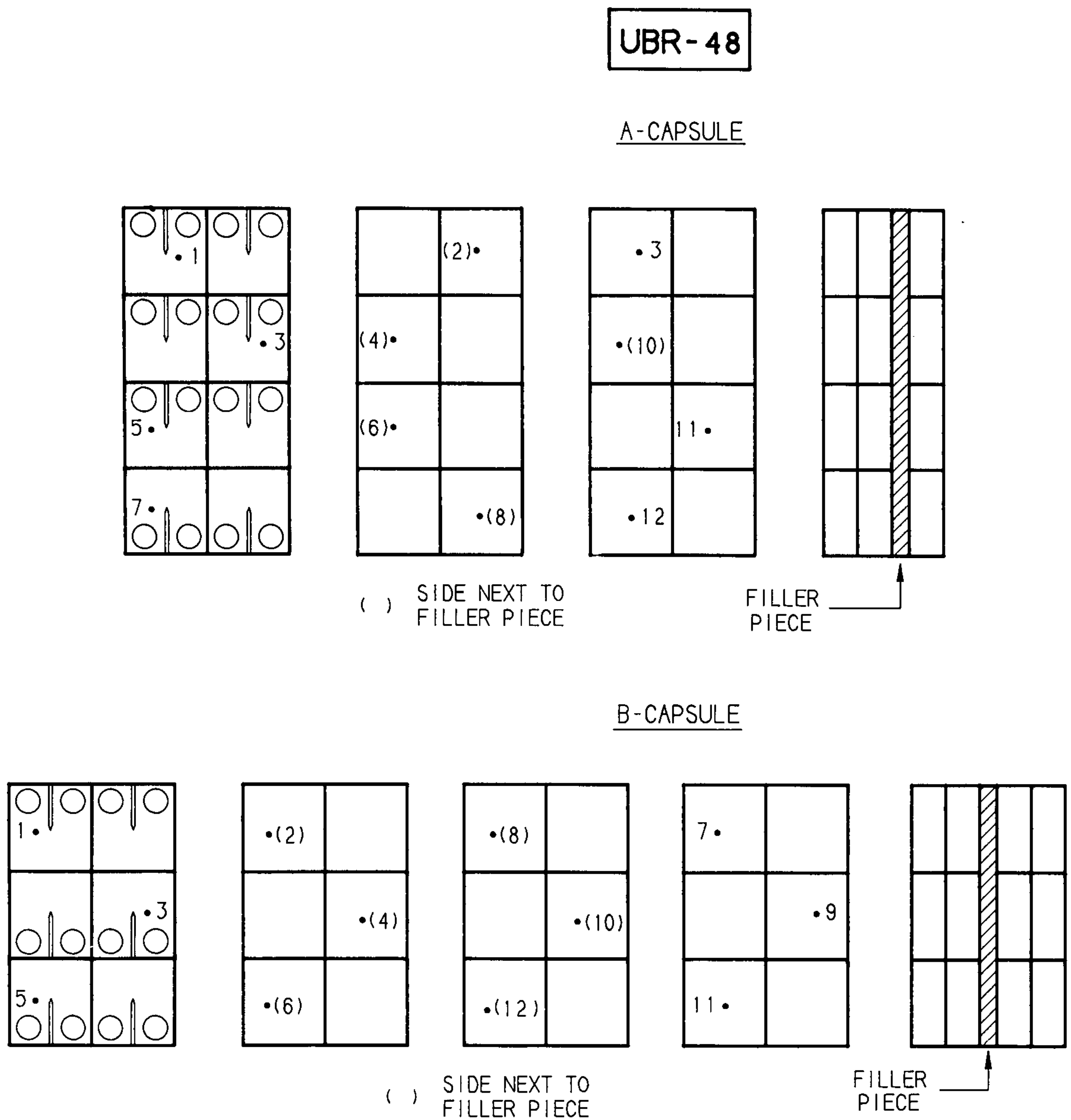

Fig. 18 Thermocouple Placements on Compact Tension Specimens in Experiment UBR-48 (Capsules A and B).

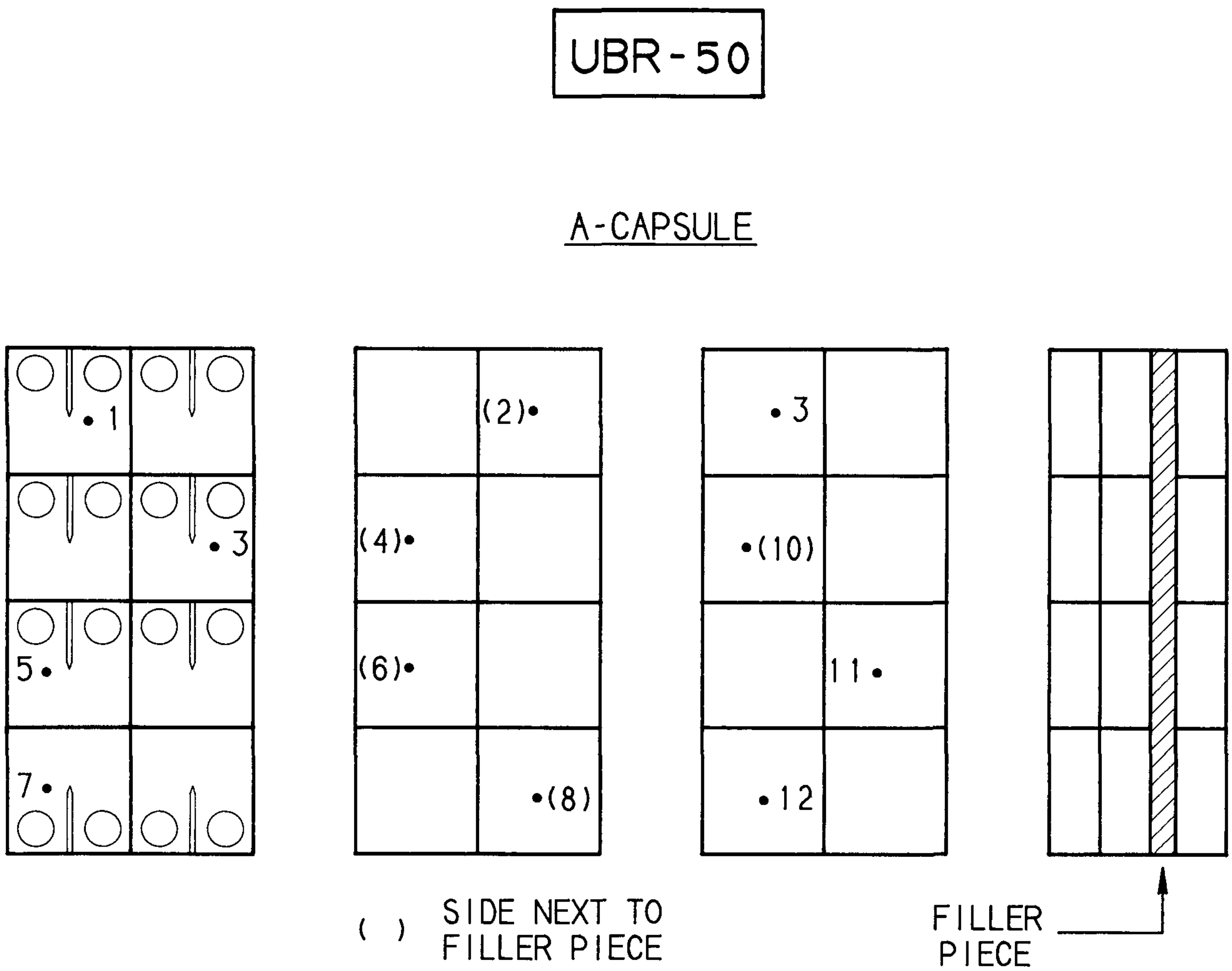

Fig. 19 Thermocouple Placements on Compact Tension; Specimens in Experiment UBR-50 (Capsule B).

Table 4 Irradiation Exposure of Experiment Assemblies

Irradiation Assembly No.	UBR Experiment (Capsule No.)	Condition[a]	Fluence (n/cm^2, E > 1 MeV) Cycle 1 ($x10^{19}$)	Cycle 2 ($x10^{19}$)	Total ($x10^{19}$)
IAR-1C	UBR-41C	I	1.34	----	1.34
IAR-2C	UBR-42C	I	2.03	----	2.03
IAR-3C	UBR-43C	I	2.72	----	2.72
IAR-6C	UBR-55C	I	3.25	----	3.25
IAR-1A	UBR-41A	IAR	1.32	0.32	1.64
IAR-1B	UBR-41B	IAR	1.44	0.75	2.19
IAR-2A	UBR-42A	IAR	1.28	0.96	2.24
IAR-2B	UBR-42B	IAR	1.46	1.49	2.95
IAR-6B	UBR-55B	IAR	2.63	0.61	3.24
IAR-6A	UBR-55A	IAR	2.67	1.43	4.10
IAR-7A	UBR-48A	I	2.10	----	2.10
IAR-7B	UBR-48B	IAR	1.48	0.74	2.22
IAR-8A	UBR-50A	I	1.50	----	1.50

[a] U = Unirradiated
I = Irradiated
IAR = Irradiated + Annealed + Reirradiated

Fission spectrum averaged cross section values for neutrons having energies greater than 1 MeV are assumed to be 115.2 and 156.8 millibarns, for the two respective dosimeter types.

5. TENSION TEST RESULTS

Yield strength and ultimate tensile strength determinations at 24°C for the various material conditions are listed in Tables 5 and 6, and are illustrated in Fig. 20.

A sharp rise in strength with 288°C irradiation to a fluence of 1.2 x 10^{19} n/cm^2 was observed. Above this fluence, the rate of strength elevation with additional fluence was much less as expected. The data moreover, show a clear benefit of the IAR treatment toward minimizing the yield strength and tensile strength change with a given total fluence. Of interest, the yield strength elevation with IAR for a total fluence of 4.1 x 10^{19} n/cm^2 (Irradiation Assembly IAR-6A) is about the same for the Weld W8A and the Weld W9A, that is, 147.5 MPa (21.4 ksi) vs. 129.7 MPa (18.8 ksi). Preirradiation yield strengths of the welds, however, differed by 76.5 MPa (11.1 ksi).

Referring to the data from the low first cycle fluence capsule set, the strength patterns for the Weld W8A describe a strong tendency toward radiation effects saturation. On the other hand, the data for the Weld W9A do not provide as clear an indication of this tendency. The data for the low first cycle fluence capsule set vs. the high first cycle fluence capsule set suggest that there is no particular effect of first cycle fluence level on subsequent IAR yield strength level or tensile strength level at high fluence.

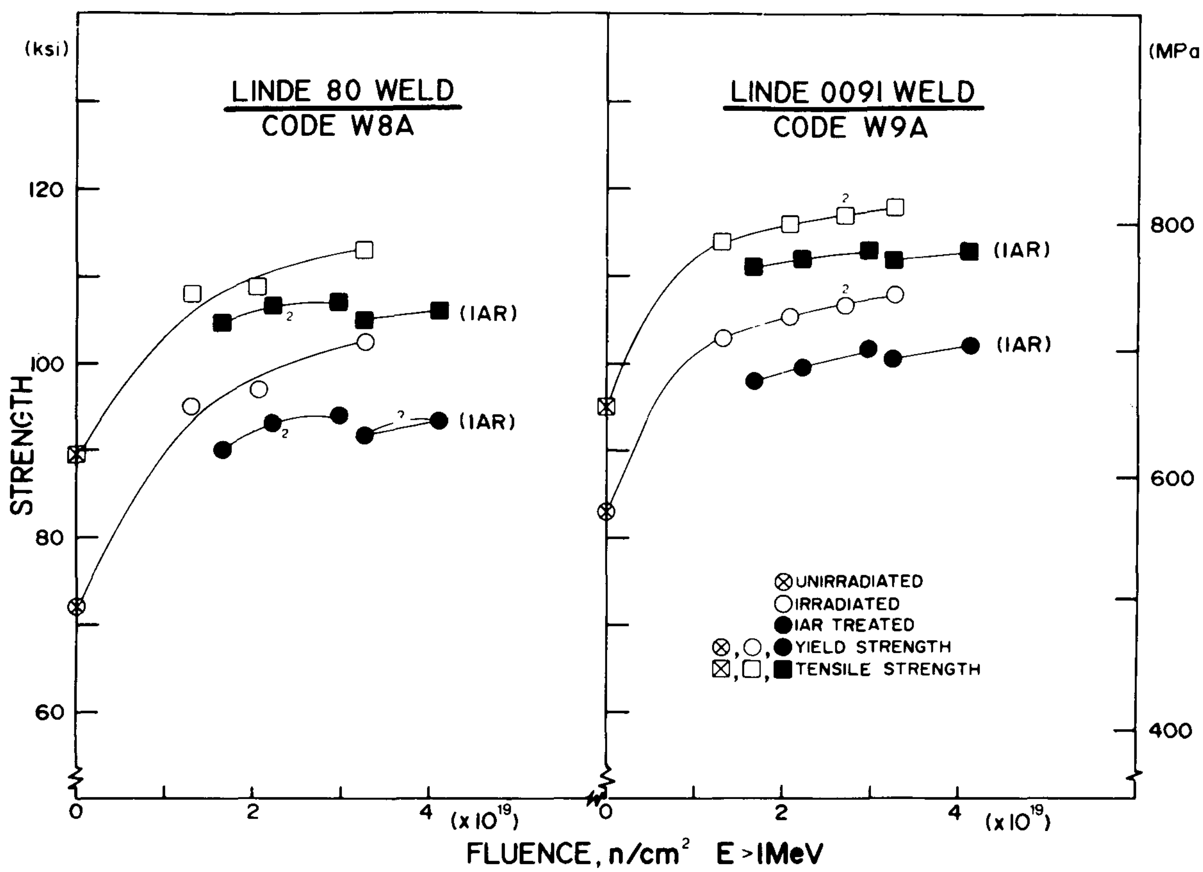

Fig. 20 Yield strength and tensile strength changes with irradiation (I) vs. irradiation-anneal-reirradiation (IAR) observed for the Linde 80 submerged-arc weld (left) and the Linde 0091 submerged-arc weld (right). Open and filled symbols refer, respectively, to I and IAR test results.

Table 5 Yield and Tensile Strength Changes of Weld W8A with Irradiation and IAR Treatments

Material Code	Irradiation Assembly No.	Condition[a]	Fluence (n/cm^2, E > 1 MeV) Cycle 1 ($\times 10^{19}$)	Cycle 2 ($\times 10^{19}$)	Total ($\times 10^{19}$)	Yield Strength (MPa at 24°C)	Yield Strength (ksi at 75°F)	Tensile Strength (MPa at 24°C)	Tensile Strength (ksi at 75°F)
W8A	------	U	----	----	----	497.8	72.2[b]	617.1	89.5[b]
(Linde 80 ϕ)	IAR-1C	I	1.34	----	1.34	657.1	95.3	743.9	107.9
	IAR-2C	I	2.03	----	2.03	668.1	96.9	749.5	108.7
	IAR-3C	I	2.72	----	2.72	-----[c]	----[c]	-----[c]	-----[c]
	IAR-6C	I	3.25	----	3.25	706.0	102.4	778.4	112.9
	IAR-1A	IAR	1.32	0.32	1.64	621.9	90.2	721.2	104.6
	IAR-1B	IAR	1.44	0.75	2.19	641.9	93.1	734.3	106.5
	IAR-2A	IAR	1.28	0.96	2.24	641.2	93.0	735.0	106.6
	IAR-2B	IAR	1.46	1.49	2.95	647.4	93.9	736.4	106.8
	IAR-6B	IAR	2.63	0.61	3.24	630.9	91.5	723.3	104.9
	IAR-6A	IAR	2.67	1.43	4.10	645.3	93.6	733.6	106.4

[a] U = Unirradiated
I = Irradiated
IAR = Irradiated + annealed + reirradiated

[b] Average of duplicate tests

[c] Not available

Table 6 Yield and Tensile Strength Changes of Weld W9A with Irradiation or IAR Treatments

Material Code	Irradiation Assembly No.	Condition[a]	Fluence (n/cm^2, E > 1 MeV) Cycle 1 ($\times 10^{19}$)	Cycle 2 ($\times 10^{19}$)	Total ($\times 10^{19}$)	Yield Strength (MPa at 24°C)	Yield Strength (ksi at 75°F)	Tensile Strength (MPa at 24°C)	Tensile Strength (ksi at 75°F)
W9A	------	U	----	----	----	497.3	83.3[b]	656.4	95.2[b]
(Linde 0091 ϕ)	IAR-1C	I	1.34	----	1.34	708.8	102.8	784.6	113.8
	IAR-2C	I	2.03	----	2.03	726.0	105.3	799.1	115.9
	IAR-3C	I	2.72	----	2.72	735.7	106.7[b]	803.9	116.6[b]
	IAR-6C	I	3.25	----	3.25	744.6	108.0	815.6	118.3
	IAR-1A	IAR	1.32	0.32	1.64	676.4	98.1	764.6	110.9
	IAR-1B	IAR	1.44	0.75	2.19	686.0	99.5	770.8	111.8
	IAR-2A	IAR	1.28	0.96	2.24	701.2	101.7	779.1	113.0
	IAR-2B	IAR	1.46	1.49	2.95	-----[c]	-----[c]	-----[c]	-----[c]
	IAR-6B	IAR	2.63	0.61	3.24	691.5	100.3	774.3	112.3
	IAR-6A	IAR	2.67	1.43	4.10	704.0	102.1	781.2	113.3

[a] U = Unirradiated
I = Irradiated
IAR = Irradiated + annealed + reirradiated

[b] Average of duplicate tests

[c] Not available

6. CHARPY-V NOTCH DUCTILITY TEST RESULTS

6.1 Overview

The C_v notch ductility determinations for the welds are summarized in Tables 7 and 8. Trends in 41-J transition temperature change with fluence for the I-condition and the IAR-condition are illustrated in Figs. 21 and 22. Companion trends in C_v USE change with fluence are illustrated in Figs. 23 and 24.

Brittle-ductile transition curves and data points for the individual material conditions are shown in Figs. 25 to 34. The curves shown are visual best-fits to the data. Individual specimen data are given in Appendix D. Computer-curve fits of the data and values of curve fitting parameters are also given in Appendix E. In general, the hand-drawn vs. computer-fit curves show a close agreement in their 41-J transition temperature determination. In the text below, comparisons are based on 41-J and USE values derived from the hand-drawn curves.

6.2 I-Condition and IA-Condition Observations

Figures 25 and 26 provide the C_v data for the welds in the unirradiated condition, the low fluence first cycle irradiated (I) condition and 399°C postirradiation annealed (IA) condition. All annealing heat treatments were of 168 hour duration. In general, low data scatter is evident which aided the determination of 41-J transition and USE properties.

Comparisons were made with unirradiated and as-irradiated condition properties observed for the welds used in the IAR Phase 1 program (see Figs. 35 and 36). Close similarities were found. For example, the transition temperature elevations for the Weld W8A and Weld W9A were 119°C and 96°C respectively; those for the Weld V84 and Weld V86 were 117°C and 119°C respectively, at about the same fluence. An important difference, however was noted in the degree of transition temperature recovery by 399°C annealing. In the present case, the recovery was on the order of 35 to 45 percent whereas 70 percent recovery was observed with the same heat treatment for Welds V84 and V86. Accordingly, a potential for large differences in recovery with 399°C annealing exists among welds. Welding flux type does not appear to be a causative factor based on the comparable recovery (~42 percent) of Weld W8A and Weld W9A.

Judicious use of specimens from each irradiation capsule permitted a reservation of some specimens for exploratory postirradiation annealing (or post-reirradiation annealing) tests at 454°C. Figures 29 and 30 present and compare these results to the 399°C-168 hour annealing data from the various capsules. For both welds, the residual embrittlement of the annealing would appear to be independent of the prior irradiation history (I or IAR). A second observation is that 454°C-168 hour annealing did not produce full 41-J transition temperature recovery for either weld. Recent assessments of the effectiveness of 454°C-168 hour annealing, using other welds and plate

(text continues on pg. 53)

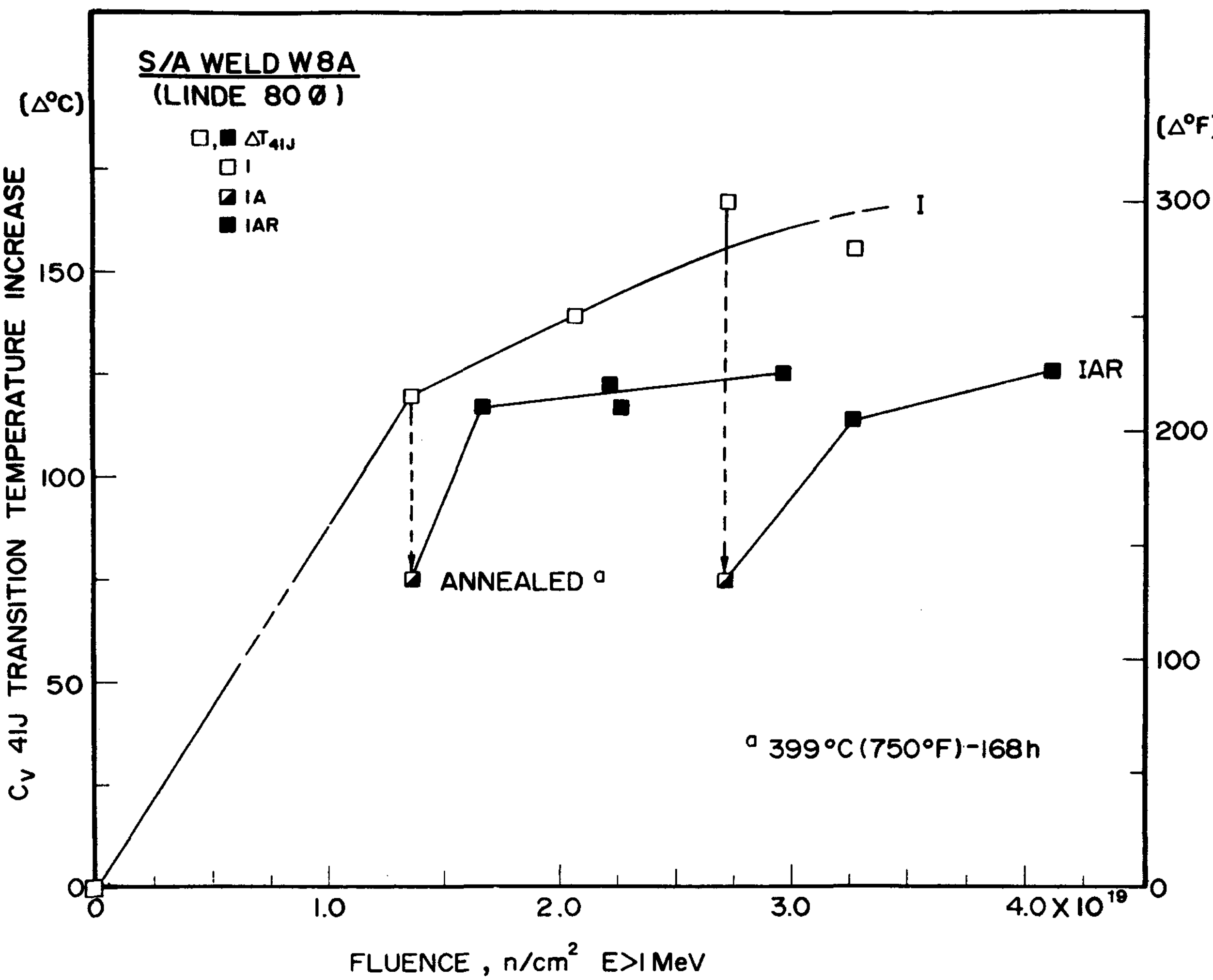

Fig. 21 Summary of C_v 41-J transition temperature observations for Weld W8A (I and IAR conditions).

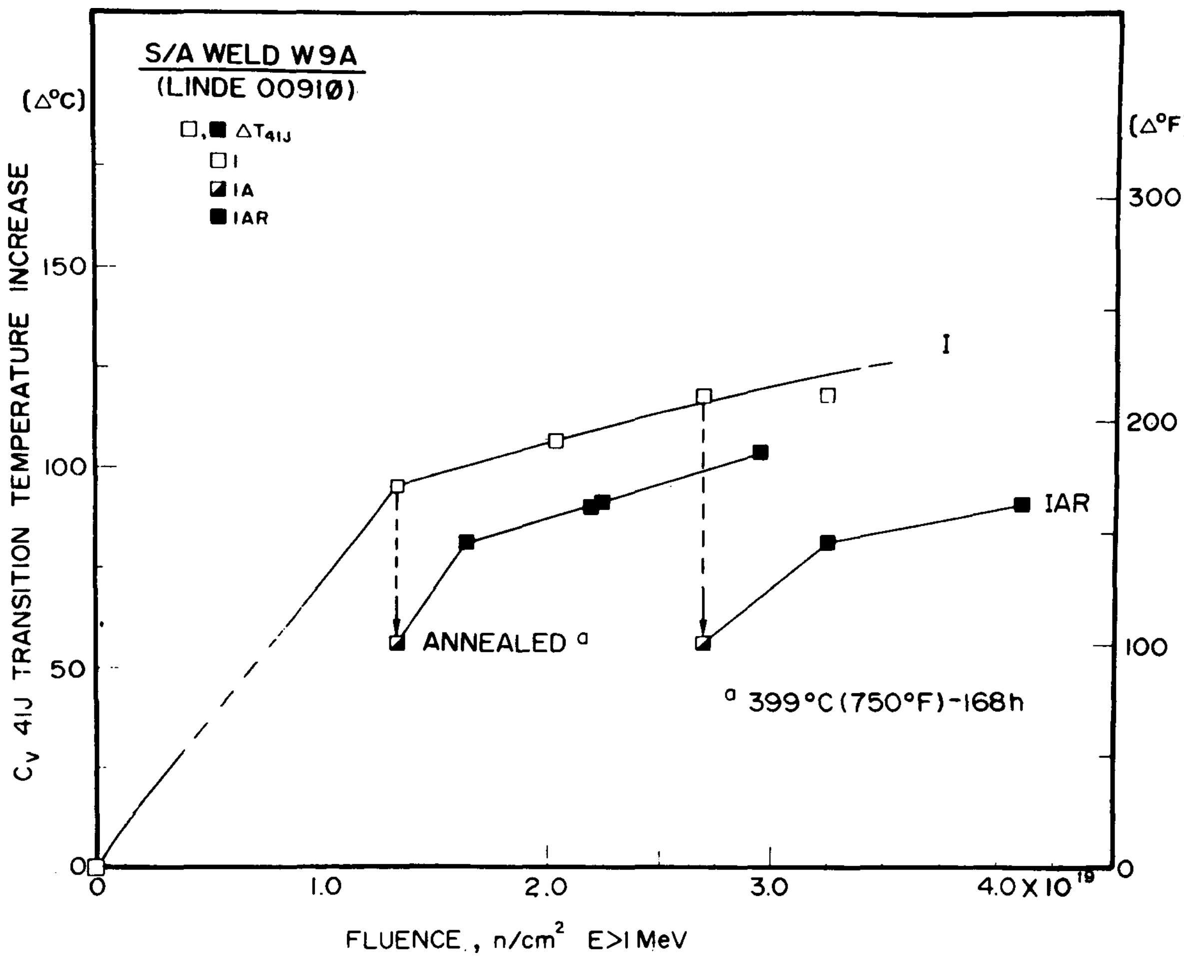

Fig. 22 Summary of C_v 41-J transition temperature observations for Weld W9A (I and IAR conditions).

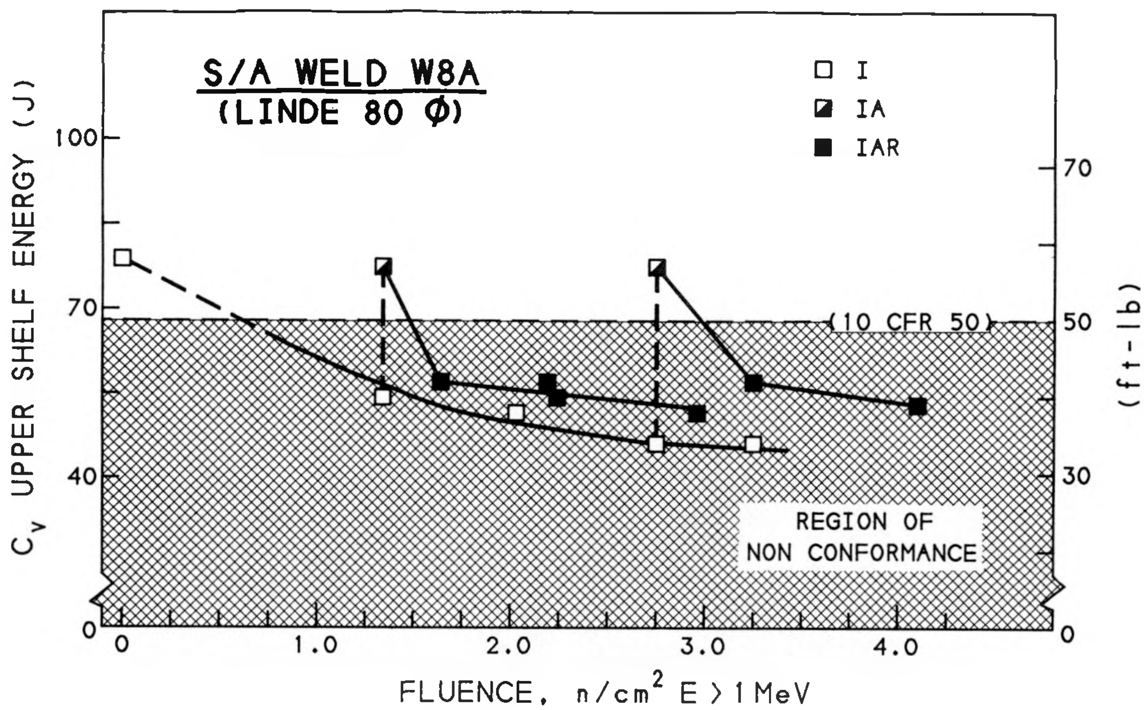

Fig. 23 Summary of C_v upper shelf energy observations for Weld W8A (I and IAR conditions).

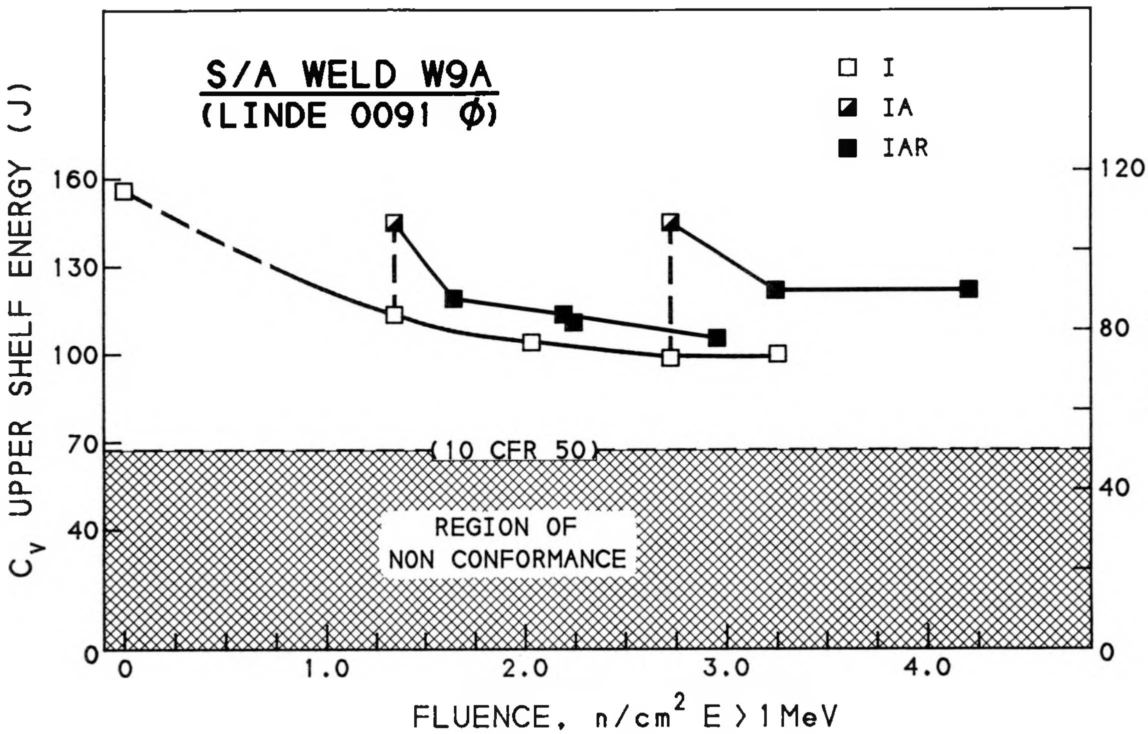

Fig. 24 Summary of C_v upper shelf energy observations for Weld W9A (I and IAR conditions).

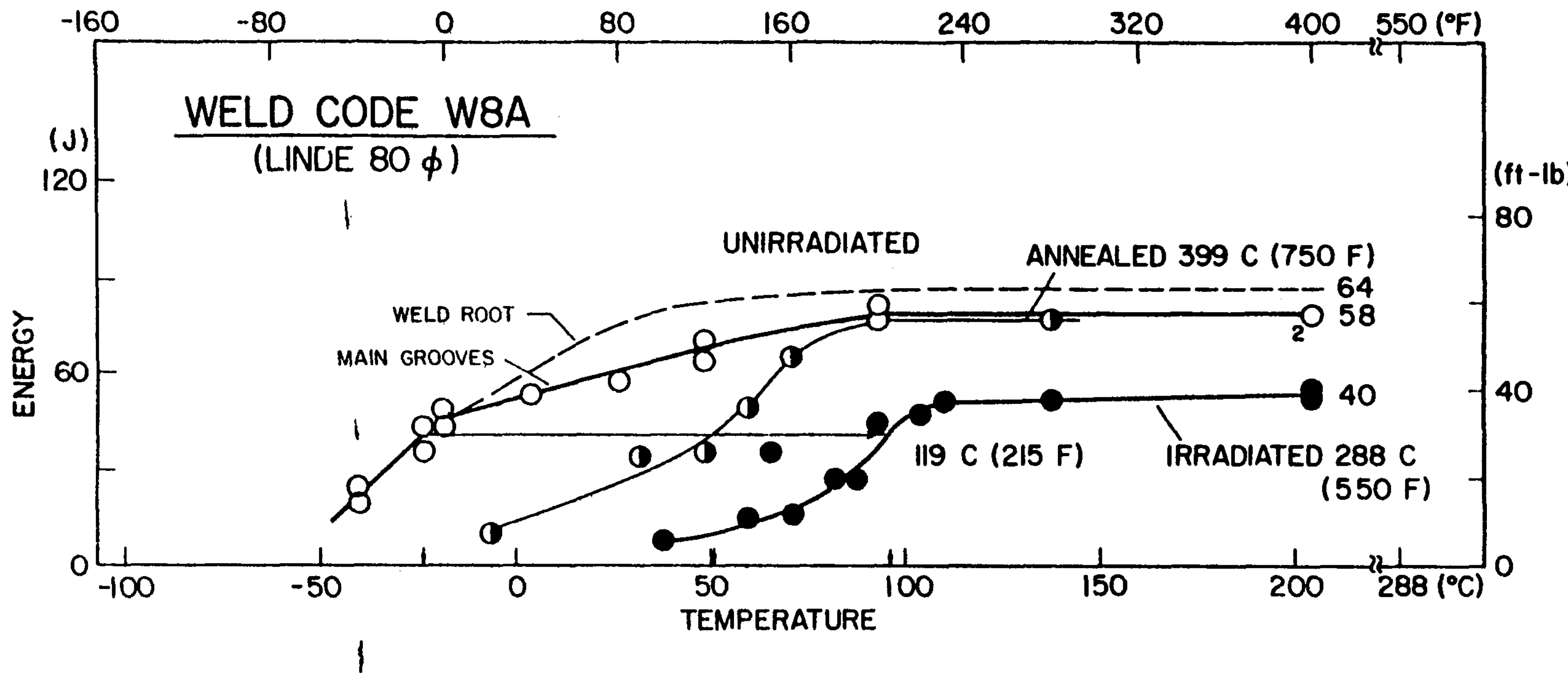

Fig. 25 Notch ductility of Weld W8A before and after irradiation and after postirradiation annealing. (low first cycle fluence case)

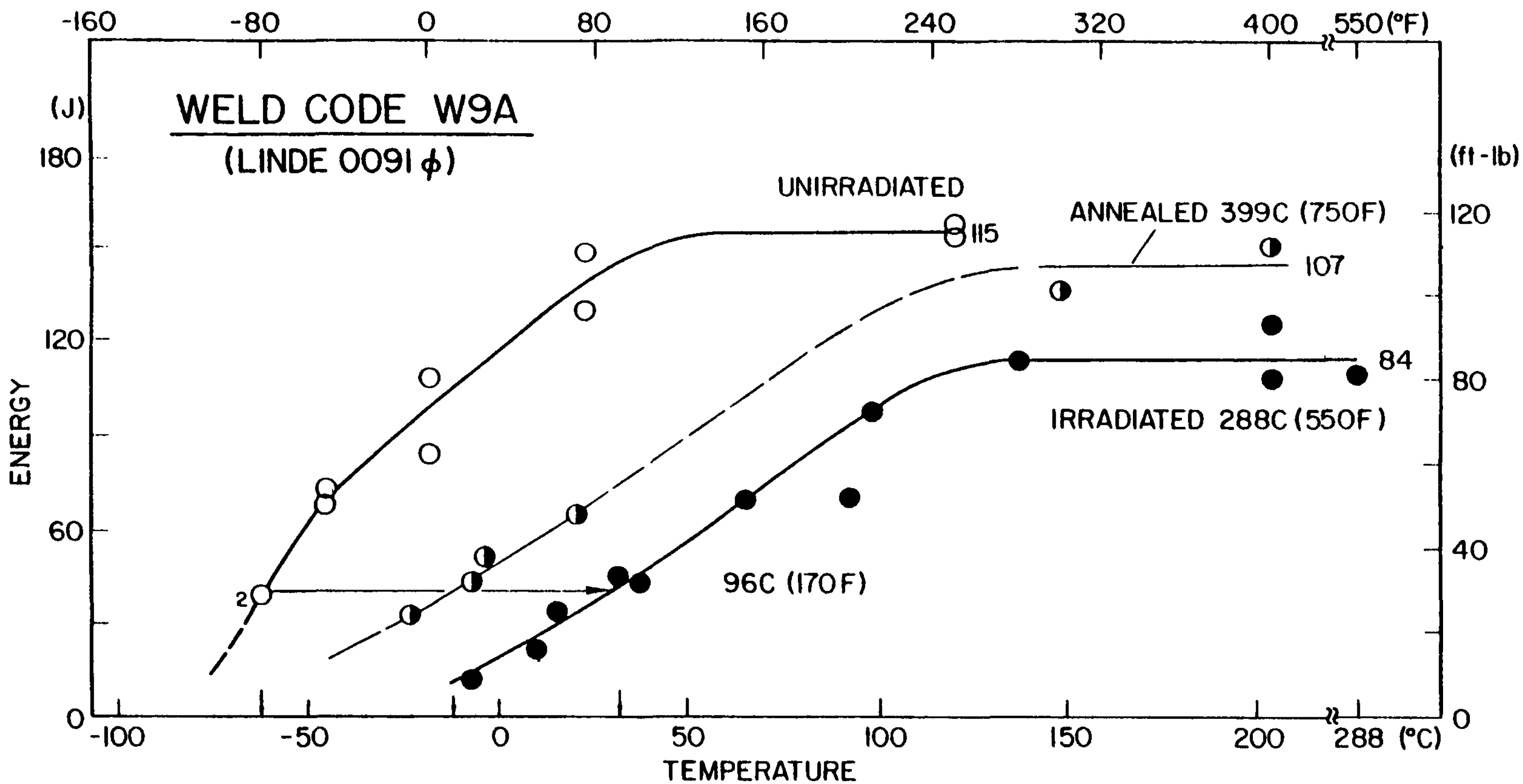

Fig. 26 Notch ductility of Weld W9A before and after irradiation and after postirradiation annealing. (low first cycle fluence case)

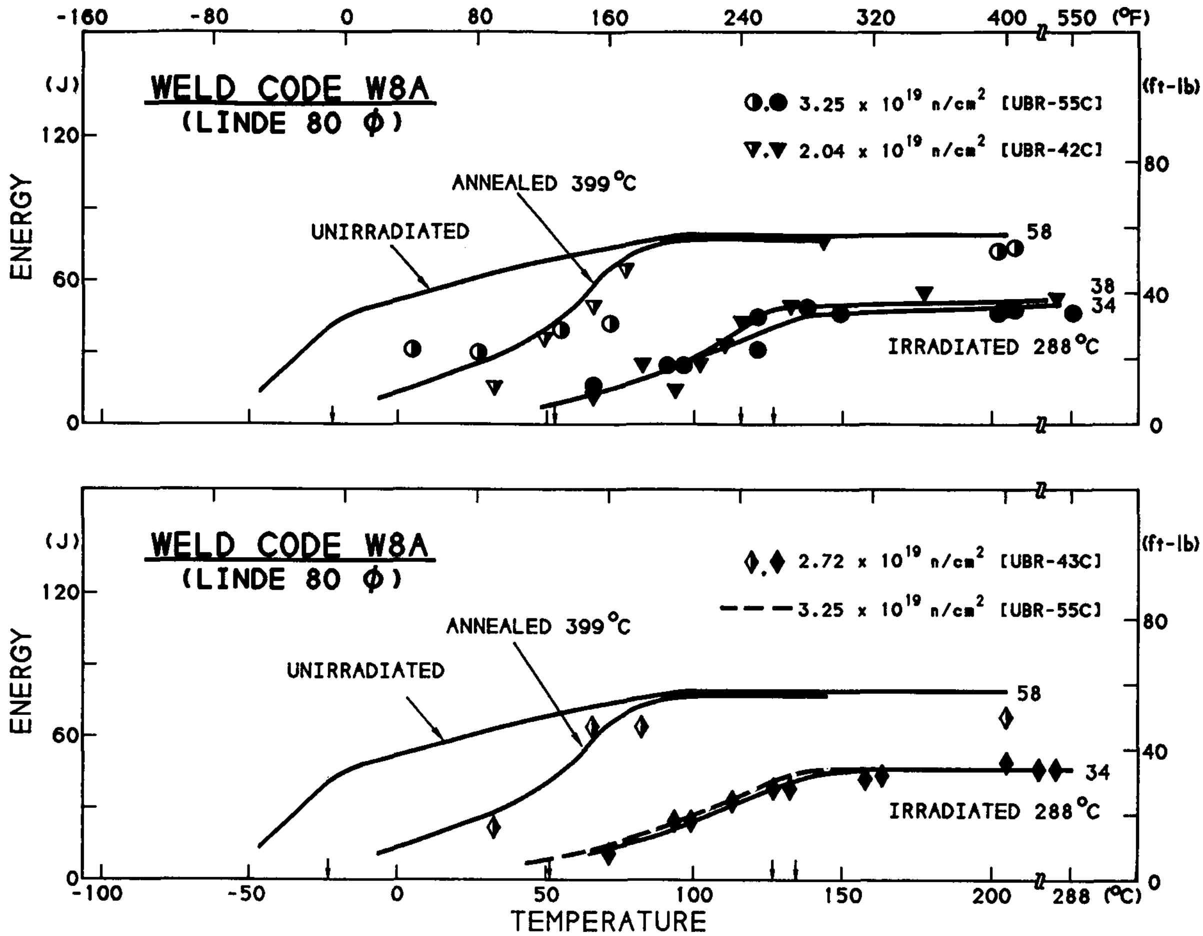

Fig. 27 Notch ductility of Weld W8A before and after irradiation and after postirradiation annealing. (high fluence case)

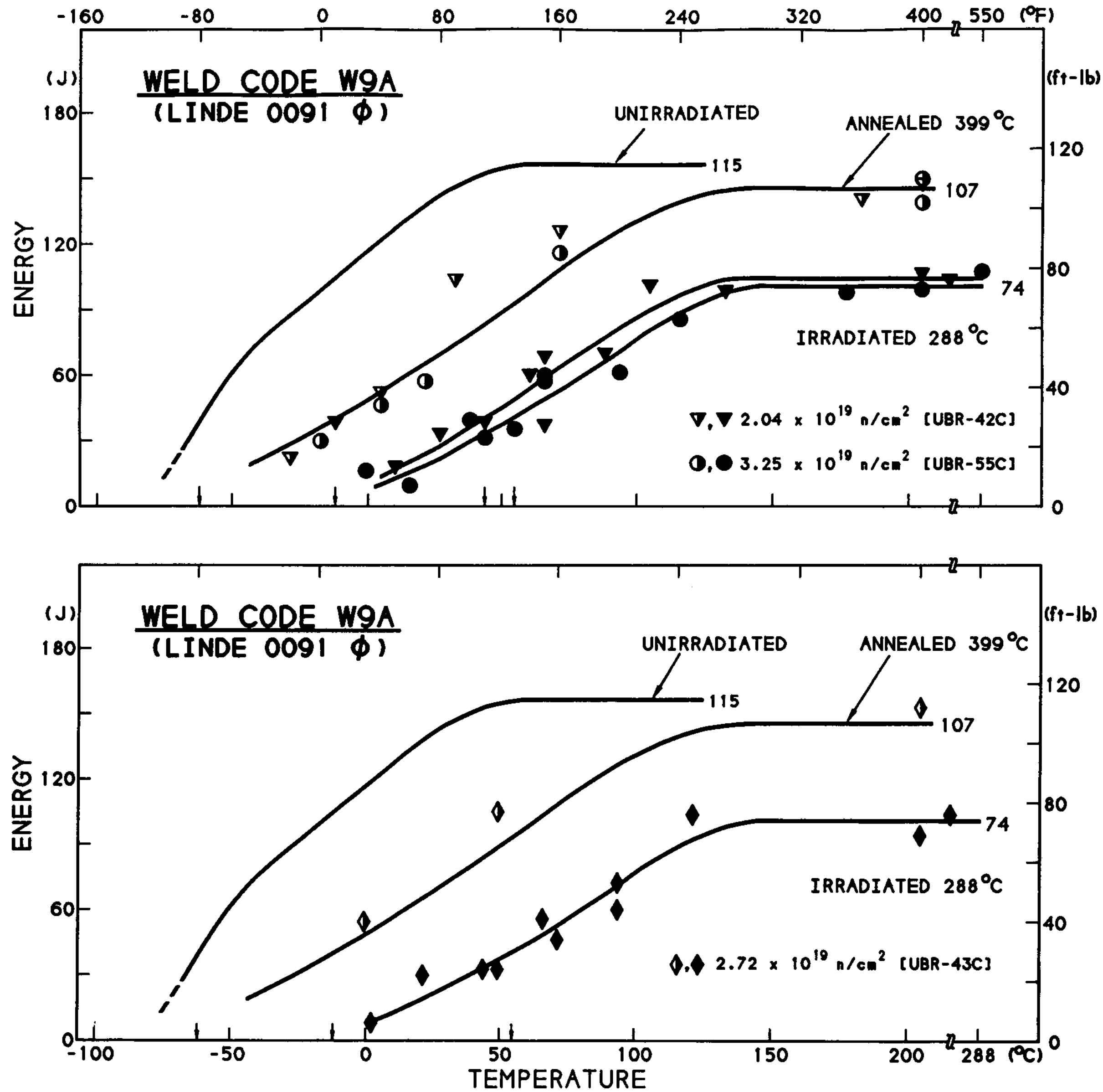

Fig. 28 Notch ductility of Weld W9A before and after irradiation and after postirradiation annealing. (high fluence case)

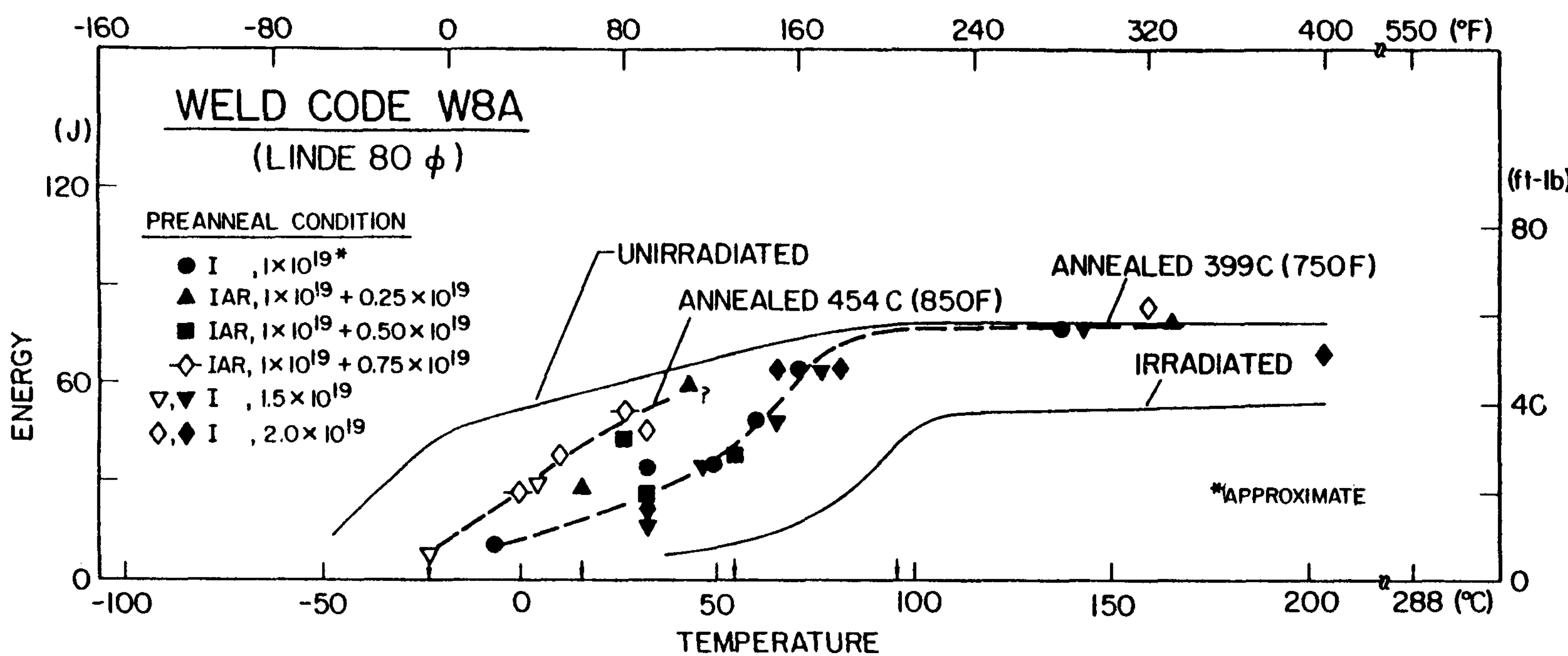

Fig. 29 Observations on effectiveness of 399^0 C and 454^0 C annealing for Weld W8A. Results for several I and IAR experiments are shown.

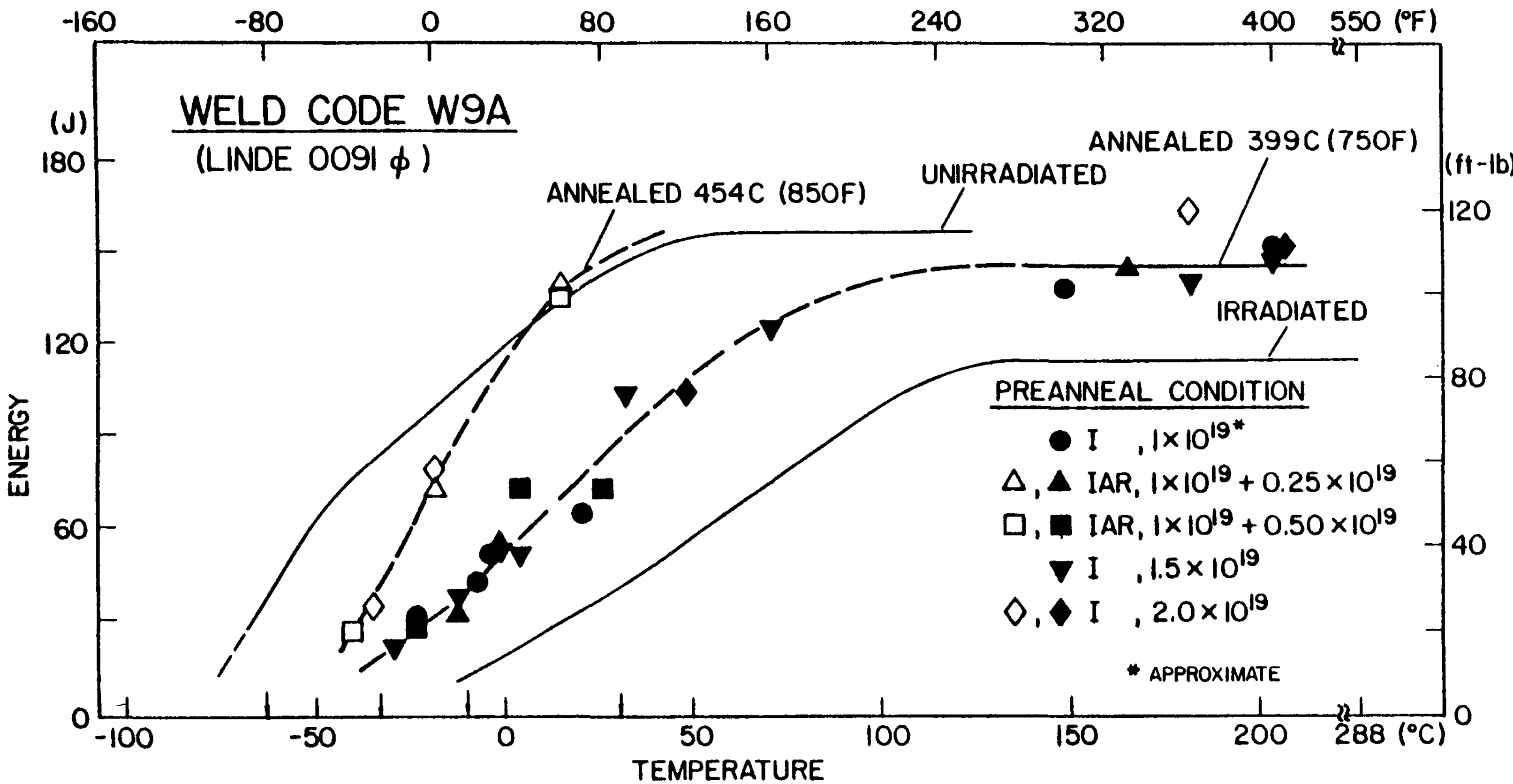

Fig. 30 Observations on effectiveness of 399 ^{0} C and 454 ^{0} C annealing for Weld W9A. Results for several I and IAR experiments are shown.

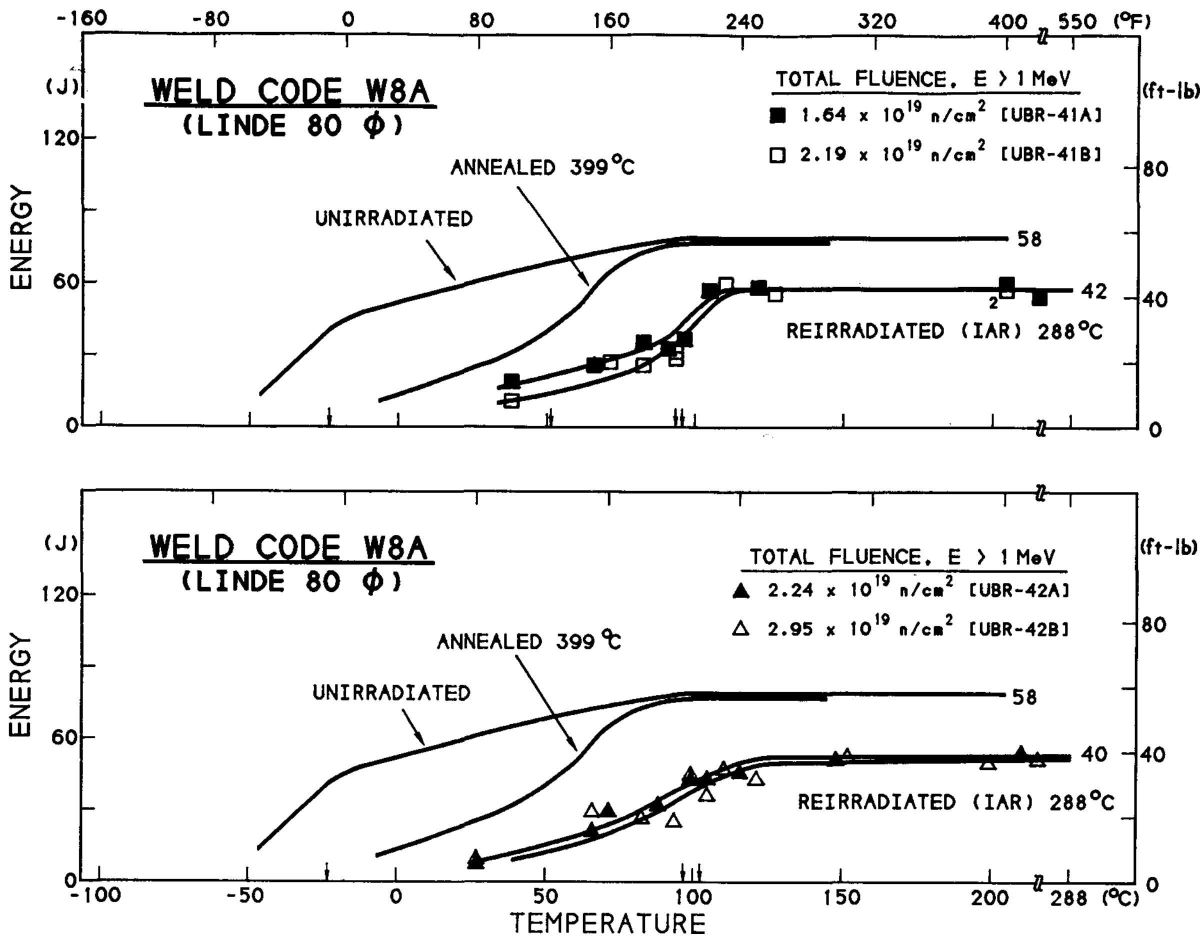

Fig. 31 Notch ductility of Weld W8A after reirradiation referenced to the unirradiated condition and the 399°C postirradiation annealed condition (Low first cycle fluence case). In this figure and later figures, the curve for the postirradiation annealed condition of Weld W8A is based on data from Irradiation Assembly IAR-1C (only).

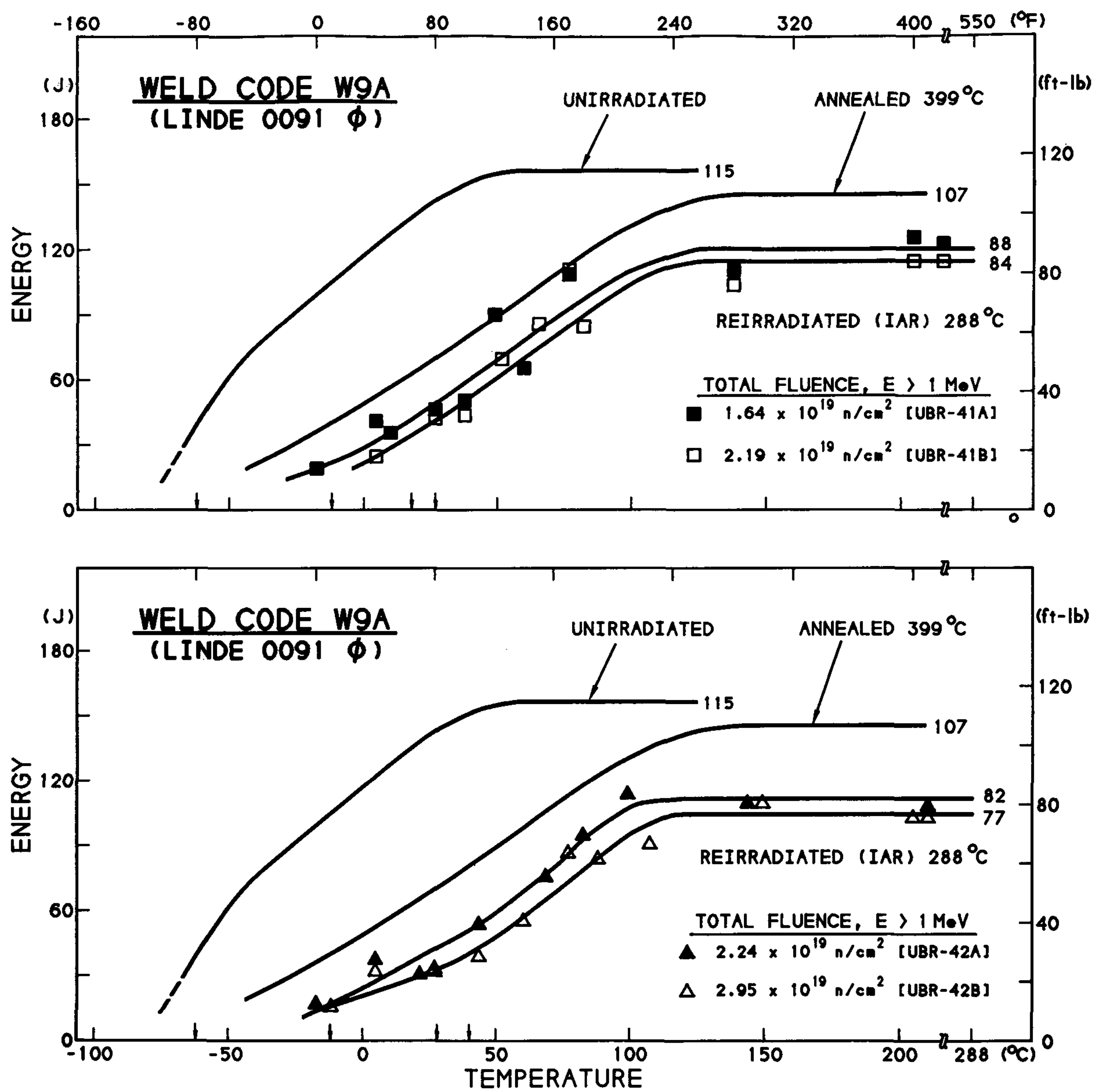

Fig. 32 Notch ductility of Weld W9A after reirradiation referenced to the unirradiated condition and the 399°C postirradiation annealed condition (Low first cycle fluence case). In this figure and later figures, the curve for the postirradiation annealed condition of Weld W9A is based on data from Irradiation Assembly IAR-1C (only).

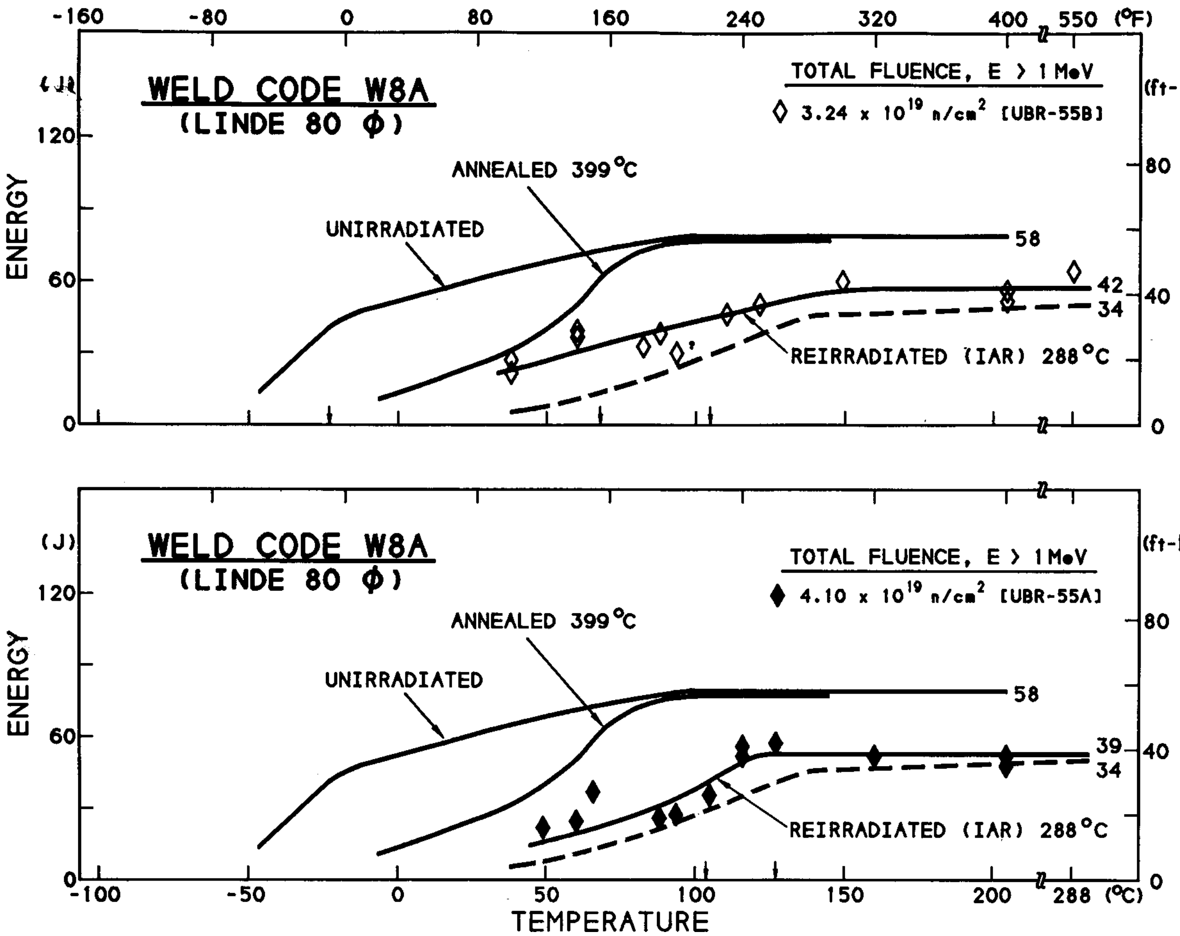

Fig. 33 Notch ductility of Weld W8A after reirradiation referenced to the unirradiated condition and the 399°C postirradiation annealed condition (High first cycle fluence case). The dashed curve depicts I-condition data from UBR-55C.

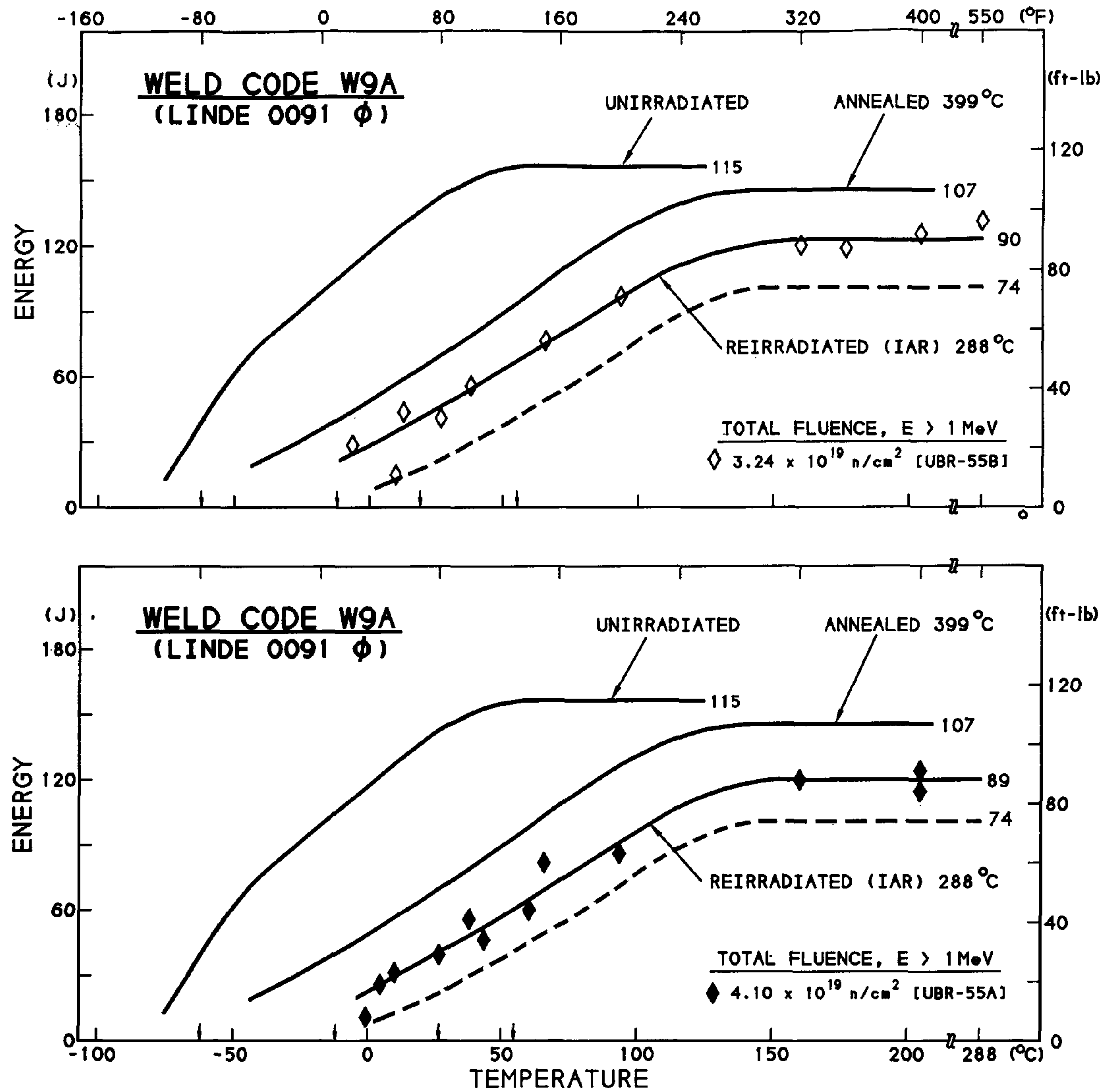

Fig. 34 Notch ductility of Weld W9A after reirradiation referenced to the unirradiated condition and the 399°C postirradiation annealed condition (High first cycle fluence case). The dashed curve depicts I-condition data from UBR-55C.

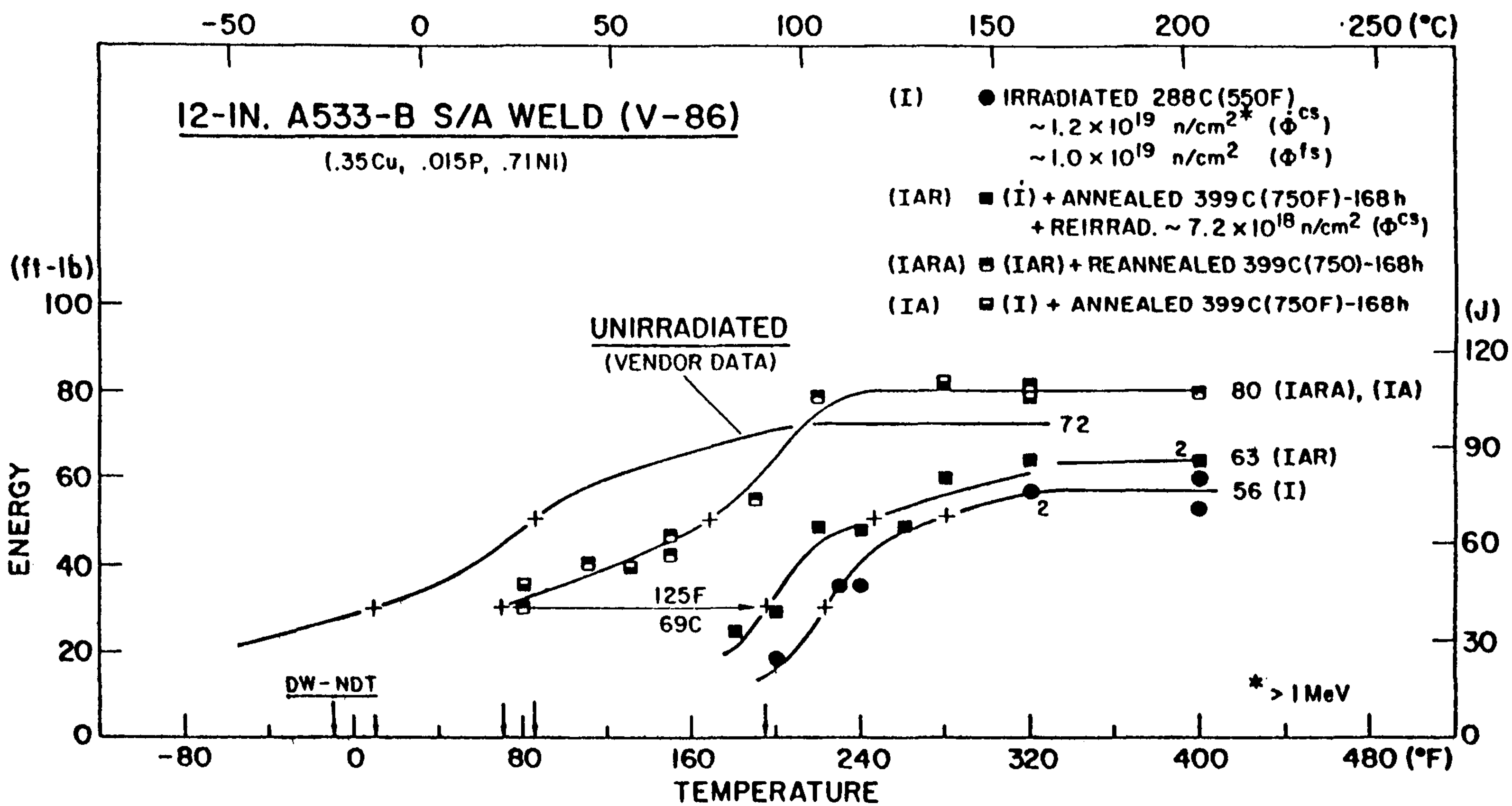

Fig. 35 Notch ductility of Weld V86 (Phase 1 Study) after irradiation, intermediate annealing and reirradiation. Limited results for reannealing are also shown. The transition temperature elevation of the I-condition is 117°C (210°F).

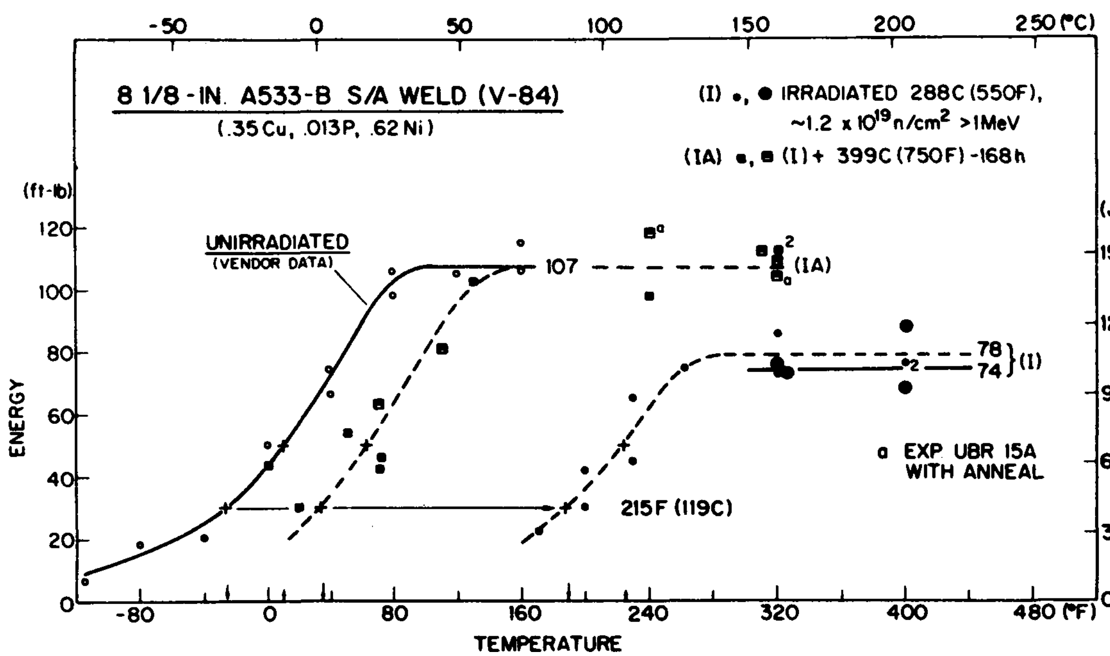

Fig. 36 Notch ductility of Weld V84 (Phase 1 Study) after irradiation, intermediate annealing and reirradiation. Limited results for reannealing are also shown.

Table 7 Summary of Observations for Weld W8A (Linde 80 ϕ)
(IAR Phase 2 Experiments)

Irradiation Assembly No.	Condition[a]	Fluence (n/cm^2 E > 1 MeV)			C_v 41 J Temperature[b,c] Increase				C_v USE Decrease[b,c]			
		Cycle 1	Cycle 2	Total	Over Initial 41-J Temp		Over Annealed 41-J Temp		Below Initial		Below Annealed	
		($\times 10^{19}$)	($\times 10^{19}$)	($\times 10^{19}$)	(Δ°F)	(Δ°C)	(Δ°F)	(Δ°C)	(Δft-lb)	(ΔJ)	(Δft-lb)	(ΔJ)
IAR-1C	I	1.34	----	1.34	215	119	---	---	18	25	--	--
IAR-2C	I	2.03	----	2.03	250	139	---	---	20	27	--	--
IAR-3C	I	2.72	----	2.72	300	167	---	---	24	33	--	--
IAR-6C	I	3.25	----	3.25	280	156	---	---	24	33	--	--
IAR-1A	IAR	1.32	0.32	1.64	210	117	70	39	16	22	15	20
IAR-1B	IAR	1.44	0.75	2.19	220	122	80	44	16	22	15	20
IAR-2A	IAR	1.28	0.96	2.24	210	117	70	39	18	25	17	23
IAR-2B	IAR	1.46	1.49	2.95	225	125	85	47	20	27	19	26
IAR-6B	IAR	2.63	0.61	3.24	205	114	65	36	16	22	15	20
IAR-6A	IAR	2.67[d]	1.43[d]	4.10[d]	~225[d]	125[d]	85[d]	47[d]	19	26	18	24

[a] U = Unirradiated I = Irradiation only IAR = Irradiated, Annealed, Reirradiated
[b] Radiation-induced change
[c] Initial C_v Properties 41 J = -23°C (-10°F)
USE = 79 J (58 ft-lb)
[d] Preliminary

Table 8 Summary of Observations for Weld W9A (Linde 0091 d) (IAR Phase 2 Experiments)

Irradiation Assembly No.	Condition[a]	Fluence (n/cm^2 E > 1 MeV)			C_v 41 J Temperature Increase[b,c]				C_v USE Decrease[b,c]			
		Cycle 1	Cycle 2	Total	Over Initial 41-J Temp		Over Annealed 41-J Temp		Below Initial		Below Annealed	
		($\times 10^{19}$)	($\times 10^{19}$)	($\times 10^{19}$)	(Δ°F)	(Δ°C)	(Δ°F)	(Δ°C)	(Δft-lb)	(ΔJ)	(Δft-lb)	(ΔJ)
IAR-1C	I	1.34	----	1.34	170	94	---	---	31	42	--	--
IAR-2C	I	2.03	----	2.03	190	106	---	---	38	52	--	--
IAR-3C	I	2.72	----	2.72	210	117	---	---	42	57	--	--
IAR-6C	I	3.25	----	3.25	210	117	---	---	41	56	--	--
IAR-1A	IAR	1.32	0.32	1.64	145	81	50	28	~27	37	19	26
IAR-1B	IAR	1.44	0.75	2.19	160	89	65	36	31	42	23	31
IAR-2A	IAR	1.28	0.96	2.24	160	89	65	36	33	45	25	34
IAR-2B	IAR	1.46	1.49	2.95	185	103	90	50	38	52	30	41
IAR-6B	IAR	2.63	0.61	3.24	145	81	50	28	25	34	17	23
IAR-6A	IAR	2.67[d]	1.43[d]	4.10[d]	160	89	65	36	25	34	17	23

[a] U = Unirradiated I = Irradiation only IAR = Irradiated, Annealed, Reirradiated
[b] Radiation-induced change
[c] Initial C_v Properties 41 J = -62°C (-80°F)
USE = 156 J (115 ft-lb)
[d] Preliminary

materials, have revealed that percentage recovery in transition temperature with 454°C annealing is material dependent (Refs. 11 and 12).

6.3 IAR-Condition Observations

6.3.1 Low First Cycle Fluence Capsule Set

Figures 31 and 32 illustrate the C_v data from specimens contained in the four IAR capsules having the low first cycle fluence target, (~1.2 x 10^{19} n/cm^2).

A relatively rapid reembrittlement with fluence after annealing is revealed for both welds. A fluence of only ~0.3 x 10^{19} n/cm^2 is seen to reduce a large portion of the annealing benefit. The results for a reirradiation fluence of ~0.8 x 10^{19} n/cm^2, nevertheless, reinforce the earlier Phase 1 finding that, at this fluence level, reembrittlement with IAR is not more than the embrittlement induced by the first cycle of irradiation. Moreover, the 41-J transition temperature elevation with IAR is significantly less than that by irradiation without annealing for a total fluence of 2.2 x 10^{19} n/cm^2. A good reproducibility of data for the IAR condition is demonstrated by the results for irradiation assemblies IAR-1B and IAR-2A. The total fluence of these assemblies were essentially identical; fluences received during the second irradiation cycle differed somewhat (see Table 7).

Of special interest, the reembrittlement trend for the Weld W8A is highly indicative of a tendency toward an embrittlement plateau. This observation mirrors that found with the tensile properties trend with IAR cited above. In contrast, a tendency toward embrittlement saturation with IAR is not described by the C_v data for the Weld W9A; the observation here is likewise supported by the tensile properties trend with IAR. Accordingly, an influence of welding flux type on reirradiation property trends is indicated. Examination of Figs. 21 and 22 further reveals that the benefit of IAR was greater for the Linde 80 Weld W8A than for the Linde 0091 Weld W9A. Whether or not this is a generic effect of welding flux type remains to be established.

6.3.2 High First Cycle Fluence Capsule Set

Figures 33 and 34 provide the C_v data from specimens contained in the two IAR capsules having the high first cycle fluence target, ~2.4 x 10^{19} n/cm^2.

Reirradiation fluence intervals initially were to match those of the low first cycle fluence capsule set; however, the observation of embrittlement saturation tendencies for Weld W8A in the latter capsule set led to a reconsideration of the reirradiation fluence target for Irradiation Assembly IAR-6A at mid-program. To obtain a more critical test of saturation tendencies for both welds, the target reirradiation fluence was increased from ~0.6 x 10^{19} n/cm^2 to 1.4 x 10^{19} n/cm^2.

The actual reirradiation fluence of 1.43 x 10^{19} n/cm^2 was found to increase only slightly the 41-J transition temperature of the Weld W8A and Weld W9A over that produced by a reirradiation fluence of 0.6 x 10^{19} n/cm^2. Also, the 41-J transition temperature elevation in this IAR condition was about the same order of magnitude as that produced by a fluence of ~1.3 x 10^{19} n/cm^2 without annealing. The benefit of intermediate 399°C annealing is obvious in the summary figures (Figs. 21 and 22). The 41-J temperature elevations determined with Assemblies IAR-3C and IAR-6C representing the I-condition (2.7 to 3.3 x 10^{19} n/cm^2) and those determined with Assembly IAR-6A representing the IAR-condition (4.1 x 10^{19} n/cm^2) suggest that the IAR benefit is about the same for the two weld types (36°C vs. 28°C). In this regard, it is noted that a close determination of the 41-J temperature for the Weld W8A at high fluence is made difficult (if not precluded) by the low upper shelf level of the material in this condition. The difficulty is compounded by data scatter at upper shelf temperatures.

Referring next to the data from Irradiation Assembly IAR-6B, a confirmation of the tendency of both welds to exhibit relatively rapid reembrittlement with fluence after 399°C annealing is provided. That is, the tendency appears to be independent of the fluence received before annealing for the range investigated: ~1.3 x 10^{19} to ~2.6 x 10^{19} n/cm^2.

6.3.3 Reproducibility of I-Condition and IA-Condition

A follow-on study of IAR benefits to the Weld W8A and Weld W9A for 454°C vs. 399°C intermediate annealing has been reported (Ref. 11). The first cycle fluence at 288°C was approximately the same as that used for the present study; also, the duration of the 399°C heat treatment investigated was identical. Accordingly, an assessment of experiment reproducibility can be made for the I and IA conditions. (Experimental reproducibility for the IAR-condition was discussed in Section 6.3.1.)

The results of the follow-on study are shown in Figs. 37 and 38. The dashed curves in each figure indicate the data trends from the present investigations. Very close agreement is indicated. The fluence level for the follow-on study was 1.44 x 10^{19} vs. 1.34 x 10^{19} n/cm^2 here.

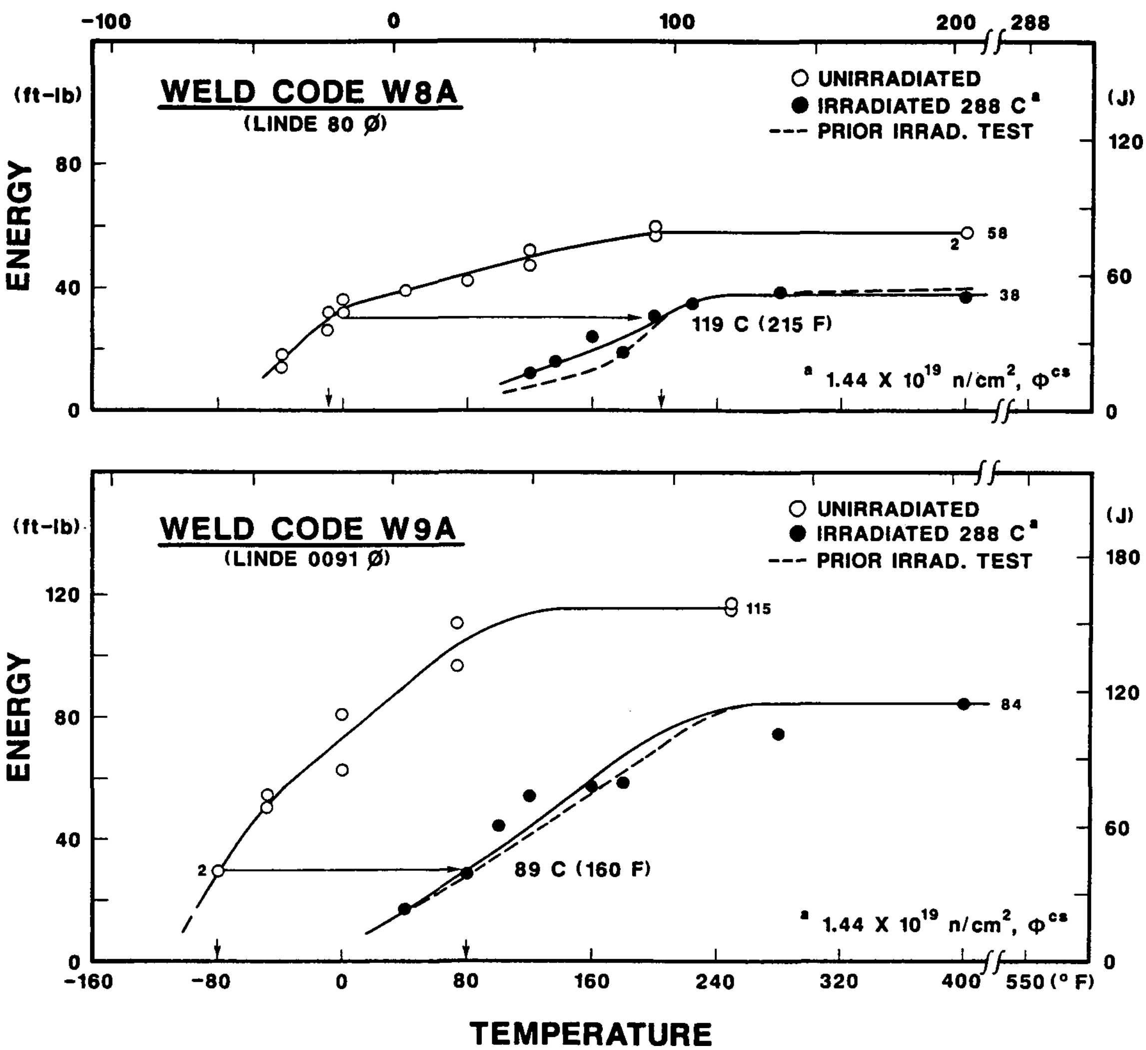

Fig. 37 Charpy-V notch ductility of Weld W8A (upper graph) and Weld W9A (lower graph) before and after irradiation in Assembly HTA-1 (UBR-62). The data points for the irradiated condition agree well with the data trends observed in the present study (dashed curves).

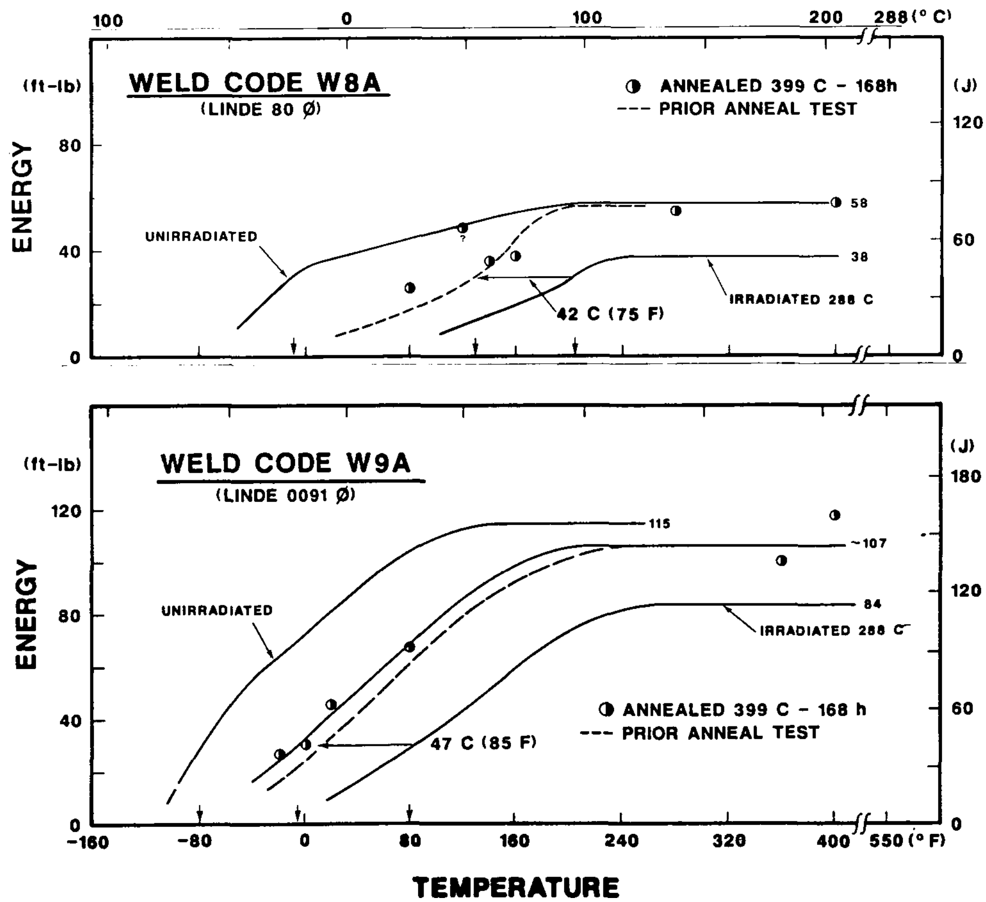

Fig. 38 Charpy-V notch ductility of Weld W8A (upper graph) and Weld W9A (lower graph) before and after irradiation and after postirradiation annealing at 399 °C (Assembly HTA-1). The dashed curves indicate 399°C annealing trends from the present study.

7. FRACTURE TOUGHNESS DETERMINATIONS

7.1 Specimen Design

The fracture toughness determinations were made using 0.5T-CT specimens with a thickness of 12.7 mm (Fig. 7). This design is similar to that recommended in ASTM E 813-81 (Ref. 13) where load-line displacement is measured on the specimen. (Suitability of this specimen design for testing is discussed in Section 7.4.)

Precracking was performed in the preirradiation condition for all tests, with K_{max} below 22 MPa$\sqrt{m}$ for the last 1 mm (0.04 in.). Side grooves were applied only to those specimens for which ductile failure (i.e., J-R curve development) was anticipated. The side grooving was targeted to a total depth of 2.54 mm, 1.27 mm per side, or 20% of the gross specimen thickness. All side grooving of the irradiated specimens was performed after irradiation, with actual depths on the irradiated specimens from 19% to 26%. Razor blades were spot welded to the flats located on the load line, to allow accurate measurement of the load-line displacement.

7.2 Test Procedures

Although definitions of upper shelf (ductile, J-R curve) and transition (cleavage, K_{Ic} or K_J) behavior were desired in this program, the testing procedures for both types of tests were identical. Specifically, a 50-kN (110-kip) servohydraulic test frame was used, with either a strain-gaged clip gage or a capacitance-type clip gage for displacement measurements. In all cases, a computerized data acquisition system was used, with digital load-displacement pairs stored on magnetic media for later retrieval or analysis. In addition, an analog load-displacement trace was recorded for each test. The $\dot{K}$ for these tests was ~ 44 MPa$\sqrt{m}$/min, with monotonic loading of the specimen until the ASTM E 399 (Ref. 14) 5% secant line was intersected, at which time the single specimen compliance (SSC) technique was utilized to track the crack length during the remainder of the test (Refs. 15 to 17). Successive crack length determinations were made at intervals sufficient to accurately characterize the J-R curve behavior of the specimen.

After completion of the J-R curve tests, the specimens were heat tinted at ~ 300°C to mark the end of the stable growth, cooled to liquid nitrogen temperature, and then fractured. This procedure allows for an undistorted characterization of the fracture surface, as it was upon test termination. For the unirradiated tests, the resultant crack lengths (initial and final) were measured using a microscope and an X-Y table (accurate to 0.025 mm). The irradiated fracture surfaces were photographed, with the crack lengths then digitized using an X-Y digitizer. The latter technique has been found accurate to within 0.05 mm, based on optical and photographic measurements of unirradiated fracture surfaces.

7.3 Data Analysis Procedures

7.3.1 Cleavage/No Stable Crack Growth

For those tests resulting in cleavage failure with no stable crack growth, an ASTM E 399 (Ref. 14) analysis was performed to determine K_Q, and to assess if $K_Q = K_{Ic}$.

In addition, the J integral was used to calculate toughness for these tests. The form of the J integral used was the ASTM E 813-81 form (Ref. 18):

$$J = \frac{A}{B_N b_o} f(a_o/W) \tag{1}$$

with

$$f(a_o/W) = 2(1 + \alpha) / (1 + \alpha^2)$$

$$\alpha = [(2a_o/b_o)^2 + 2 (2a_o/b_o) + 2]^{1/2} - (2a_o/b_o + 1)$$

A = total area under the load-load line displacement curve

B_N = net specimen thickness

a_o = initial (precrack) crack length

$b_o = W - a_o$

Specifically, the J value at the cleavage point was termed J_{Crit}, and a K_{Jc} value was calculated from

$$K_{Jc} = \sqrt{E \, J_{Crit} / (1 - \nu^2)} \tag{2}$$

where E is the modulus of elasticity and ν is Poisson's ratio, taken to be 0.3 in all cases. (In the data tables, the J_{Crit} values are listed under J_{Ic}.)

Since the specimens used here were small and precluded the determination of valid K_{Ic} values above 60 $MPa\sqrt{m}$, the K_{Jc} values were adjusted using the Irwin β_{Ic} procedure (Ref. 19). As recommended by Merkle (Ref. 20), these tests were conducted in displacement control, cleavage was the failure mode in every case, and conditions at the cleavage point were used to calculate the unadjusted fracture toughness values. The adjusted fracture toughness values, termed $K_{\beta c}$ and thought to provide a better approximation to K_{Ic}, were calculated from:

$$\beta_c = \beta_{Ic} + 1.4 \, \beta_{Ic}^3 \tag{3}$$

where

$$\beta_c = \frac{1}{B} \left(\frac{K_c}{\sigma_y}\right)^2$$

$$\beta_{Ic} = \frac{1}{B} \left(\frac{K_{\beta c}}{\sigma_y}\right)^2$$

and

B = specimen thickness

σ_y = 0.2% offset yield strength at temperature

K_c = "non-plane strain fracture toughness" = K_{Jc}

$K_{\beta c}$ = to be solved for

Rearranged, Eq. 3 gives:

$$\beta_{Ic}^3 + (5/7)\, \beta_{Ic} - (5/7)\, \beta_c = 0 \qquad (4)$$

Several parameters can be defined

$$m = (5/14)\, \beta_c$$

$$A_1 = \sqrt{m^2 + \frac{(5/7)^3}{27}} + m$$

$$A_2 = A_1 - 2m$$

β_{Ic} can be calculated from

$$\beta_{Ic} = A_1^{1/3} - A_2^{1/3}$$

and finally $K_{\beta c} = \sigma_y \sqrt{B\, \beta_{Ic}}$.

Since the magnitude of the β_{Ic} adjustment is inversely proportional to the yield strength, unirradiated data are adjusted significantly more than irradiated data, due to strengthening typically associated with irradiation embrittlement. This in turn results in irradiation-induced transition temperature increases (ΔT's) which should be lower (by definition) than ΔT's from K_{Jc} data. While the β_{Ic} data are reported in the data tables, no other use of the data are made in this report.

7.3.2 Ductile/Stable Crack Growth

The J integral resistance curve (J-R curve) was used for upper shelf characterizations. The test procedure used was in general conformance with ASTM Standard E 1152-87 (Ref. 21) and the J_{Ic} test procedure, ASTM E 813-81 (Ref. 13).

As noted previously, the unloading compliance technique was used for crack length (and crack growth) determinations. For J-integral calculations, the modified J integral, J_M, was used (Ref. 22):

$$J_M = J_D - \int_{a_o}^{a} \frac{\partial (J_D - G)}{\partial a} \bigg|_{\delta_{pl}} da \qquad (5)$$

with

J_D = deformation theory J

G = Griffith linear elastic energy release rate

a_o,a = the initial and current crack lengths, respectively

δ_{pl} = the plastic part of the displacement

Reference 17 gives a detailed listing of the computations required to calculate J_M. Additionally, Refs. 17 and 22 provide justification for the use of this non-path independent integral whereby small specimen data using J_M are seen to give better corresondence with large specimen data (using path independent J_D or J_M) than do small specimen data using J_D. Since one intent of this study is to develop data relevant to structural integrity applications, J_M is considered the appropriate formulation of the J integral.

The format for the presentation and analysis of these J-R curves is illustrated in Fig. 39. The left most J_{Ic} value is determined using ASTM E 813-81 procedures (Ref. 13), whereby selected data are fit to a linear equation, which is then extrapolated back to the blunting line (as given by $J = 2\,\sigma_f\,\Delta a$, with σ_f the flow strength, the average of the yield and ultimate strengths). The intersection of the linear equation and the blunting line is defined as J_Q, which becomes J_{Ic} if various validity criteria are satisfied.

In a similar fashion, the power-law definition of J_{Ic} used in this report is the intersection of the 0.15-mm exclusion line with a power-law fit to the test data. The power law is given by

$$J = C\,\Delta a^n \qquad (6)$$

with C and n determined through regression analysis. This power-law method is considered preferable to the ASTM linear method in that the actual J-R curve behavior is modeled better using the power law than using a linear equation, and power-law intersection represents a true intersection and not an extrapolated intersection. In addition, the cited power law method gives J_{Ic} values which are generally within 10% of the E 813-81 values, instead of the larger differences found with the power law method given in E 813-87, which uses a 0.2 mm offset to define J_{Ic}.

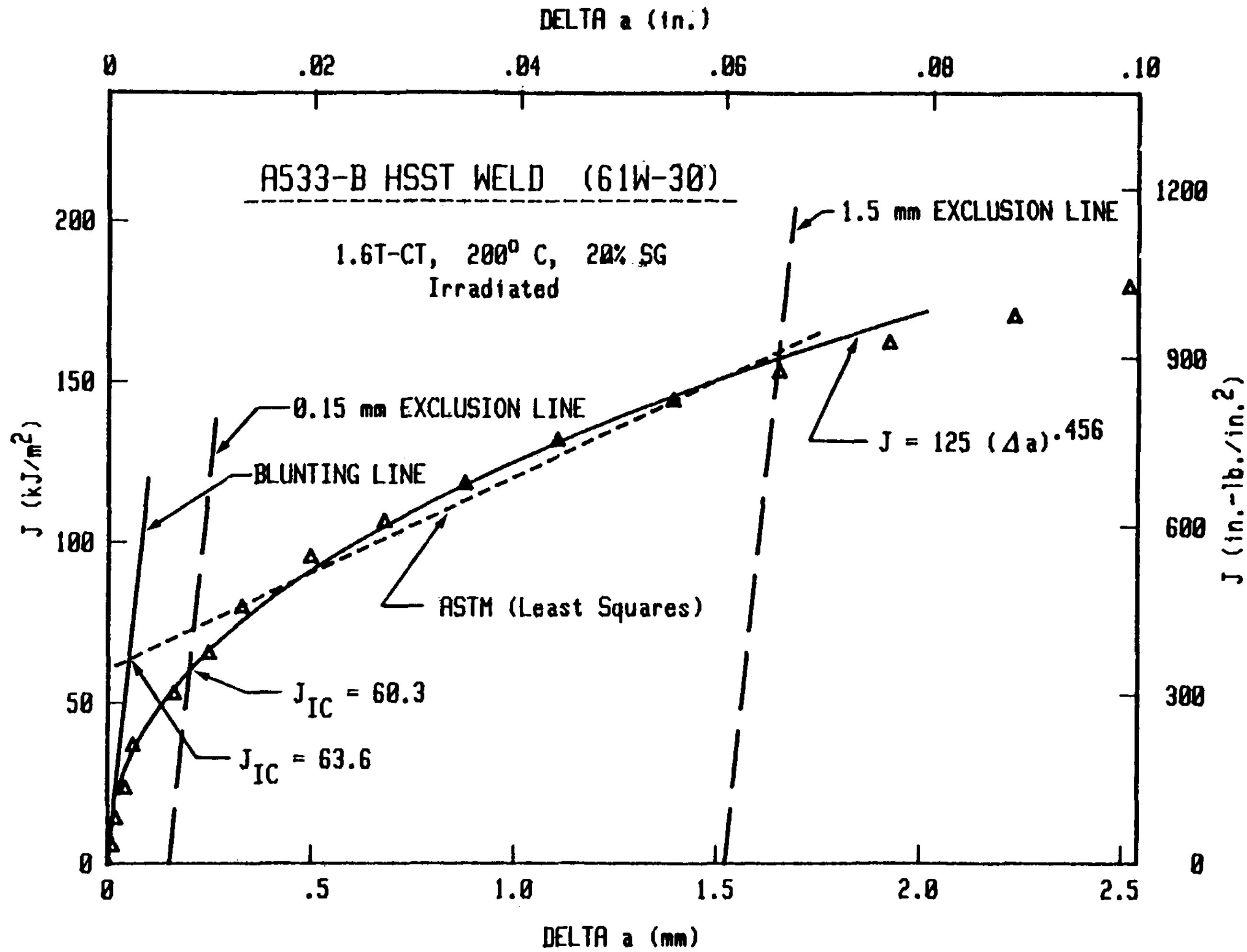

Fig. 39 Schematic illustration of the J-R curve format used with these data. The J_{Ic} data labeled "P.L." are determined as in the 60.3 kJ/m^2 value, whereas those labeled "ASTM" are determined as in the 63.6 kJ/m^2 value.

Another parameter used to define J-R curves is the tearing modulus (T), as given by (Ref. 23):

$$T = \frac{E}{\sigma_f^2} \frac{dJ}{da} \qquad (7)$$

where dJ/da is the slope of the J-R slope. While T changes continuously with crack growth, an average value of T between the 0.15- and 1.5-mm exclusion lines, T_{avg}, has been defined (in Appendix H of Ref. 17) for use in referencing fracture toughness differences.

7.4 Specimen Size Selection

The IAR Phase I fracture toughness determinations (Ref. 6) were made using 1T-CT specimens having a thickness of 25.4 mm (1 in.). Since eight 0.5T-CT specimens can be machined and irradiated in the same space as a single 1T-CT specimen, the feasibility of using the smaller specimens was assessed for the present study. It was expected that an increase in transition region toughness would result from the use of smaller specimens, but this effect was thought to have only a minimal effect on changes (increases) in transition temperature (at a specific index) due to irradiation. The question of size effect on upper shelf (J-R curve) toughness was approached by comparing data from 1T-CT and 0.5T-CT specimens from a single submerged arc weld.

The weld used for this study was Weld E24 from earlier work at the U. S. Naval Research Laboratory (Ref. 24). This weld was made using Linde 0091 flux and has a pre-irradiation C_v upper shelf level of 179 J, 15% higher than that of Weld W9A.

Three specimens of each size (0.5T- and 1T-CT) were prepared and tested at 200°C. These specimens were precracked per Section 7.1, with each specimen side-grooved by 20%. As illustrated in Fig. 40, this side-groove percentage was sufficient to minimize crack-front tunneling in all cases.

As illustrated in Fig. 41 for both J_M and J_D, the J_M-R curves for the six specimens are similar to one another, although the data from 1T-CT specimens appear to be slightly lower for Δa up to ~ 1 mm and slightly higher for Δa greater than ~ 2 mm. In contrast, J_D indicates a consistent size dependence, as the slope of the J_D-R curve diminishes with increasing Δa for the 0.5T-CT specimens in comparison to that for the 1T-CT specimens. At the end of the J_D-R curves, significant differences exist in the J_D levels for the two specimen sizes.

The observations found for J_M are confirmed in Table 9, as the 0.5T-CT specimens yield higher J_{Ic} values and slightly lower T_{avg} values, on average using J_M.

On the basis of the generally good agreement of the J_M-R curves, 0.5T-CT specimens were selected for use in this program.

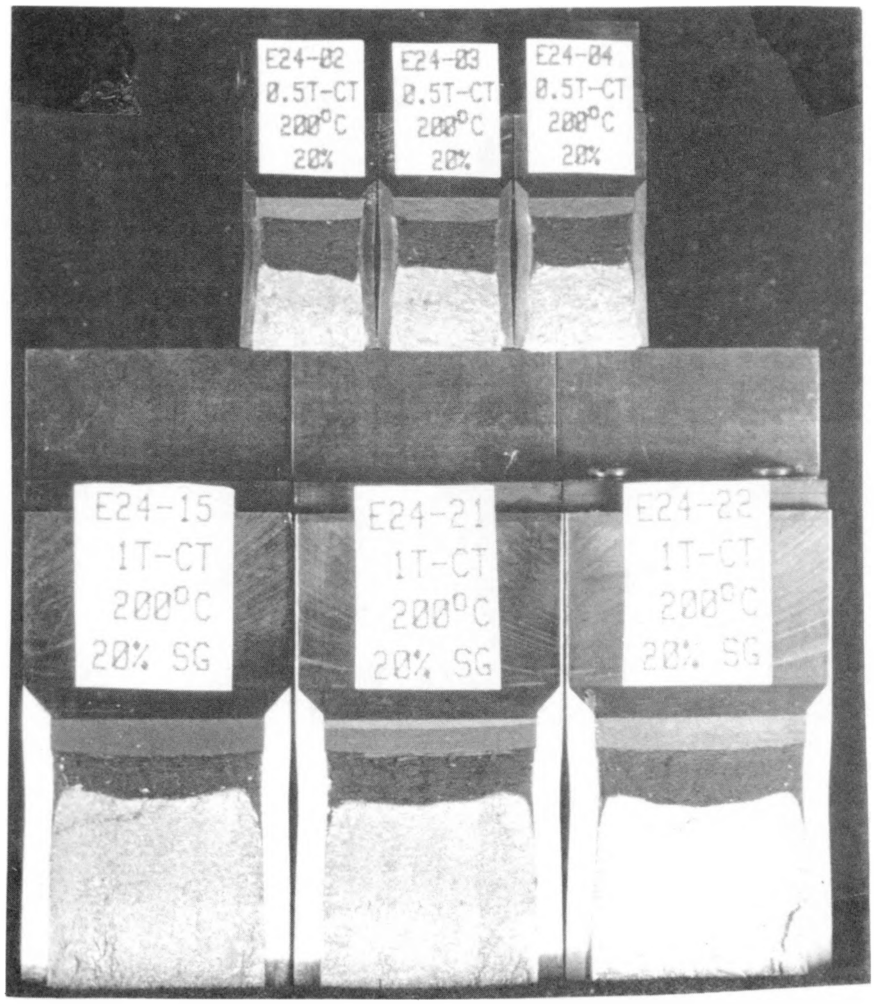

Fig. 40 Photographs of the fracture surfaces from the size effect study using the E24 weld. The 1T-CT surfaces indicate some reverse tunneling at the tips of the side grooves.

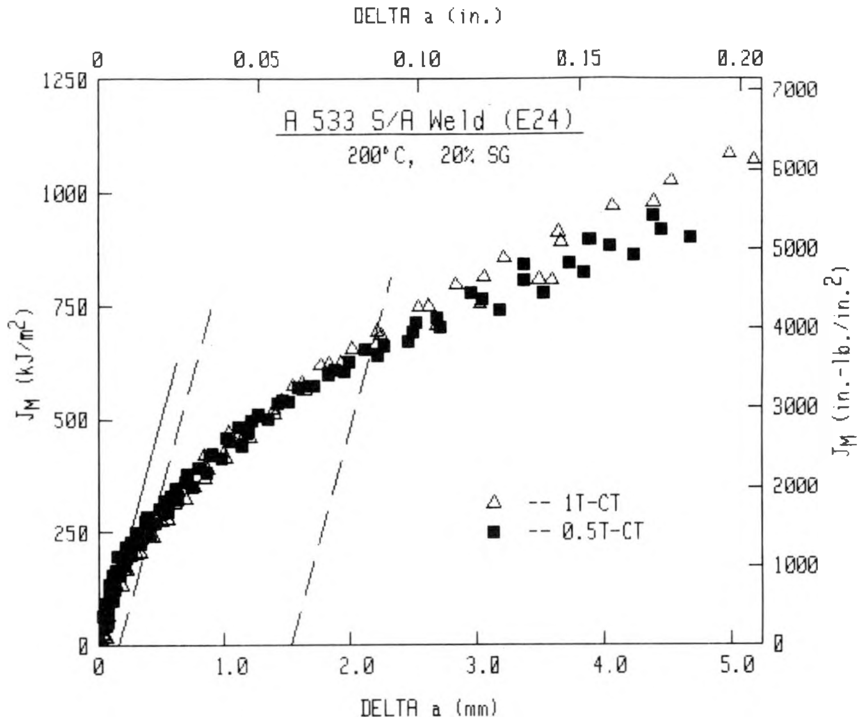

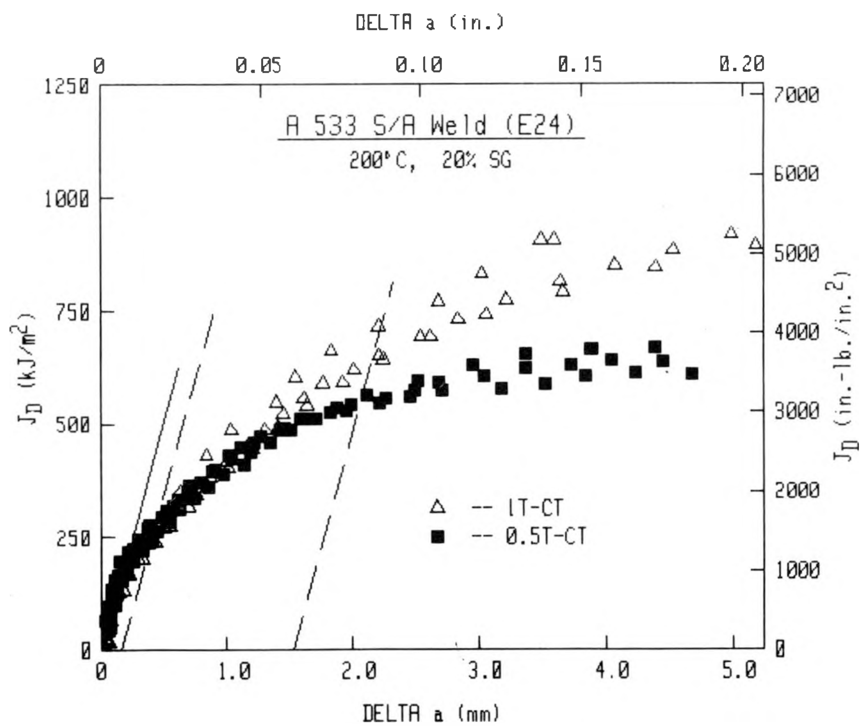

Fig. 41 J_M- and J_D-R curves for the size effect study. The J_M curves indicate good agreement in J levels for crack growth levels up to ~ 2 mm, whereas the J_D curves indicate a divergence starting at lower crack growth levels.

Table 9 IAR Size-Effect Study - 200°C, 20% SG

Specimen No.	Specimen Size	J_{Ic} (kJ/m^2)	T_{avg}	Δa_p[a] (mm)	Δa_m[b] (mm)	$\Delta a_p - \Delta a_m$ (mm)
E24-02	0.5T-CT	253.5	163	4.68	5.13	-0.45
-03	0.5T-CT	295.4	154	4.45	4.70	-0.25
-04	0.5T-CT	304.3	152	4.39	4.75	-0.36
	Average	284.4	156			
E24-15	1T-CT	210.9	180	4.14	3.96	+0.18
-21	1T-CT	239.0	187	4.99	4.87	+0.12
-22	1T-CT	224.5	182	5.18	4.95	+0.23
	Average	224.8	183			

[a] Δa predicted by the unloading compliance method.

[b] Δa optically measured on the fracture surface.

[c] J_{Ic} is invalid according to specimen size requirement from ASTM E 813-81.

7.5 Fracture Toughness Results

The fracture toughness data are summarized in Tables 10 and 11 for welds W8A and W9A, respectively. Fracture surface photographs are illustrated in Figs. 42 to 49 for each data set (in some cases photographs are not available). While in only a few cases did cleavage tests result in valid K_{Ic} values per ASTM E 399, in virtually every case a ductile test resulted in a valid J_{Ic} value per ASTM E 813-81. The results will be treated here by looking at the transition regime first and then the upper shelf region.

As a note, validity of fracture toughness data and evaluation of J_{Ic} and T_{avg} require the use of tensile properties, specifically the yield strength (σ_y) and the flow strength (σ_f). For the unirradiated condition, full curves of strength as a function of temperature were made. In contrast, limited testing was possible for the irradiated conditions. To provide strength data at each test temperature, the strength results for the unirradiated condition were fit to a quadratic equation. For the irradiated conditions, the same overall curvature of the strength vs. temperature curve was used (i.e., the same quadratic equation), with the constant adjusted to account for differences in strengths between the unirradiated condition and each irradiated condition. For weld W8A, the following equations were used for yield and ultimate (σ_u) strength:

$$\sigma_y = (0.0003025\ T^2 - 0.132\ T + 75.44) \times 6.894757 \ \text{MPa}$$

$$\sigma_u = (0.0003390\ T^2 - 0.117\ T + 91.63) \times 6.894757 \ \text{MPa}$$

where T is the test temperature in °C and the resultant strengths are in MPa. The constant 75.44 is changed to 98.34 for UBR-50, 99.94 for UBR-48A and 96.14 for UBR-48B. The constant 91.63 is changed to 109.99 for UBR-50, 110.79 for UBR-48A and 108.59 for UBR-48B.

For weld W9A, the following equations were used for yield and ultimate (σ_u) strength :

$$\sigma_y = (0.000369\ T^2 - 0.162\ T + 85.35) \times 6.894757 \ \text{MPa}$$

$$\sigma_u = (0.000332\ T^2 - 0.124\ T + 96.98) \times 6.894757 \ \text{MPa}$$

where T is the test temperature in °C and the resultant strengths are in MPa. The constant 85.35 is changed to 107.88 for UBR-50, 110.38 for UBR-48A and 104.58 for UBR-48B. The constant 96.98 is changed to 116.63 for UBR-50, 118.73 for UBR-48A and 114.63 for UBR-48B.

The transition region data have been curve-fit to an exponential equation of the form:

$$K = A_o + A_1 \ \text{EXP} \ [(T-T_o)/A_2] \qquad (8)$$

with A_o, A_1 and A_2 constants for each data set as determined through a non-linear regression analysis, and T_o is 0°C or 32°F. Table 12 summarizes the regression constants for each material and each

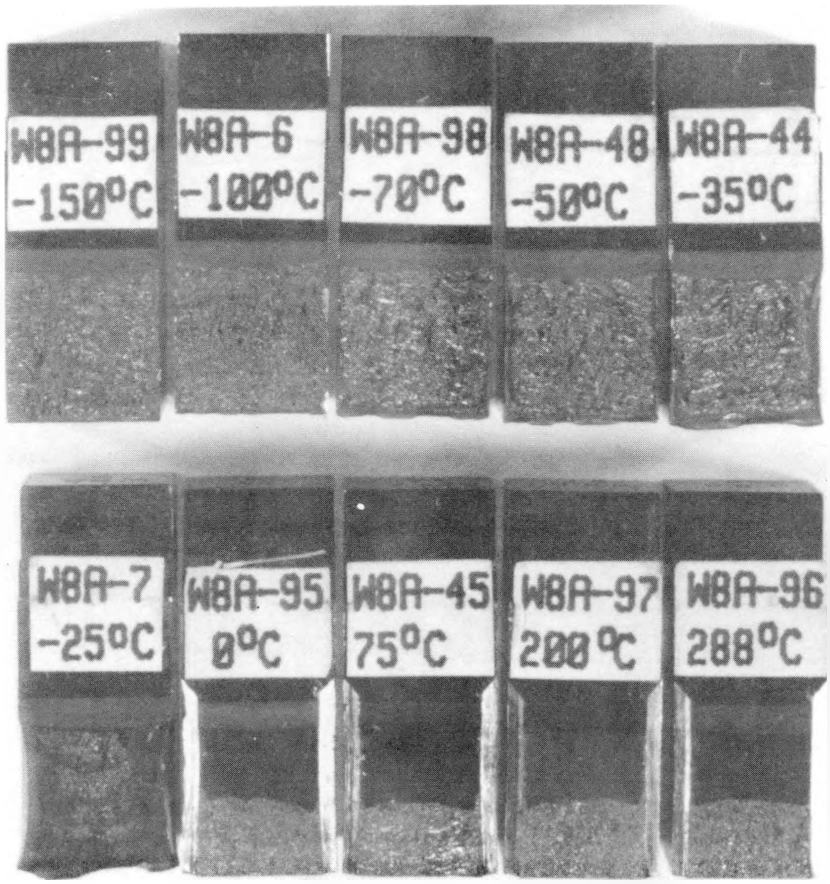

Fig. 42 Fracture surfaces for the Linde 80 weld (W8A), in the unirradiated condition.

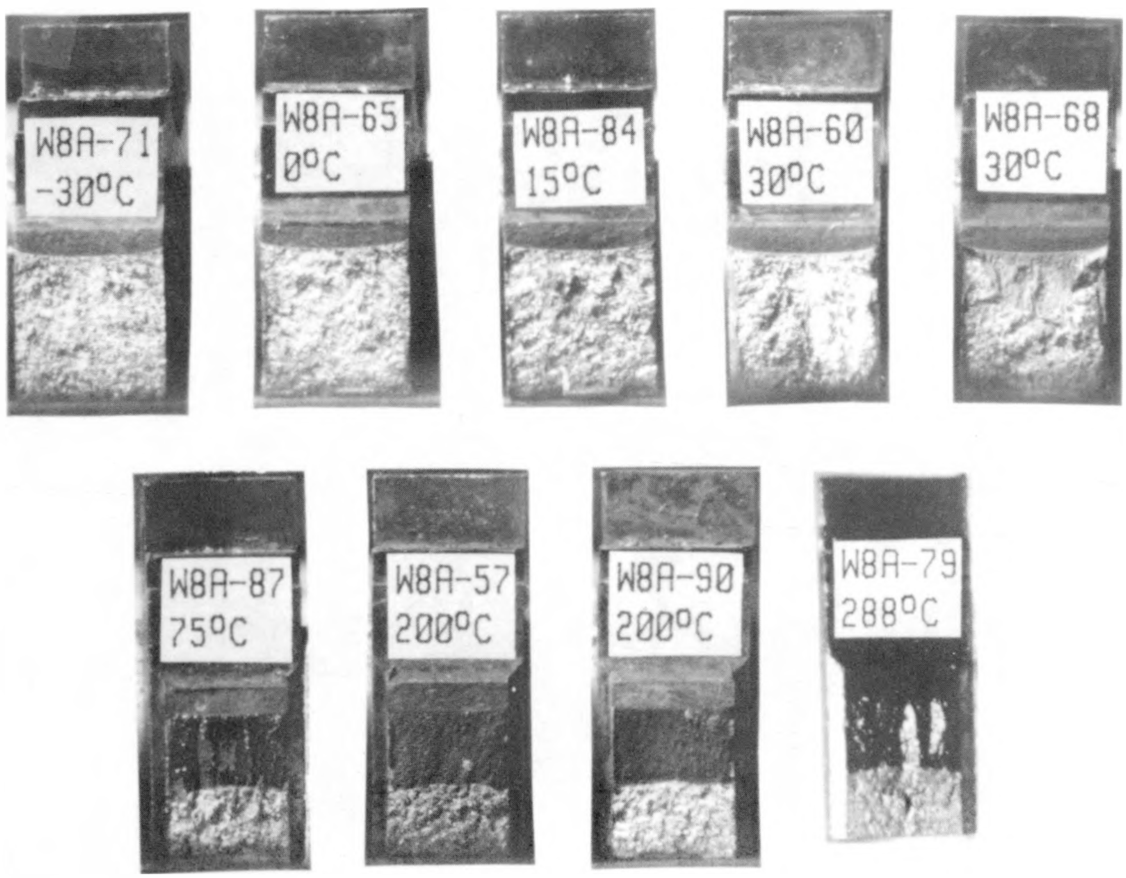

Fig. 43 Fracture surfaces for the Linde 80 weld (W8A), in the I condition to a fluence of 1.5×10^{19} n/cm^2.

Fig. 44 Fracture surfaces for the Linde 80 weld (W8A), in the I condition to a fluence of 2.1×10^{19} n/cm^2.

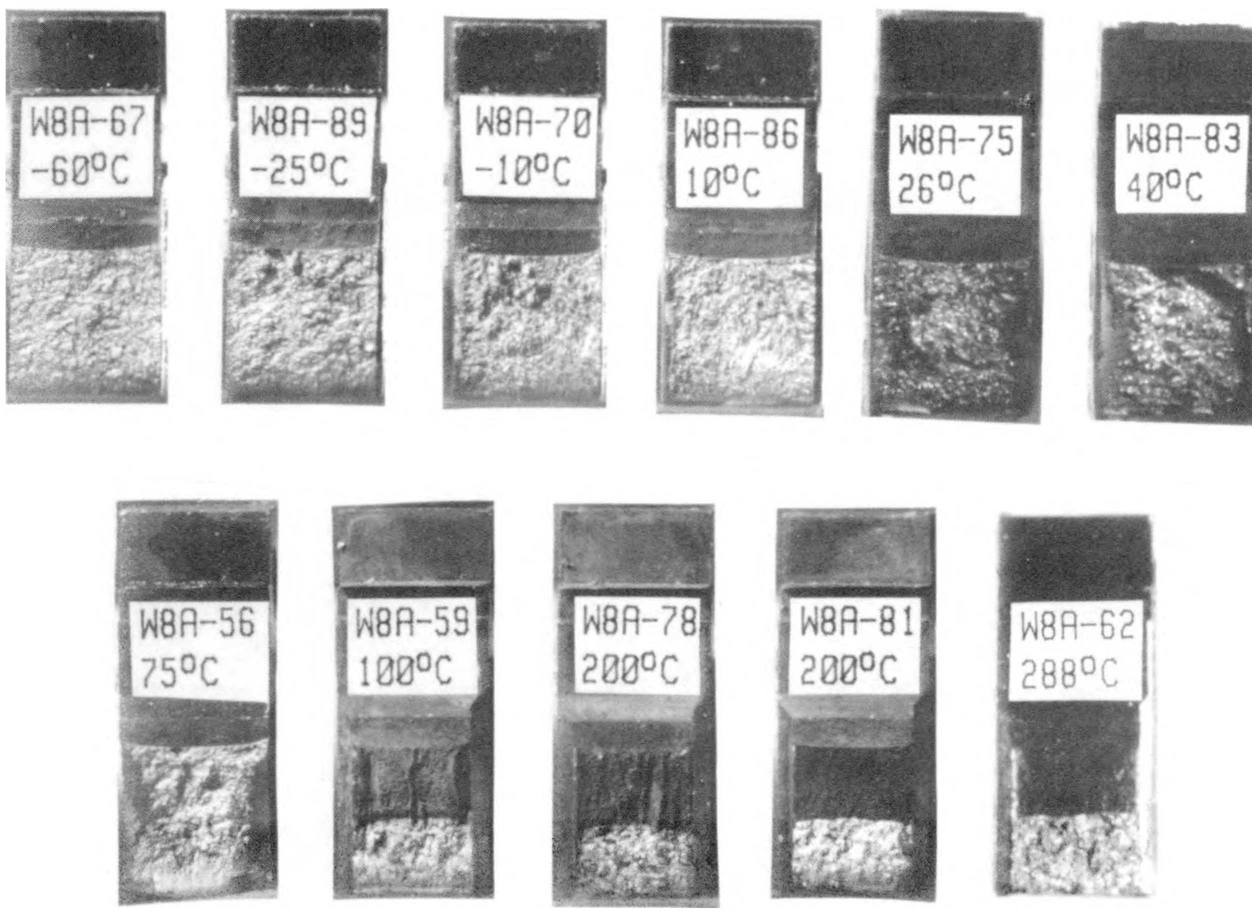

Fig. 45 Fracture surfaces for the Linde 80 weld (W8A), in the IAR condition to a total fluence of 2.2×10^{19} n/cm^2.

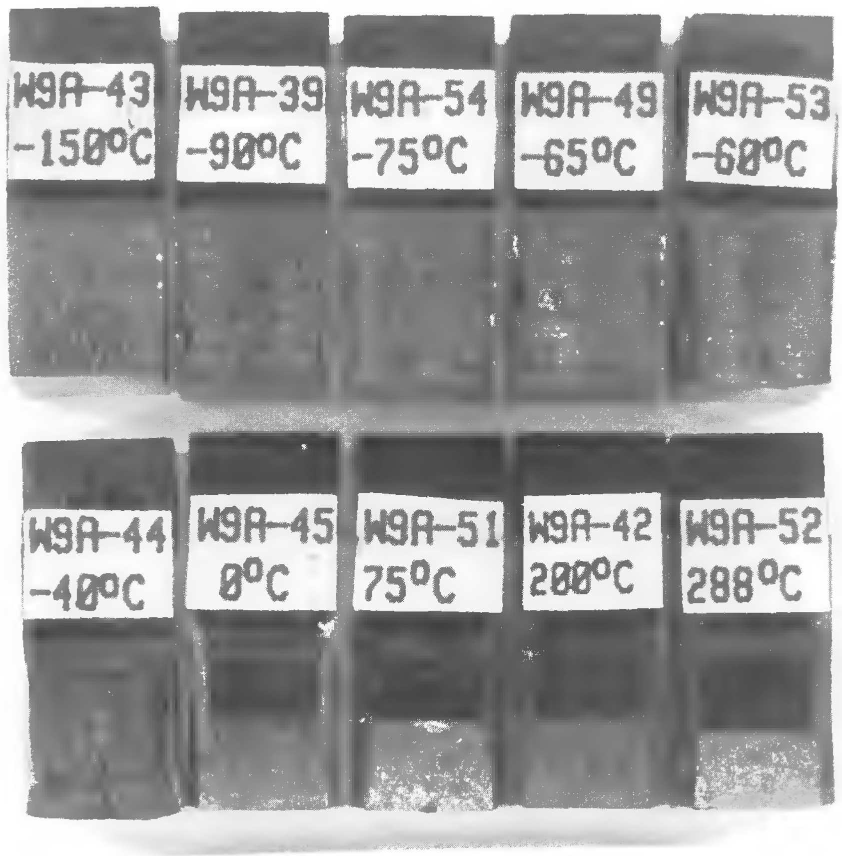

Fig. 46 Fracture surfaces for the Linde 0091 weld (W9A), in the unirradiated condition.

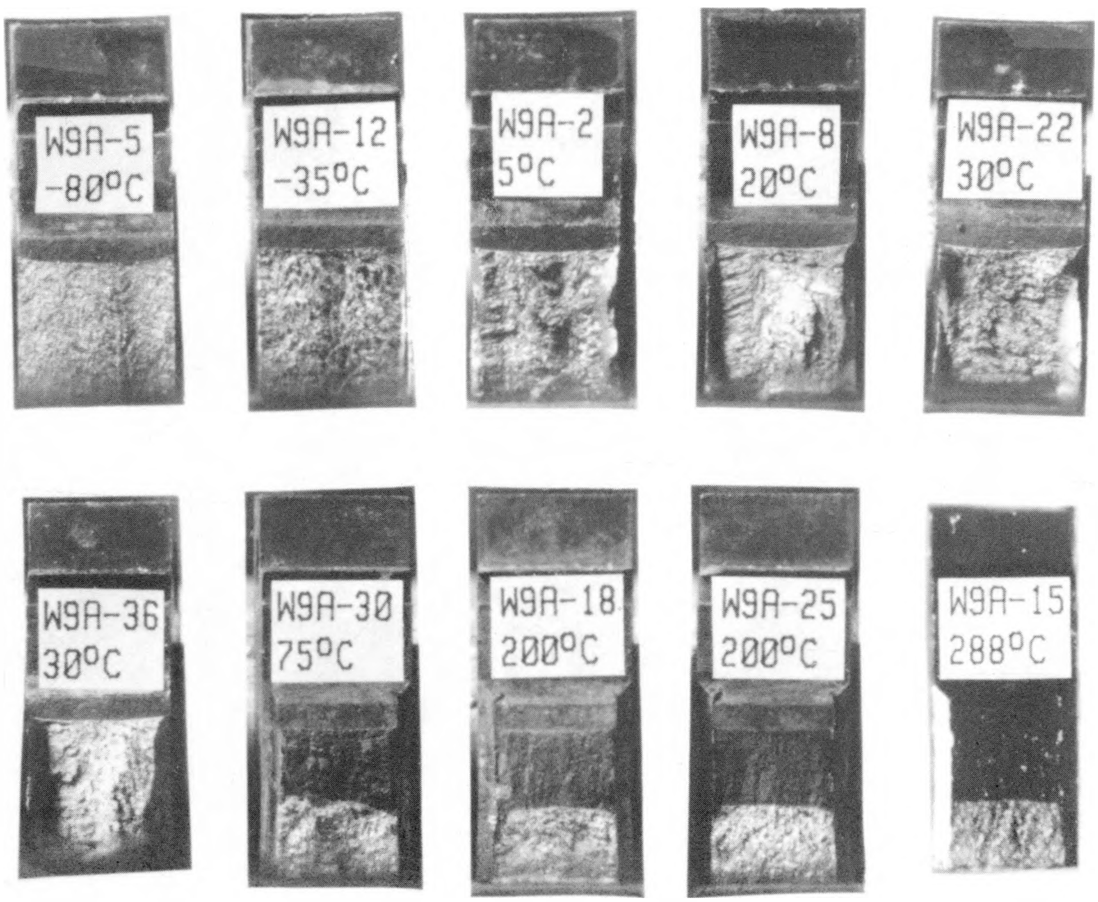

Fig. 47 Fracture surfaces for the Linde 0091 weld (W9A), in the I condition to a fluence of 1.5×10^{19} n/cm^2.

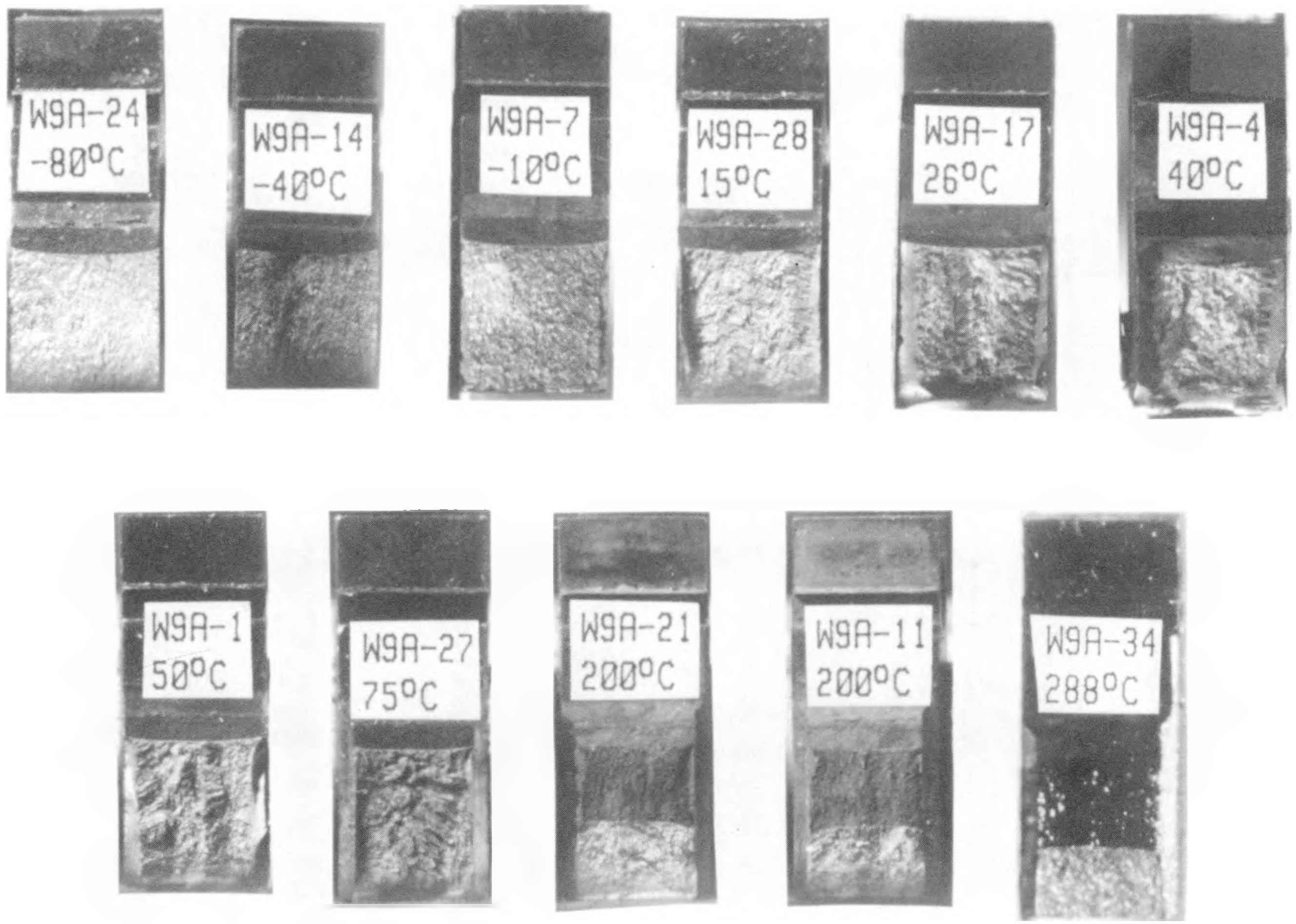

Fig. 48 Fracture surfaces for the Linde 0091 weld (W9A), in the I condition to a fluence of 2.1×10^{19} n/cm^2.

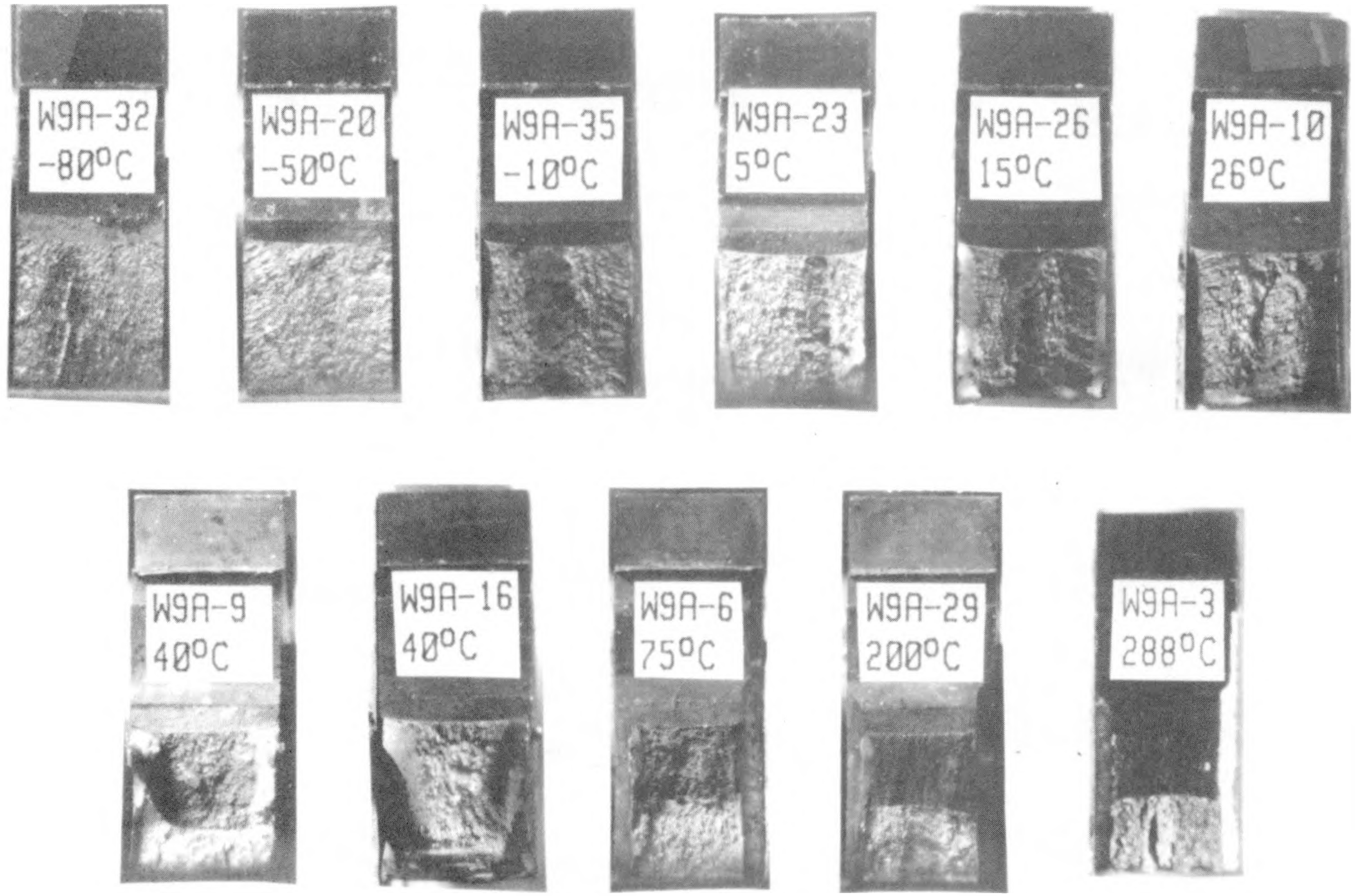

Fig. 49 Fracture surfaces for the Linde 0091 weld (W9A), in the IAR condition to a fluence of 2.2×10^{19} n/cm^2.

Table 10 Fracture Toughness Results for W8A

Specimen Number	Test Temp (°C)	Φ^a	$(a/W)_o^b$	Δa_m^c (mm)	Δa_p^d (mm)	$\Delta a_p - \Delta a_m$ (mm)	J_{Ic} P.L. (kJ/m²)	J_{Ic} ASTM (kJ/m²)	K_{Jc} P.L. (MPa√m)	K_{Jc} ASTM (MPa√m)	$K_{\beta c}$ (MPa√m)	T_{avg} P.L.	σ_y (MPa)	σ_f (MPa)
UNIRRADIATED														
W8A-99	-150	----	0.511	----	----	-----	6.7	-----	40.0	40.3[g]	38.5	--	703.6	754.5
W8A-93	-110	----	0.519	----	----	-----	12.7	-----	54.6	53.2	48.4	--	645.5	697.2
W8A-6	-100	----	0.509	----	----	-----	35.4	-----	90.9	55.3	64.9	--	632.0	683.9
W8A-98	-70	----	0.513	----	----	-----	31.5	-----	85.5	49.4	61.0	--	594.0	646.9
W8A-48	-50	----	0.509	----	----	-----	43.5	-----	100.2	53.4	64.5	--	570.8	624.4
W8A-91	-50	----	0.518	----	----	-----	28.7	-----	81.5	55.9	58.4	--	570.8	624.4
W8A-44	-35	----	0.511	----	----	-----	78.7	-----	134.5	48.2	72.1	--	554.5	608.7
W8A-7	-25	----	0.516	----	----	-----	128.1	-----	171.4	43.6	78.5	--	544.2	598.8
W8A-92	-15	----	0.523	----	----	-----	60.0	-----	117.2	53.8	66.6	--	534.2	589.2
W8A-95	0	----	0.518	6.02	5.98	-0.04	102.9	104.4[f]	153.1	154.2	----	72	520.1	575.9
W8A-45[e]	75	----	0.516	6.41	6.39	-0.02	94.2	94.4[f]	144.9	145.1	----	81	463.6	524.0
W8A-97[e]	200	----	0.522	5.87	5.70	-0.17	80.2	79.7[f]	131.4	131.0	----	57	421.5	492.7
W8A-96[e]	288	----	0.521	5.83	5.92	+0.09	54.2	58.6[f]	106.6	110.8	----	34	431.0	512.2
IRRADIATED (UBR-48A, 2.1 x 10^{19} n/cm², E > 1 MeV)														
W8A-66[k]	-10	1.95	0.514	----	----	-----	5.9	-----	36.7	36.1[g]	35.7	--	698.4	735.3
W8A-72	26	2.11	0.510	----	----	-----	15.8	-----	59.8	57.4	52.0	--	666.8	705.6
W8A-85	50	2.34	0.504	----	----	-----	26.5	-----	77.2	58.4	58.5	--	648.8	689.1
W8A-55	55	1.98	0.501	----	----	-----	25.1	-----	75.6	61.7	59.4	--	645.3	685.9
W8A-69[j]	60	2.30	0.507	----	----	-----	61.8	-----	117.6	53.0	73.9	--	641.9	682.9
W8A-61[j]	75	2.04	0.497	----	----	-----	71.2	-----	126.0	57.6	78.4	--	632.5	674.5
W8A-74[e,k]	100	1.99	0.508	h	h	h	41.5	-----	95.9	53.9	----	--	618.9	662.7
W8A-88[e]	125	2.16	0.522	6.25	6.39	+0.14	66.6	69.9[f]	119.5	124.0	----	16	607.9	653.7
W8A-58[e]	200	2.07	0.514	6.27	6.50	+0.23	52.3	54.1[f]	106.1	107.9	----	14	590.4	643.2
W8A-80[e]	288	2.25	0.542	5.94	5.86	-0.08	37.0	38.6[f]	88.1	90.0	----	9	599.9	662.7
W8A-82 IA[i]	30	2.17	0.510	----	----	-----	60.8	-----	117.2	48.5	75.2	--	663.3	702.7

[a] 10^{19} n/cm² (E > 1 MeV)
[b] Pre-test a/W
[c] Measured crack growth
[d] Crack growth predicted by compliance
[e] Side grooved
[f] Valid J_{Ic}, per ASTM E 813-81
[g] Valid K_{Ic}, per ASTM E 399-81
[h] Cleavage failure precluded determination of this quantity
[i] Annealed at 399°C for 168 hours
[j] Cleavage pop took Δa past exclusion area
[k] Cleavage pop took Δa past J_{Ic}, then total cleavage

Table 10 Fracture Toughness Results for W8A
(Continued)

Specimen Number	Test Temp (°C)	Φ[a]	$(a/W)_o$[b]	Δa_m[c] (mm)	Δa_p[d] (mm)	$\Delta a_p - \Delta a_m$ (mm)	J_{Ic} P.L. (kJ/m^2)	J_{Ic} ASTM (kJ/m^2)	K_{Jc} P.L. (MPa$\sqrt{m}$)	K_{Jc} ASTM (MPa$\sqrt{m}$)	$K_{\beta c}$ (MPa$\sqrt{m}$)	T_{avg} P.L.	σ_y (MPa)	σ_f (MPa)
IRRADIATED-ANNEALED-REIRRADIATED (UBR-48B, 1.5 x 10^{19} + 0.7 x 10^{19} = 2.2 x 10^{19} n/cm^2, E > 1 MeV)														
W8A-67	-60	2.21	0.513	----	----	-----	6.2	----	37.9	38.2[g]	36.8	--	725.0	765.2
W8A-89	-25	2.21	0.509	----	----	-----	14.0	----	56.7	54.7	50.6	--	686.9	728.6
W8A-70	-10	2.15	0.511	----	----	-----	35.4	----	89.9	54.5	66.5	--	672.2	714.6
W8A-86	10	2.19	0.513	----	----	-----	26.0	----	76.8	63.5	60.2	--	654.0	697.4
W8A-75	26	2.26	0.500	----	----	-----	34.2	----	87.9	66.0	64.2	--	640.6	684.9
W8A-83	40	2.31	0.517	----	----	-----	36.2	----	90.3	54.1	64.5	--	629.8	675.0
W8A-64	55	2.27	0.500	----	----	-----	41.2	----	96.1	51.2	66.0	--	619.1	665.2
W8A-56	75	2.24	0.527	----	----	-----	84.5	----	137.3	57.3	76.6	--	606.3	653.8
W8A-59[e]	100	2.21	0.523	6.35	6.31	-0.04	81.5	86.3[f]	134.3	138.2	----	22	792.7	642.0
W8A-78[e]	200	2.16	0.514	6.43	6.45	+0.02	65.8	70.6[f]	119.0	123.2	----	20	564.2	622.6
W8A-81[e]	200	2.19	0.522	6.20	6.32	+0.12	70.8	76.2[f]	123.4	128.0	----	16	564.2	622.6
W8A-62[e]	288	2.37	0.514	5.86	5.84	-0.02	51.5	53.0[f]	103.9	105.4	----	10	573.7	642.0
IRRADIATED (UBR-50A, 1.5 x 10^{19} n/cm^2, E > 1 MeV)														
W8A-76	-60	1.36	0.510	----	----	-----	5.6	----	36.0	36.2	35.2	--	740.1	777.6
W8A-71	-30	1.55	0.510	----	----	-----	20.6	----	68.8	54.7	58.2	--	707.2	745.9
W8A-65	0	1.38	0.506	----	----	-----	20.0	----	67.5	56.6	56.6	--	678.0	718.2
W8A-84	15	1.53	0.509	----	----	-----	25.4	----	75.9	54.2	59.6	--	664.8	705.8
W8A-60	30	1.54	0.522	----	----	-----	79.7	----	134.2	75.9	79.1	--	652.6	694.4
W8A-68	30	1.51	0.526	--[h]--	--[h]--	--[h]--	109.1	80.8[f]	157.0	135.1	----	54	652.6	694.4
W8A-87[e]	75	1.61	0.525	6.27	6.18	-0.09	84.8	84.6[f]	137.5	137.3	----	28	621.5	666.2
W8A-57[e]	200	1.33	0.522	6.25	6.36	+0.11	61.5	60.0[f]	115.0	113.6	----	17	579.4	635.0
W8A-90[e]	200	1.39	0.513	6.17	6.35	+0.18	54.5	57.4[f]	108.3	111.1	----	18	579.4	635.0
W8A-79[e]	288	1.47	0.503	6.47	6.48	+0.01	42.1	41.6[f]	94.0	93.4	----	11	588.9	654.4
W8A-63 IA[i]	-30	1.42	0.510	----	----	-----	19.9	----	67.6	54.1	57.5	--	707.2	745.9
W8A-73 IAA[j]	5	1.34	0.515	----	----	-----	50.9	----	107.6	41.0	76.6	--	701.9	745.0

a 10^{19} n/cm^2 (E > 1 MeV)
b Pre-test a/W
c Measured crack growth
d Crack growth predicted by compliance
e Side grooved
f Valid J_{Ic}, per ASTM E 813-81
g Valid K_{Ic}, per ASTM E 399-81
h Cleavage failure precluded determination of this quantity (Δa is beyond 1.5-mm exclusion line)
i Annealed at 399°C for 168 hours
j Annealed at 399°C for 168 hours, then at 454°C for 168 hours

Table 11 Fracture Toughness Results for W9A

Specimen Number	Test Temp (°C)	Φ^a	$(a/W)_o$ [b]	Δa_m [c] (mm)	Δa_p [d] (mm)	$\Delta a_p - \Delta a_m$ (mm)	J_{Ic} P.L. (kJ/m²)	J_{Ic} ASTM (kJ/m²)	K_{Jc} P.L. (MPa√m)	K_{Jc} ASTM (MPa√m)	$K_{\beta c}$ (MPa√m)	T_{avg} P.L.	σ_y (MPa)	σ_f (MPa)
UNIRRADIATED														
W9A-43	-150	----	0.505	----	----	-----	5.3	-----	35.4	35.2[g]	34.9	---	813.2	830.8
W9A-46	-110	----	0.510	----	----	-----	22.5	-----	72.7	64.3	61.3	---	742.1	766.3
W9A-39	-90	----	0.513	----	----	-----	40.8	-----	97.6	53.1	71.2	---	709.6	736.9
W9A-54	-75	----	0.509	----	----	-----	48.7	-----	106.4	62.0	73.1	---	686.5	716.1
W9A-49	-65	----	0.503	----	----	-----	73.0	-----	130.1	57.5	79.3	---	671.8	702.9
W9A-53	-60	----	0.506	----	----	-----	123.8	-----	169.3	56.9	88.2	---	664.6	696.4
W9A-44	-40	----	0.506	--h--	--h--	--h--	397.1	207.4	302.4	218.5	-----	---	637.2	671.9
W9A-45[e]	0	----	0.517	5.21	4.98	-0.23	267.4	255.0[f]	246.7	241.0	----	173	588.5	628.6
W9A-51[e]	75	----	0.514	5.26	5.10	-0.16	230.4	195.9[f]	226.6	209.0	----	170	519.0	568.2
W9A-42[e]	200	----	0.512	5.39	5.21	-0.18	161.7	147.9[f]	186.5	178.4	----	130	466.8	528.0
W9A-52[e]	288	----	0.510	6.31	5.97	-0.34	111.4	92.9	152.8	139.6	----	120	477.8	545.1
W9A-40[e]	288	----	0.518	6.65	6.45	-0.20	131.6	116.0[f]	166.1	156.0	----	97	477.8	545.1
IRRADIATED (UBR-48A, 2.1 x 10^{19} n/cm², E > 1 MeV)														
W9A-24	-80	2.17	0.525	----	----	-----	8.8	-----	45.2	44.1[g]	44.0	---	866.7	884.2
W9A-14	-40	2.07	0.511	----	----	-----	14.3	-----	57.4	55.9[g]	53.2	---	809.8	833.1
W9A-7	-10	2.04	0.514	----	----	-----	13.5	-----	55.5	53.7[g]	51.3	---	772.5	799.9
W9A-28	15	2.30	0.501	----	----	-----	23.3	-----	72.7	68.9	61.4	---	744.8	775.6
W9A-17	26	2.16	0.493	----	----	-----	59.4	-----	115.9	63.2	78.9	---	733.7	765.8
W9A-4	40	1.99	0.520	----	----	-----	79.2	-----	133.5	61.4	83.4	---	720.4	754.3
W9A-1	50	1.98	0.499	----	----	-----	69.6	-----	125.0	59.9	80.4	---	711.5	746.6
W9A-27[e]	75	2.11	0.498	--h--	--h--	--h--	155.0	156.2	185.9	186.6	----	42	691.6	729.5
W9A-11[e]	200	1.95	0.509	6.65	6.57	-0.08	118.5	124.1[f]	159.7	163.4	----	37	639.4	689.3
W9A-21[e]	200	2.29	0.492	6.40	6.47	+0.07	144.0	147.7[f]	176.0	178.3	----	40	639.4	689.3
W9A-34[e]	288	2.25	0.511	6.53	6.47	-0.06	85.7	81.5[f]	134.0	130.7	----	31	650.4	706.3
W9A-31 IA[i]	5	2.34	0.510	----	----	-----	48.5	-----	105.0	65.8	76.2	---	755.5	785.0

a 10^{19} n/cm² (E > 1 MeV)
b Pre-test a/W
c Measured crack growth
d Crack growth predicted by compliance

e Side grooved
f Valid J_{Ic}, per ASTM E 813-81
g Valid K_{Ic}, per ASTM E 399-81
h Cleavage failure precluded determination of this quantity

i Annealed at 399°C for 168 hours

Table 11 Fracture Toughness Results for W9A
(Continued)

Specimen Number	Test Temp (°C)	Φ[a]	$(a/W)_o$[b]	Δa_m[c] (mm)	Δa_p[d] (mm)	$\Delta a_p - \Delta a_m$ (mm)	J_{Ic} P.L. (kJ/m^2)	J_{Ic} ASTM (kJ/m^2)	K_{Jc} P.L. (MPa$\sqrt{m}$)	K_{Jc} ASTM (MPa$\sqrt{m}$)	$K_{\beta c}$ (MPa$\sqrt{m}$)	T_{avg} P.L.	σ_y (MPa)	σ_f (MPa)
IRRADIATED-ANNEALED-REIRRADIATED (UBR-48B, 1.5 x 10^{19} + 0.7 x 10^{19} = 2.2 x 10^{19} n/cm^2, E > 1 MeV)														
W9A-32	-80	2.19	0.499	----	----	-----	14.2	-----	57.5	52.3[g]	53.6	--	826.7	850.0
W9A-20	-50	2.19	0.496	----	----	-----	17.0	-----	62.6	59.2	56.4	--	783.2	811.0
W9A-35[l]	-10	2.15	0.501	----	----	-----	14.3	-----	57.1	53.9	51.8	--	732.5	765.8
W9A-23	5	2.21	0.518	----	----	-----	29.4	-----	81.8	68.7	64.9	--	715.5	750.8
W9A-26	15	2.37	0.510	----	----	-----	69.5	-----	125.6	65.9	80.2	--	704.9	741.5
W9A-10	26	2.26	0.501	----	----	-----	53.7	-----	110.2	58.3	74.8	--	693.7	731.7
W9A-9	40	2.31	0.525	---[h]	---[h]	---[h]	190.3	-----	207.0	111.1	----	--	680.4	720.1
W9A-16	40	2.21	0.488	---[h]	---[h]	---[h]	120.9	-----	165.0	111.4	----	--	680.4	720.1
W9A-6[e]	75	2.24	0.493	6.56	6.43	-0.13	163.7	161.6[f]	191.0	189.8	----	46	651.6	695.4
W9A-29[e]	200	2.16	0.525	6.12	6.10	-0.02	140.6	136.7[f]	173.9	171.5	----	41	599.4	655.2
W9A-3[e]	288	2.27	0.514	5.91	5.67	-0.24	82.4	77.4[f]	131.4	127.4	----	40	610.4	672.2
IRRADIATED (UBR-50A, 1.5 x 10^{19} n/cm^2, E > 1 MeV)														
W9A-5	-80	1.51	0.522	----	----	-----	8.0	-----	42.5	43.7[g]	41.5	--	849.4	868.3
W9A-12	-35	1.33	0.492	----	----	-----	24.0	-----	74.3	67.6	63.3	--	779.6	805.7
W9A-2[k]	5	1.38	0.498	----	----	-----	37.7	-----	92.6	56.3	70.5	--	738.3	769.1
W9A-8	20	1.55	0.494	----	----	-----	150.2	-----	184.4	59.1	95.9	--	722.5	755.2
W9A-22[l]	30	1.36	0.481	----	----	-----	42.3	-----	97.7	58.7	71.4	--	712.6	746.6
W9A-36	30	1.53	0.502	----	----	-----	112.6	-----	159.5	59.9	89.6	--	712.6	746.6
W9A-30[e]	75	1.42	0.503	6.22	6.10	-0.12	170.7	167.7[f]	195.1	193.4	----	52	674.3	713.6
W9A-18[e]	200	1.39	0.507	6.47	6.54	+0.07	145.4	146.4[f]	176.9	177.5	----	46	622.2	673.5
W9A-25[e]	200	1.47	0.501	6.17	6.40	+0.23	134.4	127.2[f]	170.1	165.4	----	47	622.2	673.5
W9A-15[e]	288	1.54	0.502	6.34	6.14	-0.20	101.0	96.1[f]	145.5	141.9	----	36	633.1	690.5
W9A-19 IA[i]	-60	1.34	0.510	----	----	-----	17.5	-----	63.6	62.4	57.7	--	820.0	841.8
W9A-33 IAA[j]	-15	1.61	0.505	5.15	4.31	-0.84	167.3	104.2	195.6	154.4	----	110	-----	770.8

a 10^{19} n/cm^2 (E > 1 MeV)
b Pre-test a/W
c Measured crack growth
d Crack growth predicted by compliance
e Side grooved
f Valid J_{Ic}, per ASTM E 813-81
g Valid K_{Ic}, per ASTM E 399-81
h Cleavage failure precluded determination of this quantity
i Annealed at 399°C for 168 hours
j Annealed at 399°C for 168 hours, then at 454°C for 168 hours
k Cleavage pop took Δa past exclusion area
l Cleavage pop took Δa past J_{Ic}, then total cleavage

Table 12 Transition Temperature Fit Results ($K = A_o + A_1 \, EXP \, [(T-T_o)/A_2]$)[a]

Code	Condition c	Fluence d	A_0 (MPa$\sqrt{m}$)	A_1 (MPa$\sqrt{m}$)	A_2 (°C)	Temperature (°C) At Index Level of 75[b]	100[b]	150[b]	Shift (°C) At Index Levels of 75[b]	100[b]	150[b]
W8A	U	---	-27.03	187.75	149.72	-91	-58	-9	---	---	---
	I	1.5	51.38	11.55	15.36	11	22	33	102	80	42
	I	2.1	21.16	19.82	44.29	44	61	-[e]-	135	119	-[e]-
	IAR	2.2	-14.89	87.63	157.30	4	43	-[e]-	95	101	-[e]-
W9A	U	---	22.40	519.22	44.24	-101	-84	-62	---	---	---
	I	1.5	24.97	84.57	52.46	-28	-6	21	73	78	83
	I	2.1	34.24	39.55	52.19	2	27	-[e]-	103	111	-[e]-
	IAR	2.2	53.32	28.14	29.63	-8	15	-[e]-	93	99	-[e]-

a T_o is 0°C or 32°F

b MPa$\sqrt{m}$

c U = Unirradiated
I = Irradiated
IAR = Irradiated-Annealed-Reirradiated

d 10^{19} n/cm^2 (E > 1 MeV)

e Cannot be determined

condition. Curve-fit sheets for each data set are given in Appendix F. Figures 50 to 55 compare each irradiated data set to the appropriate unirradiated condition data set. Temperatures at 100 $MPa\sqrt{m}$ are given for each data set in Table 13, as determined for the mean curve and the 95% upper and lower bound confidence curves in each case. As indicated, the lower and upper bounds have significant differences in each case.

For the unirradiated condition, data for Weld W9A indicate little scatter, in contrast to the larger scatter for Weld W8A. One possible cause for the variability in the data for the Linde 80 weld is that the specimens were selected from a greater length of the weld with a greater chance for more scatter. In addition, Specimen W8A-6 tested at -100°C exhibits a cleaner fracture appearance than the other specimens, possibly indicating higher toughness. In contrast, the Linde 0091 specimens were more closely arranged in the weld, helping to minimize the inherent variability.

Somewhat surprisingly, the transition data of Weld W8A for the irradiation conditions are not highly scattered. For the two I conditions, several specimens were annealed (at 399°C for 168 h) and tested in the IA condition. In each case some recovery is apparent from the mean curve of the I condition. However, for UBR-50 (fluence of 1.5 x 10^{19} n/cm^2) the IA condition exhibits identical toughness to that for an I condition specimen at the same temperature. A specimen tested in the IAA condition (an anneal at 399°C for 168 h followed by an anneal at 454°C for 168 h) demonstrated similar minimal recovery in toughness. Somewhat greater recovery results for an anneal after an initial fluence of 2.1 x 10^{19} n/cm^2.

Comparison of the K_{Jc} data for all three conditions indicates some benefit of the IAR treatment (Fig. 56), with the overall curvature of the data for the IAR condition yielding a shallower slope with increasing temperature.

For Weld W9A, variability in transition region data for the irradiation conditions is somewhat greater than that for the unirradiated condition. For UBR-50 (fluence of 1.5 x 10^{19} n/cm^2), two specimens tested at 30°C (86°F) demonstrate significantly different toughness. As illustrated in Fig. 57, the lower toughness of the two is due to a pop-in during the initial portion of the test, in contrast to the higher load and displacement reached by the other specimen prior to cleavage fracture. However, the specimen exhibiting lower initiation toughness ends up with significant additional stable crack growth, with a resistance curve out to ~1.8 mm of crack growth (Fig. 58). Therefore, the specimen exhibiting nominally lower toughness in actuality exhibits somewhat higher toughness in that significant stable crack growth results for this test.

For this same irradiation condition, specimens were annealed for this weld as for the Linde 80 weld. As with W8A, the IA condition test does not exhibit significant recovery. However, the IAA condition results in a J-R curve at -15°C (5°F), where only cleavage behavior had been found for the I condition. The initial part of the resultant

(text continues on pg. 91)

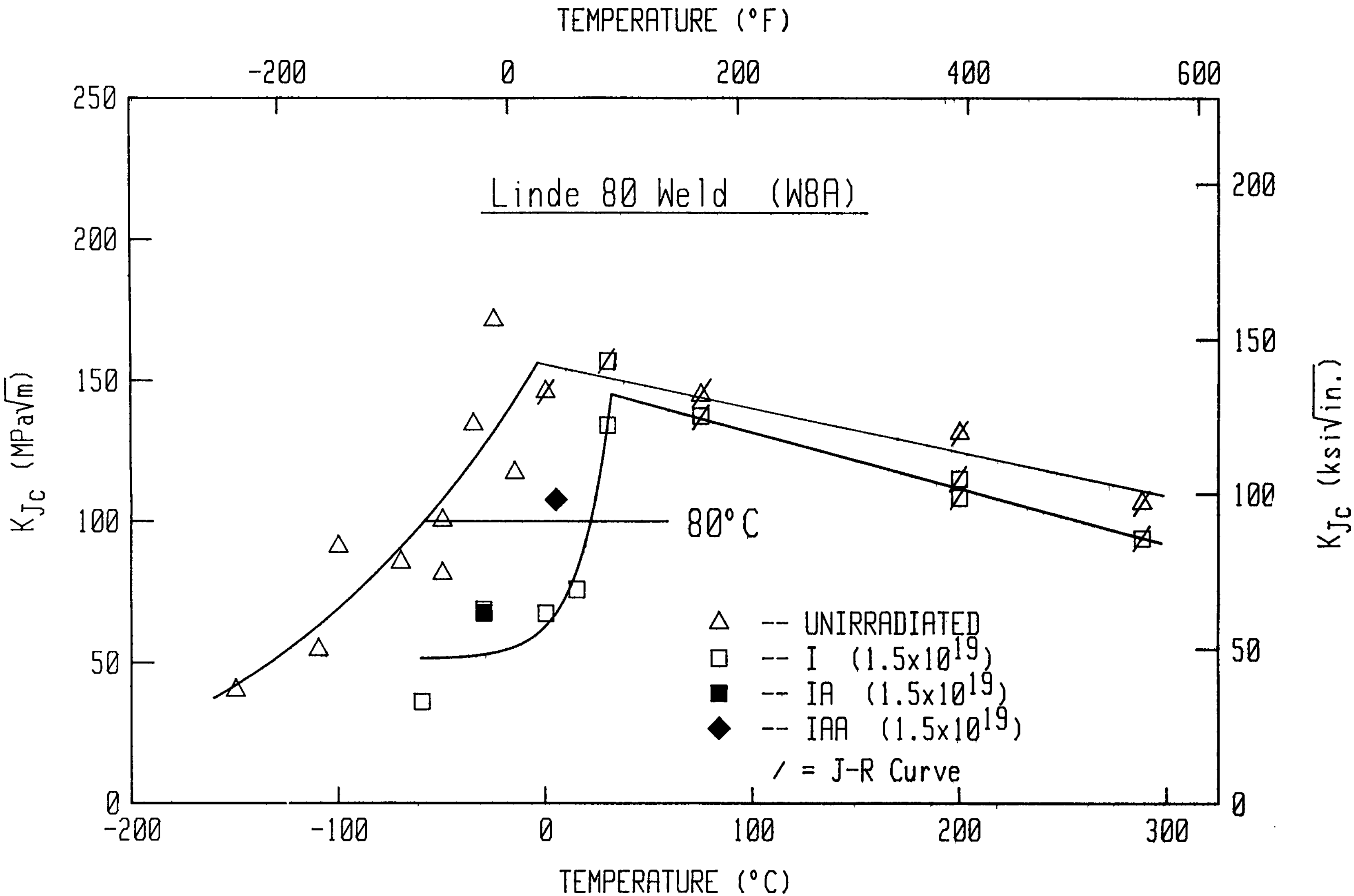

Fig. 50 For the Linde 80 weld (W8A), K_{Jc} data for the I condition to a fluence of 1.5×10^{19} n/cm^2 indicates a ΔT of 80°C and a moderate decrease in upper shelf.

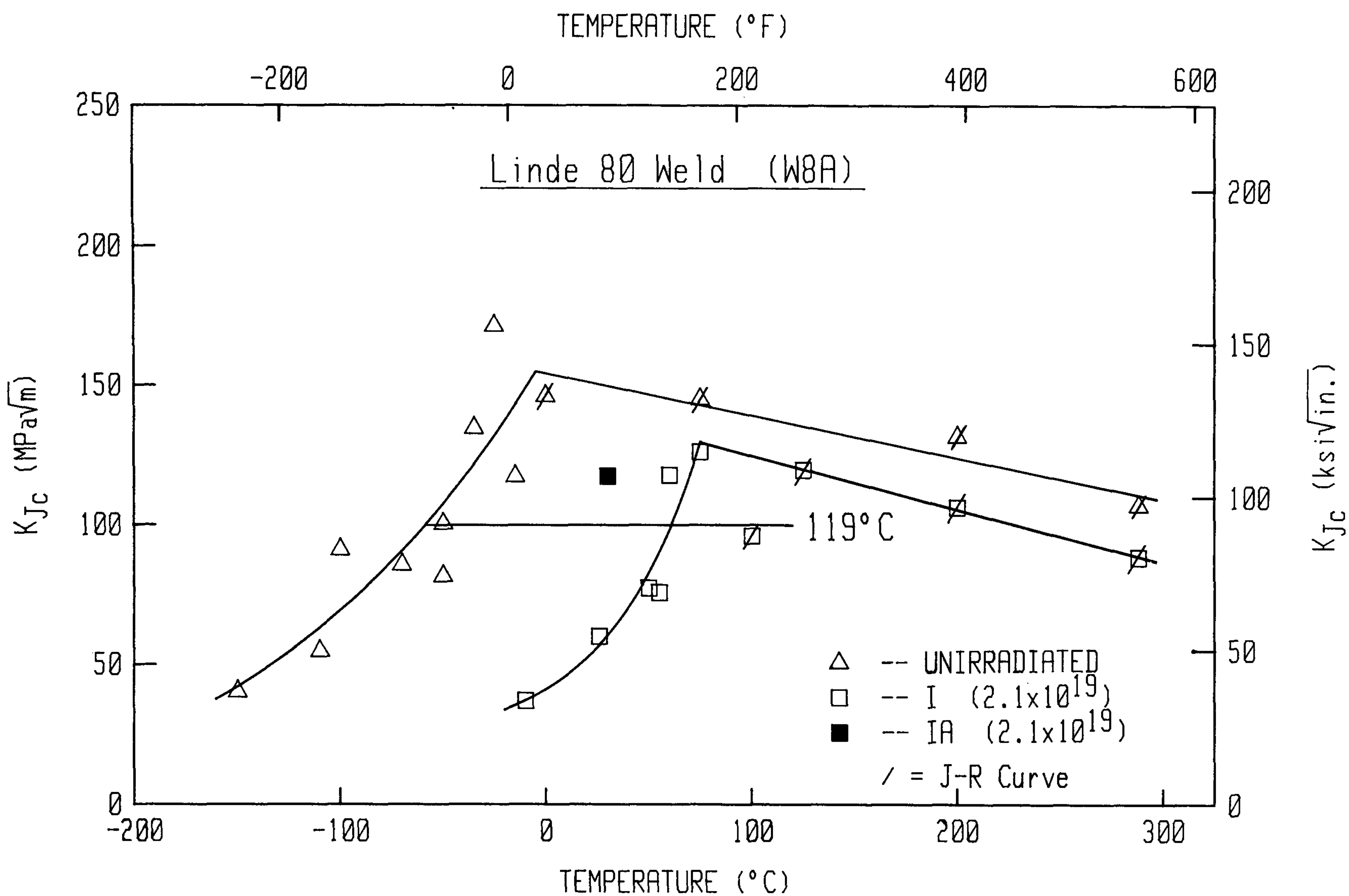

Fig. 51 For the Linde 80 weld (W8A), K_{Jc} data for the I condition to a fluence of 2.1×10^{19} n/cm^2 indicates a ΔT of 119°C and a moderate decrease in upper shelf.

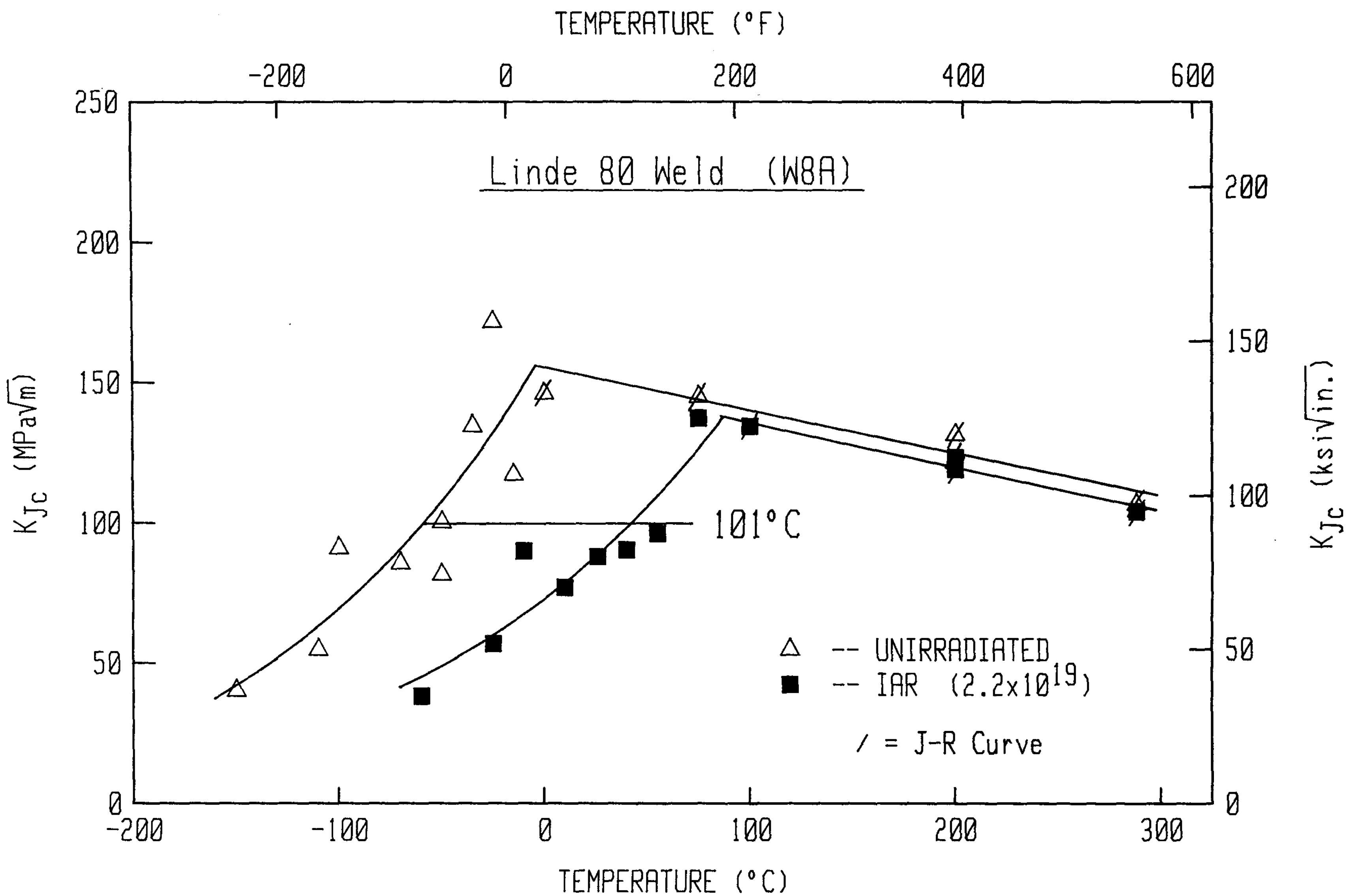

Fig. 52 For the Linde 80 weld (W8A), K_{Jc} data for the IAR condition to a total fluence of 2.2 x 10^{19} n/cm^2 indicates a ΔT of 101°C and a small decrease in upper shelf toughness

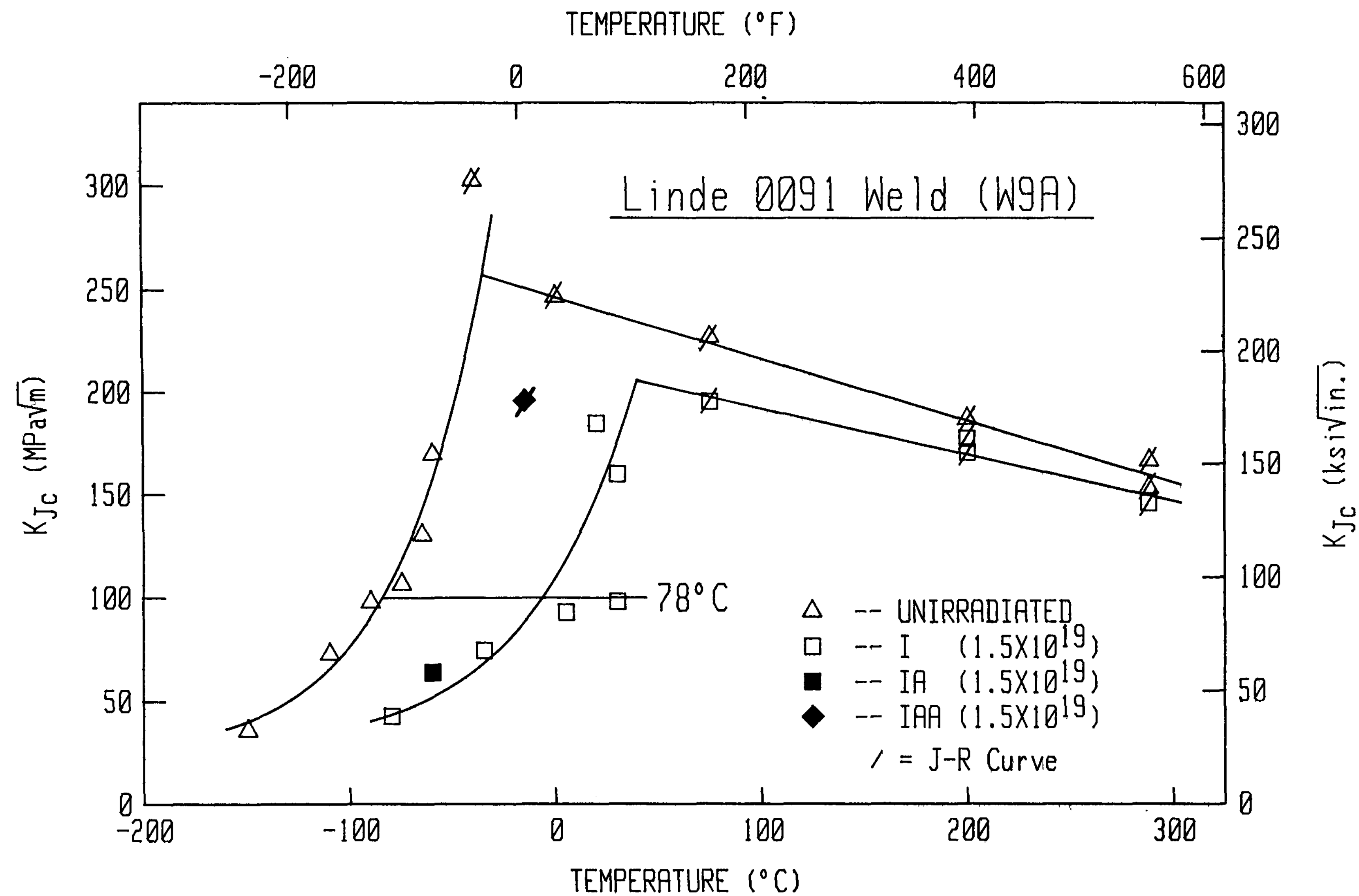

Fig. 53 For the Linde 0091 weld (W9A), K_{Jc} data for the I condition to a fluence of 1.5×10^{19} n/cm^2 indicates a ΔT of 78°C and a moderate decrease in upper shelf.

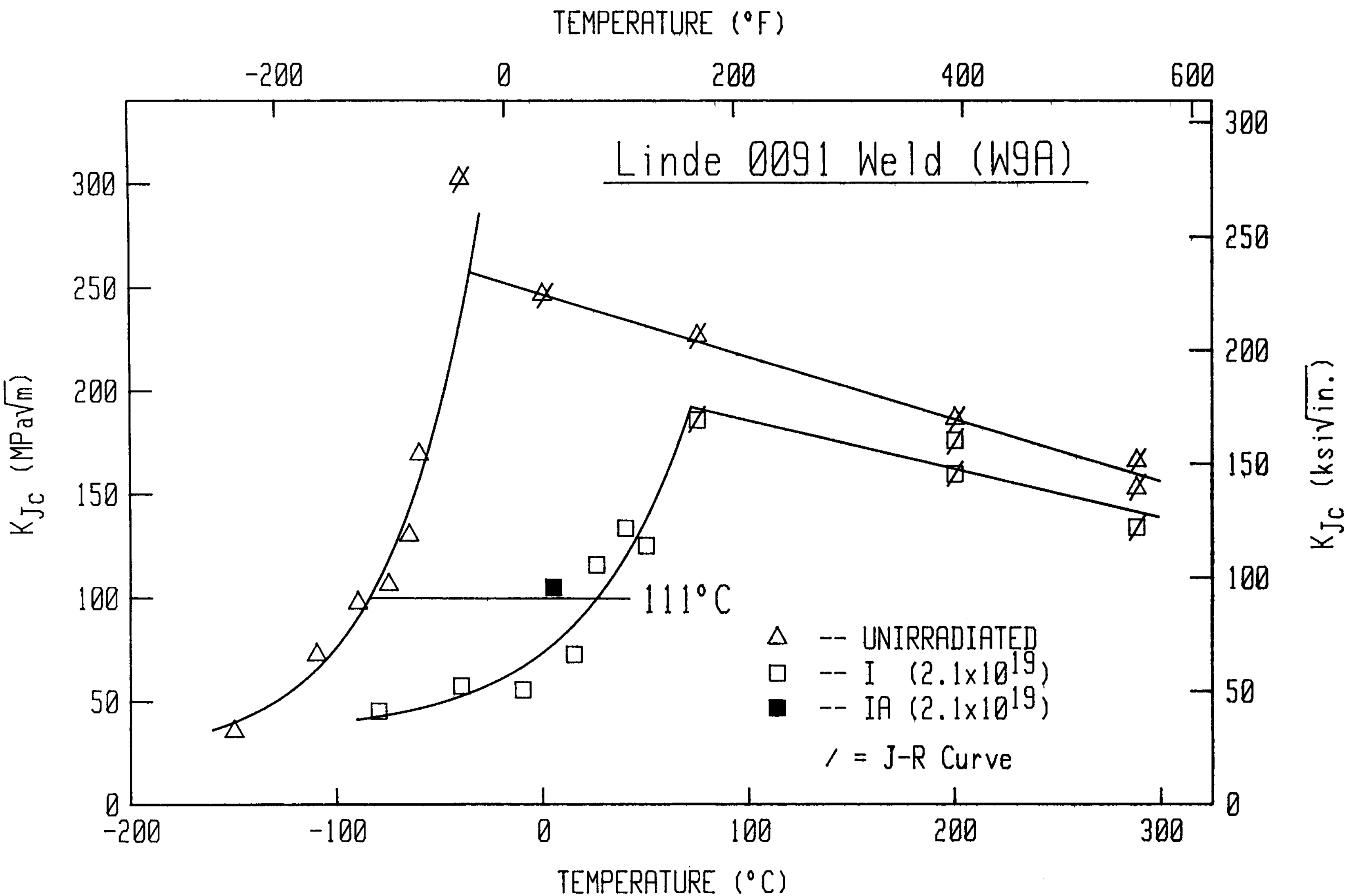

Fig. 54 For the Linde 0091 weld (W9A), K_{Jc} data for the I condition to a fluence of 2.1×10^{19} n/cm^2 indicates a ΔT of 111°C and a moderate decrease in upper shelf.

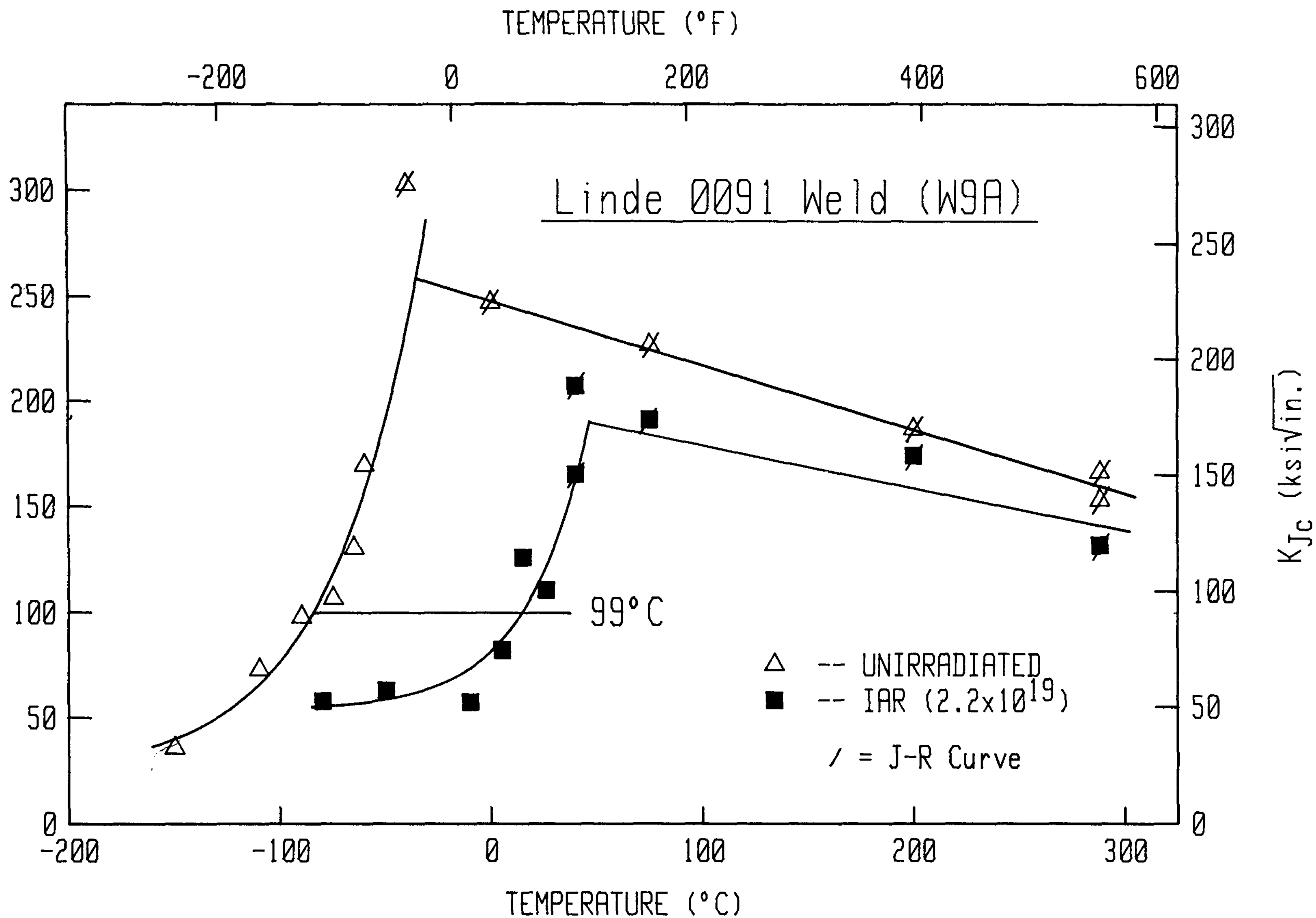

Fig. 55 For the Linde 0091 weld (W9A), K_{Jc} data for the IAR condition to a total fluence of 2.2×10^{19} n/cm^2 indicates a ΔT of 99°C and a moderate decrease in upper shelf toughness.

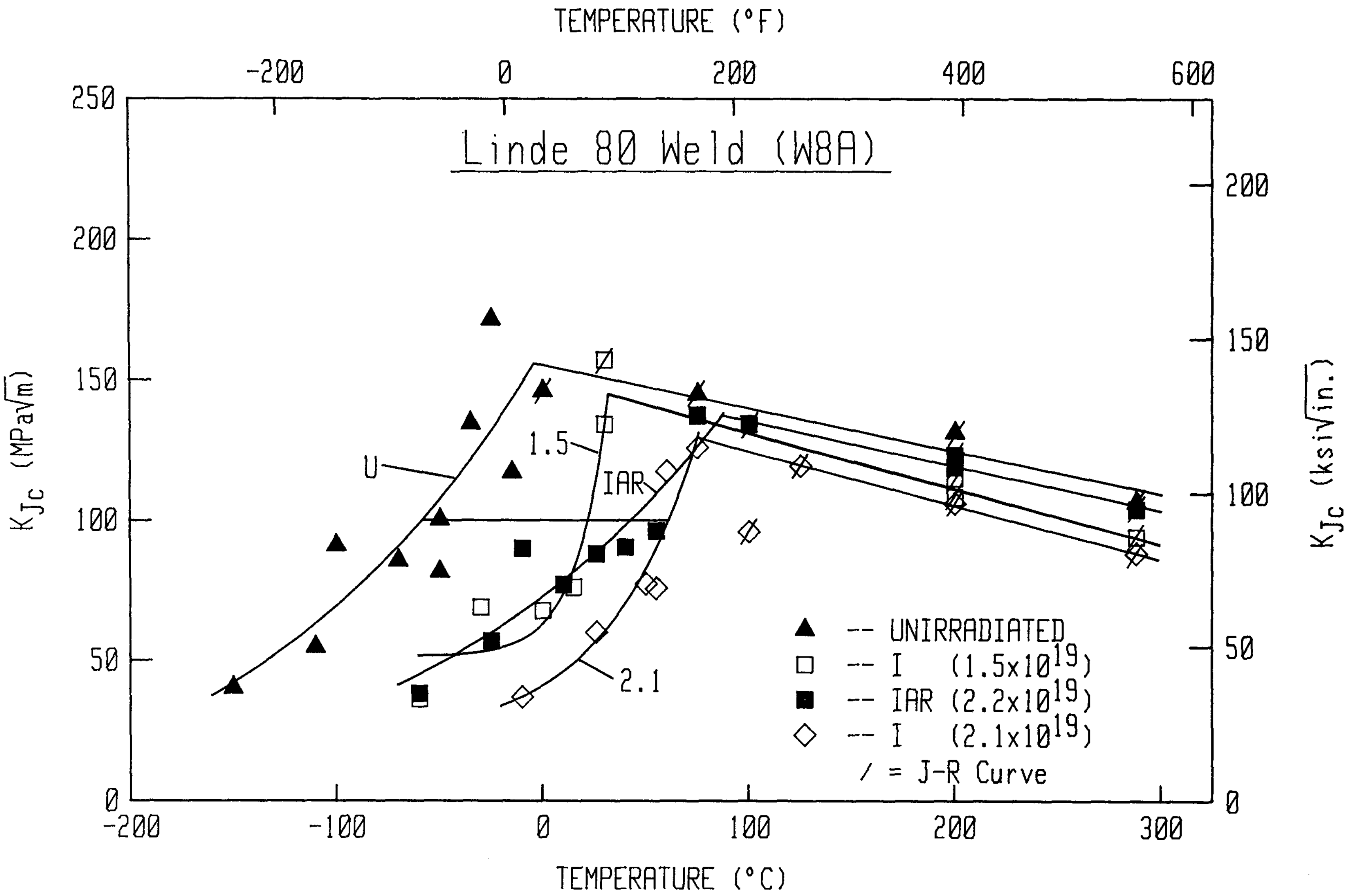

Fig. 56 Comparison of all of the K_{Jc} data for the Linde 80 weld (W8A).

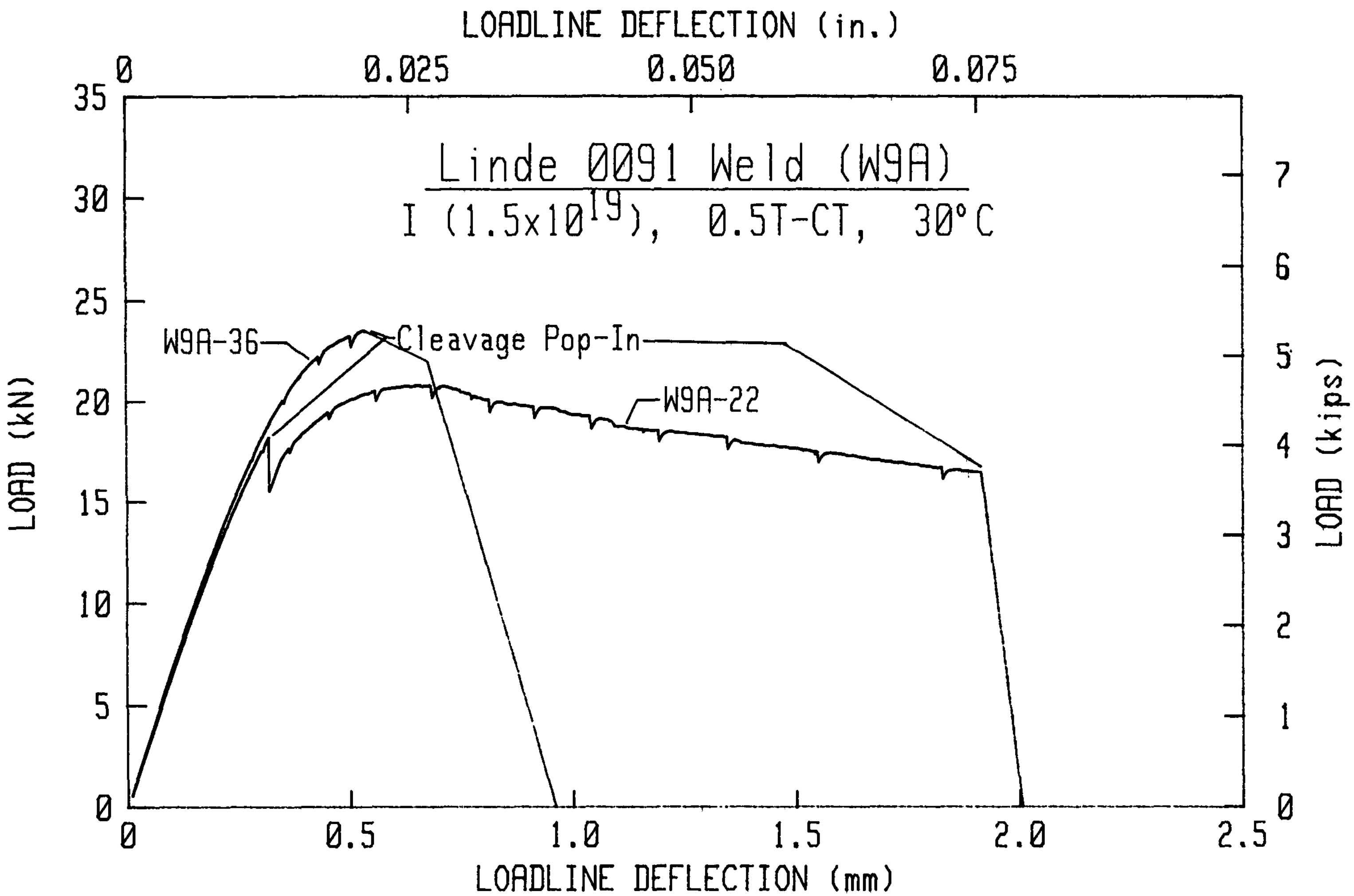

Fig. 57 For the Linde 0091 weld (W9A), comparison of load-displacement curves for two tests at 30°C of the I condition (fluence of 1.5 x 10^{19} n/cm^2). Both tests exhibit cleavage pop-in behavior, with the specimen exhibiting the lower pop-in load eventually giving substantial amounts of stable crack growth.

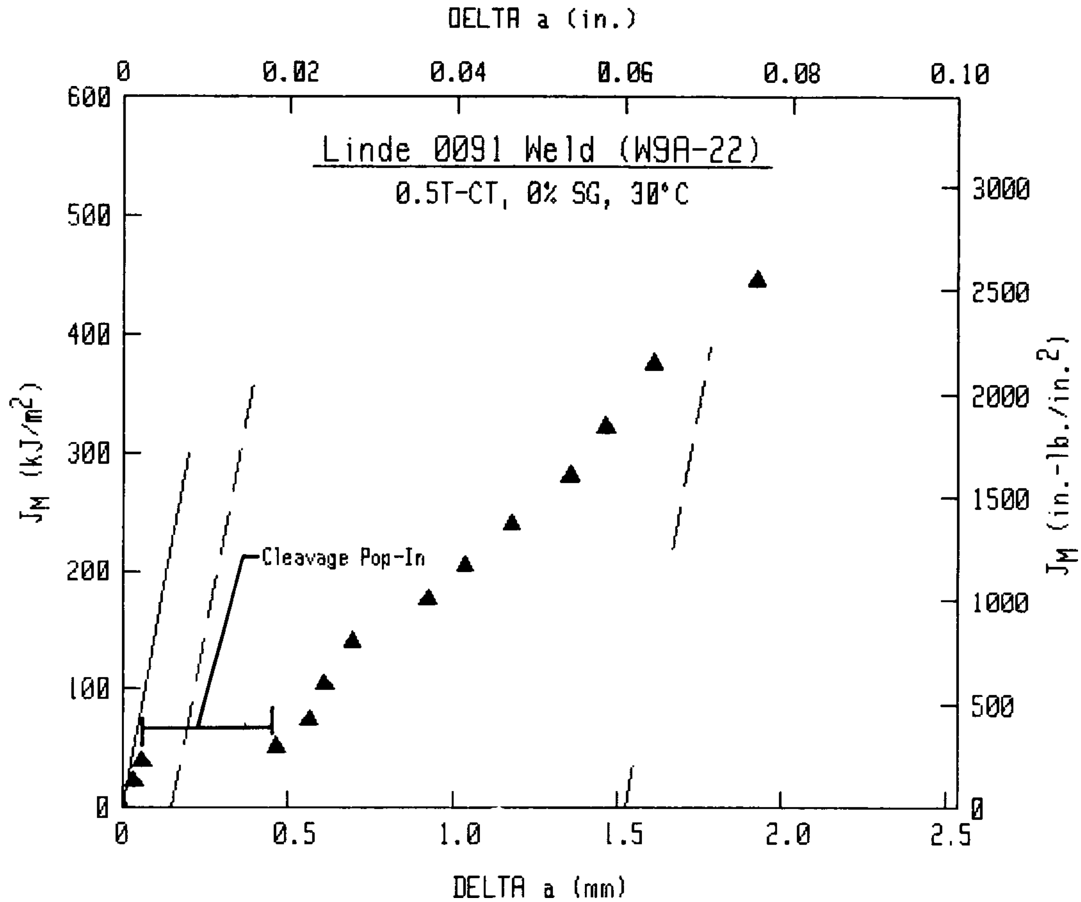

Fig. 58 Of the tests for which the load-displacement curves are illustrated in Fig. 57, specimen W9A-22 exhibited the lowest K_{Jc} value and gave this J_M-R curve. In contrast, specimen W9A-36 gave the highest K_{Jc} value but the J_M-R curve never moved off of the blunting line.

Table 13 Summary of Transition Temperature Upper and Lower Bounds

Code	Condition [a]	Fluence [b]	Temperature (°C) At 100 MPa√m Upper Bound	Temperature (°C) At 100 MPa√m Mean Curve	Temperature (°C) At 100 MPa√m Lower Bound	Shifts (°C) at 100 MPa√m Minimum	Shifts (°C) at 100 MPa√m Mean	Shifts (°C) at 100 MPa√m Maximum
W8A	U	---	-85	-58	-39	---	---	---
	I	1.5	13	22	28	42	80	113
	I	2.1	54	61	69	93	119	154
	IAR	2.2	27	43	59	66	101	144
W9A	U	---	-93	-84	-77	---	---	---
	I	1.5	-40	-6	14	37	78	107
	I	2.1	13	27	37	90	111	130
	IAR	2.2	-1	15	--[c]	76	99	--[c]

[a] U = Unirradiated
I = Irradiated
IAR = Irradiated-Annealed-Reirradiated

[b] 10^{19} n/cm^2 (E > 1 MeV)

[c] Cannot be determined.

J-R curve exhibits a relatively low J_{Ic} level (Fig. 59), much lower than those for the unirradiated condition.

No significant surprises are apparent for the I condition with a fluence of 2.1 x 10^{19} n/cm^2. An IA condition test demonstrates little recovery in toughness.

For the IAR condition, surprisingly little scatter results. The only noteworthy test is at -10°C (14°F), where a small pop-in occurs at a relatively low toughness, prior to final fracture at a much higher load. At the final fracture, the K_{Jc} is 86.9 MPa$\sqrt{m}$, in contrast to 57.1 MPa$\sqrt{m}$ at the pop-in (Fig. 60).

For Weld W9A, the IAR treatment does result in some recovery over that of an I condition to about the same fluence (Fig. 61).

No consistent trend emerges for the welds in terms of K_{Jc} curve-shape change. Weld W8A exhibits an unusual trend in that the I-conditions exhibited somewhat steeper curves than the unirradiated condition. In contrast, the IAR condition exhibited a much shallower slope. Weld W9A is opposite to that, as the I conditions exhibit somewhat of a shallower slope, and the IAR condition exhibits similar curvature to the unirradiated condition.

With the upper shelf (i.e., J-R curve) data, two overall trends emerge for each weld. Increasing the test temperature tends to result in lower J levels in each case, and the I condition with the highest fluence (UBR-48A, 2.1 x 10^{19} n/cm^2) tends to give the lowest J-R curves. As will be seen in some of the J_M-R curves, an inflection point ("hook" or "up-sweep") occurs near the end of the data, indicating an end to J_M validity.

J-R curves for weld W8A are illustrated in Figs. 62 to 65 for each condition. In each case, the J levels are reduced with increasing test temperature. For UBR-50 and UBR-48B, duplicate tests at 200°C (392°F) indicate excellent reproducibility. For several of the curves, the end of the curve indicates an increasing slope or a "hook-up" behavior, which has been found to indicate the loss of validity for J_M.

Comparisons of J-R curves from each condition at the same temperature demonstrate a consistent trend of the unirradiated condition exhibiting much higher J levels than the other conditions (Figs. 66 to 68). At each temperature, the highest fluence I condition gives the lowest curves overall.

For Weld W9A (Figs. 69 to 72), good reproducibility results for the cases of duplicate tests, for the case of side-grooved specimens. The one case in which good agreement does not occur is for UBR-48B, where two plane-sided specimens were tested at 40°C (104°F). As illustrated in Fig. 73, both of these tests indicate significant stable tearing which is interrupted by a cleavage pop-in. For Specimen W9A-9, the test is continued to greater crack growth, while for Specimen W9A-16 the test is terminated after the pop-in.

(text continues on pg. 107)

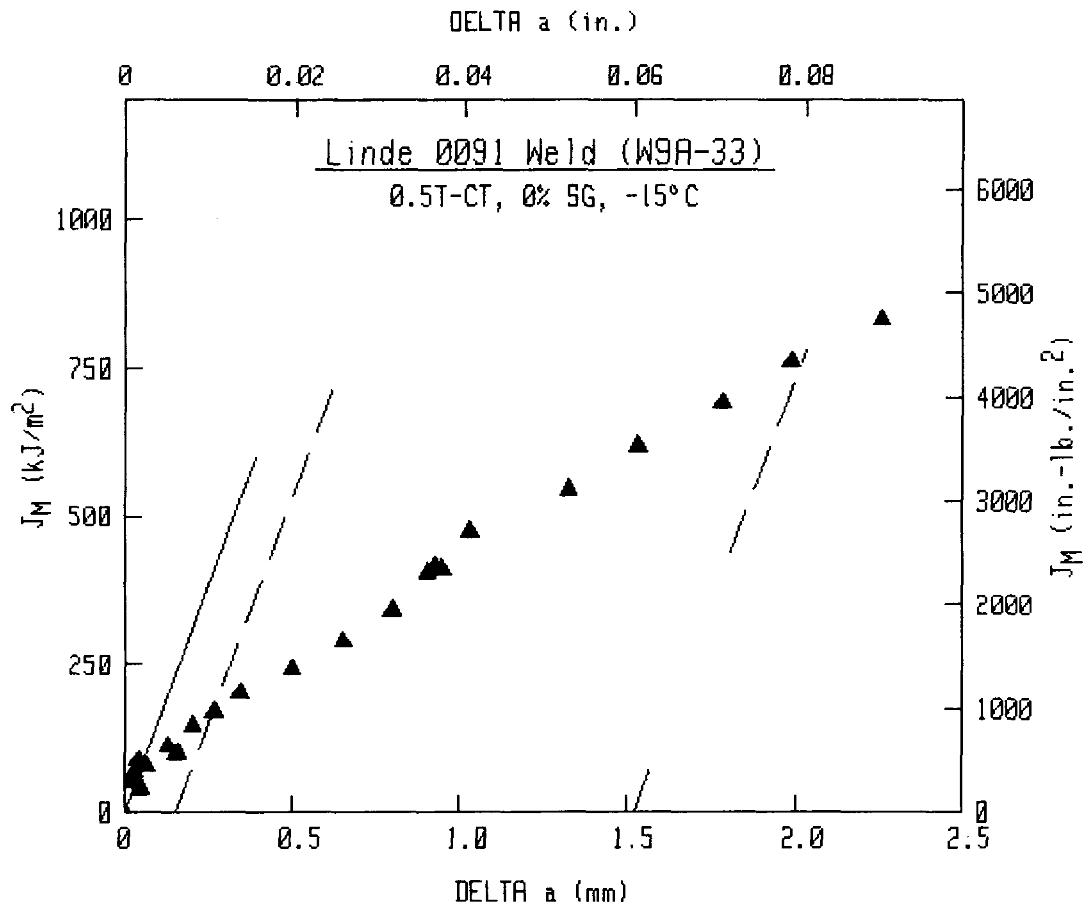

Fig. 59 For the Linde 0091 weld (W9A), an IAA condition (fluence of 1.5×10^{19} n/cm^2) test at -15°C resulted in this J_M-R curve, which is characterized by a low initiation J level.

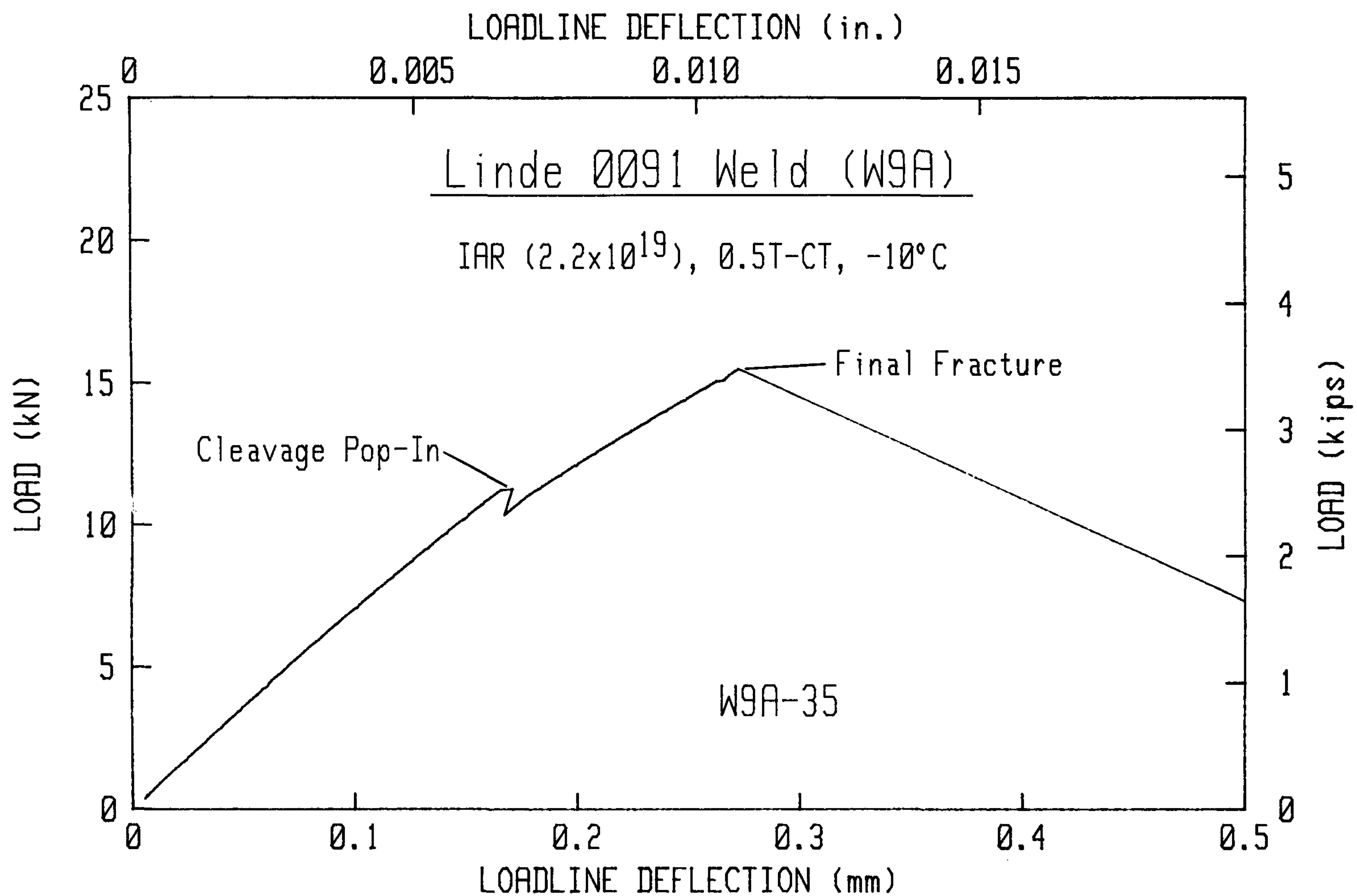

Fig. 60 For the Linde 0091 weld (W9A), an IAR condition test at $-10^{\circ}C$ (total fluence of 2.2 x 10^{19} n/cm^2) exhibited a cleavage pop-in at ~ 12 kN and then final fracture at a higher load.

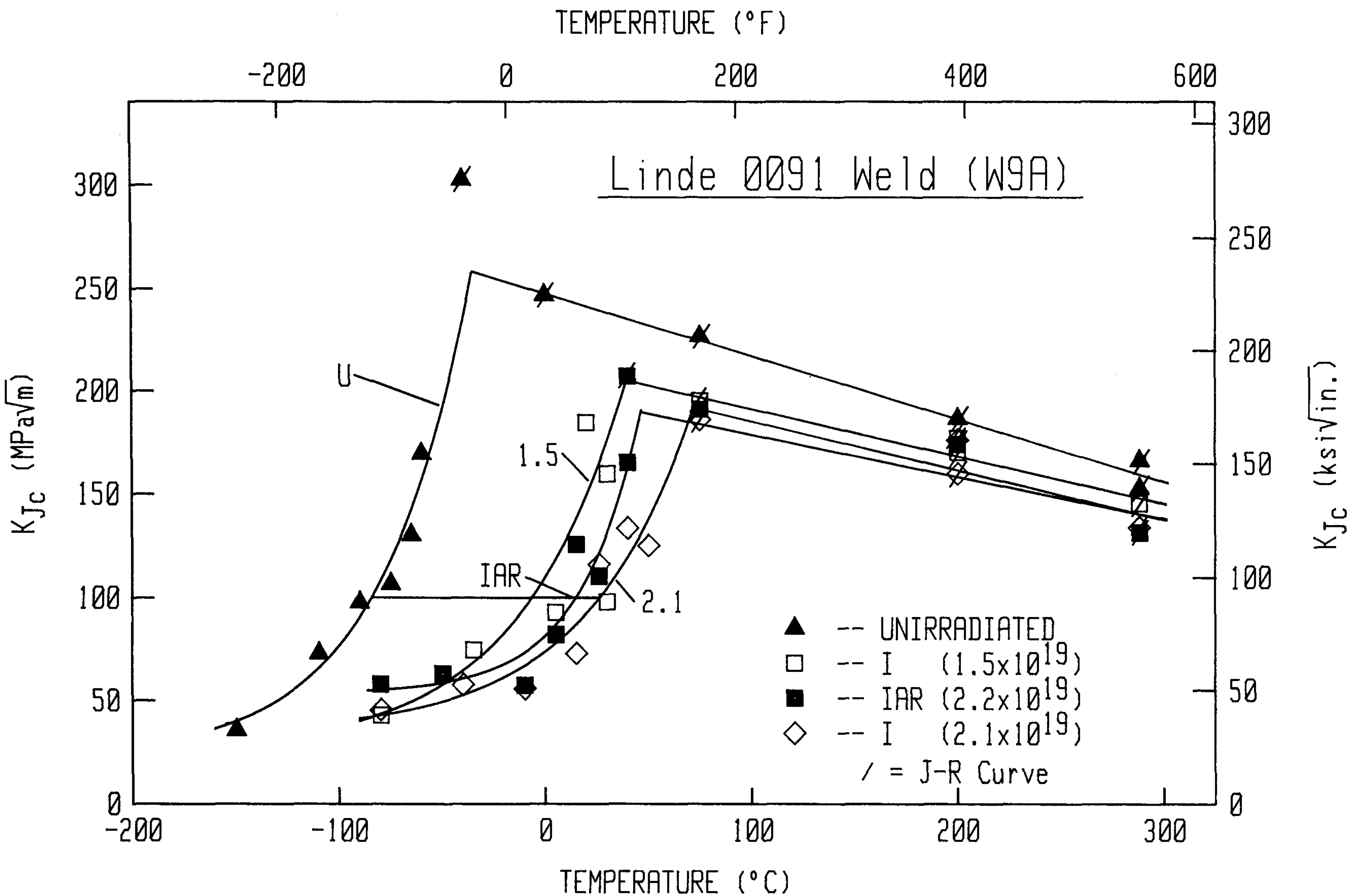

Fig. 61 Comparison of all of the K_{Jc} data for the Linde 0091 weld (W9A).

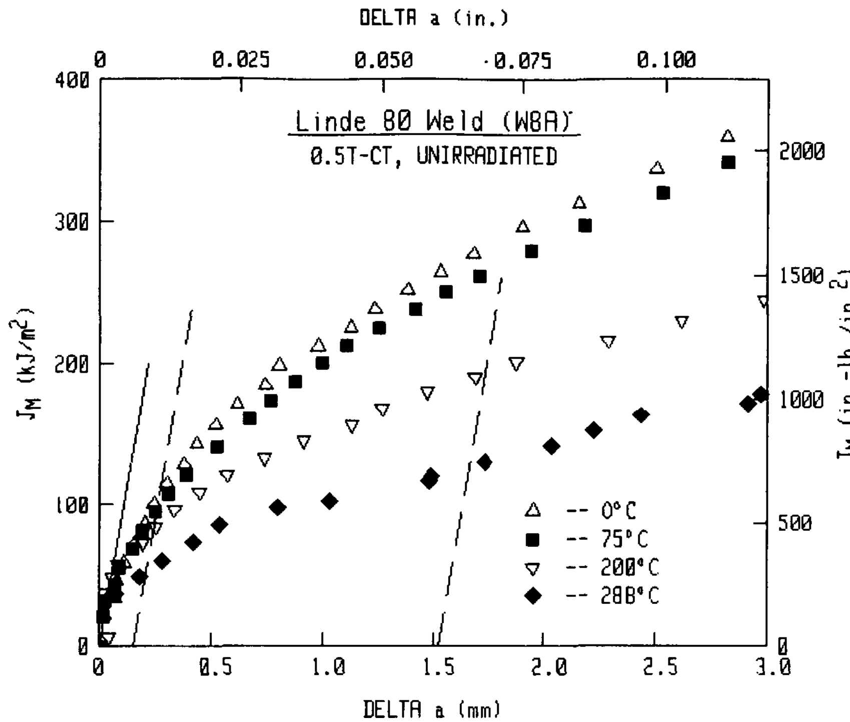

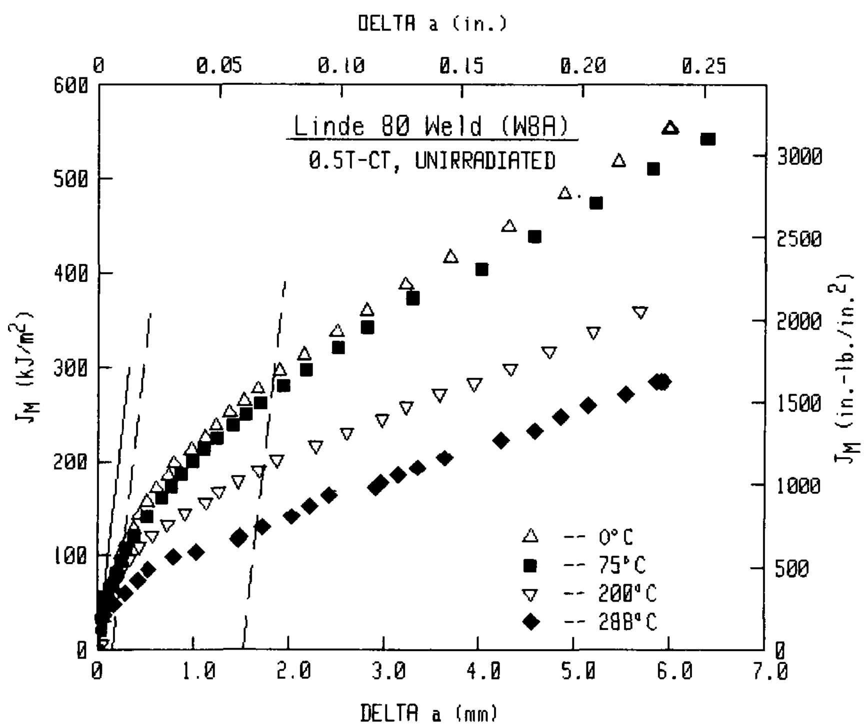

Fig. 62 Comparison of the J_M-R curves for the Linde 80 weld (W8A) in the unirradiated condition.

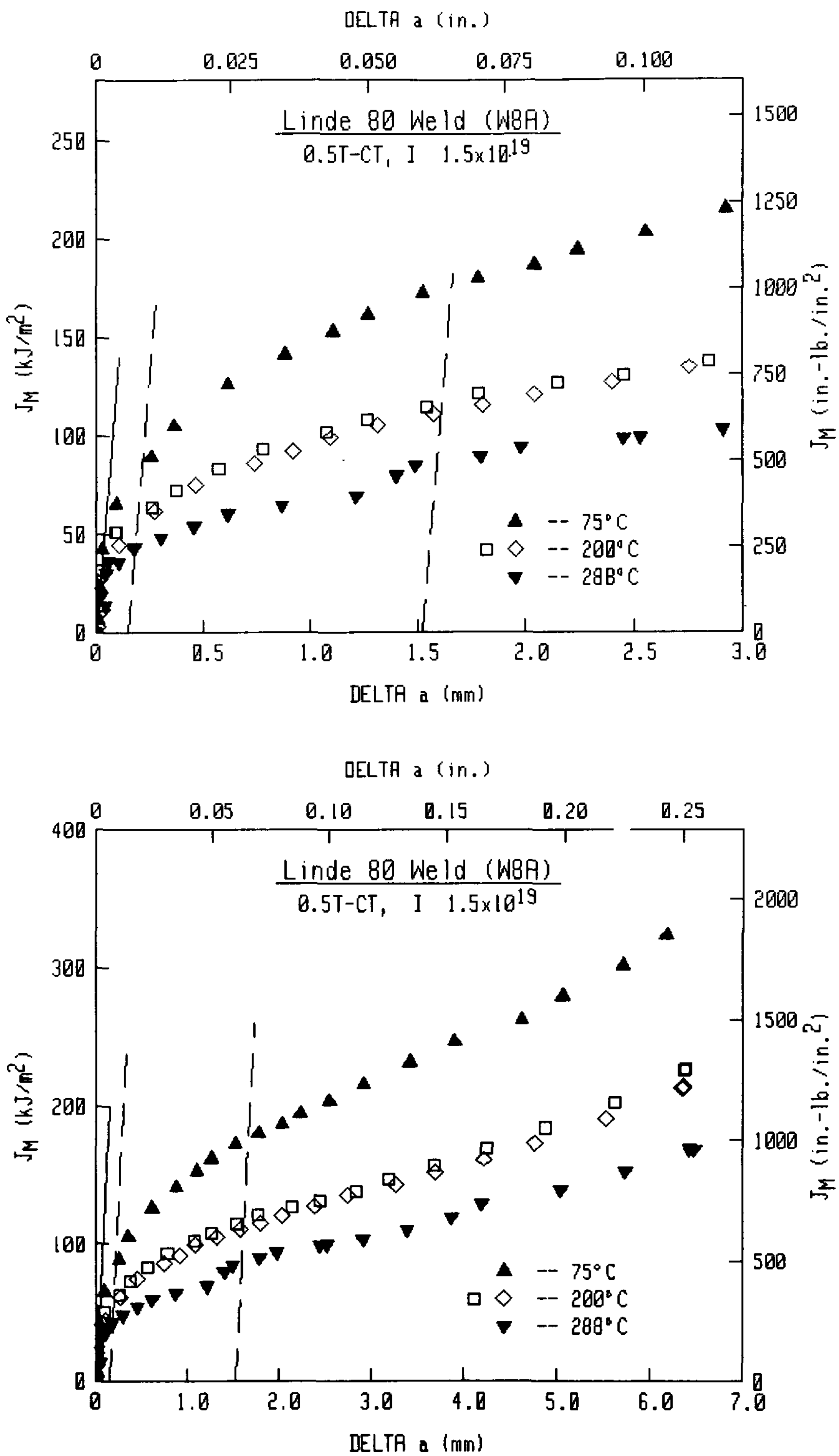

Fig. 63 Comparison of the J_M-R curves for the Linde 80 weld (W8A) in the I condition (1.5×10^{19} n/cm^2).

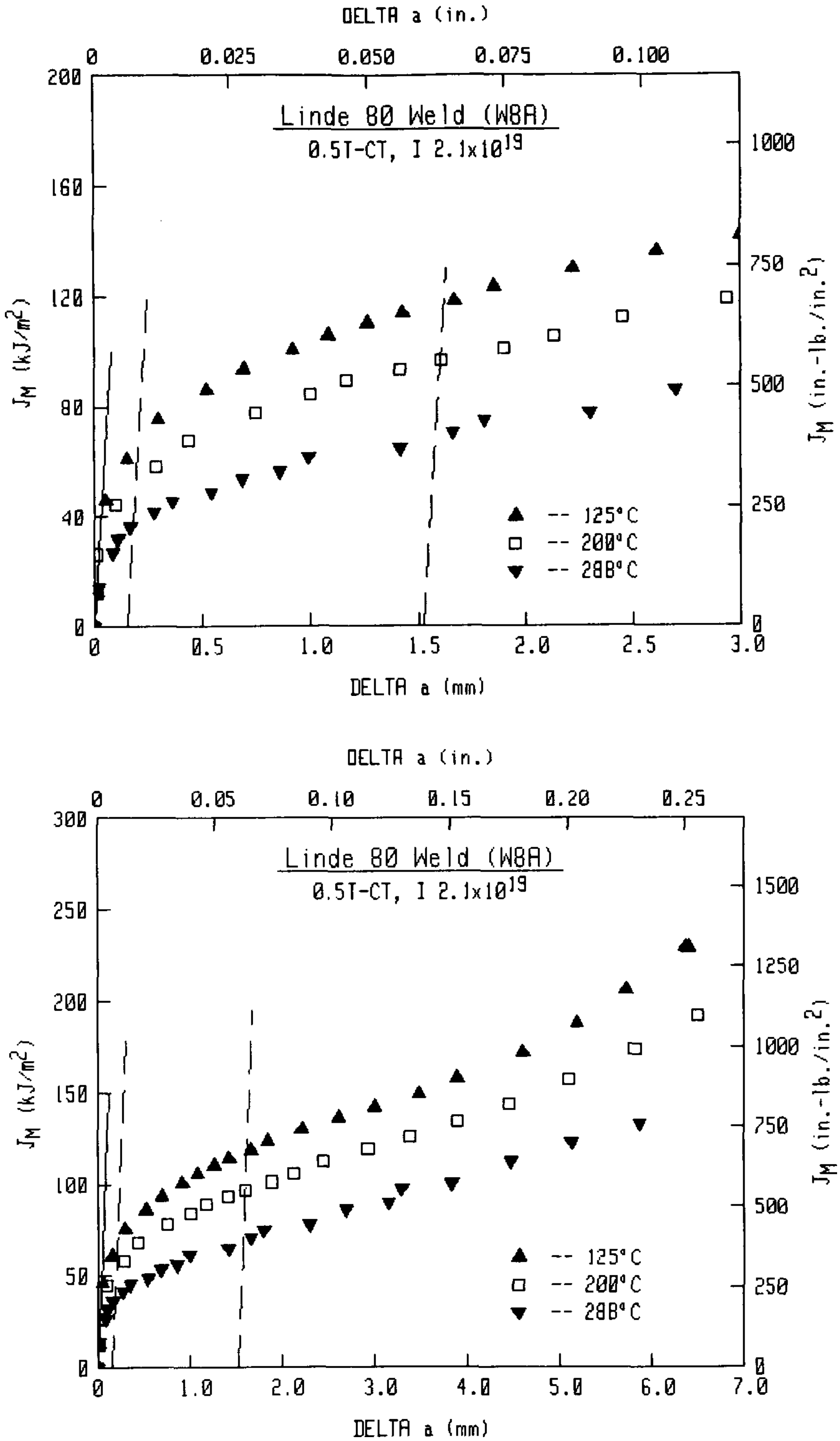

Fig. 64 Comparison of the J_M-R curves for the Linde 80 weld (W8A) in the I condition (2.1×10^{19} n/cm^2).

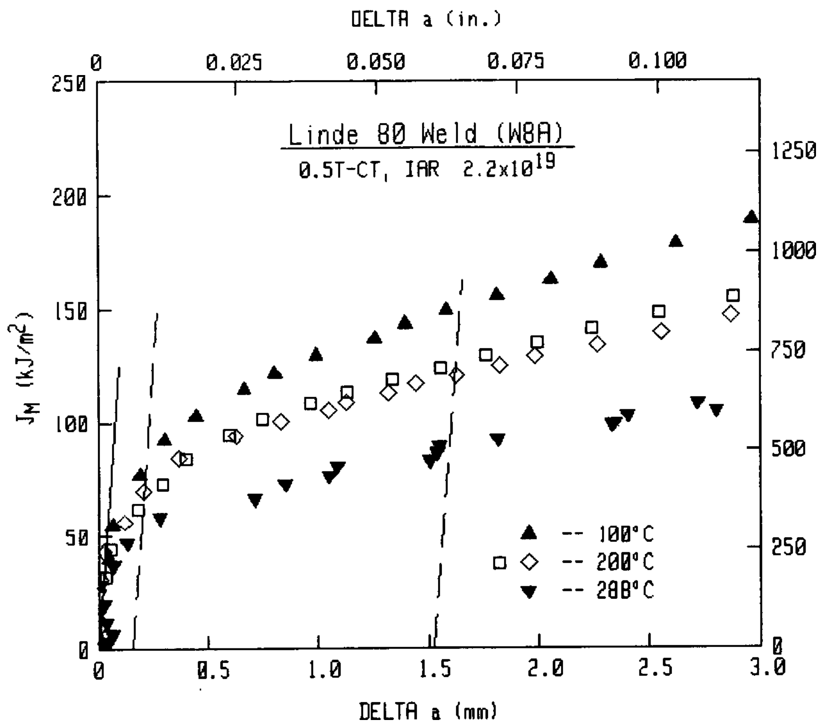

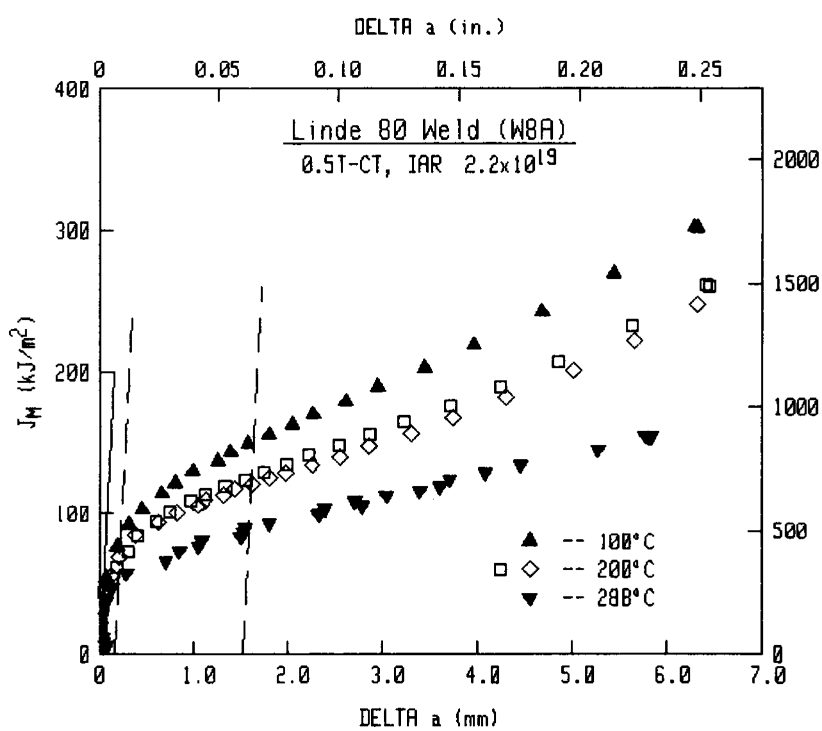

Fig. 65 Comparison of the J_M-R curves for the Linde 80 weld (W8A) in the IAR condition (total 2.2×10^{19} n/cm^2).

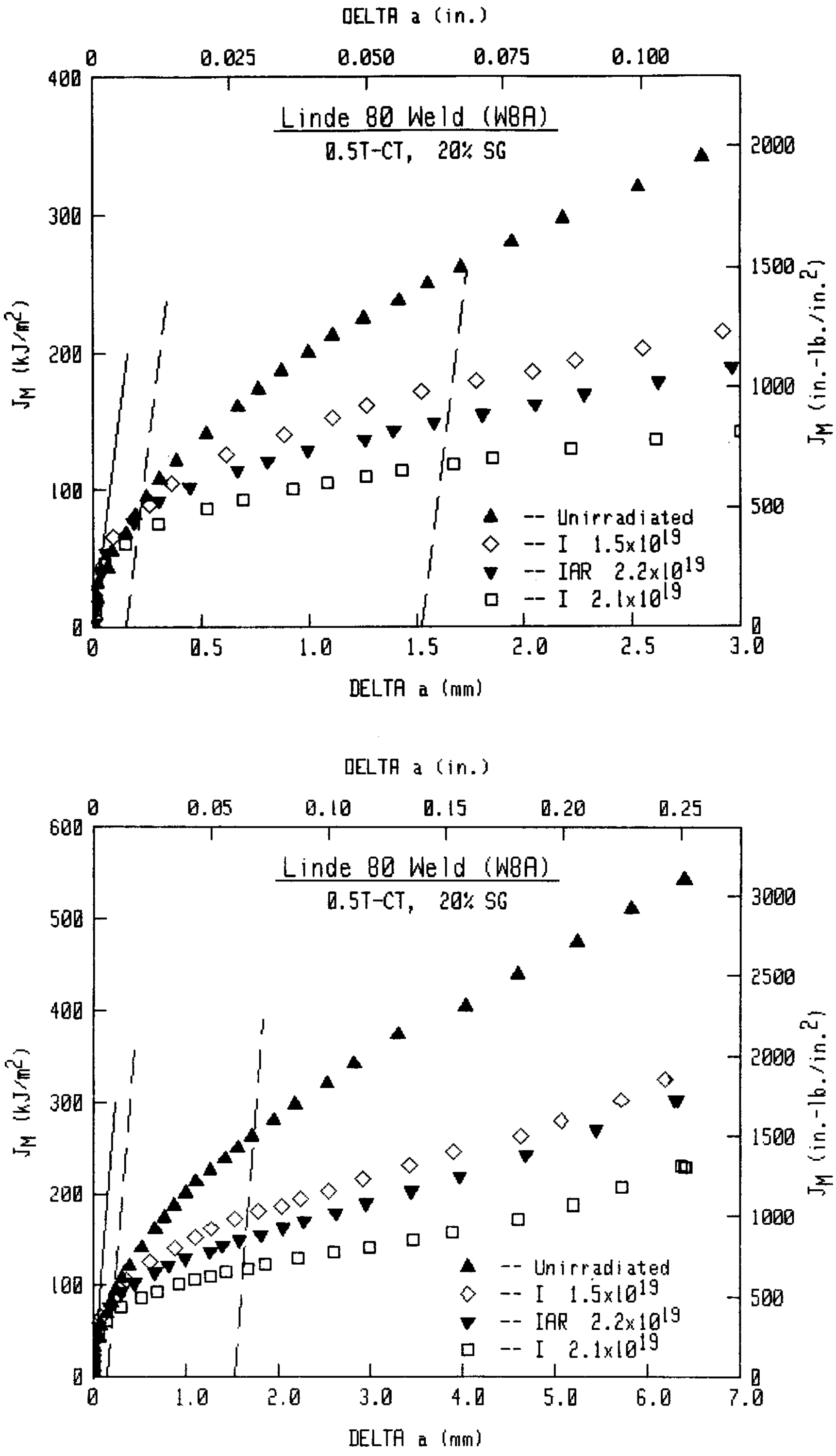

Fig. 66 Comparison of the J_M-R curves for the Linde 80 weld (W8A) at the lowest upper shelf test temperatures, ranging from 75°C to 125°C. The slight differences in test temperature should not have a significant impact on the relative placement of these curves.

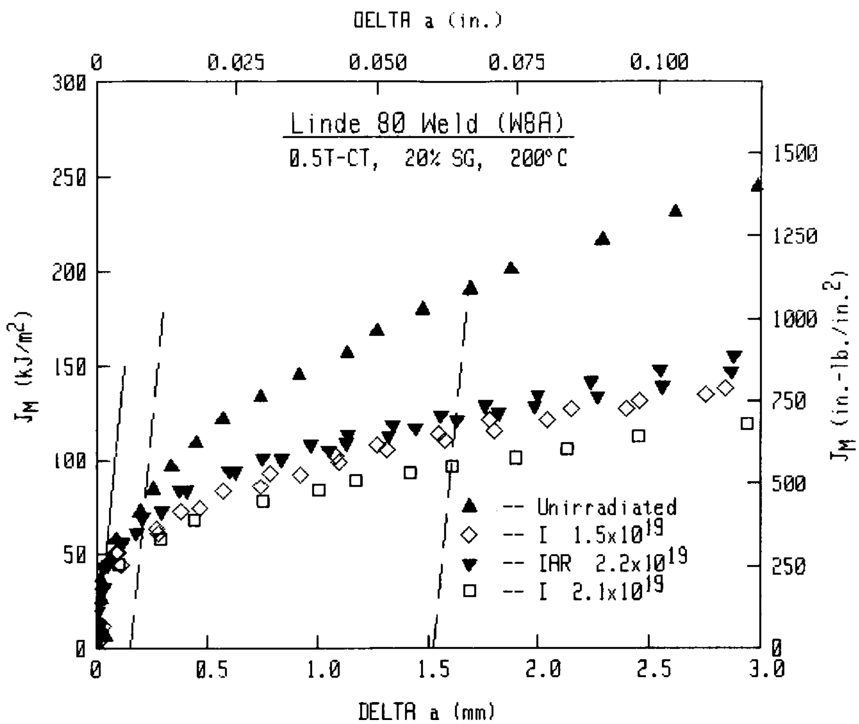

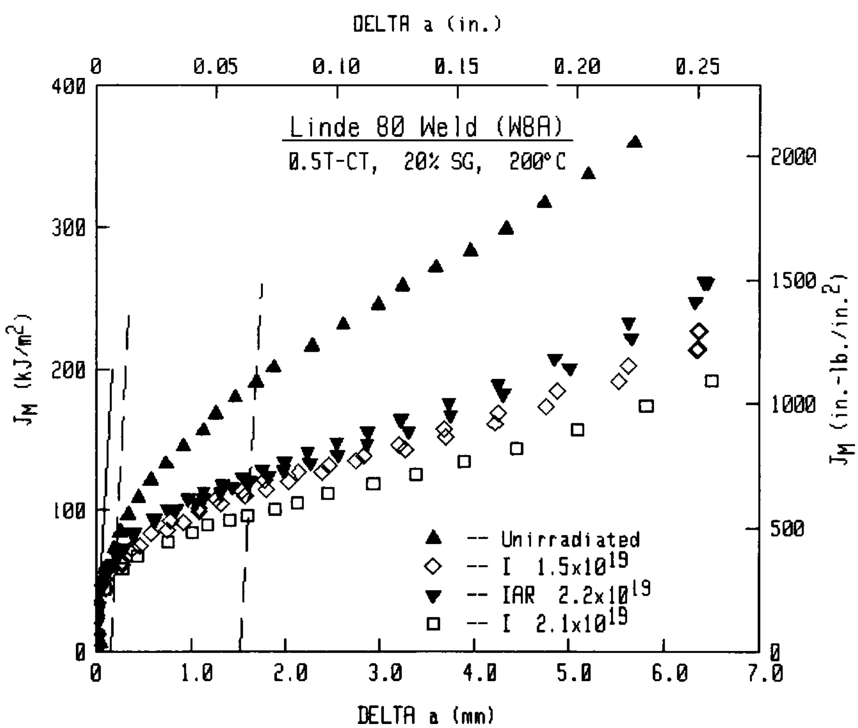

Fig. 67 Comparison of the J_M-R curves for the Linde 80 weld (W8A) at 200°C.

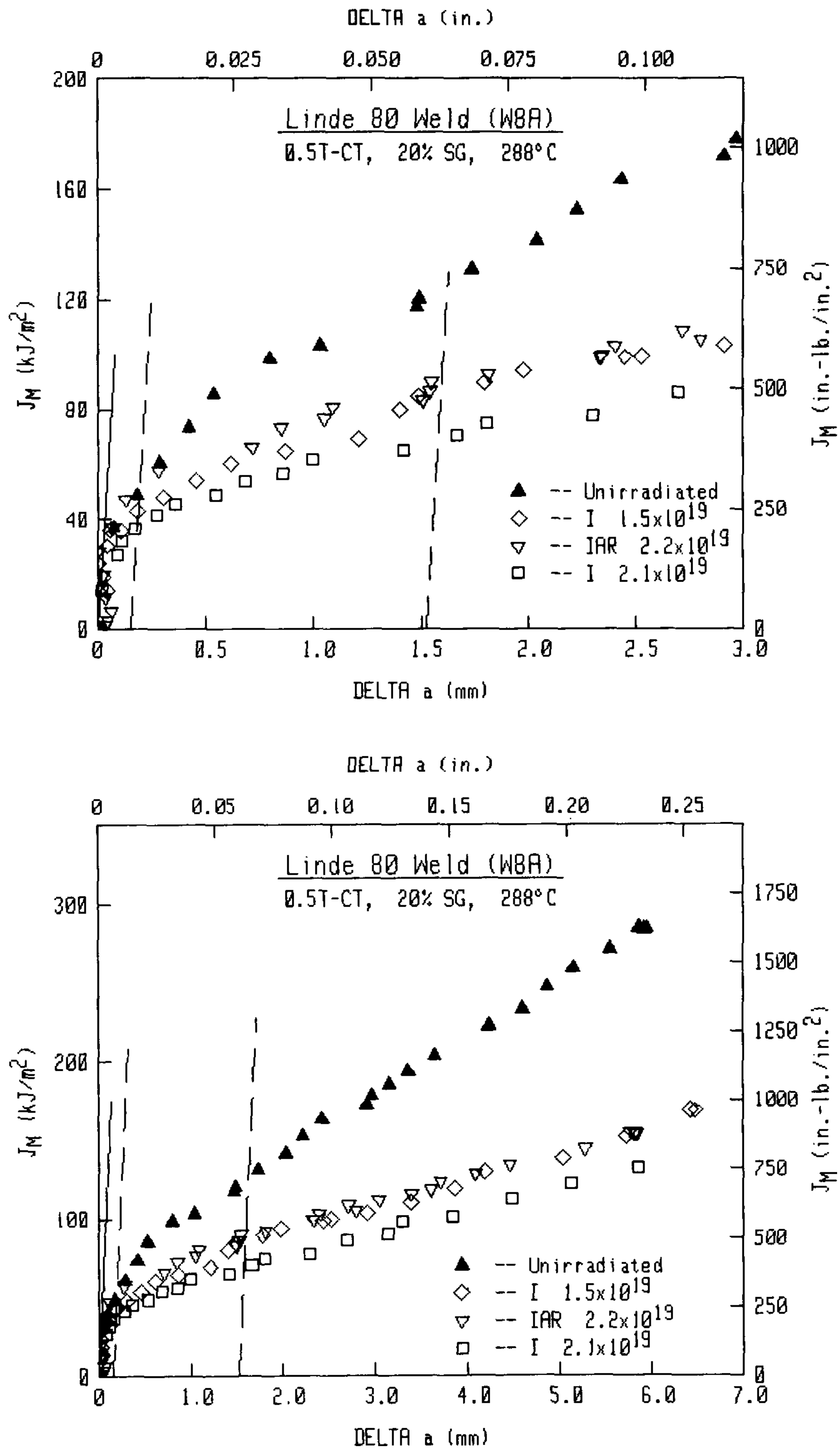

Fig. 68 Comparison of the J_M-R curves for the Linde 80 weld (W8A) at 288 °C.

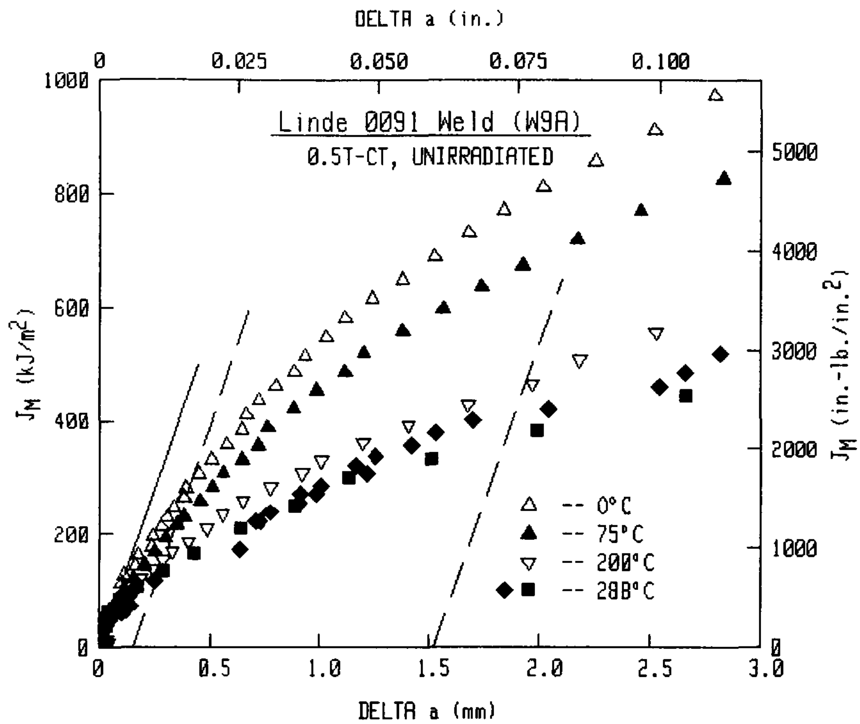

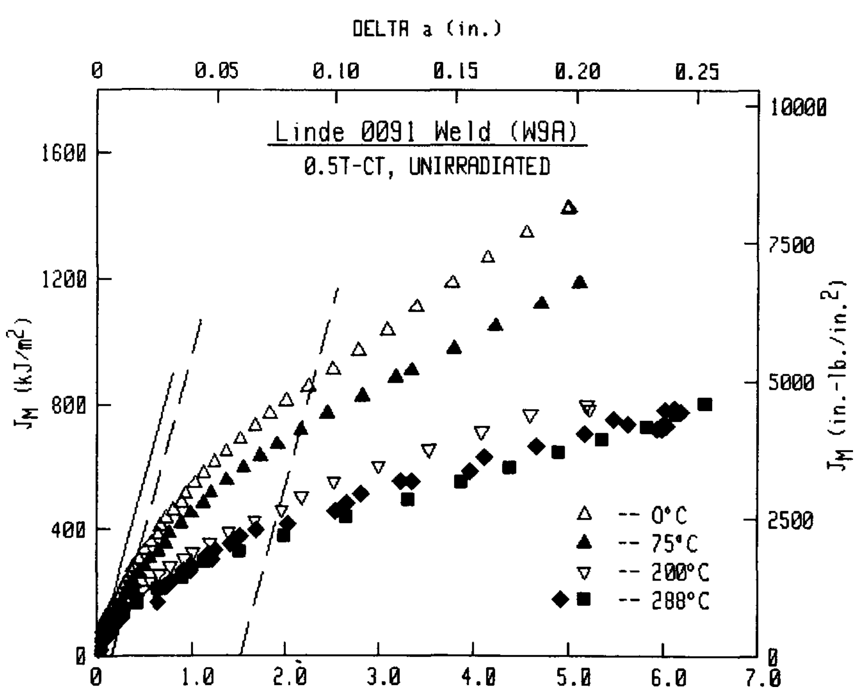

Fig. 69 Comparison of the J_M-R curves for the Linde 0091 weld (W9A) in the unirradiated condition.

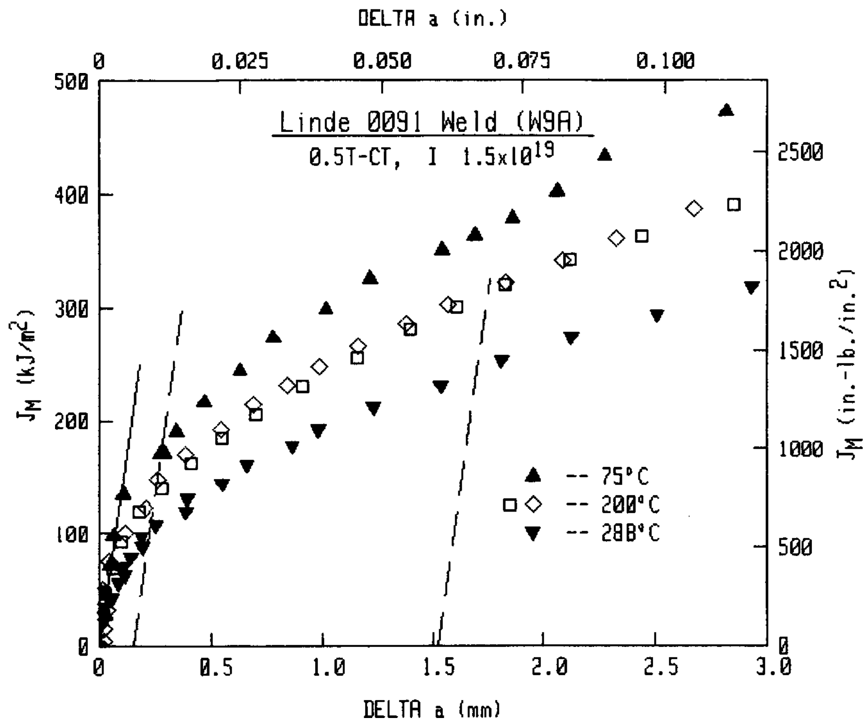

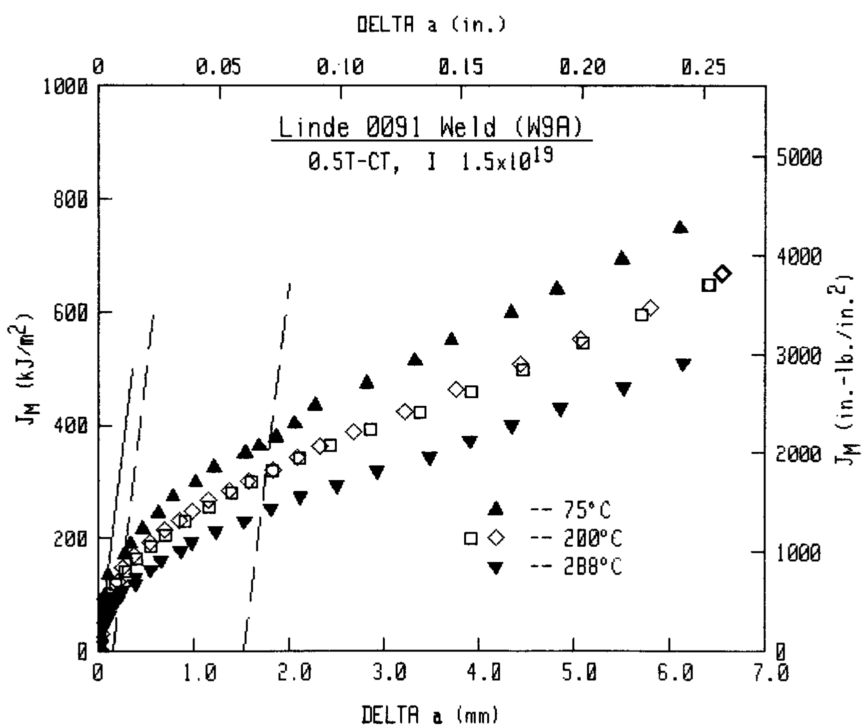

Fig. 70 Comparison of the J_M-R curves for the Linde 0091 weld (W9A) in the I condition (1.5×10^{19} n/cm^2).

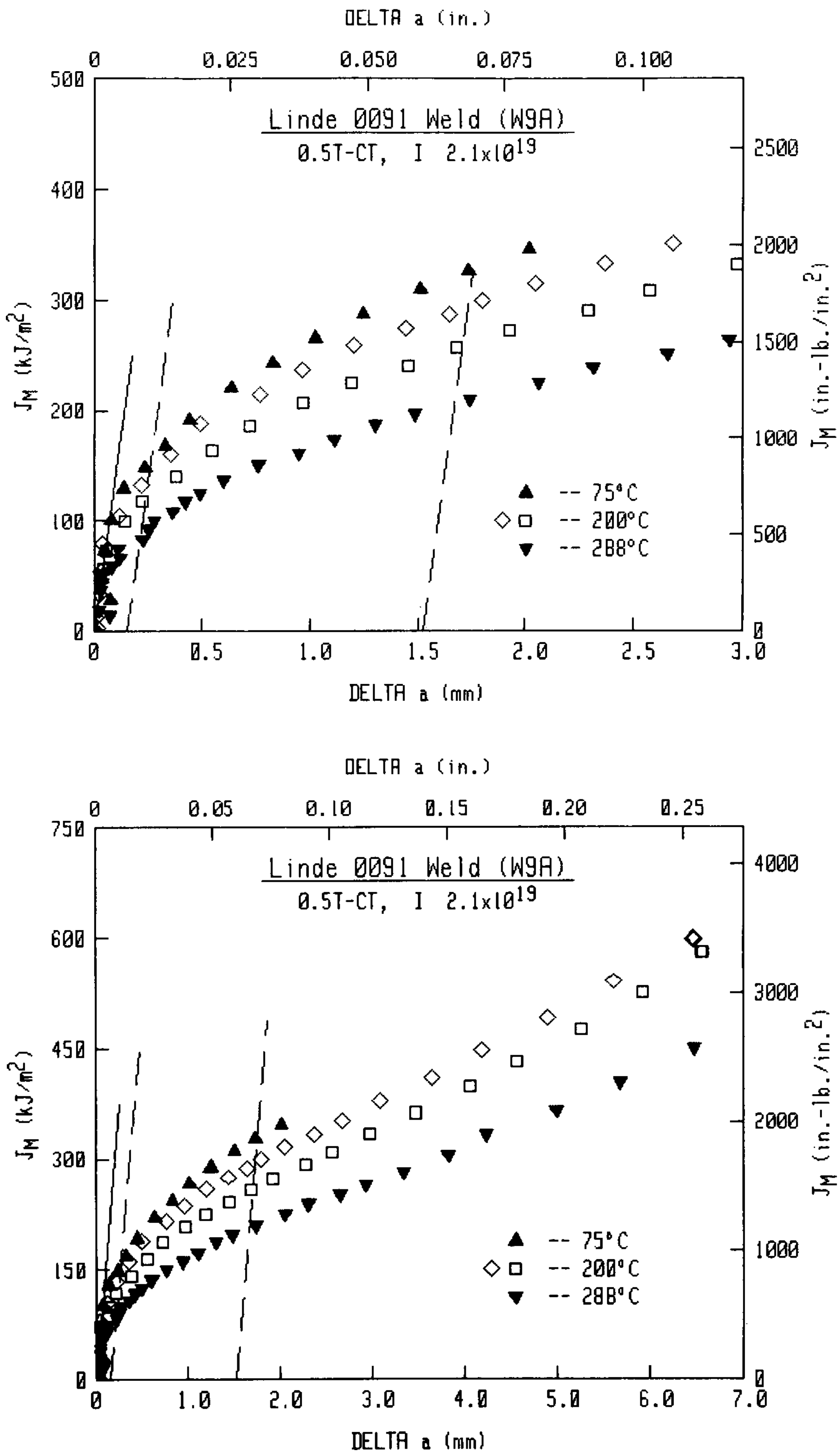

Fig. 71 Comparison of the J_M-R curves for the Linde 0091 weld (W9A) in the I condition (2.1×10^{19} n/cm^2).

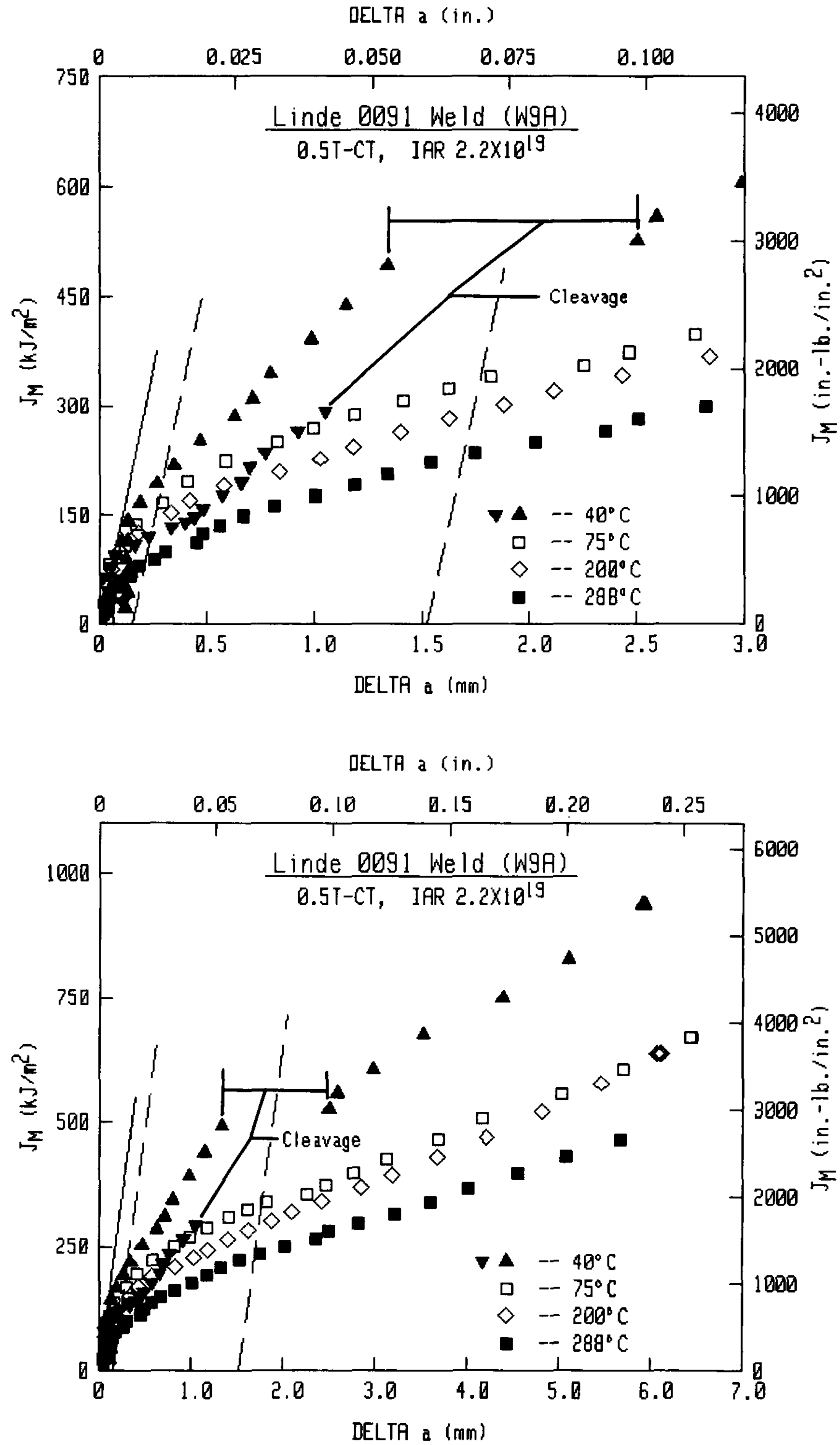

Fig. 72 Comparison of the J_M-R curves for the Linde 0091 weld (W9A) in the IAR condition (total 2.2×10^{19} n/cm²).

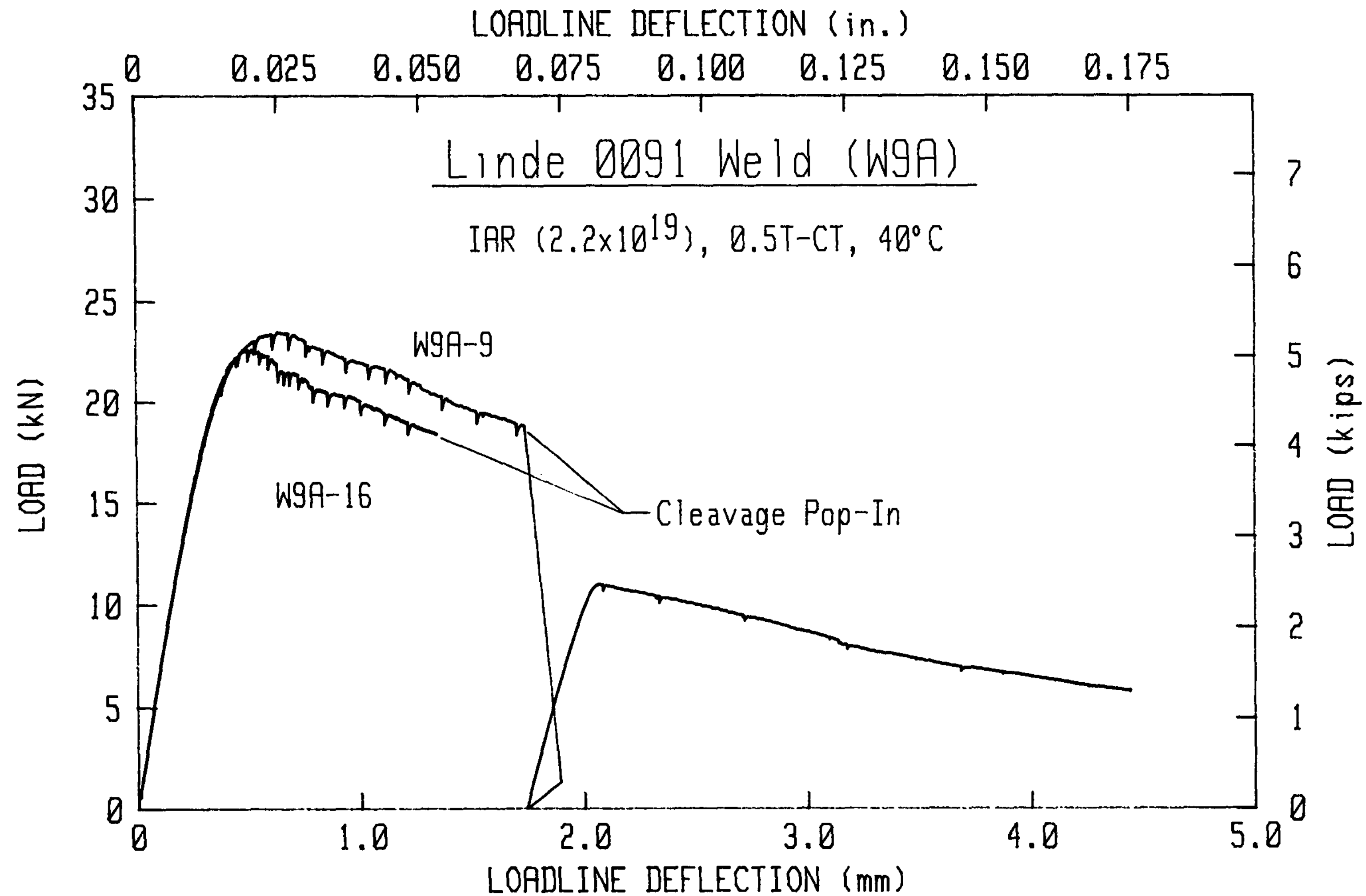

Fig. 73 For the IAR condition (2.2 x 10^{19} n/cm^2) of Linde 0091 weld (W9A), two tests at 40°C exhibited cleavage pop-ins, as illustrated in Fig. 72.

Comparisons of J-R curves for each condition at the same temperature (Figs. 74 to 76) demonstrate a similar trend to that found with Weld W8A. Specifically, the unirradiated condition exhibits much higher J levels than any of the irradiated conditions. In fact, all three of the irradiation conditions exhibit similar J levels, although the lowest fluence I condition and the IAR condition exhibit somewhat higher J levels than the highest fluence I condition. At 75°C (167°F), the test from UBR-48A exhibits ~2 mm of stable tearing which is interrupted by cleavage fracture.

Comparisons of T_{avg} with temperature for each weld confirm the high toughness of the unirradiated condition as opposed to the irradiated conditions (Figs. 77 and 78). As illustrated, the IAR conditions exhibit similar levels to those for the lowest fluence I condition. One cautionary note concerning the use of T_{avg} is the strong dependence of this quantity on the material flow strength. As indicated in Eq. 7, the flow strength is included as a squared term in the formula for T_{avg}. As well, the flow strength enters the calculation of T_{avg} by changing the Δa range over which T_{avg} is evaluated, by changing the placement (actually the slope) of the exclusion lines. Since one consequence of irradiation is an increase in flow strength, then, assuming the same J-R curve data, the exclusion line modification would tend to elevate T_{avg} (since a steeper portion of the J-R curve would be used), whereas the term in Eq. 7 would give a large reduction in T_{avg}. In general, combining the two effects tends to give large reductions in T_{avg}. As an example, for each weld at 288°C the largest flow strength increase results in a 40% reduction in T_{avg} due to Eq. 7. Therefore, a portion of the reductions illustrated for each weld are simply due to the flow strength increases after irradiation.

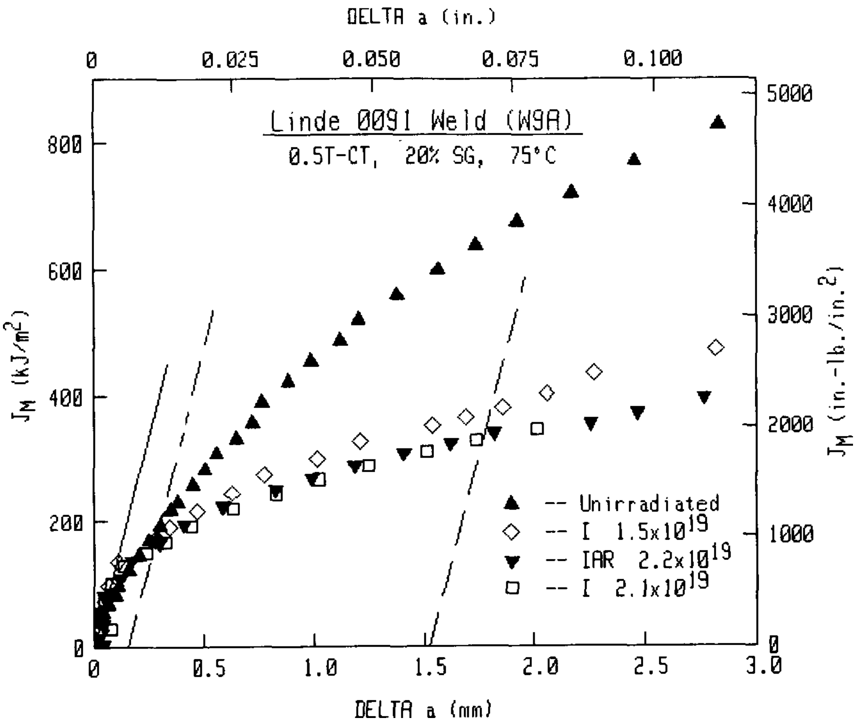

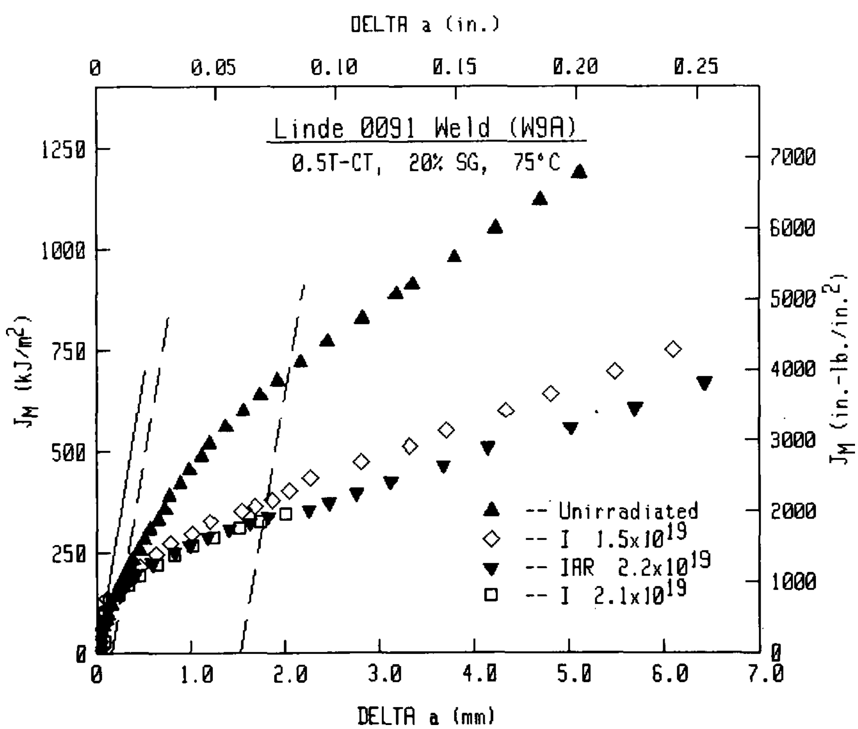

Fig. 74 **Comparison of the J_M-R curves for the Linde 0091 weld (W9A) at 75°C.**

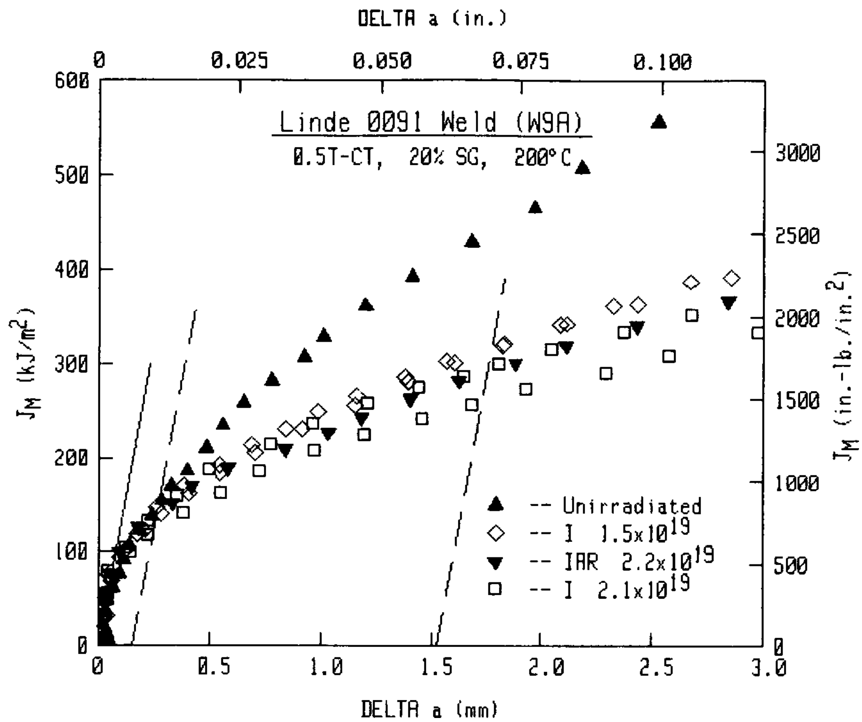

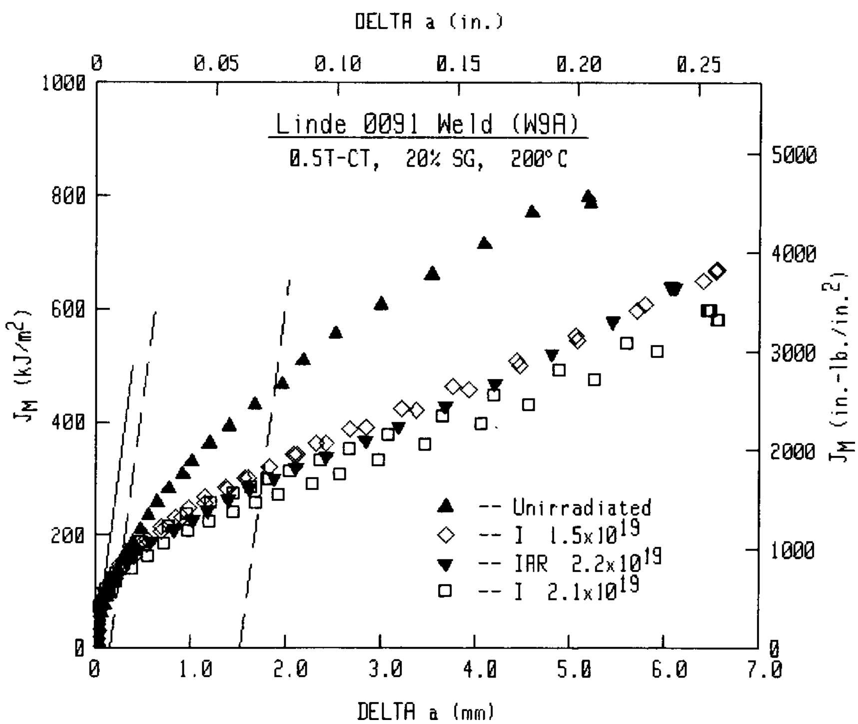

Fig. 75 Comparison of the J_M-R curves for the Linde 0091 weld (W9A) at 200°C.

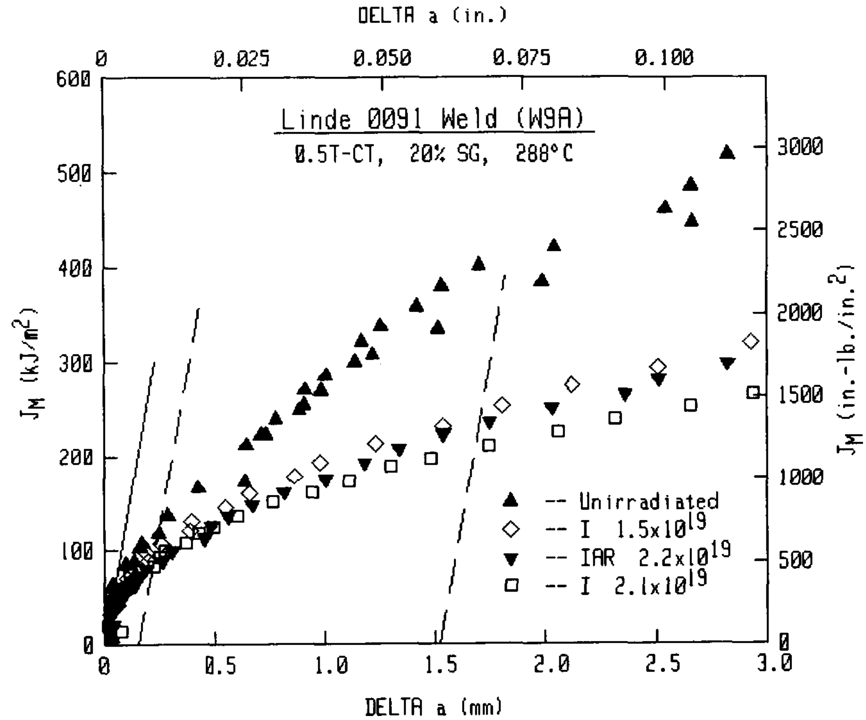

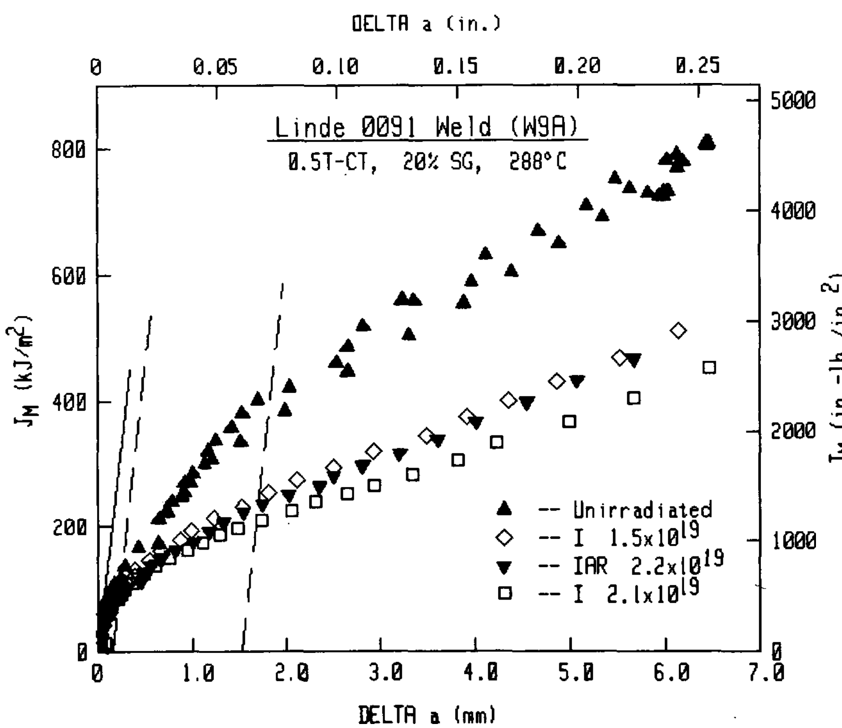

Fig. 76 Comparison of the J_M-R curves for the Linde 0091 weld (W9A) at 288 °C.

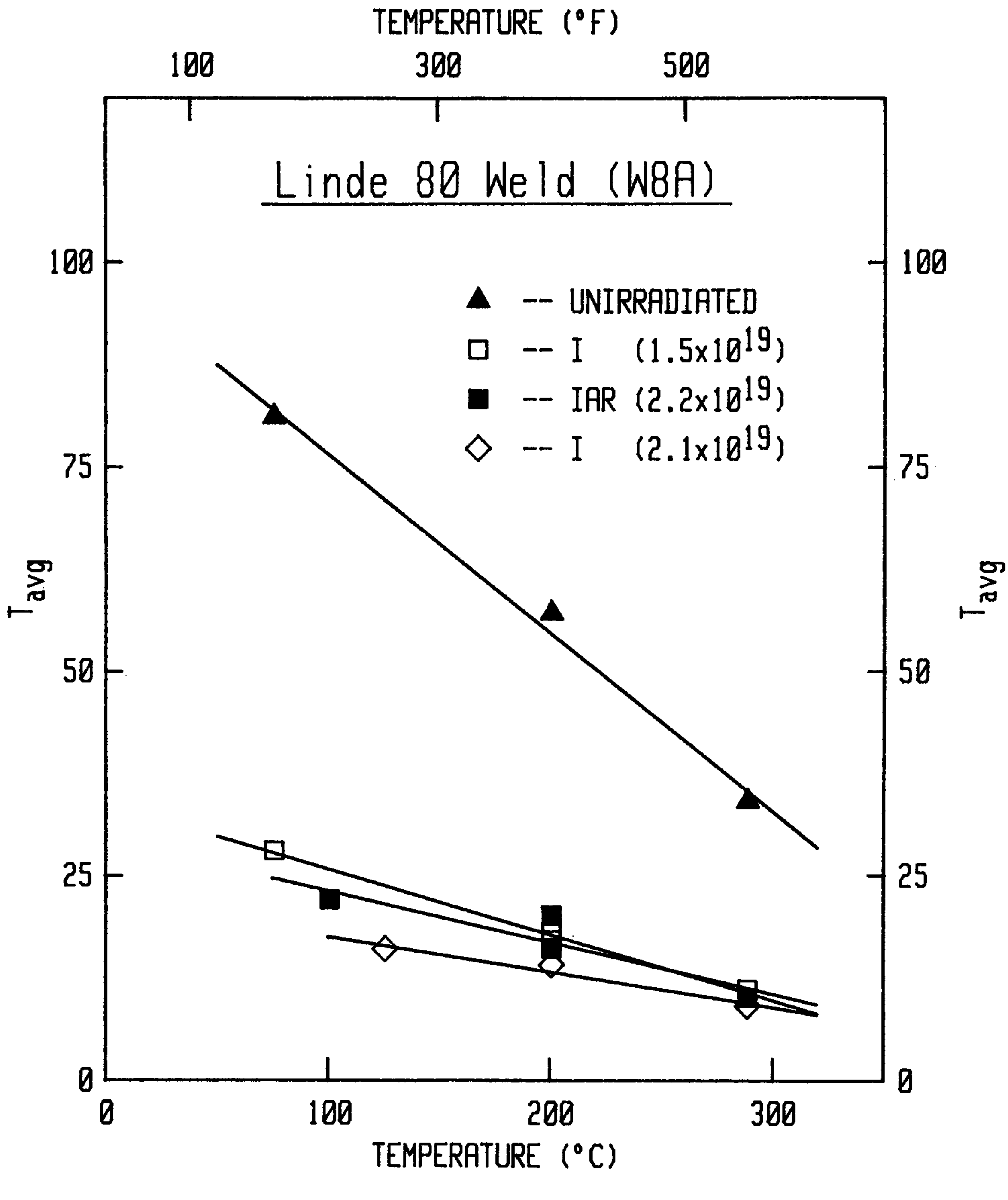

Fig. 77 Comparison of T_{avg} data for the Linde 80 weld (W8A). Substantial reductions in this quantity are apparent for all of the irradiated conditions. All conditions indicate indicate reductions in T_{avg} as the test temperature increases.

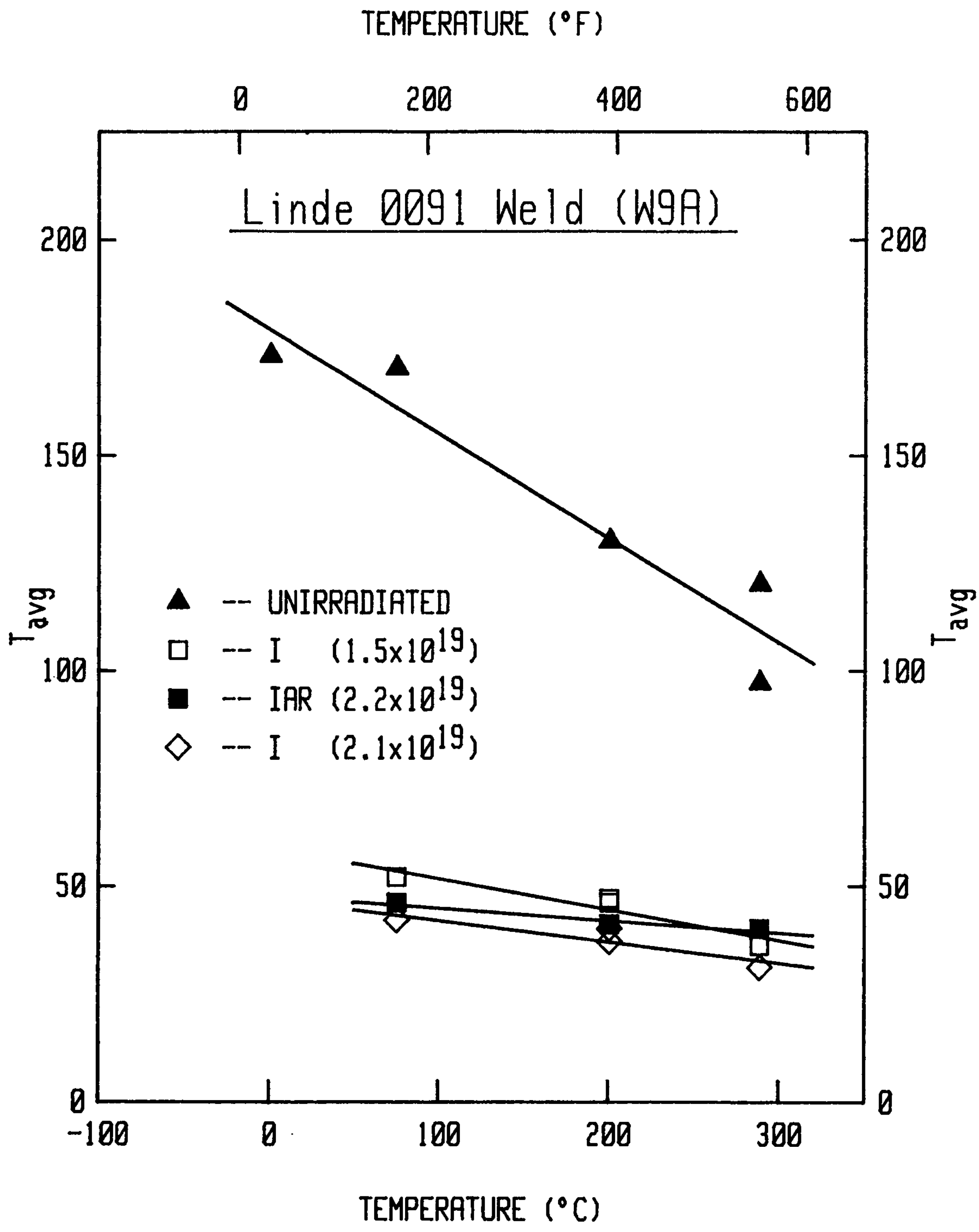

Fig. 78 Comparison of T_{avg} data for the Linde 0091 weld (W9A). Substantial reductions in this quantity are apparent for all of the irradiated conditions. All conditions indicate indicate reductions in T_{avg} as the test temperature increases.

8. DISCUSSION

Certain dissimilarities in the radiation embrittlement trends and reirradiation susceptibilities of the Weld W8A and Weld W9A have been pointed out in the data presentations above. Specimens of the welds, were commingled in each irradiation assembly to enable 1:1 comparisons of properties behavior. The two welds were made with identical welding materials except for welding flux type, and with essentially identical welding parameters. Accordingly, the dissimilarities can be related to welding flux differences and in particular, the difference in as-deposited weld compositions resulting from their use.

The role of composition in properties recovery by post irradiation annealing and reirradiation embrittlement trends is just beginning to be understood. Recent studies have shown that copper but not phosphorus has an influence on the residual embrittlement after a 399°C-168 hour anneal (Ref. 25). An influence of copper content on sensitivity to reirradition embrittlement 288°C is suspected (Ref. 11), but has not yet been confirmed by systematic materials evaluations. It is possible that the effectiveness of copper in influencing annealing recovery and reirradiation embrittlement sensitivity is a function of the amount of alloying present. A dependency of the 288°C radiation sensitivity of RPV steel plates on their Cu:Mn, Cu:Mo and Cu:Ni ratio, as well as their copper content has been shown experimentally (Ref. 26). In turn, an influence of such ratios on properties recovery and reirradiation behavior becomes suspect.

The present results contribute significantly to the growing body of evidence in favor of IAR procedures for properties maintenance in pressure vessels, if needed. The procedure has, in fact, been applied successfully to the Belgian BR3 reactor vessel and several power reactor vessels in the USSR. Because of certain factors such as vessel operating temperatures or steel types involved, these examples are not ideal examples of the potential benefits of IAR for USA commercial reactor vessels. However, it is becoming evident from the recent experiences that annealing heat treatments do not necessarily involve unacceptably-long reactor outages with attendant costs.

The agreement in properties trend directions found in tensile vs. C_v test determinations is encouraging. In general, the fracture toughness results are consistent with those from C_v tests. The radiation-induced shift in the C_v curve at 41 J (30 ft-lb) tends to exceed somewhat that found with K_{Jc} at the 100 MPa$\sqrt{m}$ level (Table 14). The exceptions to this were observed with weld W9A in the IAR condition and the highest fluence I-condition. Here the C_v shifts were within 10°C (18°F) of the shift in K_{Jc}. The results are consistent with those found for other weld metals (Ref. 27), where the shift in C_v 41-J temperature tends to exceed the shift in the 100 MPa$\sqrt{m}$ K_{Jc} temperature. In the present case, K_{Jc} data scatter is large in some instances. The measured shifts and upper shelf decreases indicated by the fracture toughness data are similar in magnitude for the two welds, indicating little or no composition dependence.

Table 14 Comparison of Transition Temperature Shifts (ΔT) from C_v and K_{Jc}

Code	Condition[a]	Fluence[b]	Temperature at 41 J (°C)	Temperature at 100 MPa$\sqrt{m}$ (°C)	Temperature Shifts at 41 J (°C)	Temperature Shifts at 100 MPa$\sqrt{m}$ (°C)
W8A	U	----/---	-23	-58	---	---
	I	1.34/1.5	96	22	119	80
	I	2.03/2.1	116	61	139	119
	IAR	2.19/2.2	99	43	122	101
W9A	U	----/---	-62	-84	---	---
	I	1.34/1.5	32	-6	94	78
	I	2.03/2.1	44	27	106	111
	IAR	2.19/2.2	27	15	89	99

[a] U = Unirradiated
I = Irradiated
IAR = Irradiated-Annealed-Reirradiated

[b] 10^{19} n/cm^2 ($E > 1$ MeV), with C_v/K_{Jc}.

In view of the generally good agreement between the C_v and the fracture toughness test data for a given weld, additional IAR work with fracture toughness specimen experiments would not appear necessary to completely define weld metal property trends. That is, C_v testing may be sufficient for characterizing overall trends of IAR. The development of fracture toughness data at key points in IAR matrices would suffice to guard against technical surprises.

9. CONCLUSIONS

This study employed two submerged arc weld deposits made with Linde 80 or Linde 0091 welding fluxes and a common lot of copper-coated weld filler wire. C_v notch ductility, yield and tensile strength, and fracture toughness property changes were investigated for 288°C irradiated, 399°C-168 hour postirradiation annealed and 288°C reirradiated conditions. Primary observations and conclusions from this study <u>for the conditions investigated</u> are as follows:

- The C_v data indicate a relatively rapid reembrittlement of both weld types with fluence immediately following annealing. A fluence of only ~0.3 x 10^{19} n/cm^2 reduced a large portion of the annealing benefit following a first cycle fluence of 1.3 x 10^{19} n/cm^2.

- In spite of the propensity toward an initially-rapid reembrittlement following the anneal, the benefit of IAR procedures to notch ductility is significant when indexed to property changes produced by irradiation without intermediate annealing.

- A strong tendency toward radiation embrittlement saturation by IAR treated material was exhibited by one of the two welds investigated (Linde 80 Weld W8A). The 41-J transition temperature elevation for the second weld (Linde 0091) with IAR was less than that produced by the first cycle fluence, even with a doubling of the fluence exposure in one test series.

- Welding flux type (Linde 80 vs. Linde 0091) or the as-deposited weld composition difference reflecting these types, appear to influence radiation embrittlement sensitivity and reirradiation embrittlement sensitivity. An influence of welding flux type on notch ductility recovery was observed but appeared to be dependent on the prior fluence level.

- Yield strength and tensile strength changes with irradiation, annealing and reirradiation describe trends mirroring those trends shown by C_v notch ductility changes.

- Residual embrittlement after annealing, as measured by the C_v test, appeared to be independent of the pre-anneal condition (I or IAR) for those cases examined. However, weld-to-weld comparisons indicate wide variability in percentage recovery produced by 399°C-168 hour annealing.

- For the welds investigated, a 454°C-168 hour anneal was much more effective than a 399°C anneal toward 41-J transition temperature recovery. Cases of incomplete recovery were found with the higher temperature anneal.

- The transition temperature shift described by the C_v data in most cases exceeds that described by the fracture toughness data.

- In general, the fracture toughness trends with I-, IA- and IAR-treatments are similar to those found in C_v testing.

REFERENCES

1. T. Griesbach, "Pressure-Temperature Limits for Pressure Vessels," The Electric Power Research Institute Journal, July/August, 1988, pp. 40-43.

2. "Fracture Toughness Requirements for Light-Water Nuclear Power Reactors," Appendix G, Federal Register, Rules and Regulations, Vol. 48 (104), May 27, 1983, pp. 24008-24011.

3. U. Potapovs, G. W. Knighton and A. S. Denton, "Critique of In-Place Annealing of SM-1A Nuclear Reactor Vessel," American Society of Mechanical Engineers, Report 67-WA/ER-3, November 1967; also, Nuclear Engineering and Design, Volume 8, 1968, pp. 39-57.

4. J. R. Hawthorne, "Survey of Postirradiation Heat Treatment as a Means to Mitigate Radiation Embrittlement of Reactor Vessel Steels," Proc. IAEA Specialists' Meeting on Analysis of Behavior of Advanced Reactor Pressure Vessel Steels Under Neutron Irradiation, Vienna, Austria, 1-2 March 1979; also, Naval Research Laboratory Report 8287, 14 February 1979.

5. J. R. Hawthorne, H. E. Watson and F. J. Loss, "Experimental Investigation of Multicycle Irradiation and Annealing Effects on Notch Ductility of A 533-B Weld Deposits," Effects of Radiation on Materials: Tenth Conference, ASTM STP 725, American Society for Testing and Materials, 1981, pp. 63-75.

6. F. J. Loss, B. H. Menke, R. A. Gray, Jr., J. R. Hawthorne and H. E. Watson, "J-R Curve Characterization of A 533-B Weld Metal with Irradiation and Postirradiation Annealing," Effects of Radiation on Materials: Tenth Conference, ASTM STP 725, American Society for Testing and Materials, 1981, pp. 76-91.

7. J. R. Hawthorne, J. J. Koziol and S. T. Byrne, "Evaluation of Commercial Production A 533-B Steel Plates and Weld Deposits with Extra-Low Copper Content for Radiation Resistance," Effects of Radiation on Structural Materials, ASTM STP 683, American Society for Testing and Materials, 1979, pp. 235-251.

8. E. P. Lippincott, "Buffalo Light Water Reactor Calculation," Letter Communication Serial No. 7754977, Hanford Engineering Development Laboratory, Richland, WA, to J. R. Hawthorne, dated November 16, 1977.

9. E. P. Lippincott, L. S. Kellogg, W. N. McElroy, and C. A. Baldwin, "Evaluation of Neutron Exposure Conditions for the Buffalo Reactor," Proceedings of the Fifth International ASTM-Euratom Symposium, Geesthacht, Federal Republic of Germany, September 24-28, 1984.

10. G. Prillinger, E. D. McGarry, and J. R. Hawthorne, "Neutron Spectra Calculations for Ex-Core Irradiation Experiments at the Buffalo Reactor," presented at the ASTM Fourteenth International Symposium on Effects of Radiation on Material, Andover, MA, June 1988.

11. J. R. Hawthorne, "Irradiation-Anneal-Reirradiation (IAR) Studies of Prototypic Reactor Vessel Weldments: Final Report," USNRC Report NUREG/CR-5469, November 1989.

12. J. R. Hawthorne, "Exploratory Assessment of Postirradiation Heat Treatment Variables in Notch Ductility Recovery of A 533-B Steel," USNRC Report NUREG/CR-3229, April 1983.

13. ASTM E 813-81, "Standard Test for J_{Ic}, A Measure of Fracture Toughness," ASTM Book of Standards, Part 10, 1981, pp. 810-828.

14. ASTM E 399-81, "Standard Method for Plane-Strain Fracture Toughness of Metallic Materials," ASTM Book of Standards, Part 10, 1981, p. 589.

15. F. J. Loss, B. H. Menke and R. A. Gray, "Development of J-R Curve Procedures," in The NRL-EPRI Research Program (RP886-2), Evaluation and Prediction of Neutron Embrittlement in Reactor Pressure Vessel Materials: Annual Report for CY 1978, Naval Research Laboratory, Report 8327, Aug. 30, 1979, pp. 30-57.

16. F. J. Loss, et al., "J-R Curve Characterization of Irradiated and Annealed Weld Deposits," in Structural Integrity of Water Reactor Pressure Boundary Components, Annual Report, FY 1979, USNRC Report NUREG/CR-1128, Dec. 31, 1979, pp. 4-36.

17. A. L. Hiser, F. J. Loss and B. H. Menke, "J-R Curve Characterization of Irradiated Low Upper Shelf Welds," USNRC Report NUREG/CR-3506, April 1984.

18. G. A. Clarke and J. D. Landes, "Evaluation of J for the Compact Specimen," Journal of Testing and Evaluation, Vol. 7(5), Sept. 1979, pp. 264-269.

19. G. R. Irwin, "Fracture Mode Transition for a Crack Traversing a Plate," J. of Basic Eng., ASME, Vol. 82(2), 1960, pp. 417-425.

20. J. G. Merkle, "An Examination of the Size Effect and Data Scatter Observed in Small-Specimen Cleavage Fracture Toughness Testing," ORNL/TM-9800, USNRC Report NUREG/CR-3672, April 1984.

21. ASTM E 1152-87, "Standard Test Method for Determining J-R Curves," Annual Book of ASTM Standards, Volume 03.01, 1989, pp. 814-824.

22. H. A. Ernst, "Material Resistance and Instability Beyond J-Controlled Crack Growth," Elastic-Plastic Fracture, ASTM STP 803 Vol. 1, American Society for Testing and Materials, 1983, pp. 191-213.

23. P. C. Paris, H. Tada, A. Zahoor, and H. Ernst, "The Theory of Instability of the Tearing Mode of Elastic-Plastic Crack Growth," Elastic-Plastic Fracture, ASTM STP 668, American Society for Testing and Materials, March 1979, pp. 5-36.

24. J. R. Hawthorne, et al., "Evaluation and Prediction of Neutron Embrittlement in Reactor Pressure Vessel Materials," EPRI NP-2782, The Electric Power Research Institute, Dec. 1982.

25. J. R. Hawthorne, "Steel Impurity Element Effects on Post-irradiation Properties Recovery by Annealing: Final Report," USNRC Report NUREG/CR-5388, August 1989.

26. J. R. Hawthorne, "An Exploratory Study of Element Interactions and Composition Dependencies in Radiation Sensitivity Development: Final Report," USNRC Report NUREG/CR-5357, April 1989.

27. A. L. Hiser, "Correlation of C_v and K_{Ic}/K_{Jc} Transition Temperature Increases Due to Irradiation," USNRC Report NUREG/CR-4395, November 1985.

APPENDIX A

Fabrication of Weldments: Materials and Procedures

Fabrication of Weldments W8A and W9A

1. General

The weldments were produced commercially by Lukens Steel Company under contract. The welds were made using buyer-supplied 210-mm (8.25-in.) thick A 533 Grade B Class 1 plate and contractor-supplied welding fluxes and filler wire. The filler wire was copper-coated by other subcontractors to the buyer (see Section 4, below). The purchase specifications for the plate are given in Attachment 1; the mill test report is given as Attachment 2. The purchase specifications for the set of Linde 80 welds which included Weld W8A are given in Attachment 3; the same specifications except for welding flux type were used for the Linde 0091 Weld, W9A.

The same lot of weld filler wire was used for both welds. The wire was made from Steel Melt 3P8393. The filler wire composition before copper coating as determined by Airco Welding Products is given in Attachment 4. The weld joint design is shown in Figure A-1.

2. Fabrication of Weld W8A

The Lukens Steel Company report documenting fabrication details for Weld W8A is given as Attachment 5. No particular problems were encountered in the production of this weld.

The post welding stress relief anneal (SRA) of 621°C (1150°F) for 24 hours was performed by the buyer after weld receipt, using a recirculating air furnace. Workpiece temperatures were monitored using chromel-alumel thermocouples attached to the weldment at several locations. Cooling rates after the SRA were less than 56°C (100°F) hour.

3. Fabrication of Weld W9A

The Lukens Steel Company report documenting fabrication details for Weld W9A is given as Attachment 6. No particular problems were encountered in the production of this weld.

The post welding SRA of 621°C (1150°F) for 24 hours was performed by the buyer after weld receipt using the same furnace and procedures employed for Weld W8A (above).

4. Special Note on Copper Coating of Filler Wire

Copper-coated Hi Mn-Mo-Ni filler wire was no longer available at the time this project commenced. The acquisition of wire that was prototypic of the copper-coated wire used in early vessel construction proved very difficult and time-consuming.

The first subcontractor, Airco Welding Products, resurrected equipment from storage and after considerable effort, was only able to provide one-half of the total wire lot in an acceptable coated condition. The remainder of the wire lot either did not have the required coating thickness or had a poorly adherent coating which easily flaked off in the welder wire feed apparatus.

The second subcontractor, Techalloy Maryland, Inc. reprocessed the remainder of the wire successfully but with difficulties stemming from two sources. One difficulty was the attainment of sufficient coating thickness determination of "as-deposited" copper content without production of an actual weld. Trial weld pads provided inconsistent copper content results; the production of "button melts" for spectrographic determinations gave highly misleading results. In the case of the latter, it was subsequently determined that the cross sections of the melts were highly inhomogeneous with regard to copper content. Ultimately, the problem of copper content determinations for the clad wire was solved by resorting to wet chemistry determinations. Each coil produced was checked at the start-end and at the finish-end. Because of the extreme difficulties encountered in the production of copper-clad wire yielding uniform as-deposited copper contents in the range of 0.30% Cu or higher, it is recommended for any future efforts of this type, that close attention be given to <u>all</u> details in the production of such wire and its usage.

Attachment No. 1

BASE PLATE PURCHASE SPECIFICATIONS

1. Melt/Chemical Composition

Lukens Steel Company Melt No. D-2819 representing electric furnace, vacuum degassed melting practice will be the source melt for the ASTM A 533 Grade B plates. The copper content will be in the range of 0.20% to 0.26% Cu; the nickel content will be in the range of 0.60% to 0.65% Ni.

2. Dimensions of Plate Sections

Thickness: 210-mm (8.25-in.)
Width: 406-mm (16-in.)
Length: 1829-mm (72-in.)[a]

[a] Length direction to be parallel to primary plate rolling direction.

3. Heat Treatment

The as-rolled plate will be heat treated by water quenching and tempering using Lukens procedures for A 533-B Class 1 plate. For the austenitizing treatment and the tempering treatment, the plate will be held at temperature for a minimum of 0.5 hour per inch of thickness.

4. Mechanical Property Tests

Tensile tests will be conducted to verify A 533-B Class 1 strength properties. A drop weight NDT temperature of -1°C (30°F) will be guaranteed.

5. Non-destructive Tests

Ultrasonic examinations will be conducted to determine if the plate is sonically sound and in compliance with ASME Paragraph NB 2532-1.

6. Stress Relief Anneal

Test specimens (only) will be stress relief annealed for 40 hours at 621°C (1150°F) ± 14°C (25°F) prior to testing.

7. Report

One (1) certified copy of reports from destructive and non-destructive test examinations and the verification of the source of the plate (melt number) is required.

Attachment No. 2

LUKENS STEEL COMPANY
COATESVILLE, PA. 19320
TEST CERTIFICATE

PURCHASER:

DATE: 6-15-79 FILE NO. 8195-01-01
CONSIGNEE:

MILL ORDER NO.	CUSTOMER P.O.	
66743 1	10-20-78	MP 61179 BT 5/1

THIS MATERIAL HAS BEEN MANUFACTURED AND TESTED IN ACCORDANCE WITH PURCHASE ORDER REQUIREMENTS AND SPECIFICATION(S).

A-533-76 CL.1 TYPE-B

BEND TEST HOMOGENEITY TEST

CHEMICAL ANALYSIS

MELT NO.	C	MN	P	S	CU	SI	NI	CR	MO	V	TI	XXX	XXX		BASIC PROCESS
D2819	.22	1.40	.010	.008	.20	.19	.63		.54			VIP	STEEL		ELEC.

A-4

PHYSICAL PROPERTIES

MELT NO.	SLAB. NO.	YIELD PSI X100	TENSILE PSI X100	% ELONG. IN 2"	% R.A.	BHN	IMPACTS				DESCRIPTION
D2819	6	701 782	940 970	24 22							8-1/4" X 12 X 18

LONG. DROP WEIGHT TESTS PER E208(SIZE P3) @ +30°F. EXHIBIT NO BREAK.
N.D.T. IS +20°F. OR BELOW.

PLATE AND TESTS HEATED 1625°F./1675°F. HELD 1/2 HR. PER INCH MIN. AND WATER QUENCHED, THEN TEMPERED 1220°F. HELD 1/2 HR. PER INCH MIN. AND WATER QUENCHED.

TESTS STRESS RELIEVED BY HEATING TO 1100°F./1175°F. HELD 40 HRS. AND FURNACE COOLED TO 600°F.

We hereby certify the above information is correct.

SUPERVISOR TESTING H. W. Kline

Attachment No. 3

WELDMENT PURCHASE SPECIFICATIONS

1. Submerged Arc Weld Using Linde 80 Welding Flux

Electrode diameter	:	3.18-mm (1/8-in.)
Welding flux type	:	Linde 80 (20x200, Baked) (one lot only)
Welding process	:	Submerged arc using single electrode
Filler type	:	High Mn-Mo-Ni (one melt only)
Electrode connection	:	AC
Welding voltage	:	30-35V, AC
Welding current	:	500-575A
Travel speed	:	254-305 mmpm (10-12 ipm)
Heat input	:	80 Kilojoules/in. (minimum) 95 Kilojoules/in. (maximum)
Weld joint	:	Offset double vee, 134-mm 5.25-in.) deep from one side and with 5 deg. bevel and 25.4-mm (1-in) minimum gap by mild steel spacer. Spacer to be back gouged and refilled with weld metal.
Weld joint gap	:	25.4-mm (1-in.) minimum
Weld configuration	:	Full thickness weld; weld crowns will not be removed by contractor.
Preheat temperature	:	121°C (250°F) minimum, 205°C (400°F) maximum, 149°C (300°F) aim
Interpass temperature	:	121°C (250°F) minimum, 260°C (500°F) maximum
Restraint	:	Full
Postweld stress relief	:	538°C (1000°F) maximum for 4 h, followed by slow cooling
Inspection	:	Radiograph to acceptance standards of ASME Section III (NB 5320).

Weld deposit composition (wt-%) :

Element	Minimum	Maximum	Aim
Copper	0.31	0.39	0.35
Nickel	0.60	0.80	0.70

Filler wire composition (wt-%) :

Element	Minimum	Maximum
Carbon	0.14	0.19
Manganese	1.80	2.10
Phosphorus	-	0.010
Sulfur	-	0.015
Silicon	-	0.10
Nickel	0.60	0.85
Molybdenum	0.45	0.60

Repairs : None allowed

Documentation and report : Bead-by-bead record of welding conditions and materials will be furnished together with full descriptions of filler/flux qualifications.

Attachment No. 4

Composition of Filler Wire for Fabricating Weld W8A and Weld W9A

(Before Copper Coating; Steel Melt 3P8393)

Element	Content (wt-%)[a]
Carbon	0.135
Manganese	1.98
Phosphorus	0.007
Sulfur	0.011
Silicon	0.053
Nickel	0.602
Chromium	0.110
Molybdenum	0.488
Tungsten	0.012
Niobium	0.000[b]
Vanadium	0.000[b]
Copper	0.044
Cobalt	0.013
Aluminum	0.007
Titanium	0.002
Zirconium	0.004
Tantalum	0.004
Tin	0.004
Boron	0.0009

----

[a] Determinations by Airco Welding products (1981).
[b] Content below detection limit.

Attachment No. 5

Submerged-Arc Weld in 8-1/4" Gage,
A533 Grade B Class 1 Plate

Item 1 - Base Plates #1 and #2

CONTRACT NO. N00173-79-C-0218

LUKENS STEEL COMPANY
Research Service Group
Coatesville, PA 19320
March, 1982

INDEX	Page

Materials

Buyer furnished the following base materials and wire for completion of the contract:

(A) 12 pieces - A533-B Class 1
Approximately 8-1/4" x 15" x 72" with machined bevel on one edge. Problems occurred with the spacer-bar procedure, therefore the bevels were remachined at Lukens to an unbalanced double J preparation. This will be performed on each piece.

Pieces are numbered consecutively, #1 through #12 and each pair will follow in sequence regardless of type of flux employed.

(B) 1/8" dia. copper-coated High Mn-Mo-Ni wire -
Approximately 3000 lbs. all from one heat. Since attempts by Techalloy Raco to rewind the wire from the wooden spools to 12" dia. - 60 lb. coils resulted in flaking-off of the copper-coating, a holder for the wooden spools was improvised. Some flaking of copper was also noted on the spooled wire.

(C) Linde 80 and Linde 0091 fluxes will be used in the six weldments, three welds with each flux.

There were 3000 lbs. of each purchased by Lukens Steel Co. and each type was from the same lot and control. All fluxes were baked in pans at 800°F., held 1 hour, furnace-cooled to 300°F., then air-cooled to ambient temperature to minimize moisture content.

The Certificate of Acceptance Inspection forms are presented on the next two pages.

LINDE DIVISION

P.O. Box 747, Niagara Falls, New York 14302

CERTIFICATE OF ACCEPTANCE INSPECTION

Shipped to: Lukens Steel Company
Central Stores
Coatesville, PA 19320

Shipper's No.: 024552 A
Quantity Shipped: 3,000 Lbs.
Date Shipped: 6/16/81

Your Order No.: 4543-P

REPORT OF TESTS OF GRADE 80 UNIONMELT WELDING COMPOSITION

Identification of Material Tested - Grade 80, Size 20x200,

Lot 0418, Control 8556.

This certifies that the Welding Composition identified above has been tested for conforming to specifications as follows:

Sizing:	20 Mesh		Minus 200 Mesh
	1.7%		0.4%
	5.0%		3.5%
Uniformity:	SiO_2	CaO	Al_2O_3
	37.85%	20.96%	15.47%
	32.4-39.6%	19.8-24.2%	12.4-18.6%

Lower line gives specification limits - single values are maximum.

State of New York
County of Niagara

Sworn to before me this

17 day of June, 19 81

Deborah L. Cooke

DEBORAH L. COOKE
Notary Public, State of New York
Qualified in Niagara County
My Commission Expires March 30, 1983

[signature]
Consumables Quality - Electric Welding

UNION CARBIDE CORPORATION
LINDE DIVISION

P.O. Box 747, Niagara Falls, New York 14302

CERTIFICATE OF ACCEPTANCE INSPECTION

Shipped to: Lukens Steel Company
Central Stores -
Coatesville, PA 19320

Shipper's No.: 024552 A
Quantity Shipped: 3,000 Lbs.
Date Shipped: 6/16/81

Your Order No.: 4543-P

REPORT OF TESTS OF GRADE 0091 UNIONMELT WELDING COMPOSITION

Identification of Material Tested - Grade 0091, Size 65x200,

Lot 0204, Control 3756.

This certifies that the Welding Composition identified above has been tested for conforming to specifications as follows:

Sizing:	32 Mesh	48 Mesh	Minus 200 Mesh
	0.4% / 5%	24.2% / 40%	15.0% / 10-20%
Uniformity:	SiO_2	CaO	
	38.01% / 34-40%	44.40% / 43-49%	

Lower line gives specification limits - single values are maximum.

State of New York
County of Niagara

Sworn to before me this

17 day of June, 19 81

Consumables Quality - Electric Welding

DEBORAH L. COOKE
Notary Public, State of New York
Qualified in Niagara County
My Commission Expires March 30, 19 83

Preparation for Welding

Base plates were grit-blasted prior to re-machining of the bevels. The pair of base plates to be used in each weldment were aligned on edge so the 1/2" lands would be aligned, making the fit-up of each weldment simpler and at the same time compensating for the slight out-of-flatness of the plates.

Two lifting lugs were welded to the long edge (72" dimension) of one plate of the pair to facilitate the turning-over of the weldment several times during the fabrication of the test.

Since the lugs were always kept at the back side of the test, the start end and finish end of the passes were reversed with each turn.

The start end and finish end, however, were standardized for orientation purposes as being those on the face side.

Run-out tabs were welded at start end and finish end on the deepest side (face side), six (6) passes deposited, then the weldment turned over, moved to cutting table, arc-air'd from root side to sound metal and ground, then set-up and aligned on welding table (root side up), and at this point the run-outs were welded at both ends of the weld test on the root side.

A 1/2" thick carbon steel plate was employed in the run-outs as an extension of the 1/2" land. Upon arc-airing of the root side, only a small distance (1/2" to 1") was arc-aired in the 1/2" plate. This was reflected in the junction chemical analysis for copper and nickel in the run-outs due to dilution with the mild steel.

Welding Procedure

Item 1 - Base Plates 1 & 2 Linde 80 (Baked)

Preheat 300°F. - Interpass 325°F. - Heat Input 85,000 Joules/Inch

Pass #	(AC) Amps	Volts	Speed(ipm)	Start Copper and Spool No.		Wire Consumed (lbs.)
1	500	33	16	.39	14	
2	500	33	11			
3 to 6	500	34	12			
	Turn - Arc-Air 1/2" deep - Grind					
7	500	34	16			
8	500	34	14			
9 to 14	500	34	12			
	Turn					
15 to 22	500	34	12			
	Turn					
23 to 33	500	34	12	.33	13	(thru pass #27) 53
	Turn					
34 to 66	500	34	12	.44 .42	15 chk. 15	(thru pass #62) 63
	Turn					
67 to 101	500	34	12	.37 .33	end 15 16	(thru pass #99) 64
102	500	34	16			
	Turn					
103 to 140	500	34	12	.35	17	(thru pass #135) 65 (thru pass #140) 8
					Total =	253 Lbs.

1 Defect - Face side, pass #138, lack of fusion with bevel, 2-1/4" from start end - 7/8" long, approximately 1/8" deep.

Base Plates 1 and 2 .

Item 1

Spool or Coil 14, 13, 15, 16, 17

Flux Linde 80

Wire Consumed 253 lbs.

Ht. Input 85,000

Sfe.

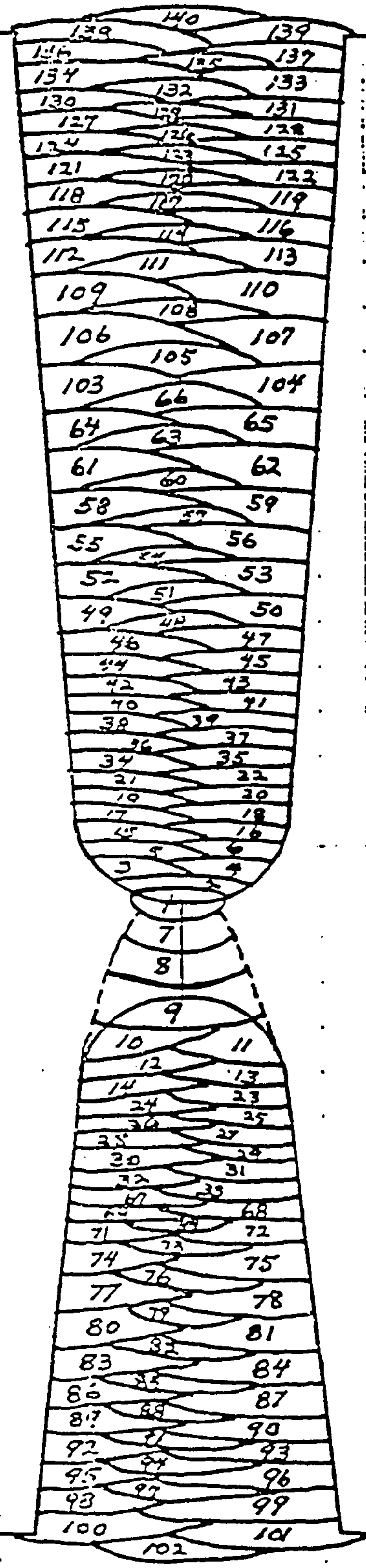

Location		Cu	Ni	Cu	Ni	Location
Start Run-out	* 1	.43	.69	.39	.66	Finish Run-ou
	* 2	.40	.66	.43	.74	
1/4L	* 3	.43	.69	.43	.66	
	* 4	.40	.66	.41	.68	
CL	* 5	.43	.68	.40	.60	
Junction	* 6	.41	.56	.36	.49	
1/4L	* 7	.43	.68	.45	.70	
	* 8	.43	.68	.44	.69	
Root Side	* 9	.40	.65	.40	.65	

Start Date 1/26/82

Finish Date 2/10/82

Post-Weld Heating

Upon completion of the welding, the weldment was draped with asbestos blankets and maintained at 375°F. for 24 hours. The heat was then turned off and the asbestos blanket was kept on the surface of the weldment which slowly cooled to ambient temperature (approx. 70°F.).

Run-Outs

Both start end and finish end (based on face side) run-outs were band-saw cut off and identified by stamping as follows: start, surface, root, and base plate numbers.

A 1/2" thick x 1-1/4" wide x full weld thickness section was saw-cut and ground in preparation for spectrographic checks of nickel and copper throughout the total weld metal, surface to surface, adjacent to the main weld.

The results of these analyses are contained in the bead-by-bead record.

The remainder of each identified run-out was sent to the attention of Mr. R. Hawthorne.

Preparation for Radiography

The two lifting lugs were removed by flame-cutting and the weldment was shipped to the Birdsboro Corporation for radiography per ASME Section V, Article 2, NB5000.

Upon completion, the films were sent to Lukens Steel Company for evaluation and interpretation by the Inspection personnel.

The weldment was held at Birdsboro until the evaluation of the films was determined to be of satisfactory quality. The weldment was then shipped

The reinforcement varied from essentially none to 1/8" maximum on both the face and root sides.

Film Interpretation

The films were interpreted by Level II personnel. The non-fused area at the top surface (pass #138) was noted at Position V1-V2 and a small crack-like indication noted at Position V5-V6. A copy of the interpretation is presented on the next page.

The films were sent to Mr. Russ Hawthorne

Form No. 332 (R10/78)

LUKENS STEEL COMPANY

RADIOGRAPHY INTERPRETATION

N00173-79-C-0218

FABRICATION	(TEST Block) Item 1 - Base Plates 1 & 2								
M.O.				CUSTOMER P.O. 16226-D					
MELT & SLAB				PC NO. 1		MK		SUB	
SURFACE	FLUSH		SMOOTH		AS WELDED		GA		
WELDING	MANUAL		AUTOMATIC		VERTAMATIC		OSCILLATOR		
SOURCE	X-RAY	✓	CO 60		IR 192		FILM KODAK AA		
SPEC			SECTION		PARA.		CLASS		
STATUS	ORIGINAL		RE RADIOGRAPH		AFTER H.T		AFTER REPAIR		AFTER RE STRESS

FILM	RATING	DENSITY 1	2	3	REMARKS
V1-V2		1.7	1.9	1.8	N.F.L.L. IND
V2-V3		1.79	1.93	1.68	
V4-V5		1.81	2.02	1.90	
V5-V6		1.82	2.10	1.97	CR. L. IND.
V3-V4		1.8	2.00	1.74	

A-18

A - ACCEPTABLE
R - REJECTED
RT - RETAKE

INTERPRETATION Earl Fitton LVII DATE 2/1

Attachment No. 6

Submerged-Arc Weld in 8-1/4" Gage A533 Grade B Class 1 Plate

Item 2 - Base Plates #5 and #6

CONTRACT NO. N00173-79-C-0218

LUKENS STEEL COMPANY
Research Service Group
June, 1982

UNION CARBIDE CORPORATION
LINDE DIVISION

P.O. Box 747, Niagara Falls, New York 14302

CERTIFICATE OF ACCEPTANCE INSPECTION

Shipped to: Lukens Steel Company
Central Stores
Coatesville, PA 19320

Shipper's No.: 024552 A
Quantity Shipped: 3,000 Lbs.
Date Shipped: 6/16/81

Your Order No.: 4543-P

REPORT OF TESTS OF GRADE 0091 UNIONMELT WELDING COMPOSITION

Identification of Material Tested - Grade 0091, Size 65x200,

Lot 0204, Control 3756.

This certifies that the Welding Composition identified above has been tested for conforming to specifications as follows:

Sizing:	32 Mesh	48 Mesh	Minus 200 Mesh
	0.4% / 5%	24.2% / 40%	15.0% / 10-20%
Uniformity:	SiO_2	CaO	
	38.01% / 34-40%	44.40% / 43-49%	

Lower line gives specification limits - single values are maximum.

State of New York
County of Niagara

Sworn to before me this

17 day of June, 19 81

[signature]

DONALD L. COOKE
... New York
... County
Commission Expires March 30, 1983

[signature]
Consumables Quality - Electric Welding

Welding Procedure

Item 2 - Base Plates 5 & 6 - Linde 0091 (Baked)

Preheat 300°F. - Interpass 325°F. - Heat Input 93,500 Joules/Inch

Pass #	(AC) Amps	Volts	Speed(ipm)	Copper	Spool #	Wire Consumed (lbs.)
1	550	34	15	.34	10	
2 to 6	550	34	12			
Turn - Arc-Air - Grind - 7/16" deep						
7	550	34	15			
8 to 26	550	34	12			
Turn						
27 to 43	550	34	12			(thru pass 43) 59
Turn						
44 to 49	550	34	12	.39	11	
Turn						
50 to 82	550	34	12			
Turn						
83 to 91	550	34	12			(thru pass 93)
92 & 93	550	34	10			69

Total Wire = 128 Lbs.

Base Plates 5 and 6.

Spool or Coil 10 & 11

Wire Consumed 128 lbs.

Sub-size Item 2

Flux 0091

Ht. Input 9350(

Sfe.

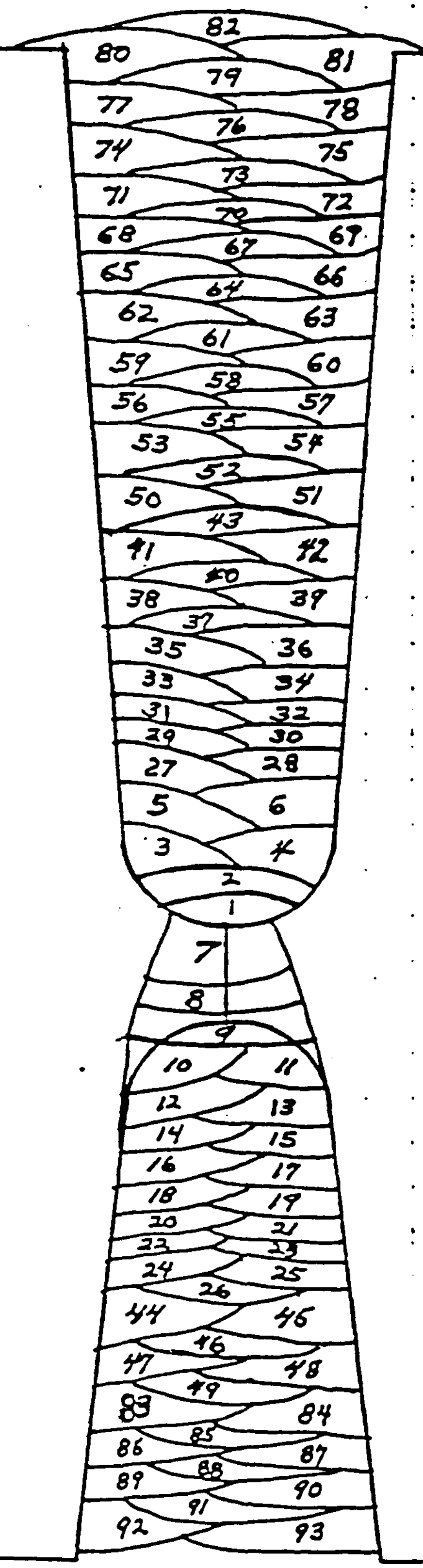

		Cu	Ni	Cu	Ni	
Start Run-out	*	.35	.60	.39	.62	Fi Ru
	*	.36	.63	.36	.62	
1/4L	*	.40	.65	.39	.62	
	*	.36	.65	.38	.63	
CL	*	.34	.58	.37	.61	
Junction	*	.28	.26	.28	.44	
1/4L	*	.39	.64	.37	.62	
	*	.37	.61	.41	.64	
Root Side	*	.40	.62	.41	.63	

Start Date 4/27/82

Finish Date 5/6/82

Form No. 332 (R10/78)

LUKENS STEEL COMPANY

RADIOGRAPHY INTERPRETATION

FABRICATION: TEST Block Item 2 - Base Plates 5 & 6

M.O. ·CUSTOMER ORDER 16226-D LUKENS - 5 - 3468 | CUSTOMER P.O. 8¼" X 32" X 38"

MELT & SLAB | PC. NO. | MK | SUB

SURFACE	FLUSH		SMOOTH		AS WELDED		GA	8¼"	
WELDING	MANUAL		AUTOMATIC		VERTAMATIC		OSCILLATOR		
SOURCE	X-RAY		CO 60		IR 192		FILM KODAK AA		
SPEC			SECTION		PARA.		CLASS		
STATUS	ORIGINAL		RE RADIOGRAPH		AFTER H.T		AFTER REPAIR		AFTER RE STRESS

FILM	RATING	DENSITY 1	2	3	REMARKS
1-2		—	—	—	1" L. L. IND.
2-3	A	2.1	2.04	1.88	
3-4	A	2.05	2.2		

A-23

A - ACCEPTABLE
R - REJECTED
- RETAKE

INTERPRETATION [signature] L V II DATE 5

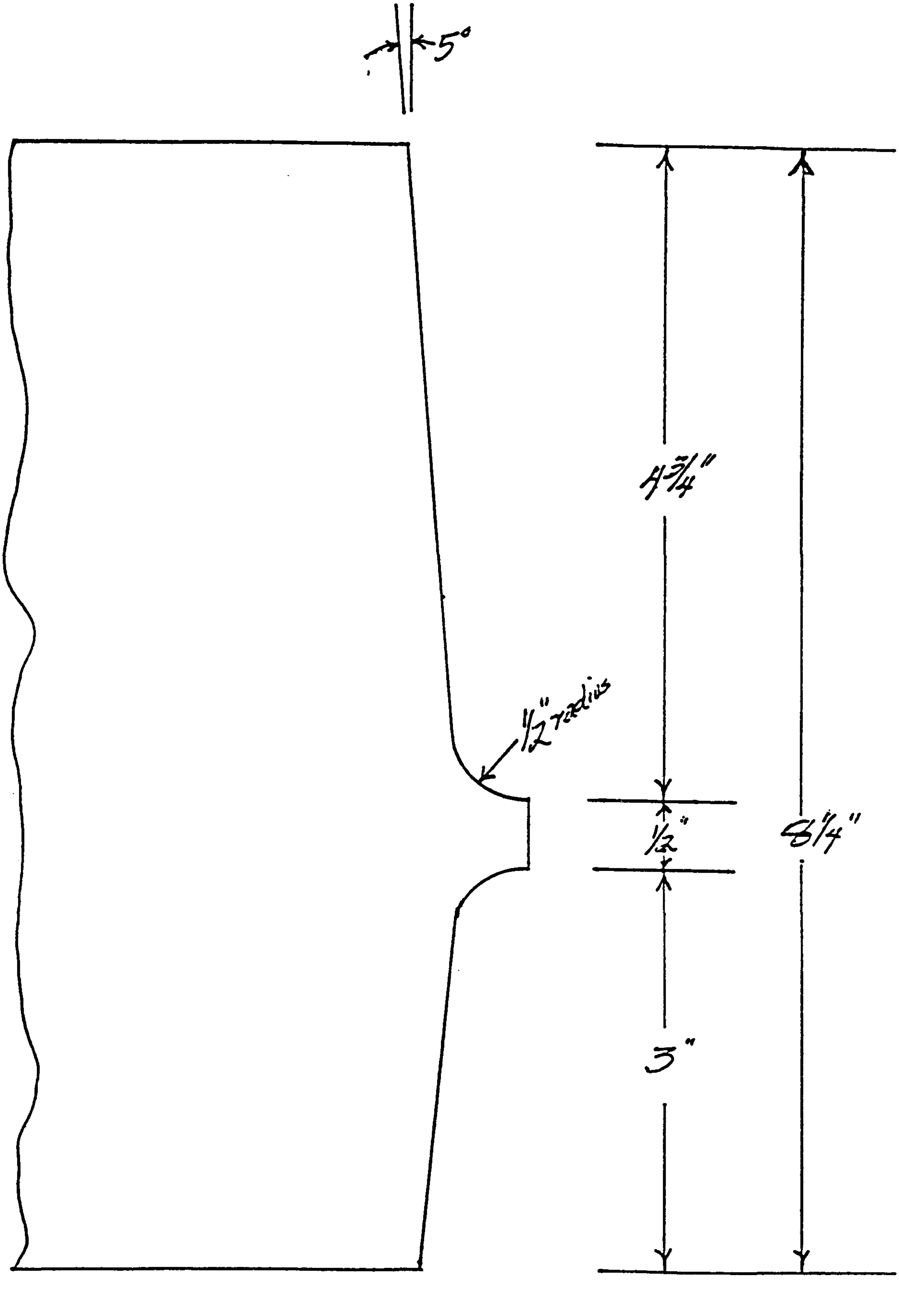

Fig. A-1 Weld joint design for Welds W8A and W9A

APPENDIX B

Neutron Dosimetry Determinations:
Irradiation Assemblies UBR-41, UBR-42, UBR-43,
UBR-48, UBR-50, and UBR-55

Neutron Fluence-Rate Determinations

Based on Fission Spectrum Assumption

For Assembly UBR-41 (Capsules A, B and C)

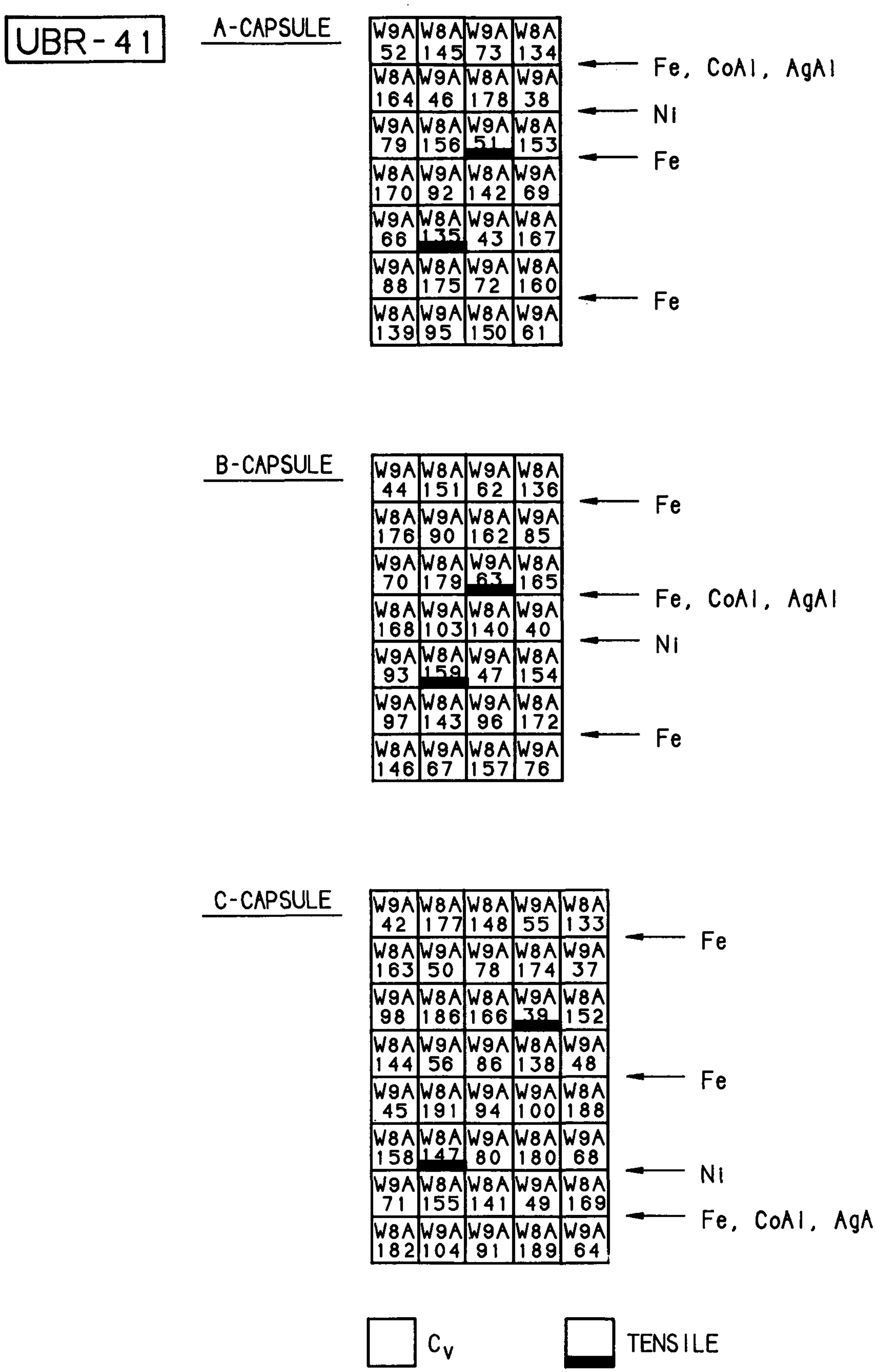

Fig. B-1 Irradiation Assembly UBR-41 showing neutron fluence-rate monitor locations

Table B-1 Irradiation Assembly UBR-41 Capsule A Fluence-Rate Monitor Results (Ref. 1)

Monitor/Segment[a]		Fluence Rate[b] x 10^{12} (Average)	Monitor Location in Specimen Array
A1	(Fe)	5.28	Between layers 1 and 2
	(AgCo)	2.30[c]	
A2	(Ni)	5.54	Between layers 2 and 3
A4	(Fe)	6.30	Between layers 6 and 7

[a] See Figure B-1 for monitor locii. The Fe and Ni results are based on > 1 MeV ^{238}U fission spectrum-averaged cross sections of 115.2 and 156.8 millibarns, respectively.

[b] Fission spectrum assumption; $n/cm^2 \cdot s^{-1}$ (E> 1 MeV) unless noted.

[c] Thermal fluence rate corrected for epithermal neutron contributions based on ^{109}Ag and ^{59}Co reaction rates and their cross sections.

Table B-2 Irradiation Assembly UBR-41 Capsule B Fluence-Rate Monitor Results (Ref. 1)

Monitor/Segment[a]		Fluence Rate[b] x 10^{12} (Average)	Monitor Location in Specimen Array
B1	(Fe)	6.91	Between layers 1 and 2
B3	(Fe)	6.91	Between layers 3 and 4
	(AgCo)	3.12[c]	
B4	(Ni)	6.97	Between layers 4 and 5
B5	(Fe)	6.85	Between layers 6 and 7

a See Figure B-1 for monitor locii. The Fe and Ni results are based on > 1 MeV ^{238}U fission spectrum-averaged cross sections of 115.2 and 156.8 millibarns, respectively.

b Fission spectrum assumption; $n/cm^2 \cdot s^{-1}$ (E> 1 MeV) unless noted.

c Thermal fluence rate corrected for epithermal neutron contributions based on ^{109}Ag and ^{59}Co reaction rates and their cross sections.

Table B-3 Irradiation Assembly UBR-41 Capsule C Fluence-Rate Monitor Results (Ref. 1)

Monitor/Segment[a]		Fluence Rate[b] x 10^{12} (Average)	Monitor Location in Specimen Array
C1	(Fe)	6.35	Between layers 1 and 2
C2	(Fe)	5.80	Between layers 4 and 5
C3	(Ni)	5.64	Between layers 6 and 7
C4	(Fe) (AgCo)	5.56 2.09[c]	Between layers 7 and 8

[a] See Figure B-1 for monitor locii. The Fe and Ni results are based on > 1 MeV ^{238}U fission spectrum-averaged cross sections of 115.2 and 156.8 millibarns, respectively.

[b] Fission spectrum assumption; $n/cm^2 \cdot s^{-1}$ (E> 1 MeV) unless noted.

[c] Thermal fluence rate corrected for epithermal neutron contributions based on ^{109}Ag and ^{59}Co reaction rates and their cross sections.

Neutron Fluence-Rate Determinations

Based on Fission Spectrum Assumption

For Assembly UBR-42 (Capsules A, B and C)

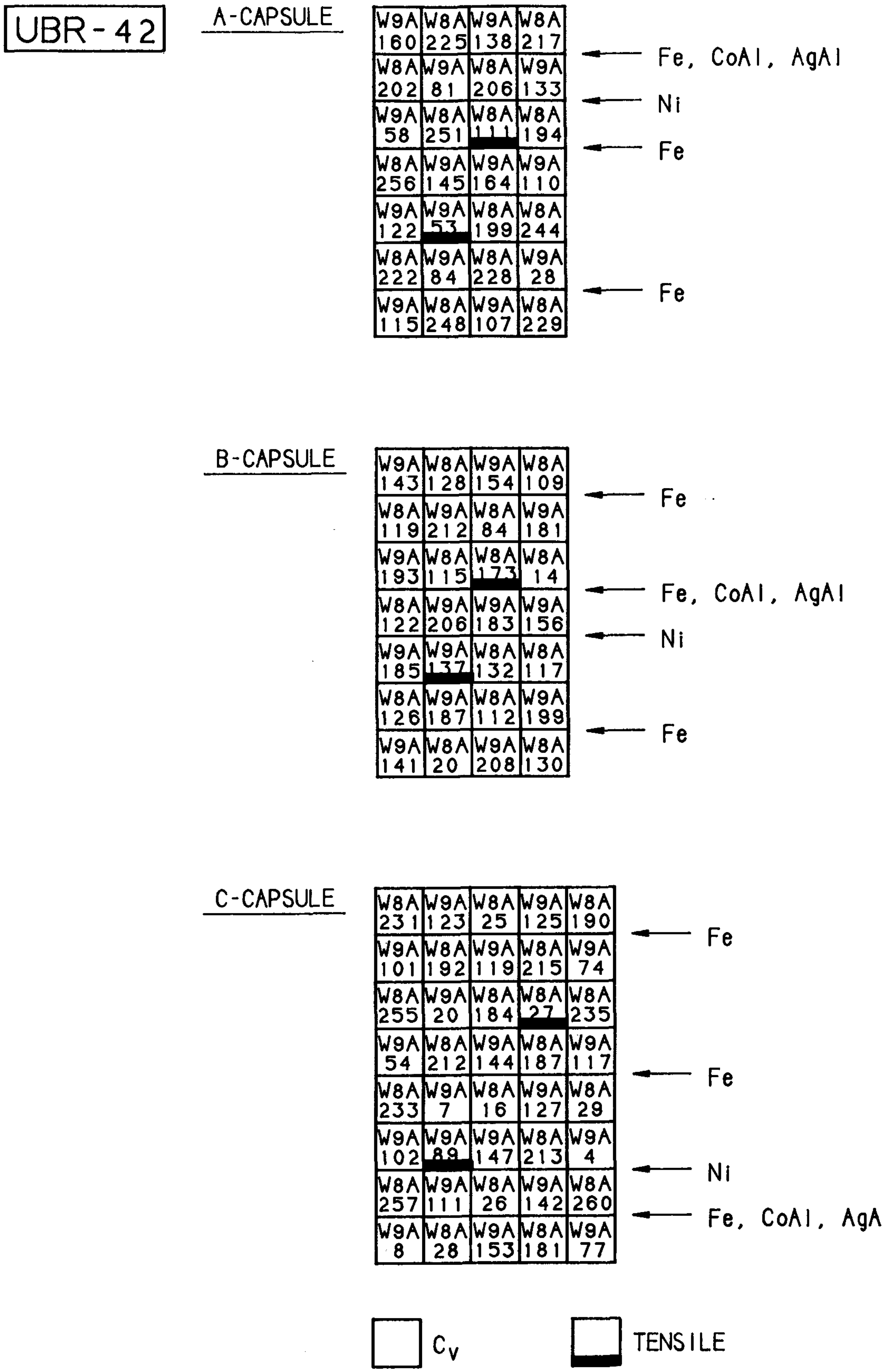

Fig. B-2 Irradiation Assembly UBR-42 showing neutron fluence-rate monitor locations

Table B-4 Irradiation Assembly UBR-42 Capsule A Fluence-Rate Monitor Results (Ref. 2)

Monitor/Segment[a]		Fluence Rate[b] x 10^{12} (Average)	Monitor Location in Specimen Array
A1	(Fe)	5.38	Between layers 1 and 2
	(AgCo)	3.07[c]	
A2	(Ni)	-[d]	Between layers 2 and 3
A3	(Fe)	5.84	Between layers 3 and 4
A4	(Fe)	6.48	Between layers 6 and 7

[a] See Figure B-2 for monitor locii. The Fe and Ni results are based on > 1 MeV ^{238}U fission spectrum-averaged cross sections of 115.2 and 156.8 millibarns, respectively.

[b] Fission spectrum assumption; $n/cm^2 \cdot s^{-1}$ (E> 1 MeV) unless noted.

[c] Thermal fluence rate corrected for epithermal neutron contributions based on ^{109}Ag and ^{59}Co reaction rates and their cross sections.

[d] Not available.

Table B-5 Irradiation Assembly UBR-42 Capsule B Fluence-Rate Monitor Results (Ref. 2)

Monitor/Segment[a]		Fluence Rate[b] x 10^{12} (Average)	Monitor Location in Specimen Array
B1	(Fe)	7.23	Between layers 1 and 2
B3	(Fe)	7.06	Between layers 3 and 4
	(AgCo)	3.69[c]	
B4	(Ni)	6.81	Between layers 4 and 5
B5	(Fe)	7.04	Between layers 7 and 8

a See Figure B-2 for monitor locii. The Fe and Ni results are based on > 1 MeV ^{238}U fission spectrum-averaged cross sections of 115.2 and 156.8 millibarns, respectively.

b Fission spectrum assumption; $n/cm^2 \cdot s^{-1}$ (E> 1 MeV) unless noted.

c Thermal fluence rate corrected for epithermal neutron contributions based on ^{109}Ag and ^{59}Co reaction rates and their cross sections.

Table B-6 Irradiation Assembly UBR-42 Capsule C Fluence-Rate Monitor Results (Ref. 1)

Monitor/Segment[a]		Fluence Rate[b] x 10^{12} (Average)	Monitor Location in Specimen Array
C1	(Fe)	6.77	Between layers 1 and 2
C2	(Fe)	6.18	Between layers 4 and 5
C3	(Ni)	6.03	Between layers 6 and 7
C4	(Fe) (AgCo)	5.80 2.20[c]	Between layers 7 and 8

a See Figure B-2 for monitor locii. The Fe and Ni results are based on > 1 MeV ^{238}U fission spectrum-averaged cross sections of 115.2 and 156.8 millibarns, respectively.

b Fission spectrum assumption; n/cm^2 -s^{-1} (E> 1 MeV) unless noted.

c Thermal fluence rate corrected for epithermal neutron contributions based on ^{109}Ag and ^{59}Co reaction rates and their cross sections.

Neutron Fluence-Rate Determinations

Based on Fission Spectrum Assumption

For Assembly UBR-43 (Capsule C)

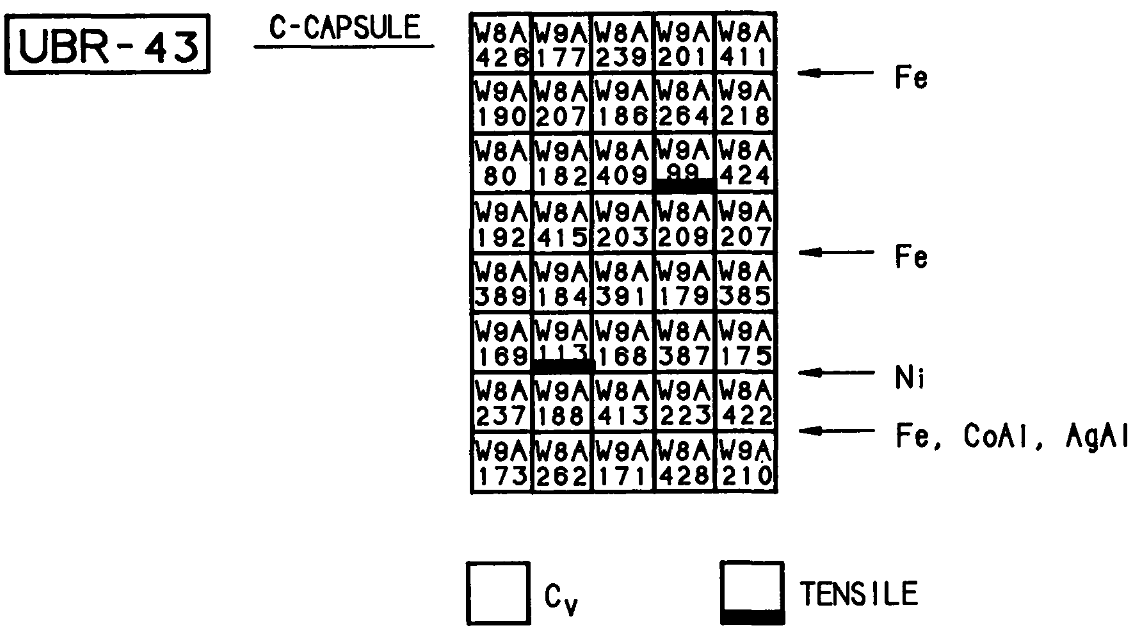

Fig. B-3 Irradiation Assembly UBR-43 showing neutron fluence-rate monitor locations

Table B-7 Irradiation Assembly UBR-43 Capsule C Fluence-Rate Monitor Results (Ref. 2)

Monitor/Segment[a]		Fluence Rate[b] x 10^{12} (Average)	Monitor Location in Specimen Array
A1	(Fe)	(not available)	Between layers 1 and 2
A2	(Fe)	6.04	Between layers 4 and 5
A3	(Ni)	5.64	Between layers 6 and 7
A4	(Fe) (AgCo)	5.73 2.60[c]	Between layers 7 and 8

[a] See Figure C-3 for monitor locii. The Fe and Ni results are based on > 1 MeV ^{238}U fission spectrum-averaged cross sections of 115.2 and 156.8 millibarns, respectively.

[b] Fission spectrum assumption; $n/cm^2 \cdot s^{-1}$ (E> 1 MeV) unless noted.

[c] Thermal fluence rate corrected for epithermal neutron contributions based on ^{109}Ag and ^{59}Co reaction rates and their cross sections.

Neutron Fluence-Rate Determination

Based on Fission Spectrum Assumption

For Assembly UBR-55 (Capsules A, B and C)

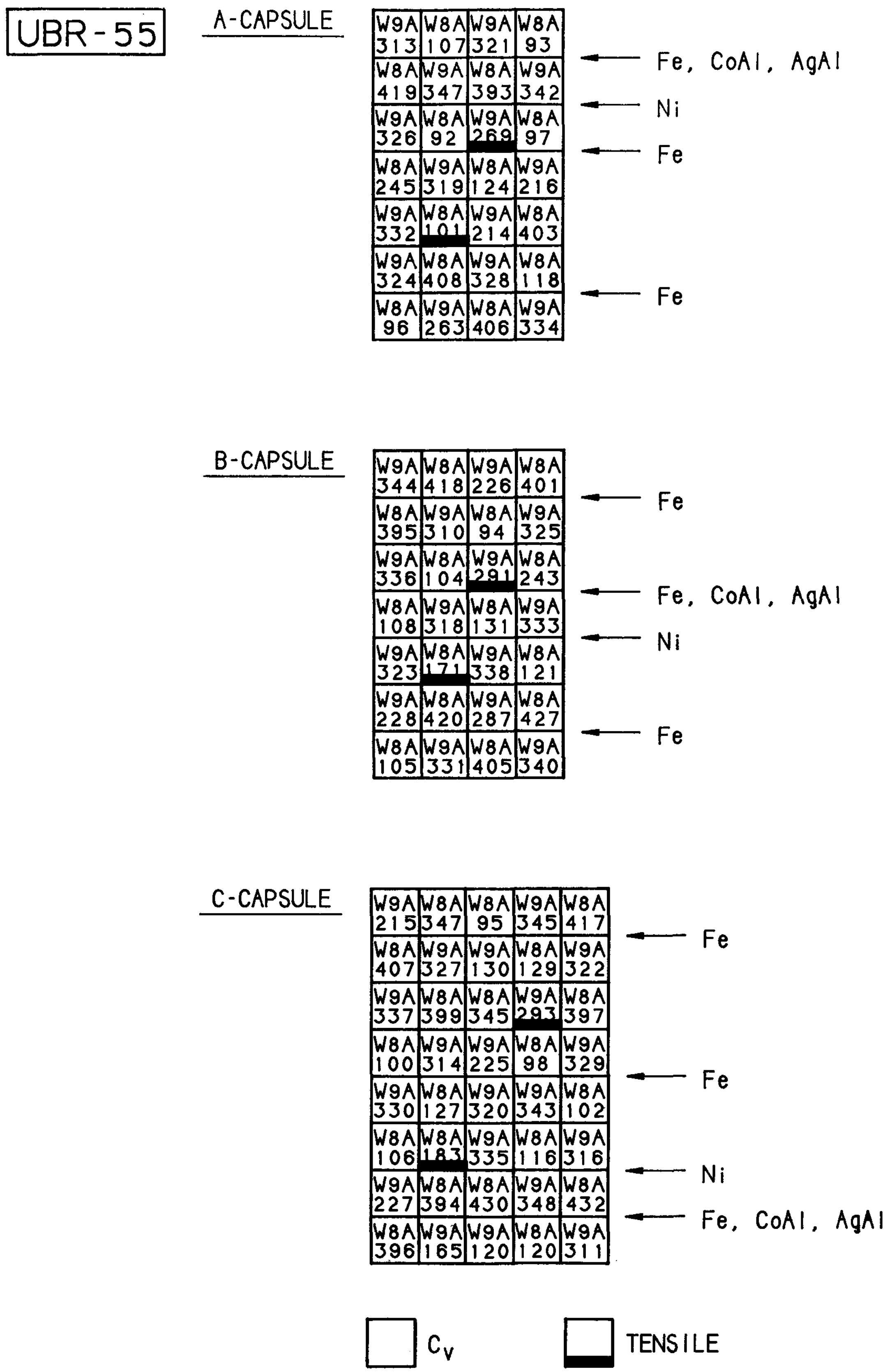

Fig. B-4 Irradiation Assembly UBR-55 showing neutron fluence-rate monitor locations

Table B-8 Irradiation Assembly UBR-55 Capsule A Fluence-Rate Monitor Results (Ref. 3)

Monitor/Segment[a]		Fluence Rate[b] x 10^{12} (Average)	Monitor Location in Specimen Array
A1	(Fe)	5.35	Between layers 1 and 2
	(AgCo)	3.09[c]	
A2	(Ni)	4.75	Between layers 2 and 3
A3	(Fe)	5.61	Between layers 3 and 4
A4	(Fe)	6.32	Between layers 6 and 7

a See Figure B-4 for monitor locii. The Fe and Ni results are based on > 1 MeV ^{238}U fission spectrum-averaged cross sections of 115.2 and 156.8 millibarns, respectively.

b Fission spectrum assumption; $n/cm^2 \cdot s^{-1}$ (E> 1 MeV) unless noted.

c Thermal fluence rate corrected for epithermal neutron contributions based on ^{109}Ag and ^{59}Co reaction rates and their cross sections.

Table B-9 Irradiation Assembly UBR-55 Capsule B Fluence-Rate Monitor Results (Ref. 3)

Monitor/Segment[a]		Fluence Rate[b] x 10^{12} (Average)	Monitor Location in Specimen Array
B1	(Fe)	6.75	Between layers 1 and 2
B3	(Fe)	6.66	Between layers 3 and 4
	(AgCo)	3.94[c]	
B4	(Ni)	5.80	Between layers 4 and 5
B5	(Fe)	6.60	Between layers 6 and 7

[a] See Figure B-4 for monitor loci. The Fe and Ni results are based on > 1 MeV ^{238}U fission spectrum-averaged cross sections of 115.2 and 156.8 millibarns, respectively.

[b] Fission spectrum assumption; $n/cm^2 \cdot s^{-1}$ (E> 1 MeV) unless noted.

[c] Thermal fluence rate corrected for epithermal neutron contributions based on ^{109}Ag and ^{59}Co reaction rates and their cross sections.

Table B-10 Irradiation Assembly UBR-55 Capsule C Fluence-Rate Monitor Results (Ref. 3)

Monitor/Segment[a]		Fluence Rate[b] x 10^{12} (Average)	Monitor Location in Specimen Array
C6	(Fe)	6.34	Between layers 1 and 2
C7	(Fe)	5.65	Between layers 4 and 5
C8	(Ni)	5.16	Between layers 6 and 7
C9	(Fe)	5.40	Between layers 7 and 8
	(AgCo)	2.46[c]	

[a] See Figure B-4 for monitor locii. The Fe and Ni results are based on > 1 MeV ^{238}U fission spectrum-averaged cross sections of 115.2 and 156.8 millibarns, respectively.

[b] Fission spectrum assumption; $n/cm^2 \cdot s^{-1}$ (E> 1 MeV) unless noted.

[c] Thermal fluence rate corrected for epithermal neutron contributions based on ^{109}Ag and ^{59}Co reaction rates and their cross sections.

Neutron Fluence-Rate Determinations

Based on Fission Spectrum Assumption

For Assembly UBR-48 (Capsules A and B)

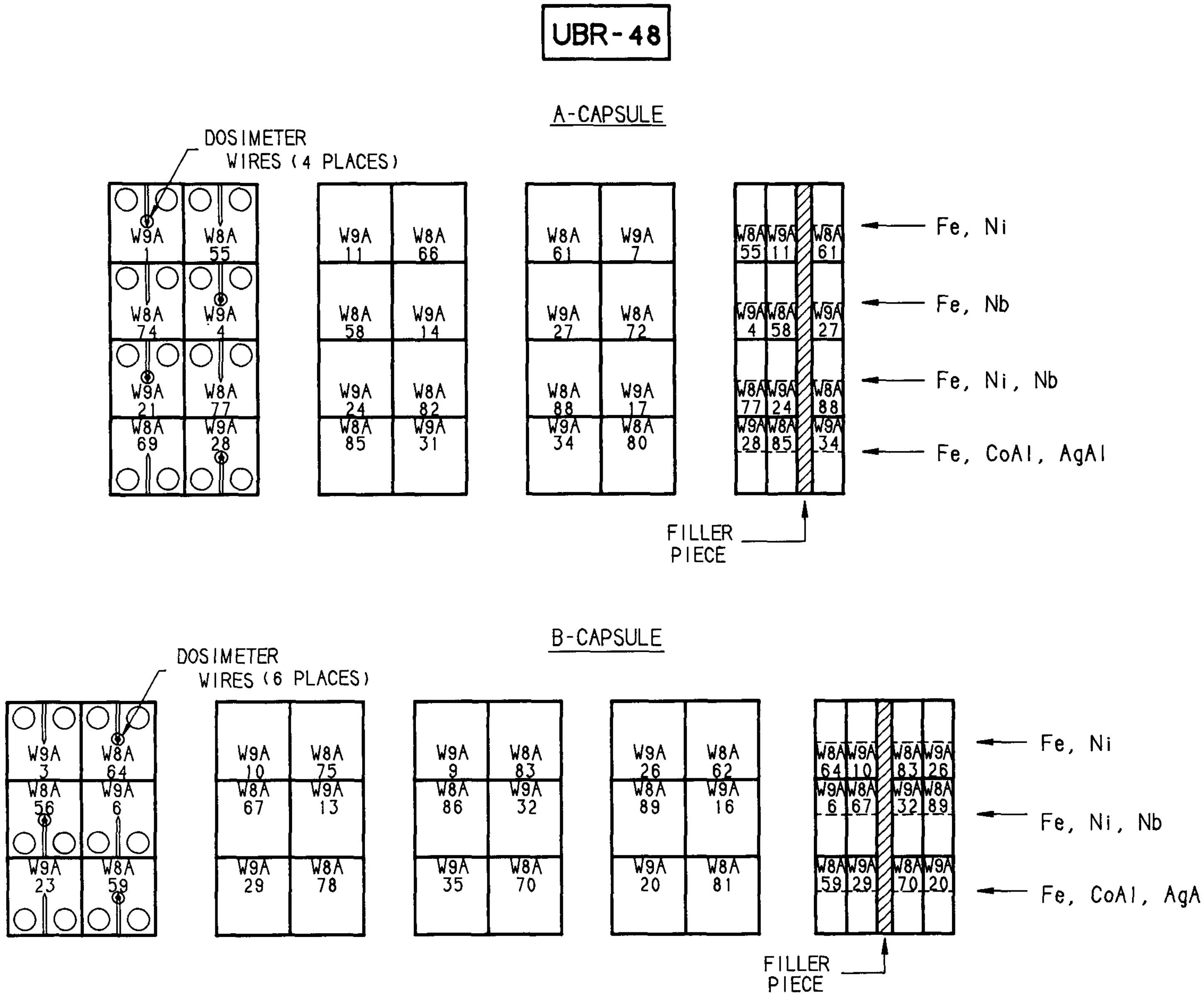

Fig. B-5 Irradiation Assembly UBR-48 showing neutron fluence-rate monitor locations

Table B-11 Irradiation Assembly UBR-48 Capsule A Fluence-Rate Monitor Results (Ref. 3)

Monitor/Segment[a]		Fluence Rate[b] x 10^{12} (Average)	Monitor Location in Specimen Array
A1	(Fe)	6.06	Specimen W9A-1, W8A-66, W9A-7
	(Ni)	6.01	
A2	(Fe)	6.58	Specimen W9A-4, W8A-58, W9A-27
A3	(Fe)	6.78	Specimen W9A-21, W8A-82, W9A-17
	(Ni)	6.84	
A4	(Fe)	7.14	Specimen W9A-28, W8A-85, W9A-34
	(AgCo)[c]	-	

[a] See Figure B-5 for monitor locii. The Fe and Ni results are based on > 1 MeV ^{238}U fission spectrum-averaged cross sections of 115.2 and 156.8 millibarns, respectively.

[b] Fission spectrum assumption; $n/cm^2 \cdot s^{-1}$ (E> 1 MeV) unless noted.

[c] Monitors lost during experiment disassembly.

Table B-12 Irradiation Assembly UBR-48 Capsule B Fluence-Rate Monitor Results (Ref. 3)

Monitor/Segment[a]		Fluence Rate[b] x 10^{12} (Average)	Monitor Location in Specimen Array
B1	(Fe)	7.04	Specimen W8A-64, W9A-10, W8A-83, W9A-26
	(Ni)	7.17	
B2	(Fe)	6.78	Specimen W8A-56, W9A-13, W8A-86, W9A-16
	(Ni)	6.84	
B3	(Fe)	6.67	Specimen W8A-59, W9A-29, W8A-70, W9A-20
	(AgCo)	2.86[c]	

[a] See Figure B-5 for monitor locii. The Fe and Ni results are based on > 1 MeV ^{238}U fission spectrum-averaged cross sections of 115.2 and 156.8 millibarns, respectively.

[b] Fission spectrum assumption; $n/cm^2 \cdot s^{-1}$ (E> 1 MeV) unless noted.

[c] Thermal fluence rate corrected for epithermal neutron contributions based on ^{109}Ag and ^{59}Co reaction rates and their cross sections.

Neutron Fluence-Rate Determinations

Based on Fission Spectrum Assumption

For Assembly UBR-50 (Capsule A)

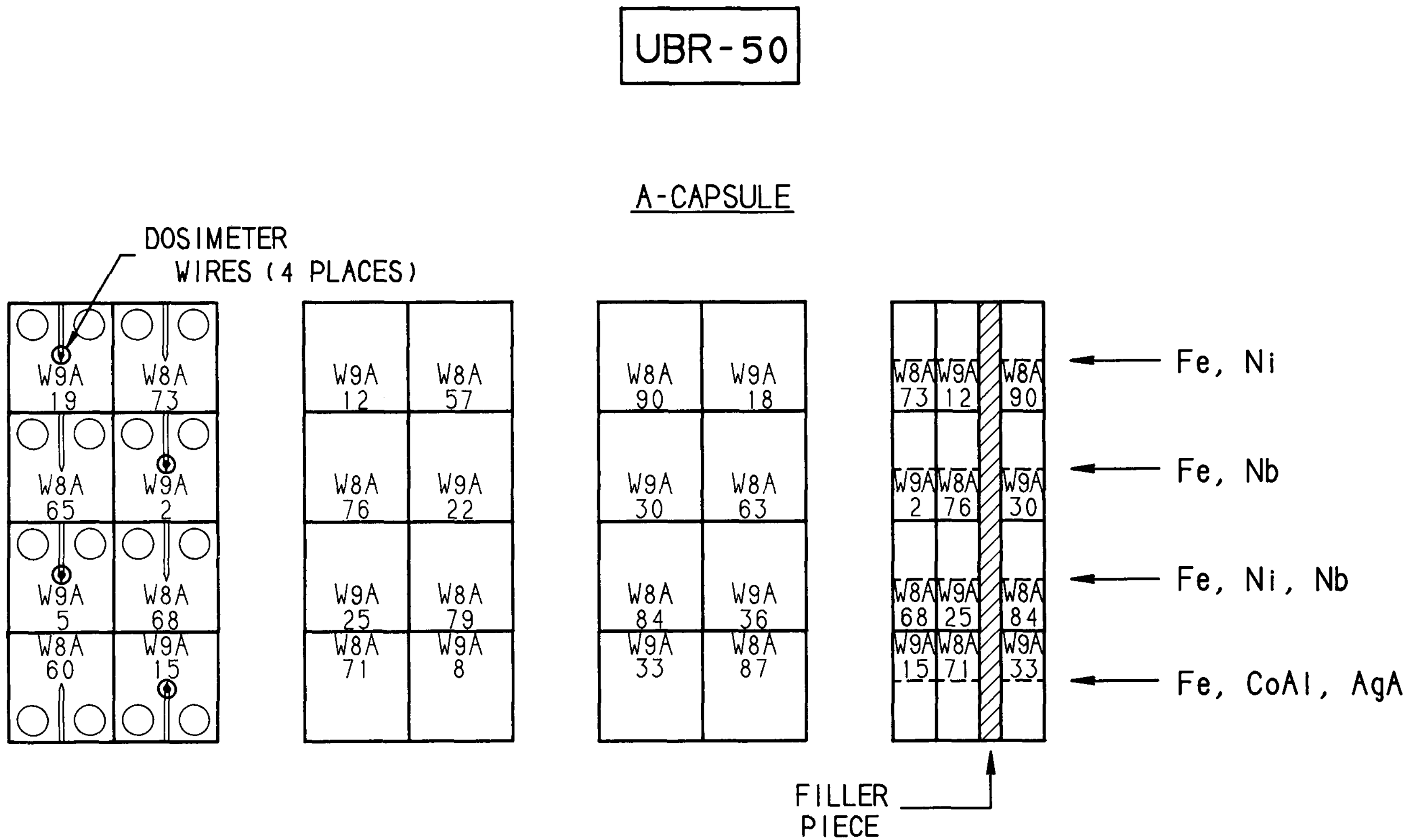

Fig. B-6 Irradiation Assembly UBR-50 showing neutron fluence-rate monitor locations

Table B-13 Irradiation Assembly UBR-50 Capsule A Fluence-Rate Monitor Results (Ref. 4)

Monitor/Segment[a]		Fluence Rate[b] x 10^{12} (Average)	Monitor Location in Specimen Array
A1	(Fe)	6.16[c]	Specimen W9A-19, W8A-57, W9A-18
	(Ni)	6.16[c]	
A2	(Fe)	6.30	Specimen W9A-2, W8A-76, W9A-30
	(Ni)	5.52	
A3	(Fe)	6.86	Specimen W9A-5, W8A-79, W9A-36
	(Ni)	6.47	
A4	(Fe)	7.50	Specimen W9A-15, W8A-71, W9A-33
	(AgCo)[c]	5.78[d]	

[a] See Figure B-6 for monitor locii. The Fe and Ni results are based on > 1 MeV ^{238}U fission spectrum-averaged cross sections of 115.2 and 156.8 millibarns, respectively.

[b] Fission spectrum assumption; n/cm^2 -s^{-1} (E> 1 MeV) unless noted.

[c] Estimate based on UBR-48A measurements.

[d] Thermal fluence rate corrected for epithermal neutron contributions based on ^{109}Ag and ^{59}Co reaction rates and their cross sections.

REFERENCES

1. A. W. Marley, "ENSA Neutron Dosimeters," Letter Report AWN-16-83, EG&G Idaho, Inc., Idaho Falls, ID, 31 May 1983.

2. A. W. Marley, "Neutron Dosimeters from Experiments UB(C2)-42, 42B(R) AND 43C(R)," Letter Report AWM-33-83, EG&G Idaho, Inc., Idaho Falls, ID, 14 November 1983.

3. J. W. Rogers, "Neutron Fluence Rates for MEA-UBR Experiments," Letter Report JWR-22-85, EG&G Idaho, Inc., Idaho Falls, ID, 28 May 1985.

4. J. W. Rogers, "Analyses of Neutron Dosimeters," Letter Report JWR-20-84, EG&G Idaho, Inc., Idaho Falls, ID, 1 March 1984.

APPENDIX C

Reactor Operations History:
Irradiation Assemblies UBR-41, UBR-42, UBR-43,
UBR-48, UBR-50 and UBR-55

Irradiation History for Experiment

UB (C2) 41A, B, C

Date In	Time In	Date Out	Time Out	Exposure (hrs.)	Accumulated Time (hrs.)	Comment
8/1/82	1725	8/2/82	1330	20.09	20.09	Location C2
8/2/82	1412	8/5/82	1112	67.50	87.59	
8/5/82	1153	8/6/82	0900	21.12	108.71	
8/8/82	1710	8/13/82	1100	113.83	222.54	Experiment rotated.
8/15/82	1714	8/20/82	1145	114.51	337.05	
8/22/82	1700	8/25/82	1500	70.00	407.05	B-Package removed from core.
8/26/82	1600	8/27/82	1100	19.00	426.05	
8/29/82	1718	8/30/82	0900	15.70	441.75	Experiment terminated.

Re Irradiation History for Experiment

UB (C2) 41A

Date In	Time In	Date Out	Time Out	Exposure (hours)	Acc. Time (hours)	Comments
10/3/82	1713	10/3/82	1842	1.48	1.48	Re-irradiation location C2 Irradiated with 42CR initially.
10/3/82	1914	10/4/82	1120	16.10	17.58	
10/4/82	1213	10/6/82	1345	49.53	67.11	41B added
10/6/82	1509	10/7/82	1637	25.47	92.58	
10/7/82	1923	10/8/82	0930	14.12	106.70	Terminated

Re Irradiation History for Experiment

UB (C2) 41B

Date In	Time In	Date Out	Time Out	Exposure (hours)	Acc. Time (hours)	Comments
10/6/82	1509	10/7/82	1637	25.47	25.47	Location C2, with 42CR and 41A
10/7/82	1923	10/8/82	0930	14.12	39.59	41A Removed
10/10/82	1647	10/13/82	0508	60.35	99.94	
10/13/82	0528	10/13/82	1030	5.03	104.97	Rotated
10/13/82	1120	10/15/82	0936	46.33	151.30	
10/15/82	1715	10/15/82	1801	0.17	151.47	
10/17/82	1650	10/20/82	0400	59.17	210.64	Terminated

Irradiation History for Experiment
UB (C2) 42A

Date In	Time In	Date Out	Time Out	Exposure (hours)	Acc.Time (hours)	Comments
						Location C2
8/30/82	1018	8/30/82	1400	3.70	3.70	
8/30/82	1440	8/30/82	1515	0.58	4.28	42B-unit removed
8/30/82	1536	9/01/82	1500	47.40	51.68	42B-unit removed
9/01/82	1524	9/03/82	1200	44.60	96.28	
9/07/82	0120	9/09/82	2140	68.34	164.62	
9/09/82	2238	9/10/82	0930	10.68	175.30	
9/12/82	1748	9/13/82	1300	19.20	194.50	Rotated
9/13/82	1330	9/17/82	0845	91.25	285.75	
9/19/82	1726	9/20/82	2056	27.49	313.24	
9/20/82	2120	9/21/82	1011	12.84	326.08	
9/21/82	1051	9/21/82	1204	1.22	327.30	
9/21/82	1232	9/24/82	1000	69.46	396.76	
9/26/82	1753	9/27/82	2000	26.12	422.88	Exp. Removed and Annealed
11/03/82	1409	11/03/82	1655	2.77	425.65	Re-irradiate with 41C and 42B
11/05/82	0913	11/05/82	1200	2.78	428.43	
11/07/83	1717	11/12/82	1100	113.72	542.15	
11/14/82	1743	11/16/82	1812	48.48	590.63	Rotated
11/16/82	1852	11/18/82	1301	42.10	632.73	
11/18/82	1440	11/19/82	0600	15.33	648.06	
11/19/82	1312	11/19/82	1500	1.80	649.86	
11/20/82	1736	11/24/82	1100	65.40	715.26	
11/24/82	1225	11/24/82	1800	5.58	720.84	
11/28/82	1715	11/25/82	1017	17.04	737.88	

Irradiation History for Experiment
UB(C2) 42B (R)

Date In	Time In	Date Out	Time Out	Exposure (hours)	Acc.Time (hours)	Comments
11/30/82	1624	12/02/82	0216	33.86	33.86	Core Location C2, Irradiated with 43C (R).
12/02/82	0235	12/03/82	1007	31.52	65.38	
12/05/82	1719	12/09 82	1825	97.10	162.48	
12/09/82	1851	12/09/82	2250	4.00	166.48	
12/12/82	1713	12/13/82	2333	30.33	196.81	Rotate
12/14/82	0007	12/17/82	2300	94.88	291.69	
12/19/82	1651	12/23/82	1320	92.82	384.51	
12/23/82	1351	12/24/82	0431	14.67	399.18	Experiment Removed
1/16/83	1720	1/18/83	1400	44.67	443.85	Experiment Reinstated Core location C2, Irradiated with 43CR
1/18/83	1530	1/20/83	1531	48.02	491.87	
1/20/83	1552	1/21/83	1415	22.38	514.25	
1/23/83	1728	1/24/83	1400	20.53	534.78	
1/24/83	1459	1/25/83	0920	18.35	553.13	
1/25/83	1002	1/26/83	0830	22.47	575.60	
1/26/83	0936	1/27/83	1912	33.60	609.20	Experiment Rotated
1/27/82	2041	1/28/83	0800	11.32	620.52	
1/28/83	1109	1/28/83	1239	1.50	622.02	
1/30/83	1723	2/04/83	0800	110.62	732.64	
2/06/83	1727	2/09/83	1900	73.55	806.19	Experiment UB(C2) 42 B (R) removed

Irradiation History for Experiment

Experiment UB(C2) 42C(R)

Date In	Time In	Date Out	Time Out	Exposure (hours)	Acc. Time (hours)	Comments
						Location C2
10/3/82	1713	10/3/82	1842	1.48	1.48	Loaded with 41A
10/3/82	1914	10/4/82	1120	16.10	17.58	
10/4/82	1213	10/6/82	1345	49.53	67.11	41B Added
10/6/82	1509	10/7/82	1637	25.47	92.58	
10/7/82	1923	10/8/82	0930	14.12	106.70	41A Removed
10/10/82	1647	10/13/82	0508	60.35	167.05	
10/13/82	0528	10/13/82	1030	5.03	172.08	Rotated
10/13/82	1120	10/15/82	0936	46.33	218.41	
10/15/82	1751	10/15/82	1801	0.17	218.58	
10/17/82	1650	10/20/82	0400	59.17	277.75	41B Removed
10/20/82	0424	10/20/82	1015	5.85	283.60	
10/20/82	1043	10/21/82	1400	27.28	310.88	
10/24/82	1715	10/29/82	1130	113.98	424.86	
11/3/82	1409	11/3/82	1655	2.77	427.63	42A and 42B Added
11/3/82	1726	11/4/82	0234	9.14	436.77	42A Removed
11/4/82	0430	11/5/82	0845	28.25	465.02	Rotated, 42A Added
11/5/82	0913	11/5/82	1200	2.78	467.80	
11/7/82	1717	11/12/82	1100	113.72	581.52	
11/14/82	1743	11/16/82	1812	48.48	630.00	Experiment Removed

Irradiation History for Experiment
UB(C2) - 43C(R)

Date In	Time In	Date Out	Time Out	Exposure (hours)	Acc.Time (hours)	Comments
11/30/82	1624	12/02/82	0216	33.86	33.86	Core Location C2,
						Irradiated with 42B (R).
12/02/82	0235	12/03/82	1007	31.52	65.38	
12/05/82	1719	12/09 82	1825	97.10	162.48	
12/09/82	1851	12/09/82	2250	4.00	166.48	
12/12/82	1713	12/13/82	2333	30.33	196.81	Rotate
12/14/82	0007	12/17/82	2300	94.88	291.69	
12/19/82	1651	12/23/82	1320	92.82	384.51	
12/23/82	1351	12/24/82	0431	14.67	399.18	
12/27/82	1012	12/28/82	2012	34.00	433.18	Experiment Removed from Core Position
1/16/83	1720	1/18/83	1400	44.67	477.85	Experiment Returned to Core location C2,
						Irradiated with 42CR
1/18/83	1530	1/20/83	1531	48.02	525.87	
1/20/83	1552	1/21/83	1415	22.38	548.25	
1/23/83	1728	1/24/83	1400	20.53	568.78	
1/24/83	1459	1/25/83	0920	18.35	587.13	
1/25/83	1002	1/26/83	0830	22.47	609.60	
1/26/83	0936	1/27/83	1912	33.60	643.20	Experiment Rotated
1/27/82	2041	1/28/83	0800	11.32	654.52	
1/28/83	1109	1/28/83	1239	1.50	656.02	
1/30/83	1723	2/04/83	0800	110.62	766.64	
2/06/83	1727	2/09/83	1900	73.55	840.19	Experiment UB(C2) 42 B (R) removed Replaced with 42B
2/09/83	1925	2/10/83	0815	12.83	853.02	
2/10/83	0854	2/10/83	1322	4.47	857.49	
2/10/83	1514	2/11/83	0800	16.75	874.24	Experiment Terminated

EXPOSURE HISTORY

UB48 A,B

date in	time in	date out	time out	exposure hours	sigma hours ~~IN REACTOR~~	core position	REMARKS
2.13.83	1740	2.18.83	0750	110.17	110.17	C-2	
2.21.83	1715	2.22.83	0919	16.07	126.24		REACTOR POWER = 2MW UNLESS OTHERWISE SPECIFIED
2.22.83	1048	2.23.83	1800	31.20	157.44		
2.23.83	1843	2.25.83	0830	37.78	195.22		
2.27.83	1720	2.28.83	0850	15.50	210.72		180° ROTATION 0850, 2.28.83
2.28.83	0917	2.28.83	1827	9.17	219.89		
2.2883	1854	3.1.83	1414	19.33	239.22		
3.1.83	1443	3.1.83	2342	8.98	248.20		
3.2.83	0010	3.2.83	1300	12.83	261.03		
3.2.83	1345	3.4.83	1015	44.50	305.53	ΣHRS PRORATED TO 2MW	
3.6.83	1702	3.7.83	1040	17.63	323.16	323.16	
3.7.83	1040	3.7.83	2000	840	331.56	330.72	REACTOR PWR = 1.8MW
3.7.83	2000	3.7.83	2100	0.95	332.51	331.62	REACTOR PWR = 1.9MW
3.7.83	2100	3.7.83	2330	2.50	335.01	334.12	REACTOR PWR = 2.0MW
3.7.83	2330	3.8.83	0100	1.35	336.36	335.34	REACTOR PWR = 1.8MW
3.8.83	0100	3.8.83	1215	11.25	347.61	346.59	REACTOR PWR = 2.0MW
3.8.83	1215	3.8.83	1345	1.35	348.96	347.80	REACTOR PWR = 1.8MW
3.8.83	1345	3.11.83	0800	66.25	415.21	414.05	
3.13.83	1721	3.13.83	2209	4.80	420.01	418.85	48A,B OUT OF CORE 3.13.83@ 2209 FOR
							ANNEAL OF B PACKAGE
3.27.83	1616	3.28.83	0945	17.48	437.49	436.33	48A,B RE-INSERTED 3.27
3.28.83	1106	3.28.83	1320	2.23	439.72	438.56	
3.28.83	1418	4.1.83	1200	93.70	533.42	532.26	180° ROTATION 1200, 4.1.84
4.5.83	1054	4.8.83	1200	73.10	606.52	605.36	
4.10.83	1655	4.11.83	1930	26.58	633.1	631.94	48A,B DISCHARGED

Exposure History

Experiment no. 50

date in	time in	date out	time out	exposure hours	sigma hours	cord position	
4/18/83	1355	4/19/83	2103	31.13	31.13	C-2	11.75" SPAC
4/19/83	2217	4/20/83	1024	12.12	43.25		ROON D
4/20/83	1054	4/22/83	1300	50.10	93.35		
4/24/83	1701	4/26/83	1630	47.48	140.83		
4/26/83	1740	4/28/83	1248	43.13	183.96		
4/28/83	1530	4/29/83	1000	18.50	202.46		
5/1/83	1707	5/2/83	0930	16.38	218.84		
		ROTATED	180°				
5/2/83	0954	5/6/83	1000	96.10	314.94		
5/8/83	1653	5/13/83	0900	112.12	427.06		
			END				

EXPOSURE HISTORY

UBR 55A

date in	time in	date out	time out	2MW exposure hours	2MW sigma hours	core position	REMARK
12.7.83	1200	12.9.83	0800	44.00	44.00	C-2	
12.11.83	1900	12.16.83	1000	111.00	155.00		
12.18.83	1713	12.20.83	0218	33.90	188.90		
12.20.83	0307	12.23.83	0900	77.88	266.78		
12.26.83	1623	12.29.83	2330	79.12	345.90		
1.2.84	1604	1.4.84	2400	55.93	401.83		
1.5.84	1013	1.5.84	1940	9.45	411.28		
1.5.84	2043	1.6.84	1300	16.28	427.56		
1.8.84	1651	1.9.84	1000	17.15	444.71		
	CAPSULE ROTATED 180°						
1.9.84	1035	1.13.84	1100	96.83	541.54		
1.15.84	1653	1.16.84	0000	7.12	548.66		
1.16.84	0000	1.19.84	1509	87.15	635.81		
1.19.84	1600	1.20.84	1030	18.50	654.31		
1.22.84	1641	1.27.84	0800	111.32	765.63		
1.29.84	1652	1.30.84	1700	24.13	789.76		
1.30.84	1838	2.3.84	1230	89.86	879.63		
	CAPSULE ANNEALED						
2.26.84	1705	2.28.84	0700	37.90	917.53		
2.29.84	1106	2.29.84	1900	7.90	925.43		
2.29.84	2002	3.2.84	1500	42.97	968.40		
3.4.84	1712	3.5.84	1000	16.80	985.20		
	CAPSULE TO POOL STORAGE						
1.25.85	1015	1.25.85	1520	5.08	990.20	C-2	
1.27.85	1658	1.28.85	0830	15.53	1005.81		
1.28.85	0948	2.1.85	1300	99.20	1105.01		
	CAPSULE ROTATED 180°						

EXPOSURE HISTORY

UBR 55A

date in	time in	date out	time out	exposure hours	sigma hours	core position	REMARK
2.3.85	1721	2.8.85	1300	115.65	1220.66	C-2	
2.10.85	1718	2.11.85	1100	17.70	1238.36		
2.17.85	1802	2.22.85	1000	112.00	1350.36		
	CAPSULE DISCHARGED						

EXPOSURE HISTORY

UBR-55B

date in	time in	date out	time out	exposure hours	sigma hours	core position	REMARKS
12.7.83	1200	12.9.83	0800	44.00	44.00	[redacted]	
12.11.83	1900	12.16.83	1000	111.00	155.00		
12.18.83	1713	12.20.83	0218	33.90	188.90		
12.20.83	0307	12.23.83	0900	77.88	266.78		
12.26.83	1623	12.29.83	2330	79.12	345.90		
1.2.84	1604	1.4.84	2400	55.93	401.83		
1.5.84	1013	1.5.84	1940	9.45	411.28		
1.5.84	2043	1.6.84	1300	16.28	427.56		
1.8.84	1651	1.9.84	1000	17.15	444.71		180° ROTATION 1.9.84
1.9.84	1035	1.13.84	1100	96.83	541.54		
1.15.84	1653	1.16.84	0000	7.12	548.66		
1.16.84	0000	1.19.84	1509	87.15	635.81		
1.19.84	1600	1.20.84	1030	18.50	654.31		
1.22.84	1641	1.27.84	0800	111.32	765.63		55B OUT OF FL FOR ANNEAL 1.27.8
2.20.84	1648	2.23.84	1450	70.03	835.66		55B INSERTED IN FLUX 2.20.84
2.23.84	1544	2.24.84	1030	18.76	854.42		
2.26.84	1705	2.28.84	0700	37.90	892.32		
2.29.84	1106	2.29.84	1900	7.90	900.22		
2.29.84	2002	3.2.84	1500	42.97	943.19		55B DISCHARGE

EXPOSURE HISTORY

UBR 55C

.te in	time in	date out	time out	exposure hours	sigma hours	core position	REMARKS
12.7.83	1200	12.9.83	0800	44.00	44.00	C-2	
12.11.83	1900	12.16.83	1000	111.00	155.00		
12.18.83	1713	12.20.83	0218	33.90	188.90		
12.20.83	0307	12.23.83	0900	77.88	266.78		
12.26.83	1623	12.29.83	2330	79.12	345.90		
1.2.84	1604	1.4.84	2400	55.93	401.83		
1.5.84	1013	1.5.84	1940	9.45	411.28		
1.5.84	2043	1.6.84	1300	16.28	427.56		
1.8.84	1651	1.9.84	1000	17.15	444.71		180° ROTATION 1.9.84
1.9.84	1035	1.13.84	1100	96.83	541.54		
1.15.84	1653	1.16.84	0000	7.12	548.66		
1.16.84	0000	1.19.84	1509	87.15	635.81		
1.19.84	1600	1.20.84	1030	18.50	654.31		
1.22.84	1641	1.27.84	0800	111.32	765.63		
1.29.84	1652	1.30.84	1700	24.13	789.76		
1.30.84	1838	2.3.84	1230	89.86	879.63		55C OUT OF FLUX, 2.3.84
2.20.84	1648	2.23.84	1450	70.03	949.66		55C INTO FLUX 2.20.84
2.23.84	1544	2.24.84	1030	18.76	968.43		
2.26.84	1705	2.28.84	0700	37.90	1006.33		
2.29.84	1106	2.29.84	1900	7.90	1014.23		
2.29.84	2002	3.2.84	1500	42.97	1057.20		
3.4.84	1712	3.5.84	1000	16.80	1074.00		
3.5.84	1022	3.6.84	0800	21.63	1095.63		55C OUT OF FLUX 0800

APPENDIX D

Tabulations of Charpy-V Notch Ductility Test Results

Charpy-V Data from Unirradiated Condition Tests

Code W8A (Unirradiated Condition)

No.	Specimen Number	Layer	Capsule	Test Temp. (°C)	Test Temp. (°F)	Energy (J)	Energy (ft-lb)	Lat. Exp. (mm)	Lat. Exp. (mils)	Shear (%)
1	4	4	---	-40	-40	19.0	14.0	0.33	13	5
2	11	11	---	-40	-40	24.4	18.0	0.43	17	5
3	30	6	---	-23	-10	35.3	26.0	(ND)	(ND)	----
4	5	5	---	-18	0	48.8	36.0	0.94	37	----
5	12	12	---	-18	0	43.4	32.0	0.79	31	20
6	18	6	---	4	40	52.9	39.0	(ND)	(ND)	----
7	10	10	---	27	80	40.7	30.0	0.74	29	35
8	3	3	---	27	80	56.9	42.0	1.09	43	45
9	6	6	---	49	120	70.5	52.0	1.27	50	80
10	1	1	---	49	120	63.7	47.0	1.19	47	60
11	9	9	---	93	200	75.9	56.0	1.47	58	100
12	2	2	---	93	200	81.3	60.0	1.55	61	100
13	15	3	---	204	400	78.6	58.0	1.68	66	100
14	22	10	---	204	400	78.6	58.0	1.52	60	100
15	9A	9	---	-23	-10	43.4	32.0	(ND)	(ND)	----

(ND) - Not Determined
(NT) - Not Tested

Code W9A (Unirradiated Condition)

No.	Specimen Number	Layer	Capsule	Test Temp. (°C)	Test Temp. (°F)	Energy (J)	Energy (ft-lb)	Lat. Exp. (mm)	Lat. Exp. (mils)	Shear (%)
1	5	5	---	-62	-80	39.3	29.0	0.71	28	20
2	15	3	---	-62	-80	38.0	28.0	0.64	25	10
3	3	3	---	-46	-50	71.9	53.0	1.09	43	50
4	19	7	---	-46	-50	67.8	50.0	1.07	42	20
5	18	7	---	24	75	130.2	96.0	1.85	73	95
6	27	3	---	24	75	149.1	110.0	1.96	77	99
7	6	6	---	71	160	154.6	114.0	2.18	86	100
8	16	4	---	204	400	169.5	125.0	2.21	87	100
9	29	5	---	204	400	169.5	125.0	2.21	87	100
10	35	11	---	204	400	168.1	124.0	2.16	85	100

(ND) - Not Determined
(NT) - Not Tested

Charpy-V Data from Irradiation Assembly UBR-41

Weld W8A (UBR-41, Capsule C, As-Irradiated) (IAR-1C)

No.	Specimen Number	Layer	Capsule	Test Temp. (°C)	Test Temp. (°F)	Energy (J)	Energy (ft-lb)	Lat. Exp. (mm)	Lat. Exp. (mils)	Shear (%)
1	155	11	41C	38	100	8.1	6.0	0.13	5	<100
2	158	2	41C	60	140	14.9	11.0	0.20	8	<100
3	152	8	41C	66	150	35.3	26.0	0.51	20	<100
4	144	12	41C	71	160	16.3	12.0	0.25	10	<100
5	174	6	41C	82	180	27.1	20.0	0.48	19	<100
6	166	10	41C	88	190	27.1	20.0	0.38	15	<100
7	188	8	41C	93	200	44.7	33.0	0.66	26	<100
8	189	9	41C	104	220	47.5	35.0	0.84	33	<100
9	177	9	41C	110	230	51.5	38.0	0.84	33	100
10	186	6	41C	138	280	51.5	38.0	0.89	35	98
11	138	6	41C	204	400	52.9	39.0	0.89	35	<100
12	191	11	41C	204	400	55.6	41.0	0.94	37	100

(ND) - Not Determined
(NT) - Not Tested

Weld W8A (UBR-41, Capsule C, Irradiated & 399 C Annealed) (IAR-1C)

No.	Specimen Number	Layer	Capsule	Test Temp. (°C)	Test Temp. (°F)	Energy (J)	Energy (ft-lb)	Lat. Exp. (mm)	Lat. Exp. (mils)	Shear (%)
1	133	1	41C	(NT)	(NT)	(NT)	(NT)	(ND)	(ND)	
2	148	4	41C	-7	20	10.8	8.0	0.15	6	<100
3	182	2	41C	32	90	33.9	25.0	0.56	22	<100
4	180	12	41C	49	120	35.3	26.0	0.71	28	<100
5	169	1	41C	60	140	48.8	36.0	0.86	34	<100
6	163	7	41C	71	160	65.1	48.0	1.09	43	<100
7	141	9	41C	138	280	77.3	57.0	1.04	41	100

(ND) - Not Determined
(NT) - Not Tested

Weld W8A (UBR-41, Capsule A, Annealed & Reirradiated) (IAR-1A)

No.	Specimen Number	Layer	Capsule	Test Temp. (°C)	Test Temp. (°F)	Energy (J)	Energy (ft-lb)	Lat. Exp. (mm)	Lat. Exp. (mils)	Shear (%)
1	*170	2	41A	16	60	28.5	21.0	0.41	16	<100
2	167	11	41A	38	100	19.0	14.0	0.30	12	<100
3	*139	7	41A	41	105	59.7	44.0	0.97	38	<100
4	178	10	41A	66	150	25.8	19.0	0.51	20	<100
5	175	7	41A	71	160	43.4	32.0	0.71	28	<100
6	160	4	41A	82	180	35.3	26.0	0.64	25	<100
7	156	12	41A	91	195	32.5	24.0	(ND)	(ND)	<100
8	134	2	41A	96	205	36.6	27.0	0.71	28	<100
9	153	9	41A	104	220	56.9	42.0	0.99	39	<100
10	164	8	41A	121	250	58.3	43.0	1.02	40	100
11	*145	1	41A	166	330	78.6	58.0	0.97	38	100
12	150	6	41A	204	400	59.7	44.0	1.14	45	100
13	142	11	41A	216	420	54.2	40.0	1.09	43	100

* Annealed at 399 C - 168 hrs.
(ND) - Not Determined
(NT) - Not Tested

Weld W8A (UBR-41, Capsule B, Annealed & Reirradiated) (IAR-1B)

No.	Specimen Number	Layer	Capsule	Test Temp. (°C)	Test Temp. (°F)	Energy (J)	Energy (ft-lb)	Lat. Exp. (mm)	Lat. Exp. (mils)	Shear (%)
1	*151	7	41B	-1	30	29.8	22.0	0.46	18	<100
2	*140	8	41B	27	80	42.0	31.0	0.69	27	<100
3	*172	4	41B	32	90	25.8	19.0	0.43	17	<100
4	143	11	41B	38	100	10.8	8.0	0.15	6	<100
5	*168	12	41B	54	130	38.0	28.0	0.64	25	<100
6	157	1	41B	71	160	27.1	20.0	0.43	17	<100
7	136	4	41B	82	180	25.8	19.0	0.41	16	<100
8	154	10	41B	93	200	28.5	21.0	0.54	21	<100
9	146	2	41B	93	200	31.2	23.0	0.58	23	<100
10	165	9	41B	110	230	59.7	44.0	0.99	39	98
11	176	8	41B	127	260	55.6	41.0	0.97	38	100
12	162	6	41B	204	400	56.9	42.0	0.89	35	100
13	179	11	41B	204	400	56.9	42.0	0.99	39	100

* Annealed at 399 C - 168 hrs.
(ND) - Not Determined
(NT) - Not Tested

Weld W9A (UBR-41, Capsule C, As-Irradiated) (IAR-1C)

No.	Specimen Number	Layer	Capsule	Test Temp. (°C)	Test Temp. (°F)	Energy (J)	Energy (ft-lb)	Lat. Exp. (mm)	Lat. Exp. (mils)	Shear (%)
1	91	7	41C	-7	20	12.2	9.0	(ND)	(ND)	<100
2	71	11	41C	10	50	21.7	16.0	0.28	11	<100
3	55	7	41C	16	60	33.9	25.0	0.43	17	<100
4	45	9	41C	32	90	44.7	33.0	0.64	25	<100
5	100	4	41C	38	100	43.4	32.0	0.58	23	<100
6	98	2	41C	66	150	69.1	51.0	1.02	40	<100
7	48	12	41C	93	200	70.5	52.0	1.02	40	<100
8	80	8	41C	99	210	97.6	72.0	1.40	55	<100
9	86	2	41C	138	280	113.9	84.0	1.40	55	<100
10	56	8	41C	204	400	126.1	93.0	1.55	61	100
11	94	10	41C	204	400	108.5	80.0	1.52	60	<100
12	50	2	41C	227	440	109.8	81.0	1.73	68	100

(ND) - Not Determined
(NT) - Not Tested

Weld W9A (UBR-41, Capsule C, Irradiated & 399 C Annealed) (IAR-1C)

No.	Specimen Number	Layer	Capsule	Test Temp. (°C)	Test Temp. (°F)	Energy (J)	Energy (ft-lb)	Lat. Exp. (mm)	Lat. Exp. (mils)	Shear (%)
1	68	8	41C	-23	-10	32.5	24.0	0.51	20	<100
2	37	1	41C	-7	20	43.4	32.0	0.58	23	<100
3	42	6	41C	-4	25	51.5	38.0	0.81	32	<100
4	49	1	41C	-1	30	32.5	24.0	0.58	23	<100
5	78	6	41C	21	70	65.1	48.0	1.04	41	<100
6	104	8	41C	149	300	136.9	101.0	1.85	73	100
7	64	4	41C	204	400	151.9	112.0	1.47	58	100

(ND) - Not Determined
(NT) - Not Tested

Weld W9A (UBR-41, Capsule A, Annealed & Reirradiated) (IAR-1A)

No.	Specimen Number	Layer	Capsule	Test Temp. (°C)	Test Temp. (°F)	Energy (J)	Energy (ft-lb)	Lat. Exp. (mm)	Lat. Exp. (mils)	Shear (%)
1	73	1	41A	-18	0	19.0	14.0	0.25	10	<100
2	*72	12	41A	-12	10	31.2	23.0	0.43	17	<100
3	79	7	41A	4	40	40.7	30.0	0.66	26	<100
4	95	11	41A	10	50	35.3	26.0	0.51	20	<100
5	66	6	41A	27	80	46.1	34.0	0.84	33	<100
6	52	4	41A	38	100	50.2	37.0	0.66	26	<100
7	69	9	41A	49	120	89.5	66.0	1.24	49	<100
8	88	4	41A	60	140	65.1	48.0	0.97	38	98
9	43	7	41A	77	170	108.5	80.0	1.42	56	<100
10	43	7	41A	77	170	108.5	80.0	1.42	56	<100
11	61	1	41A	138	280	109.8	81.0	1.78	70	98
12	*46	10	41A	166	330	143.7	106.0	1.80	71	97
13	92	8	41A	204	400	124.9	92.1	1.57	62	100
14	38	2	41A	227	440	122.0	90.0	1.57	62	100

* Annealed at 399 C - 168 hrs.
(ND) - Not Determined
(NT) - Not Tested

Weld W9A (UBR-41, Capsule B, Annealed & Reirradiated) (IAR-1B)

No.	Specimen Number	Layer	Capsule	Test Temp. (°C)	Test Temp. (°F)	Energy (J)	Energy (ft-lb)	Lat. Exp. (mm)	Lat. Exp. (mils)	Shear (%)
1	*97	1	41B	-23	-10	27.1	20.0	0.33	13	<100
2	*40	4	41B	(NT)	(NT)	(NT)	(NT)	(ND)	(ND)	<100
3	47	11	41B	4	40	24.4	18.0	0.28	11	<100
4	*103	7	41B	4	40	73.2	54.0	0.94	37	<100
5	90	6	41B	27	80	42.0	31.0	0.71	28	<100
6	*96	12	41B	27	80	73.2	54.0	0.97	38	<100
7	76	4	41B	38	100	43.4	32.0	0.66	26	<100
8	93	9	41B	52	125	69.1	51.0	1.07	42	<100
9	44	8	41B	66	150	85.4	63.0	1.22	48	<100
10	67	7	41B	82	180	84.1	62.0	1.19	47	<100
11	85	1	41B	138	280	103.0	76.0	1.52	60	100
12	62	2	41B	204	400	113.9	84.0	1.60	63	100
13	70	10	41B	227	440	113.9	84.0	1.68	66	100

* Annealed at 399 C - 168 hrs.
(ND) - Not Determined
(NT) - Not Tested

Charpy-V Data from Irradiation Assembly UBR-42

Weld W8A (UBR-42, Capsule C, As-Irradiated) (IAR-2C)

No.	Specimen Number	Layer	Capsule	Test Temp. (°C)	Test Temp. (°F)	Energy (J)	Energy (ft-lb)	Lat. Exp. (mm)	Lat. Exp. (mils)	Shear (%)
1	181	1	42C	66	150	10.8	8.0	0.15	6	<100
2	29	5	42C	82	180	24.4	18.0	0.36	14	<100
3	235	7	42C	88	190	35.3	26.0	0.53	21	<100
4	233	5	42C	93	200	13.6	10.0	0.20	8	<100
5	231	3	42C	102	215	24.4	18.0	0.41	16	<100
6	28	4	42C	110	230	32.5	24.0	0.56	22	<100
7	215	11	42C	116	240	42.0	31.0	0.66	26	<100
8	184	4	42C	132	270	48.8	36.0	0.76	30	<100
9	213	9	42C	177	350	54.2	40.0	0.86	34	100
10	26	2	42C	204	400	47.5	35.0	0.76	30	99
11	212	8	42C	221	430	51.5	38.0	0.94	37	100

(ND) - Not Determined
(NT) - Not Tested

Weld W8A (UBR-42, Capsule C, 399C Annealed) (IAR-2C)

No.	Specimen Number	Layer	Capsule	Test Temp. (°C)	Test Temp. (°F)	Energy (J)	Energy (ft-lb)	Lat. Exp. (mm)	Lat. Exp. (mils)	Shear (%)
1	16	4	42C	-23	-10	8.1	6.0	(ND)	(ND)	<100
2	255	3	42C	(NT)	(NT)	(NT)	(NT)	(ND)	(ND)	<100
3	190	10	42C	4	40	29.8	22.0	(ND)	(ND)	<100
4	25	1	42C	32	90	14.9	11.0	0.30	12	<100
5	257	5	42C	49	120	35.3	26.0	0.58	23	<100
6	192	12	42C	66	150	48.8	36.0	0.84	33	<100
7	187	7	42C	77	170	63.7	47.0	1.12	44	<100
8	260	8	42C	143	290	75.9	56.0	1.12	44	98

(ND) - Not Determined
(NT) - Not Tested

Weld W8A (UBR-42, Capsule A, Annealed & Reirradiated) (IAR-2A)

No.	Specimen Number	Layer	Capsule	Test Temp. (°C)	Test Temp. (°F)	Energy (J)	Energy (ft-lb)	Lat. Exp. (mm)	Lat. Exp. (mils)	Shear (%)
1	*229	1	42A	-1	30	28.5	21.0	(ND)	(ND)	<100
2	256	4	42A	27	80	8.1	6.0	(ND)	(ND)	<100
3	*206	2	42A	27	80	51.5	38.0	(ND)	(ND)	<100
4	225	9	42A	49	120	27.1	20.0	0.41	16	<100
5	217	1	42A	66	150	21.7	16.0	0.36	14	<100
6	222	6	42A	71	160	30.0	22.1	0.46	18	<100
7	194	2	42A	88	190	32.5	24.0	0.56	22	<100
8	199	7	42A	99	210	43.4	32.0	0.76	30	<100
9	228	12	42A	104	220	43.4	32.0	0.71	28	<100
10	244	4	42A	116	240	46.1	34.0	0.81	32	<100
11	251	11	42A	149	300	51.5	38.0	0.91	36	97
12	248	8	42A	210	410	54.2	40.0	0.94	37	99
13	202	12	42A	260	500	46.1	34.0	1.04	41	100

* Annealed at 399 C - 168 hrs.
(ND) - Not Determined
(NT) - Not Tested

Weld W8A (UBR-42, Capsule B, Annealed & Reirradiated) (IAR-2B)

No.	Specimen Number	Layer	Capsule	Test Temp.		Energy		Lat. Exp.		Shear
				(°C)	(°F)	(J)	(ft-lb)	(mm)	(mils)	(%)
1	84	12	42B	27	80	9.5	7.0	(ND)	(ND)	<100
2	115	7	42B	54	130	28.5	21.0	0.43	17	<100
3	117	9	42B	66	150	29.8	22.0	0.53	21	<100
4	14	2	42B	82	180	27.1	20.0	0.41	16	<100
5	126	6	42B	88	190	(NT)	(NT)	(ND)	(ND)	<100
6	130	10	42B	93	200	25.8	19.0	0.43	17	<100
7	128	8	42B	99	210	44.7	33.0	0.76	30	<100
8	112	4	42B	104	220	36.6	27.0	0.58	23	<100
9	119	11	42B	110	230	47.5	35.0	0.76	30	<100
10	122	2	42B	121	250	43.4	32.0	0.74	29	<100
11	20	8	42B	149	300	52.9	39.0	0.89	35	98
12	132	12	42B	199	390	50.2	37.0	0.89	35	100
13	109	1	42B	216	420	51.5	38.0	0.86	34	100

(ND) - Not Determined
(NT) - Not Tested

Weld W9A (UBR-42, Capsule C, As-Irradiated) (IAR-2C)

No.	Specimen Number	Layer	Capsule	Test Temp.		Energy		Lat. Exp.		Shear
				(°C)	(°F)	(J)	(ft-lb)	(mm)	(mils)	(%)
1	142	10	42C	10	50	17.6	13.0	0.20	8	<100
2	74	2	42C	27	80	32.5	24.0	0.48	19	<100
3	20	8	42C	43	110	38.0	28.0	0.56	22	<100
4	117	9	42C	60	140	59.7	44.0	0.84	33	<100
5	54	6	42C	66	150	67.8	50.0	0.99	39	<100
6	77	5	42C	66	150	36.6	27.0	0.53	21	<100
7	111	3	42C	88	190	69.1	51.0	1.04	41	<100
8	7	7	42C	104	220	100.3	74.0	1.22	48	<100
9	144	12	42C	132	270	97.6	72.0	1.42	56	<100
10	147	3	42C	204	400	105.8	78.0	1.57	62	99
11	125	5	42C	232	450	103.0	76.0	1.75	69	99

(ND) - Not Determined
(NT) - Not Tested

Weld W9A (UBR-42, Capsule C, Irradiated & 399 C Annealed) (IAR-2C)

No.	Specimen Number	Layer	Capsule	Test Temp. (°C)	Test Temp. (°F)	Energy (J)	Energy (ft-lb)	Lat. Exp. (mm)	Lat. Exp. (mils)	Shear (%)
1	102	6	42C	-29	-20	21.7	16.0	0.30	12	<100
2	119	11	42C	-12	10	38.0	28.0	0.53	21	<100
3	101	5	42C	4	40	51.5	38.0	0.76	30	<100
4	127	7	42C	32	90	103.0	76.0	1.42	56	<100
5	8	8	42C	71	160	124.7	92.0	1.73	68	<100
6	123	3	42C	160	320	128.8	95.0	1.65	65	99
7	4	4	42C	182	360	139.6	103.0	2.01	79	100
8	153	9	42C	204	400	146.4	108.0	1.65	65	97

(ND) - Not Determined
(NT) - Not Tested

Weld W9A (UBR-42, Capsule A, Annealed & Reirradiated) (IAR-2A)

No.	Specimen Number	Layer	Capsule	Test Temp. (°C)	Test Temp. (°F)	Energy (J)	Energy (ft-lb)	Lat. Exp. (mm)	Lat. Exp. (mils)	Shear (%)
1	133	1	42A	-18	0	17.6	13.0	0.23	9	<100
2	*138	6	42A	-18	0	71.9	53.0	0.99	39	<100
3	81	9	42A	4	40	38.0	28.0	0.51	20	<100
4	*115	7	42A	16	60	138.3	102.0	1.68	66	<100
5	122	2	42A	21	70	31.2	23.0	0.46	18	<100
6	160	4	42A	27	80	33.9	25.0	0.53	21	<100
7	58	10	42A	43	110	54.2	40.0	0.84	33	<100
8	110	2	42A	66	150	48.8	36.0	0.81	32	<100
9	28	4	42A	68	155	75.9	56.0	1.17	46	<100
10	107	11	42A	82	180	94.9	70.0	1.32	52	<100
11	164	8	42A	99	210	113.9	84.0	1.47	58	<100
12	145	1	42A	143	290	109.8	81.0	1.75	69	100
13	84	12	42A	210	410	108.5	80.0	1.80	71	100

* Annealed at 399 C - 168 hrs.
(ND) - Not Determined
(NT) - Not Tested

Weld W9A (UBR-42, Capsule B, Annealed & Reirradiated) (IAR-2B)

No.	Specimen Number	Layer	Capsule	Test Temp. (°C)	Test Temp. (°F)	Energy (J)	Energy (ft-lb)	Lat. Exp. (mm)	Lat. Exp. (mils)	Shear (%)
1	*206	2	42B	-40	-40	27.1	20.0	(ND)	(ND)	<100
2	208	4	42B	-12	10	16.3	12.0	0.18	7	<100
3	212	8	42B	4	40	32.5	24.0	0.41	16	<100
4	*143	11	42B	16	60	132.9	98.0	(ND)	(ND)	<100
5	199	7	42B	27	80	32.5	24.0	0.48	19	<100
6	156	12	42B	43	110	39.3	29.0	0.53	21	<100
7	183	3	42B	60	140	55.6	41.0	0.89	35	<100
8	187	7	42B	77	170	86.8	64.0	1.27	50	<100
9	181	1	42B	88	190	84.1	62.0	1.24	49	<100
10	185	5	42B	107	225	90.8	67.0	1.40	55	<100
11	141	9	42B	149	300	109.8	81.0	1.50	59	100
12	193	1	42B	204	400	103.0	76.0	1.57	62	100
13	154	10	42B	210	410	103.0	76.0	1.88	74	100

* Annealed at 399 C - 168 hrs.
(ND) - Not Determined
(NT) - Not Tested

Charpy-V Data from Irradiation Assembly UBR-43

Weld W8A (UBR-43, Capsule C, As-Irradiated) (IAR-3C)

No.	Specimen Number	Layer	Capsule	Test Temp. (°C)	Test Temp. (°F)	Energy (J)	Energy (ft-lb)	Lat. Exp. (mm)	Lat. Exp. (mils)	Shear (%)
1	422	2	43C	71	160	10.8	8.0	0.15	6	<100
2	239	11	43C	93	200	24.4	18.0	0.38	15	<100
3	385	1	43C	99	210	24.4	18.0	0.43	17	<100
4	80	8	43C	110	230	46.1	34.0	0.76	30	<100
5	264	12	43C	113	235	32.5	24.0	0.46	18	<100
6	424	4	43C	127	260	38.0	28.0	0.64	25	<100
7	426	6	43C	132	270	38.0	28.0	0.56	22	<100
8	209	5	43C	160	320	43.4	32.0	0.71	28	97
9	391	7	43C	160	320	42.0	31.0	0.64	25	100
10	237	9	43C	204	400	48.8	36.0	(ND)	(ND)	100
11	207	3	43C	216	420	46.1	34.0	0.87	34	100
12	262	10	43C	260	500	46.1	34.0	0.76	30	100

(ND) - Not Determined
(NT) - Not Tested

Weld W8A (UBR-43, Capsule C, Irradiated & 399 C Annealed) (IAR-3C)

No.	Specimen Number	Layer	Capsule	Test Temp. (°C)	Test Temp. (°F)	Energy (J)	Energy (ft-lb)	Lat. Exp. (mm)	Lat. Exp. (mils)	Shear (%)
1	^387	3	43C	10	50	38.0	28.0	(ND)	(ND)	<100
2	^409	1	43C	32	90	46.1	34.0	(ND)	(ND)	<100
3	*389	5	43C	32	90	21.7	16.0	0.36	14	<100
4	*415	7	43C	66	150	63.7	47.0	(ND)	(ND)	<100
5	*428	8	43C	82	180	63.7	47.0	1.02	40	<100
6	^413	5	43C	160	320	86.8	64.0	(ND)	(ND)	<100
7	*411	3	43C	204	400	67.8	50.0	1.14	45	98

* Annealed at 399 C - 168 hrs.
^ Annealed at 454 C - 168 hrs.
(ND) - Not Determined
(NT) - Not Tested

Weld W9A (UBR-43, Capsule C, As-Irradiated) (IAR-3C)

No.	Specimen Number	Layer	Capsule	Test Temp.		Energy		Lat. Exp.		Shear
				(°C)	(°F)	(J)	(ft-lb)	(mm)	(mils)	(%)
1	186	6	43C	(NT)	(NT)	(NT)	(NT)	(ND)	(ND)	
2	188	8	43C	2	35	8.1	6.0	0.05	2	<100
3	210	6	43C	21	70	29.8	22.0	0.46	18	<100
4	207	3	43C	43	110	32.5	24.0	0.53	21	<100
5	169	1	43C	49	120	32.5	24.0	0.46	18	<100
6	218	2	43C	71	160	46.1	34.0	0.74	29	<100
7	192	12	43C	93	200	59.7	44.0	0.94	37	<100
8	223	7	43C	93	200	71.9	53.0	1.07	42	<100
9	177	9	43C	121	250	103.0	76.0	1.60	63	<100
10	173	5	43C	160	320	82.7	61.0	1.30	51	98
11	190	10	43C	204	400	93.6	69.0	1.47	58	99
12	184	4	43C	216	420	103.0	76.0	1.30	51	99

(ND) - Not Determined
(NT) - Not Tested

Weld W9A (UBR-43, Capsule C, Irradiated & 399 C Annealed) (IAR-3C)

No.	Specimen Number	Layer	Capsule	Test Temp. (°C)	Test Temp. (°F)	Energy (J)	Energy (ft-lb)	Lat. Exp. (mm)	Lat. Exp. (mils)	Shear (%)
1	^171	3	43C	-34	-30	35.3	26.0	(ND)	(ND)	<100
2	^182	2	43C	-18	0	78.6	58.0	1.07	42	<100
3	*179	11	43C	-1	30	54.2	40.0	0.76	30	<100
4	*175	7	43C	49	120	104.4	77.0	(ND)	(ND)	<100
5	^168	12	43C	182	360	164.1	121.0	(ND)	(ND)	<100
6	*201	9	43C	204	400	151.9	112.0	1.98	78	98

* Annealed at 399 C - 168 hrs.
^ Annealed at 454 C - 168 hrs.
(ND) - Not Determined
(NT) - Not Tested

Charpy-V Data from Irradiation Assembly UBR-55

Weld W8A (UBR-55, Capsule C, As-Irradiated) (IAR-6C)

No.	Specimen Number	Layer	Capsule	Test Temp. (°C)	(°F)	Energy (J)	(ft-lb)	Lat. Exp. (mm)	(mils)	Shear (%)
1	394	10	55C	(NT)	(NT)	(NT)	(NT)	(ND)	(ND)	
2	432	12	55C	66	150	16.3	12.0	0.20	8	<100
3	95	11	55C	93	200	24.4	18.0	0.36	14	<100
4	397	1	55C	93	200	24.4	18.0	0.36	14	<100
5	399	3	55C	121	250	31.2	23.0	0.48	19	<100
6	116	8	55C	121	250	44.7	33.0	0.71	28	<100
7	345	9	55C	138	280	48.8	36.0	0.79	31	100
8	129	9	55C	149	300	46.1	34.0	0.81	32	100
9	100	4	55C	204	400	47.5	35.0	0.74	29	100
10	127	7	55C	204	400	(NT)	(NT)	(ND)	(ND)	100
11	120	12	55C	204	400	46.1	34.0	0.76	30	100
12	106	10	55C	288	550	46.1	34.0	0.81	32	100

(ND) - Not Determined
(NT) - Not Tested

Weld W8A (UBR-55, Capsule C, Irradiated & 399 C Annealed) (IAR-6C)

No.	Specimen Number	Layer	Capsule	Test Temp. (°C)	Test Temp. (°F)	Energy (J)	Energy (ft-lb)	Lat. Exp. (mm)	Lat. Exp. (mils)	Shear (%)
1	417	9	55C	4	40	31.2	23.0	0.51	20	<100
2	407	11	55C	27	80	29.8	22.0	0.46	18	<100
3	98	2	55C	54	130	39.3	29.0	0.61	24	<100
4	430	10	55C	71	160	42.0	31.0	0.69	27	<100
5	396	12	55C	116	240	(NT)	(NT)	(ND)	(ND)	<100
6	347	11	55C	204	400	71.9	53.0	1.14	45	100
7	102	7	55C	204	400	73.2	54.0	1.40	55	100

(ND) - Not Determined
(NT) - Not Tested

Weld W8A (UBR-55, Capsule A, Annealed & Reirradiated) (IAR-6A)

No.	Specimen Number	Layer	Capsule	Test Temp. (°C)	Test Temp. (°F)	Energy (J)	Energy (ft-lb)	Lat. Exp. (mm)	Lat. Exp. (mils)	Shear (%)
1	107	11	55A	49	120	21.7	16.0	0.30	12	<100
2	393	9	55A	60	140	24.4	18.0	0.66	26	<100
3	92	8	55A	66	150	36.6	27.0	(ND)	(ND)	<100
4	245	5	55A	79	175	(NT)	(NT)	(ND)	(ND)	<100
5	118	10	55A	88	190	25.8	19.0	(ND)	(ND)	<100
6	124	4	55A	93	200	27.1	20.0	0.38	15	<100
7	96	12	55A	104	220	35.3	26.0	0.53	21	<100
8	93	9	55A	116	240	55.6	41.0	0.91	36	97
9	403	7	55A	116	240	51.5	38.0	(ND)	(ND)	<100
10	419	11	55A	127	260	56.9	42.0	0.84	33	98
11	408	12	55A	160	320	51.5	38.0	0.84	33	100
12	97	1	55A	204	400	47.5	35.0	(ND)	(ND)	100
13	406	10	55A	204	400	51.5	38.0	0.81	32	100

(ND) - Not Determined
(NT) - Not Tested

Weld W8A (UBR-55, Capsule B, Annealed & Reirradiated) (IAR-6B)

No.	Specimen Number	Layer	Capsule	Test Temp.		Energy		Lat. Exp.		Shear
				(°C)	(°F)	(J)	(ft-lb)	(mm)	(mils)	(%)
1	418	10	55B	38	100	21.7	16.0	0.30	12	<100
2	105	9	55B	38	100	27.1	20.0	0.41	16	<100
3	405	9	55B	60	140	39.3	29.0	0.69	27	<100
4	104	8	55B	60	140	36.6	27.0	0.64	25	<100
5	401	5	55B	82	180	32.5	24.0	0.48	19	<100
6	420	12	55B	88	190	38.0	28.0	0.64	25	<100
7	94	10	55B	93	200	29.8	22.0	0.48	19	<100
8	108	12	55B	110	230	46.1	34.0	0.76	30	<100
9	243	3	55B	121	250	50.2	37.0	0.84	33	<100
10	395	11	55B	149	300	59.7	44.0	0.99	39	100
11	121	1	55B	204	400	52.9	39.0	0.94	37	100
12	427	7	55B	204	400	54.4	40.1	0.97	38	100
13	131	11	55B	288	550	63.7	47.0	1.07	42	100

(ND) - Not Determined
(NT) - Not Tested

Weld W9A (UBR-55, Capsule C, As-Irradiated) (IAR-6C)

No.	Specimen Number	Layer	Capsule	Test Temp. (°C)	Test Temp. (°F)	Energy (J)	Energy (ft-lb)	Lat. Exp. (mm)	Lat. Exp. (mils)	Shear (%)
1	165	9	55C	-1	30	16.3	12.0	0.13	5	<100
2	348	12	55C	16	60	9.5	7.0	0.13	5	<100
3	343	7	55C	38	100	39.3	29.0	0.56	22	<100
4	311	11	55C	43	110	31.2	23.0	0.41	16	<100
5	337	1	55C	54	130	35.3	26.0	0.48	19	<100
6	225	9	55C	66	150	56.9	42.0	0.81	32	<100
7	314	2	55C	66	150	59.7	44.0	0.89	35	<100
8	335	11	55C	93	200	61.0	45.0	0.91	36	<100
9	350	6	55C	116	240	85.4	63.0	1.22	48	<100
10	130	11	55C	177	350	97.6	72.0	1.57	62	100
11	327	3	55C	204	400	99.0	73.0	1.40	55	100
12	215	11	55C	288	550	107.1	79.0	1.68	66	100

(ND) - Not Determined
(NT) - Not Tested

Weld W9A (UBR-55, Capsule C, Irradiated & 399 C Annealed) (IAR-6C)

No.	Specimen Number	Layer	Capsule	Test Temp. (°C)	Test Temp. (°F)	Energy (J)	Energy (ft-lb)	Lat. Exp. (mm)	Lat. Exp. (mils)	Shear (%)
1	120	12	55C	-18	0	29.8	22.0	0.53	21	<100
2	345	9	55C	-1	30	(NT)	(NT)	(ND)	(ND)	<100
3	322	10	55C	4	40	46.1	34.0	0.71	28	<100
4	329	5	55C	21	70	56.9	42.0	0.86	34	<100
5	227	11	55C	71	160	115.2	85.0	1.65	65	<100
6	320	8	55C	204	400	149.1	110.0	1.98	78	100
7	316	4	55C	204	400	138.3	102.0	2.11	83	100

(ND) - Not Determined
(NT) - Not Tested

Weld W9A (UBR-55, Capsule A, Annealed & Reirradiated) (IAR-6A)

No.	Specimen Number	Layer	Capsule	Test Temp. (°C)	Test Temp. (°F)	Energy (J)	Energy (ft-lb)	Lat. Exp. (mm)	Lat. Exp. (mils)	Shear (%)
1	321	9	55A	-1	30	10.8	8.0	(ND)	(ND)	<100
2	328	4	55A	4	40	25.8	19.0	0.33	13	<100
3	326	2	55A	10	50	31.2	23.0	(ND)	(ND)	<100
4	347	11	55A	27	80	39.3	29.0	0.56	22	<100
5	319	7	55A	38	100	55.6	41.0	(ND)	(ND)	<100
6	263	11	55A	43	110	46.1	34.0	0.66	26	<100
7	216	12	55A	60	140	59.7	44.0	0.91	36	<100
8	332	8	55A	66	150	81.3	60.0	(ND)	(ND)	<100
9	313	1	55A	88	190	59.7	44.0	(ND)	(ND)	<100
10	214	10	55A	93	200	85.4	63.0	1.22	48	<100
11	324	12	55A	160	320	119.3	88.0	1.73	68	100
12	342	6	55A	204	400	113.9	84.0	(ND)	(ND)	100
13	334	10	55A	204	400	123.4	91.0	1.75	69	100

(ND) - Not Determined
(NT) - Not Tested

Weld W9A (UBR-55, Capsule B, Annealed & Reirradiated) (IAR-6B)

No.	Specimen Number	Layer	Capsule	Test Temp. (°C)	Test Temp. (°F)	Energy (J)	Energy (ft-lb)	Lat. Exp. (mm)	Lat. Exp. (mils)	Shear (%)
1	333	9	55B	(NT)	(NT)	(NT)	(NT)	(ND)	(ND)	
2	331	7	55B	-7	20	28.5	21.0	0.41	16	<100
3	340	4	55B	10	50	14.9	11.0	0.25	10	<100
4	287	11	55B	13	55	43.4	32.0	0.56	22	<100
5	336	12	55B	27	80	40.7	30.0	0.56	22	<100
6	338	2	55B	38	100	55.6	41.0	0.81	32	<100
7	228	12	55B	60	140	(NT)	(NT)	(ND)	(ND)	<100
8	318	6	55B	66	150	75.9	56.0	1.55	61	<100
9	323	11	55B	93	200	96.3	71.0	1.42	56	<100
10	344	8	55B	160	320	119.3	88.0	1.80	71	100
11	310	10	55B	177	350	118.0	87.0	1.68	66	100
12	325	1	55B	204	400	124.7	92.0	1.45	57	99
13	226	10	55B	288	550	130.2	96.0	1.88	74	100

(ND) - Not Determined
(NT) - Not Tested

APPENDIX E

Computer Curve Fittings of Charpy-V Test Results
(Specimen Energy Absorption vs. Temperature)

OVERVIEW

The data curve fitting procedure employed the hyperbolic tangent (Tanh) curve fitting method as given by:

$$C_V = A + B \tanh \frac{T - T_o}{C}$$

Parameters A, B, C and T_o are determined from non-linear regression analysis.

The quality of the fit to each data set generally depends upon the number of specimens tested and the availability of data defining the upper shelf and lower shelf for the data set. For many of the present data sets, both requirements are satisfied and an acceptable curve fit results. In other cases, either few tests were conducted or the data did not adequately define the lower shelf for the data set. For such cases, the lower shelf from a standard Tanh fit gives a lower shelf which is either above 27 J (20 ft-lb) or negative. Since such results are not satisfactory from either engineering or aesthetic standpoints, two modified curve fits can be applied.

Case A is the result obtained when four fictitious data points with 7 J (5 ft-lb) of energy absorption are added at a temperature that is 28°C (50°F) below the intercept with the abscissa, of a line representing a linearized transition region. The line in this case is an eyeball fit to the data; the choice of a larger temperature shift (up to 56°C or 100°F) was found not to infuence the result appreciably. Case B represents use of a fixed lower shelf of 7 J (5 ft-lb); this lower shelf is attained at a temperature of -∞.

The use of the modified curve fits serve to force the curves to a reasonably low, positive value in the lower shelf region. This device is particularly useful for those cases where data are lacking in the lower shelf region for guiding the computer in its setting of bounding conditions. It should be noted that the American Society for Testing and Materials has not issued a standard method or a standard guide for curve-fitting C_V data for the irradiated condition.

Within this appendix, the first curvefit sheet which appears for each data set represents a standard evaluation using the Tanh equation. The second curvefit sheet if present, gives the Case A results. For Case A, the fictitious data points are denoted by "O" on the graph and "*" in the data tabulation on the curvefit sheet. For both sheets, table entries marked "Test Point Not Included" identify test points for the postirradiation annealed condition and therefore are deleted here. The data for these tests are given in Appendix D.

Computer Curve Fittings of Unirradiated Condition Data

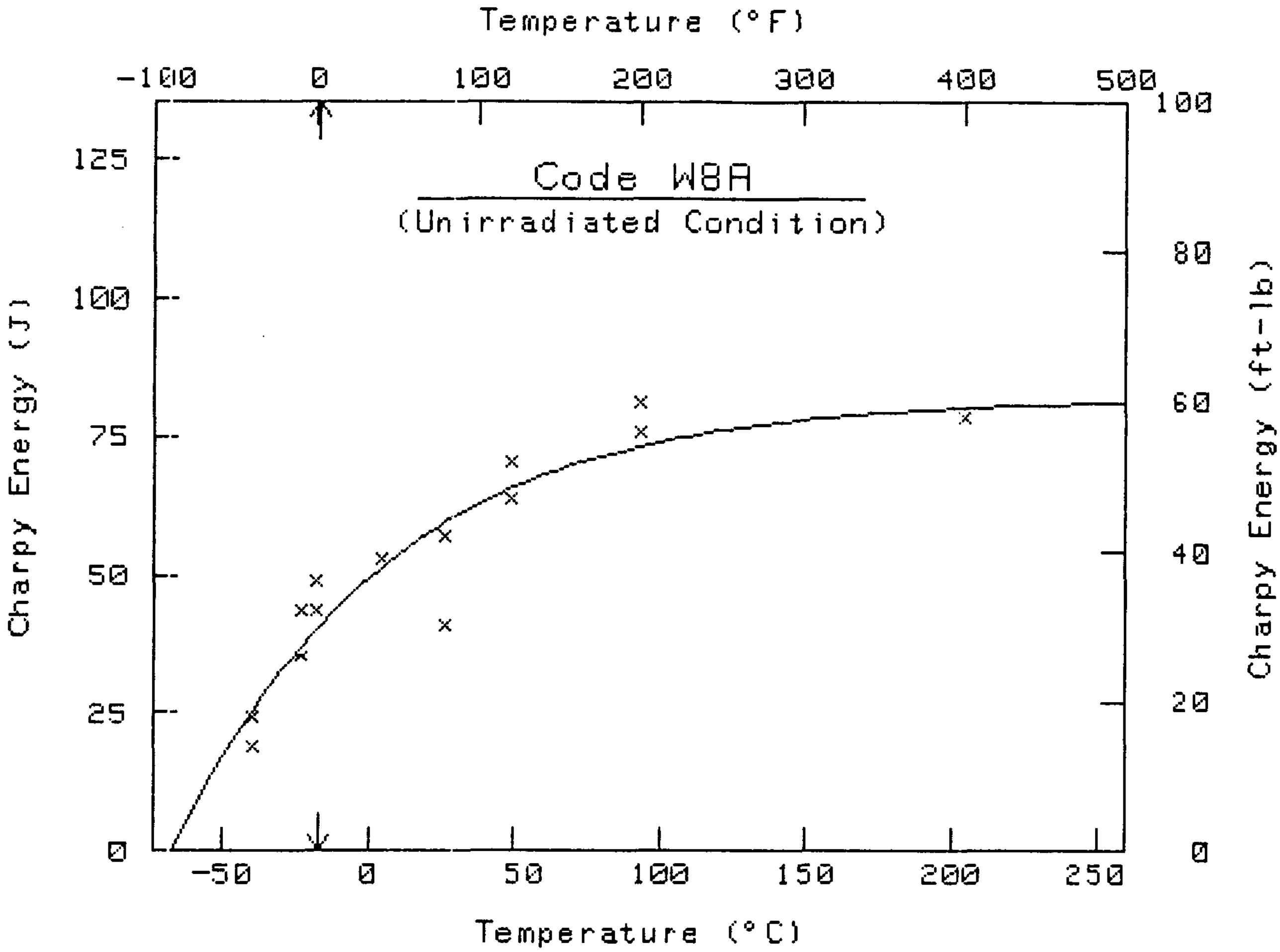

****

$$Cv = A + B \tanh[(T - To)/C]$$

		English	Metric
A	=	-355.03 ft-lb	-481.36 J
B	=	415.54 ft-lb	563.39 J
C	=	251.15 °F	139.53 °C
To	=	-408.93 °F	-244.96 °C

Cv = 30 ft-lb (41 J) at T = 1.4 °F -17.0 °C

Upper Shelf Energy = 60.5 ft-lb 82.0 J

****

PT #	Temp (°F)	Energy (ft-lb)
1	-40	14.0
2	-40	18.0
3	-10	26.0
4	-10	32.0
5	0	32.0
6	0	36.0
7	40	39.0
8	80	42.0
9	80	30.0
10	120	47.0
11	120	52.0
12	200	60.0
13	200	56.0
14	400	58.0
15	400	58.0

O = Fictitious Point Added * = Test Point Not Included

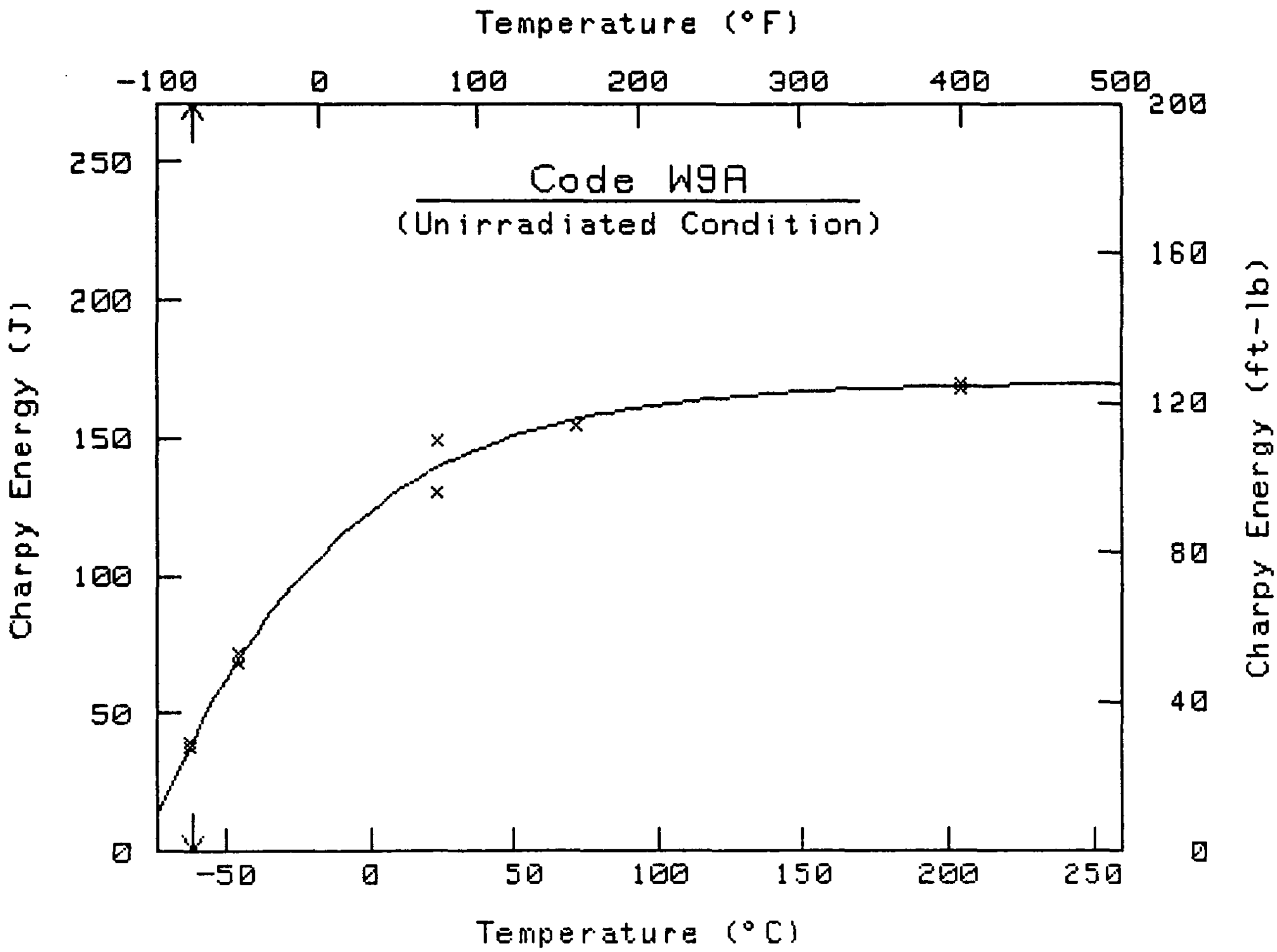

****

$C_v = A + B \tanh[(T - T_o)/C]$

		English	Metric
A	=	-395.47 ft-lb	-536.18 J
B	=	520.90 ft-lb	706.25 J
C	=	204.01 °F	113.34 °C
To	=	-312.32 °F	-191.29 °C

	English	Metric
Cv = 30 ft-lb (41 J) at T =	-78.3 °F	-61.3 °C
Upper Shelf Energy =	125.4 ft-lb	170.1 J

****

PT #	Temp (°F)	Energy (ft-lb)
1	-80	29.0
2	-80	28.0
3	-50	53.0
4	-50	50.0
5	75	96.0
6	75	110.0
7	160	114.0
8	400	125.0
9	400	125.0
10	400	124.0

O = Fictitious Point Added   * = Test Point Not Included

Computer Curve Fittings of Data from Irradiation Assembly UBR-41

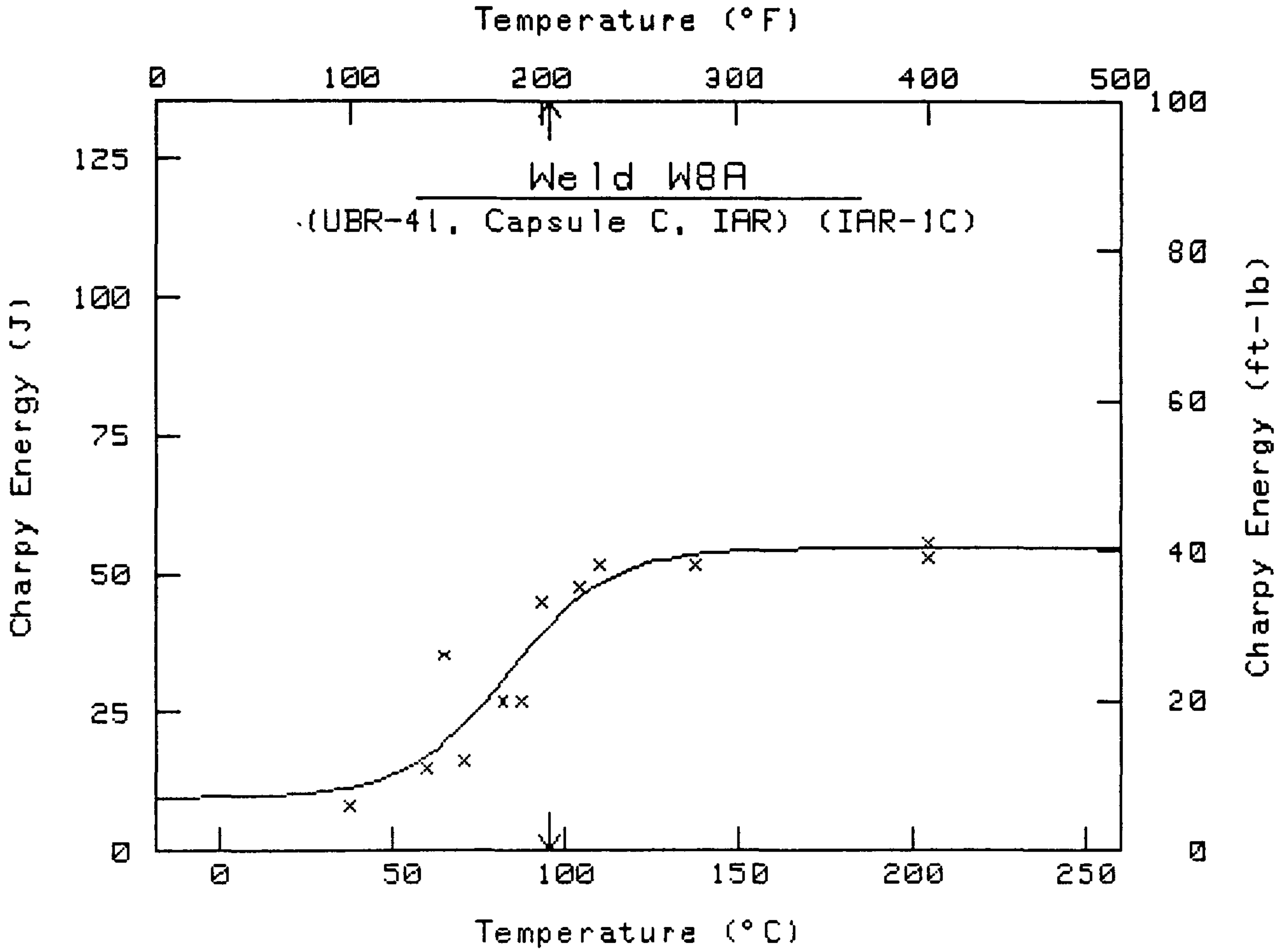

Cv = A + B tanh[(T - To)/C]

		English	Metric
A	=	23.71 ft-lb	32.15 J
B	=	16.61 ft-lb	22.52 J
C	=	52.71 °F	29.28 °C
To	=	183.21 °F	84.00 °C
Cv = 30 ft-lb (41 J) at T	=	204.2 °F	95.7 °C
Upper Shelf Energy	=	40.3 ft-lb	54.7 J

PT #	Temp (°F)	Energy (ft-lb)
1	100	6.0
2	140	11.0
3	150	26.0
4	160	12.0
5	180	20.0
6	190	20.0
7	200	33.0
8	220	35.0
9	230	38.0
10	280	38.0
11	400	39.0
12	400	41.0

O = Fictitious Point Added * = Test Point Not Included

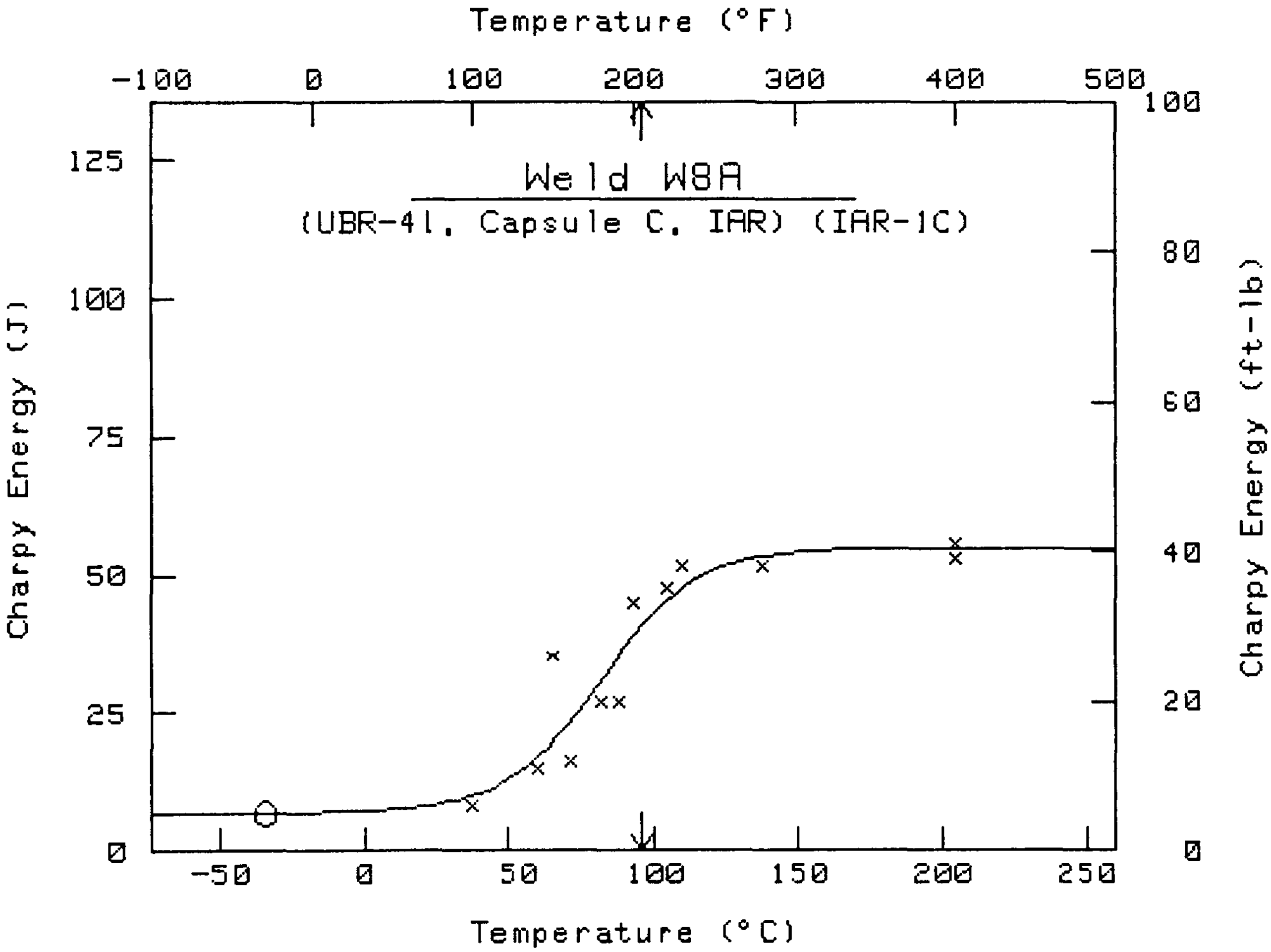

****

$$C_v = A + B \tanh[(T - T_o)/C]$$

		English	Metric
A	=	22.79 ft-lb	30.89 J
B	=	17.68 ft-lb	23.98 J
C	=	58.68 °F	32.60 °C
To	=	179.12 °F	81.73 °C

Cv = 30 ft-lb (41 J) at T =	204.5 °F	95.9 °C
Upper Shelf Energy =	40.5 ft-lb	54.9 J

****

PT #	Temp (°F)	Energy (ft-lb)	PT #	Temp (°F)	Energy (ft-lb)
1	100	6.0	9	230	38.0
2	140	11.0	10	280	38.0
3	150	26.0	11	400	39.0
4	160	12.0	12	400	41.0
5	180	20.0	13 O	-30	5.0
6	190	20.0	14 O	-30	5.0
7	200	33.0	15 O	-30	5.0
8	220	35.0	16 O	-30	5.0

O = Fictitious Point Added * = Test Point Not Included

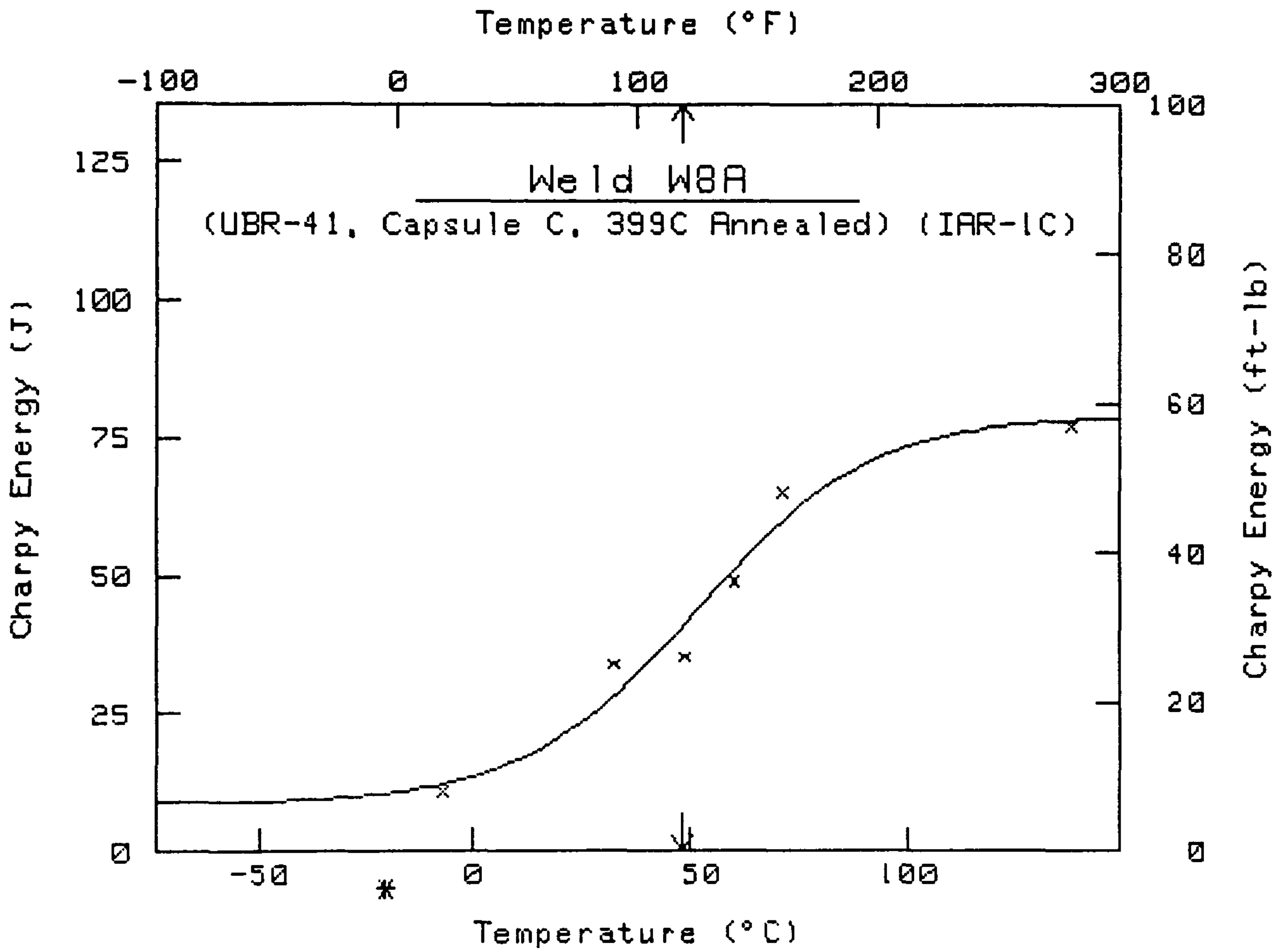

****

Cv = A + B tanh[(T - To)/C]

		English	Metric
A	=	32.42 ft-lb	43.96 J
B	=	26.00 ft-lb	35.25 J
C	=	71.90 °F	39.94 °C
To	=	125.03 °F	51.68 °C

Cv = 30 ft-lb (41 J) at T	=	118.3 °F	48.0 °C
Upper Shelf Energy	=	58.4 ft-lb	79.2 J

****

PT #		Temp (°F)	Energy (ft-lb)
1	*	-5	-5.0
2		20	8.0
3		90	25.0
4		120	26.0
5		140	36.0
6		160	48.0
7		280	57.0

O = Fictitious Point Added   * = Test Point Not Included

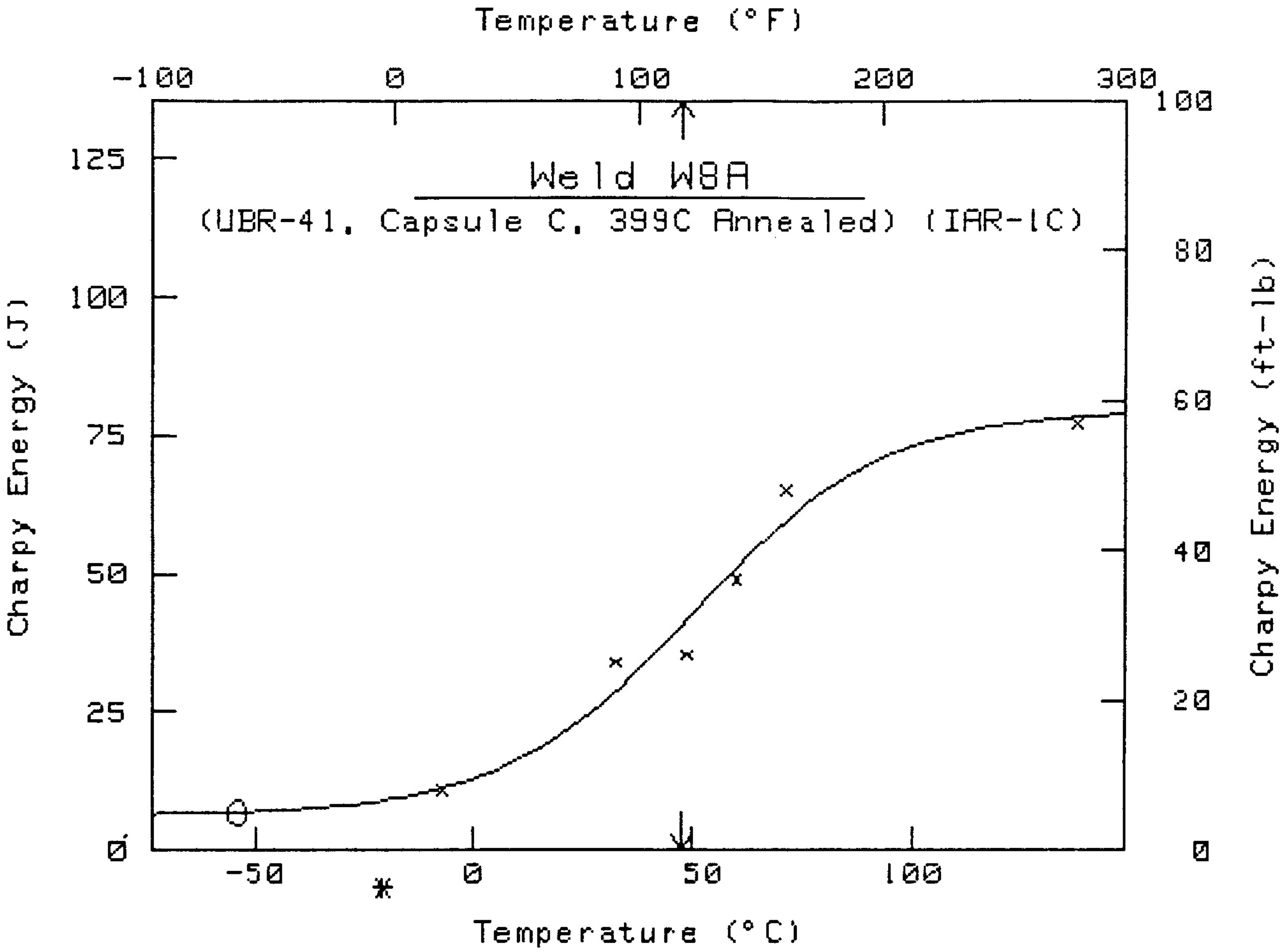

****

Cv = A + B tanh[(T - To)/C]

		English	Metric
A	=	31.69 ft-lb	42.96 J
B	=	27.00 ft-lb	36.61 J
C	=	77.58 °F	43.10 °C
To	=	122.34 °F	50.19 °C

Cv = 30 ft-lb (41 J) at T	=	117.5 °F	47.5 °C
Upper Shelf Energy	=	58.7 ft-lb	79.6 J

****

PT #		Temp (°F)	Energy (ft-lb)
1	*	-5	-5.0
2		20	8.0
3		90	25.0
4		120	26.0
5		140	36.0
6		160	48.0
7		280	57.0
8	O	-65	5.0
9	O	-65	5.0
10	O	-65	5.0
11	O	-65	5.0

O = Fictitious Point Added   * = Test Point Not Included.

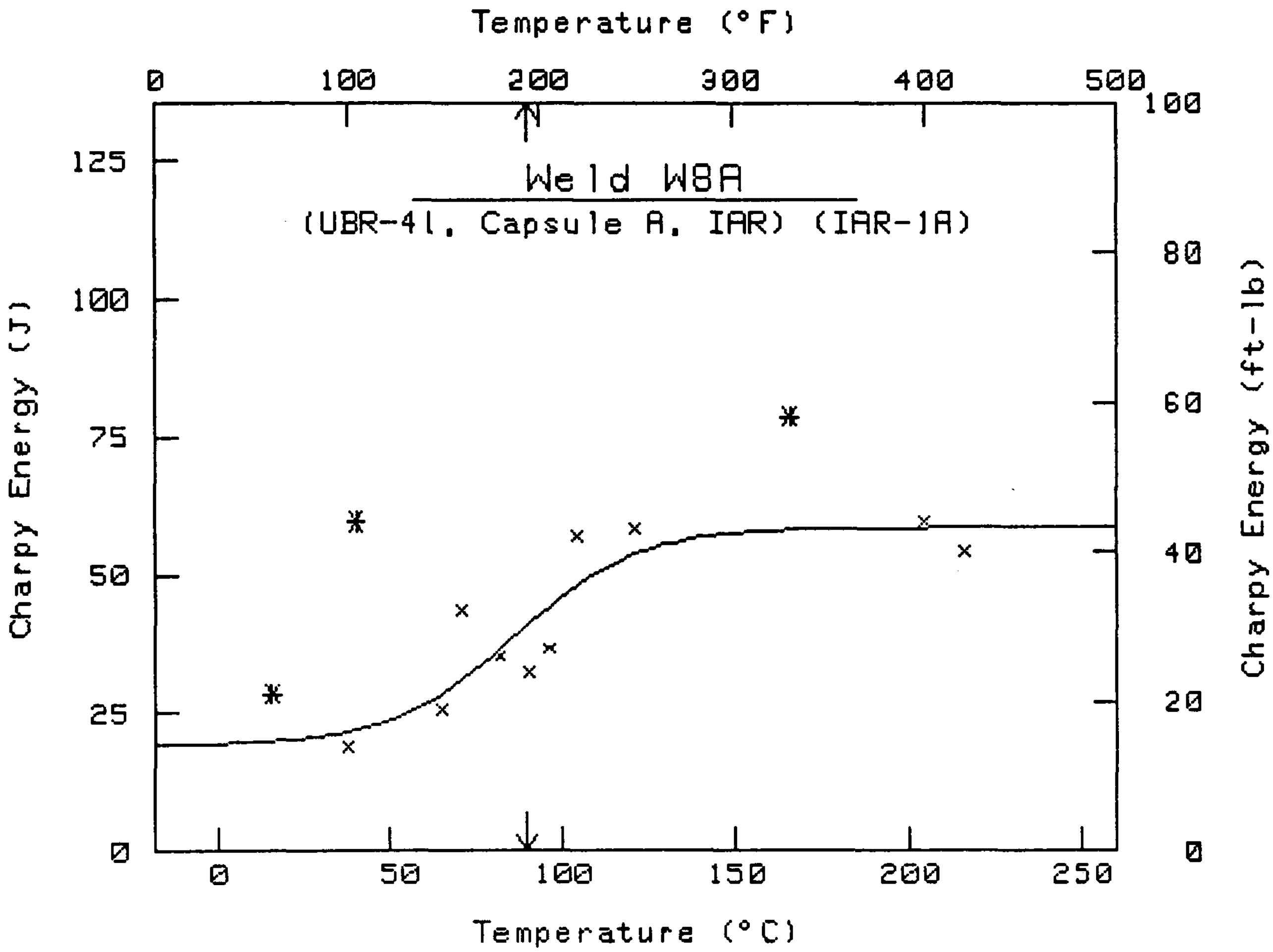

****

$$Cv = A + B \tanh[(T - To)/C]$$

		English	Metric
A	=	28.71 ft-lb	38.92 J
B	=	14.52 ft-lb	19.69 J
C	=	63.46 °F	35.26 °C
To	=	187.76 °F	86.53 °C

Cv = 30 ft-lb (41 J) at T	=	193.4 °F	89.7 °C
Upper Shelf Energy	=	43.2 ft-lb	58.6 J

****

PT #		Temp (°F)	Energy (ft-lb)
1	*	60	21.0
2		100	14.0
3	*	105	44.0
4		150	19.0
5		160	32.0
6		180	26.0
7		195	24.0
8		205	27.0
9		220	42.0
10		250	43.0
11	*	330	58.0
12		400	44.0
13		420	40.0

O = Fictitious Point Added   * = Test Point Not Included

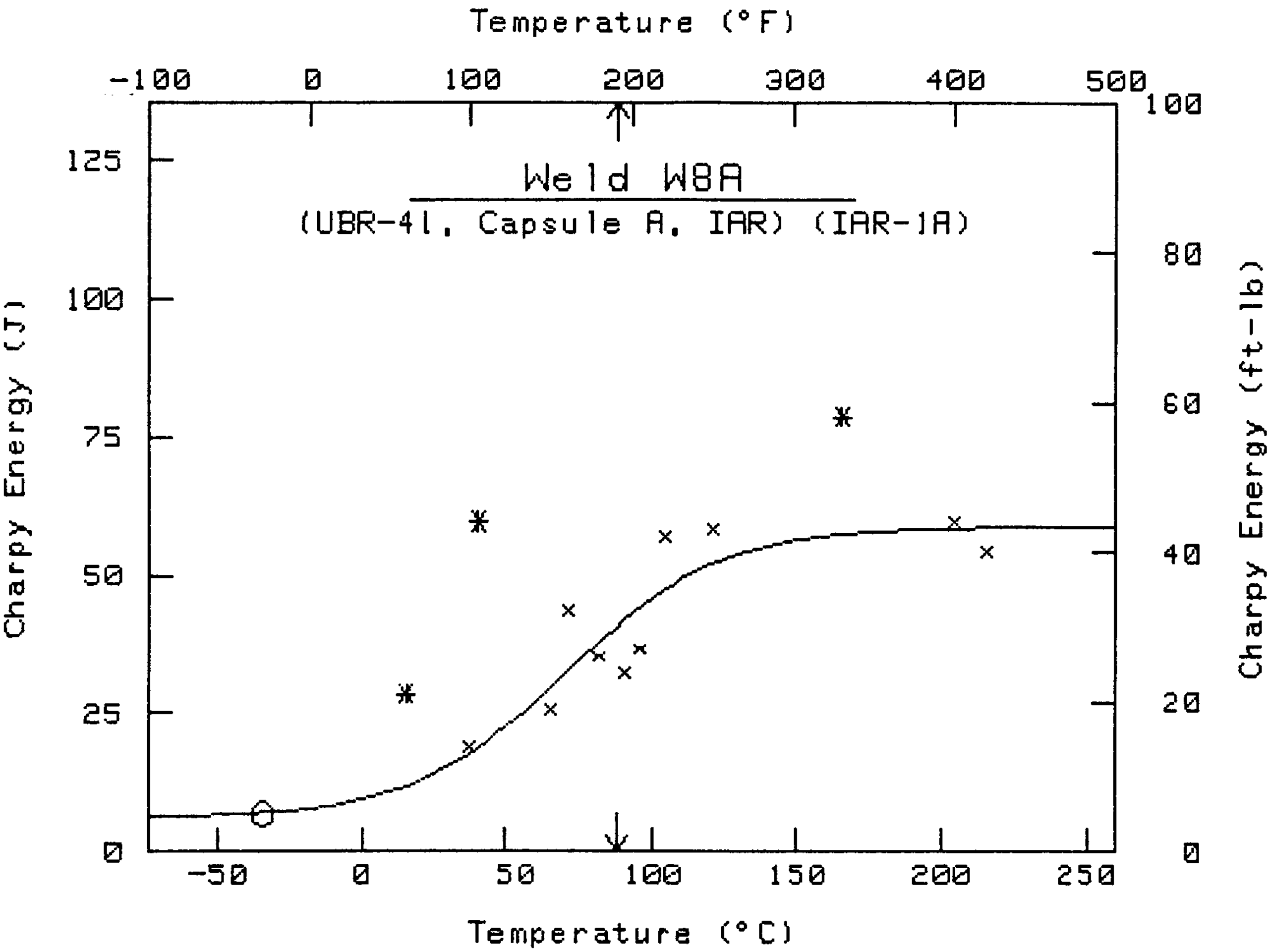

****

Cv = A + B tanh[(T - To)/C]

		English	Metric
A	=	23.94 ft-lb	32.46 J
B	=	19.42 ft-lb	26.34 J
C	=	93.49 °F	51.94 °C
To	=	159.80 °F	71.00 °C

Cv = 30 ft-lb (41 J) at T	=	190.0 °F	87.8 °C
Upper Shelf Energy	=	43.4 ft-lb	58.8 J

****

PT #	Temp (°F)	Energy (ft-lb)	PT #	Temp (°F)	Energy (ft-lb)
1 *	60	21.0	10	250	43.0
2	100	14.0	11 *	330	58.0
3 *	105	44.0	12	400	44.0
4	150	19.0	13	420	40.0
5	160	32.0	14 O	-30	5.0
6	180	26.0	15 O	-30	5.0
7	195	24.0	16 O	-30	5.0
8	205	27.0	17 O	-30	5.0
9	220	42.0			

O = Fictitious Point Added   * = Test Point Not Included

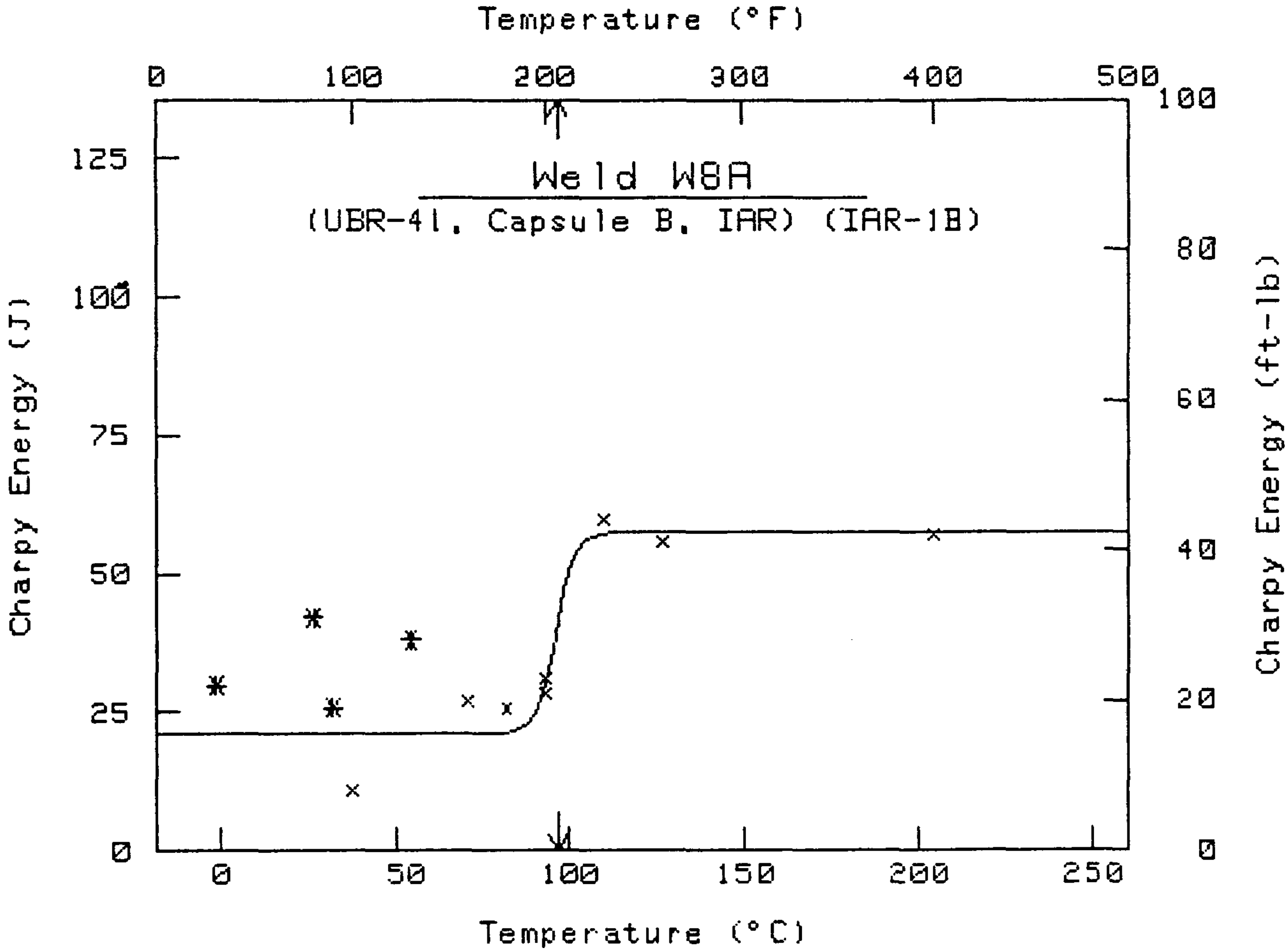

****

Cv = A + B tanh[(T - To)/C]

		English	Metric
A	=	28.93 ft-lb	39.23 J
B	=	13.35 ft-lb	18.10 J
C	=	9.52 °F	5.29 °C
To	=	205.40 °F	96.34 °C

Cv = 30 ft-lb (41 J) at T	=	206.2 °F	96.8 °C
Upper Shelf Energy	=	42.3 ft-lb	57.3 J

****

PT #		Temp (°F)	Energy (ft-lb)
1	*	30	22.0
2	*	80	31.0
3	*	90	19.0
4		100	8.0
5	*	130	28.0
6		160	20.0
7		180	19.0
8		200	21.0
9		200	23.0
10		230	44.0
11		260	41.0
12		400	42.0
13		400	42.0

O = Fictitious Point Added * = Test Point Not Included

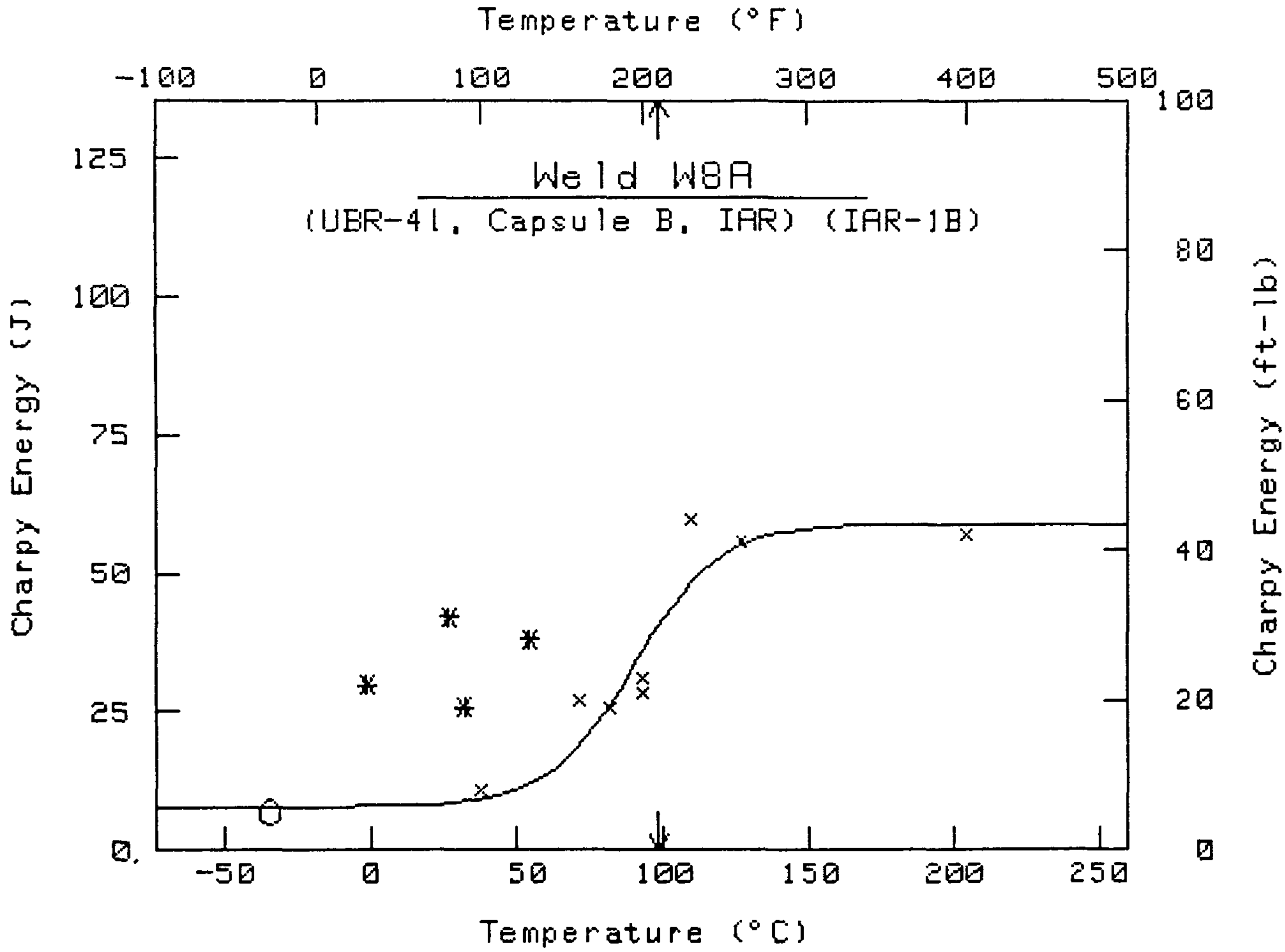

****

Cv = A + B tanh[(T - To)/C]

		English	Metric
A	=	24.64 ft-lb	33.40 J
B	=	18.84 ft-lb	25.54 J
C	=	52.57 °F	29.21 °C
To	=	194.40 °F	90.22 °C

	English	Metric
Cv = 30 ft-lb (41 J) at T =	209.8 °F	98.8 °C
Upper Shelf Energy =	43.5 ft-lb	58.9 J

****

PT #	Temp (°F)	Energy (ft-lb)	PT #	Temp (°F)	Energy (ft-lb)
1 *	30	22.0	10	230	44.0
2 *	80	31.0	11	260	41.0
3 *	90	19.0	12	400	42.0
4	100	8.0	13	400	42.0
5 *	130	28.0	14 O	-30	5.0
6	160	20.0	15 O	-30	5.0
7	180	19.0	16 O	-30	5.0
8	200	21.0	17 O	-30	5.0
9	200	23.0			

O = Fictitious Point Added   * = Test Point Not Included

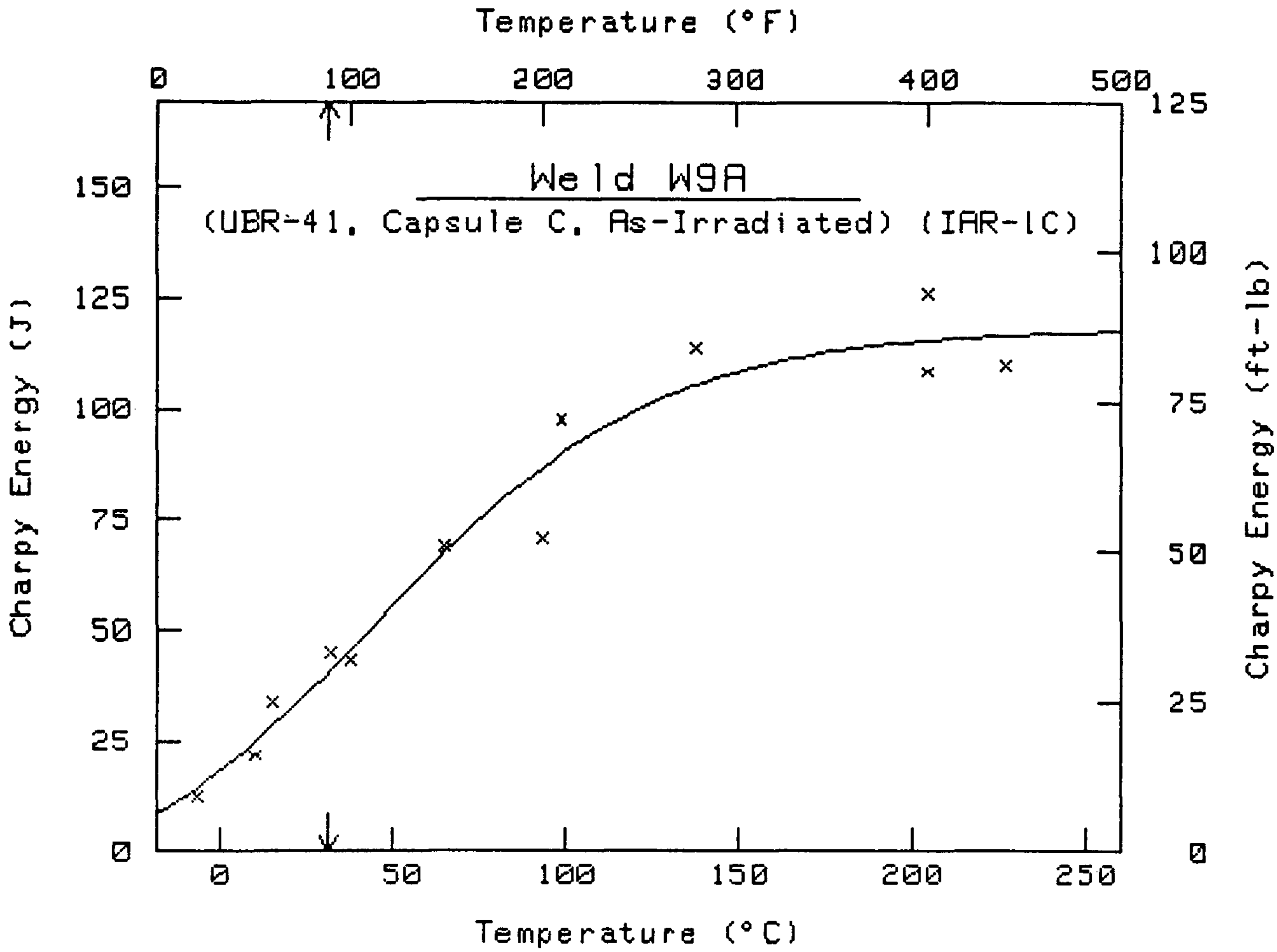

****

Cv = A + B tanh[(T - To)/C]

		English	Metric
A	=	37.74 ft-lb	51.16 J
B	=	49.53 ft-lb	67.16 J
C	=	149.34 °F	82.97 °C
To	=	112.37 °F	44.65 °C

Cv = 30 ft-lb (41 J) at T = 88.8 °F 31.6 °C

Upper Shelf Energy = 87.3 ft-lb 118.3 J

****

PT #	Temp (°F)	Energy (ft-lb)
1	20	9.0
2	50	16.0
3	60	25.0
4	90	33.0
5	100	32.0
6	150	51.0
7	200	52.0
8	210	72.0
9	280	84.0
10	400	93.0
11	400	80.0
12	440	81.0

O = Fictitious Point Added * = Test Point Not Included

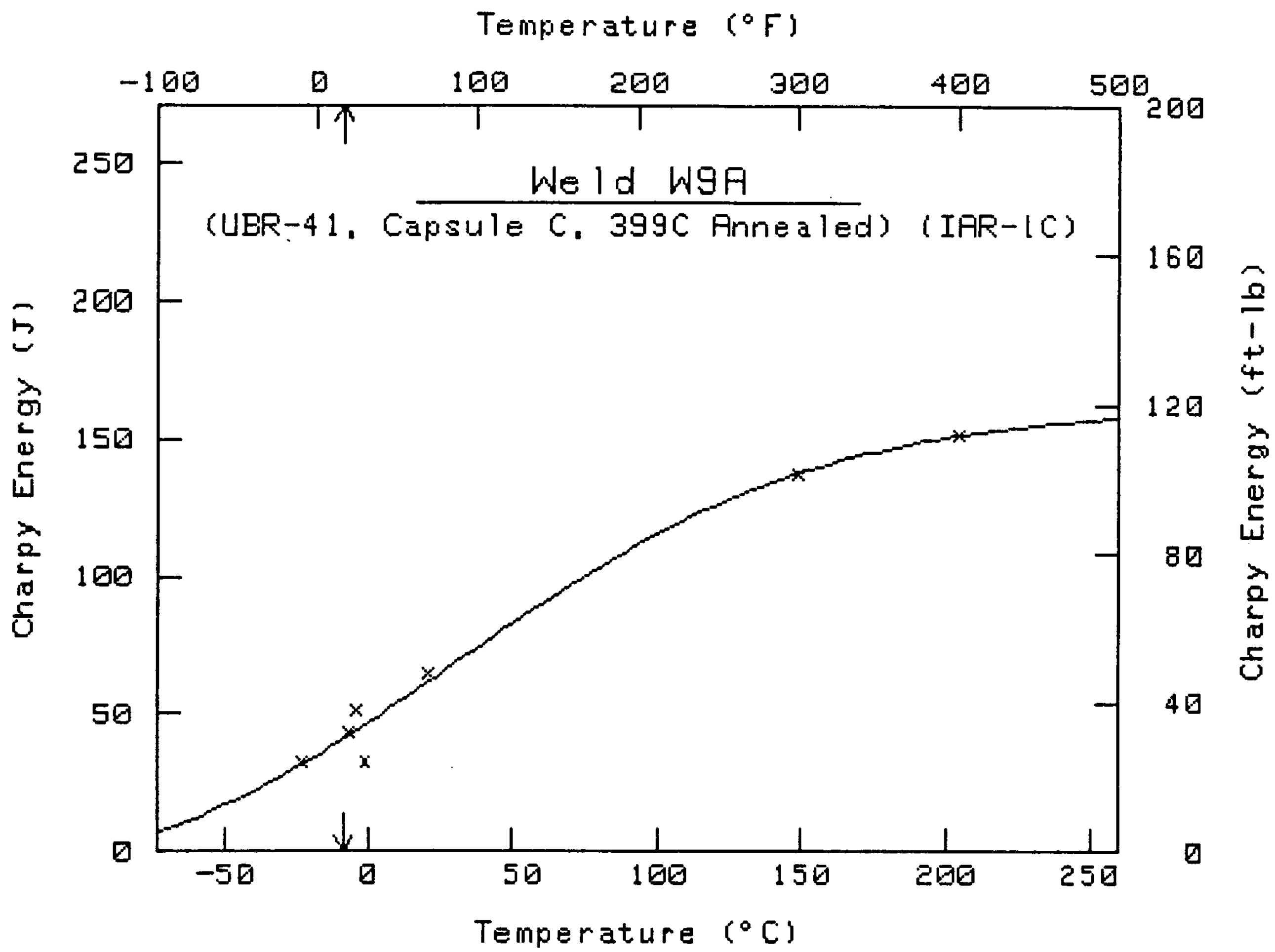

****

Cv = A + B tanh[(T - To)/C]

		English	Metric
A	=	52.08 ft-lb	70.61 J
B	=	67.68 ft-lb	91.77 J
C	=	223.59 °F	124.22 °C
To	=	92.00 °F	33.33 °C

Cv = 30 ft-lb (41 J) at T = 16.3 °F -8.7 °C

Upper Shelf Energy = 119.8 ft-lb 162.4 J

****

PT #	Temp (°F)	Energy (ft-lb)
1	-10	24.0
2	20	32.0
3	25	38.0
4	30	24.0
5	70	48.0
6	300	101.0
7	400	112.0

O = Fictitious Point Added * = Test Point Not Included

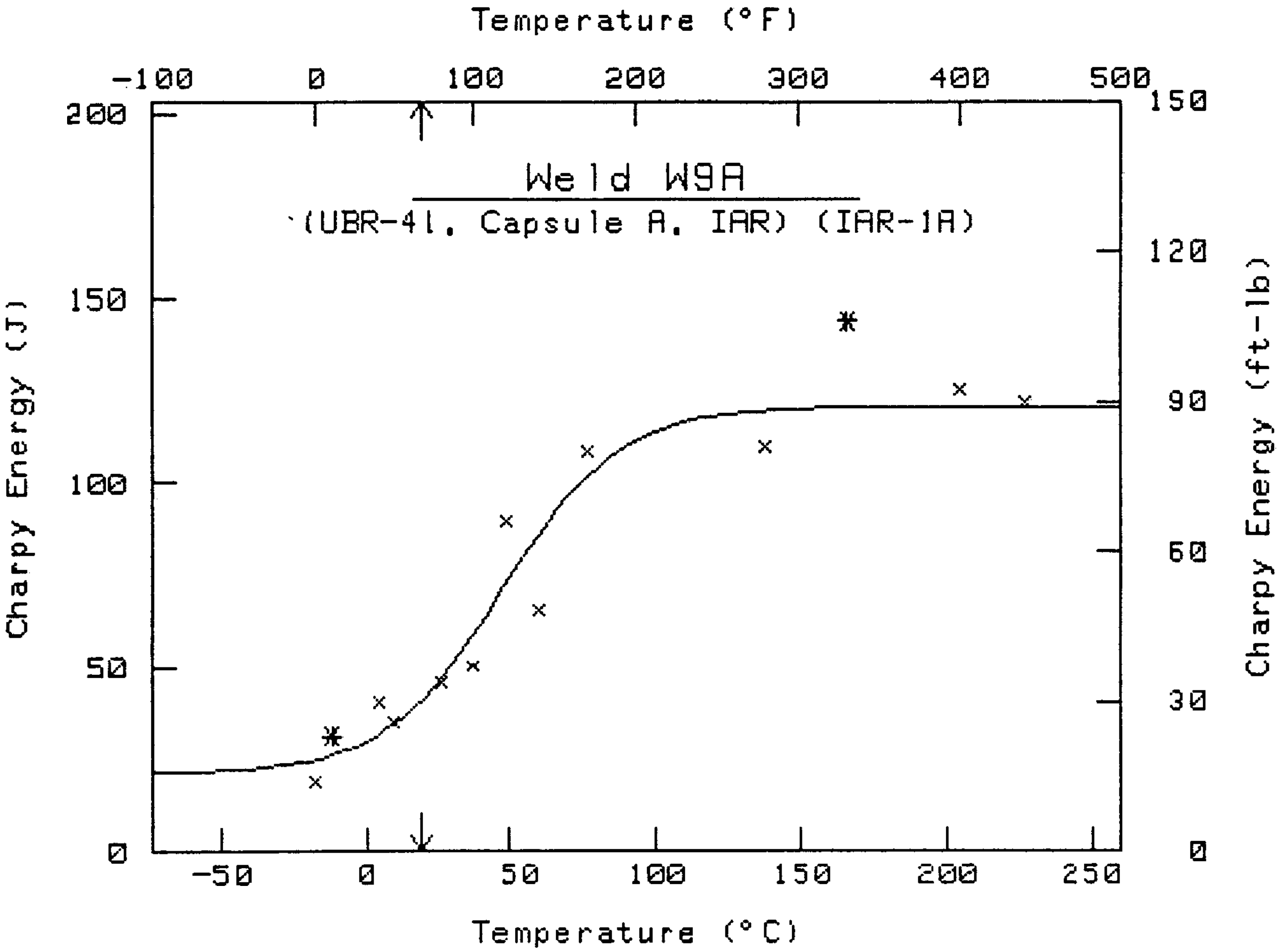

$$C_v = A + B \tanh[(T - T_o)/C]$$

		English	Metric
A	=	52.33 ft-lb	70.95 J
B	=	36.61 ft-lb	49.64 J
C	=	72.58 °F	40.32 °C
To	=	117.79 °F	47.66 °C

Cv = 30 ft-lb (41 J) at T	=	66.3 °F	19.1 °C
Upper Shelf Energy	=	88.9 ft-lb	120.6 J

PT #		Temp (°F)	Energy (ft-lb)
1		0	14.0
2	*	10	23.0
3		40	30.0
4		50	26.0
5		80	34.0
6		100	37.0
7		120	66.0
8		140	48.0
9		170	80.0
10		170	80.0
11		280	81.0
12	*	330	106.0
13		400	92.1
14		440	90.0

O = Fictitious Point Added   * = Test Point Not Included

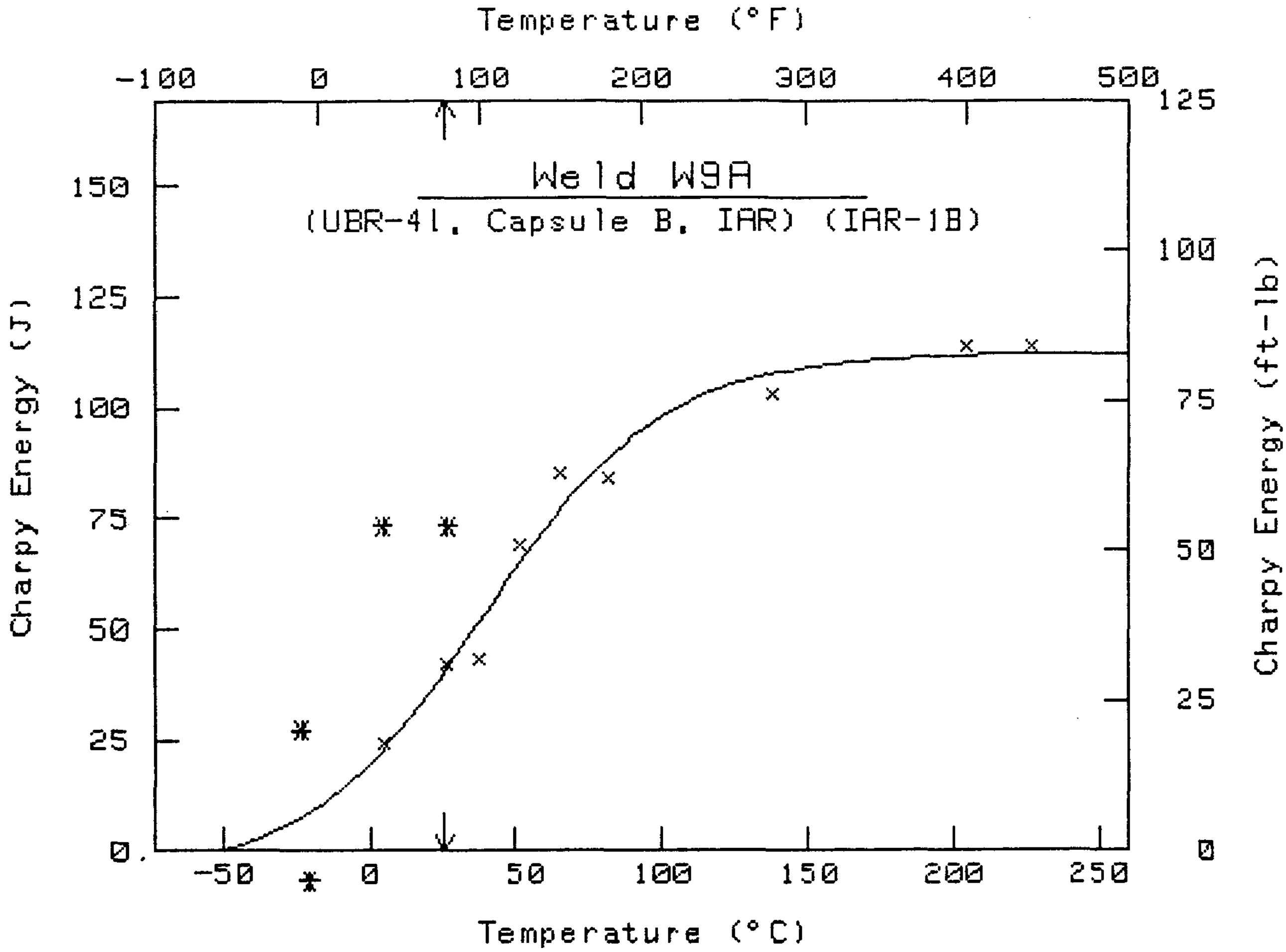

****

Cv = A + B tanh[(T - To)/C]

		English	Metric
A	=	39.04 ft-lb	52.93 J
B	=	43.81 ft-lb	59.39 J
C	=	110.96 °F	61.65 °C
To	=	101.80 °F	38.78 °C

Cv = 30 ft-lb (41 J) at T = 78.6 °F 25.9 °C

Upper Shelf Energy = 82.9 ft-lb 112.3 J

****

PT #		Temp (°F)	Energy (ft-lb)
1	*	-10	20.0
2	*	-5	-5.0
3		40	18.0
4	*	40	54.0
5		80	31.0
6	*	80	54.0
7		100	32.0
8		125	51.0
9		150	63.0
10		180	62.0
11		280	76.0
12		400	84.0
13		440	84.0

O = Fictitious Point Added * = Test Point Not Included

Computer Curve Fittings of Data from Irradiation Assembly UBR-42

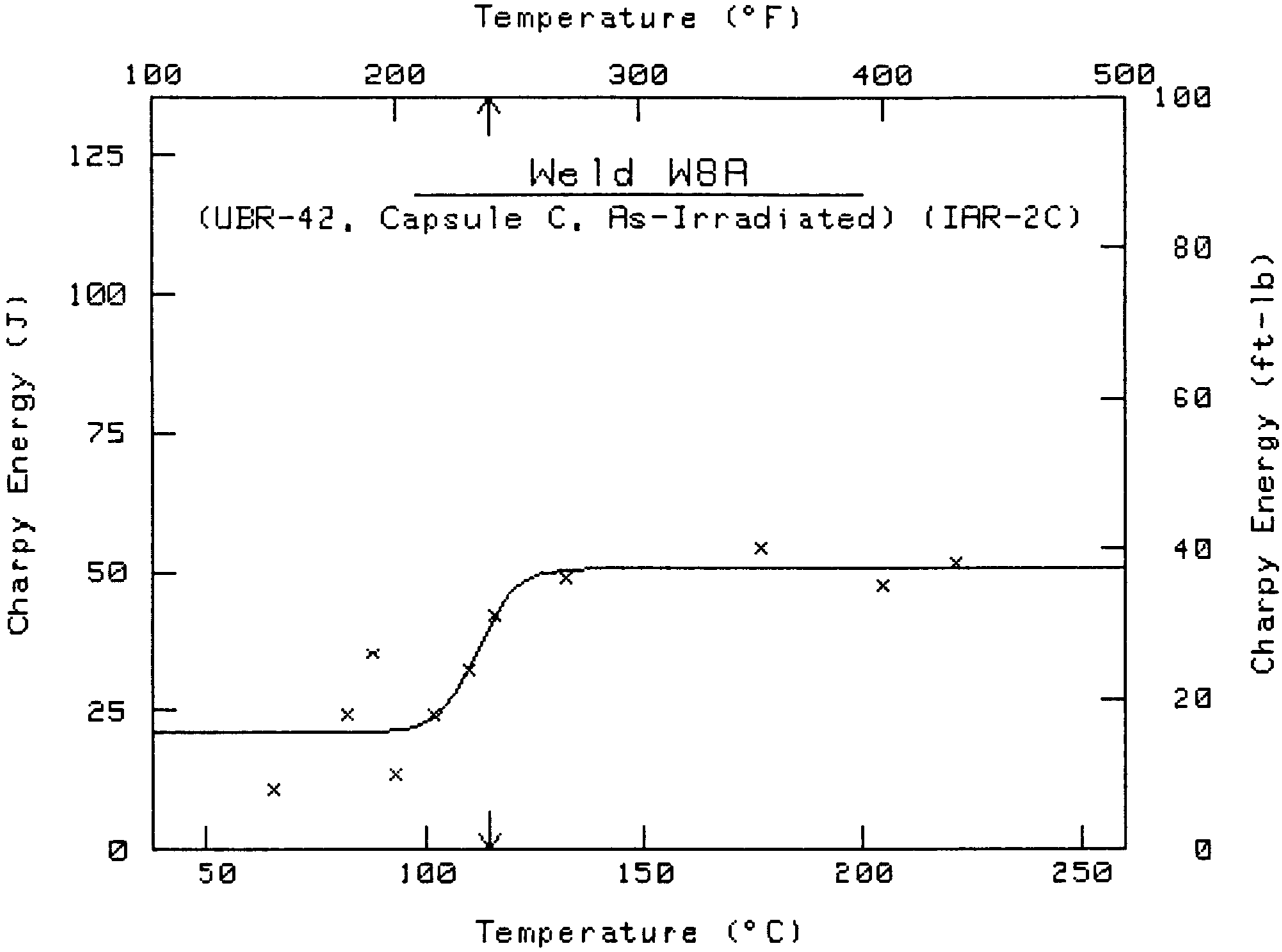

****

$$Cv = A + B \tanh[(T - To)/C]$$

		English	Metric
A	=	26.42 ft-lb	35.82 J
B	=	10.91 ft-lb	14.79 J
C	=	15.74 °F	8.74 °C
To	=	233.31 °F	111.84 °C

	English	Metric
Cv = 30 ft-lb (41 J) at T =	238.7 °F	114.8 °C
Upper Shelf Energy =	37.3 ft-lb	50.6 J

****

PT #	Temp (°F)	Energy (ft-lb)
1	150	8.0
2	180	18.0
3	190	26.0
4	200	10.0
5	215	18.0
6	230	24.0
7	240	31.0
8	270	36.0
9	350	40.0
10	400	35.0
11	430	38.0

0 = Fictitious Point Added   * = Test Point Not Included

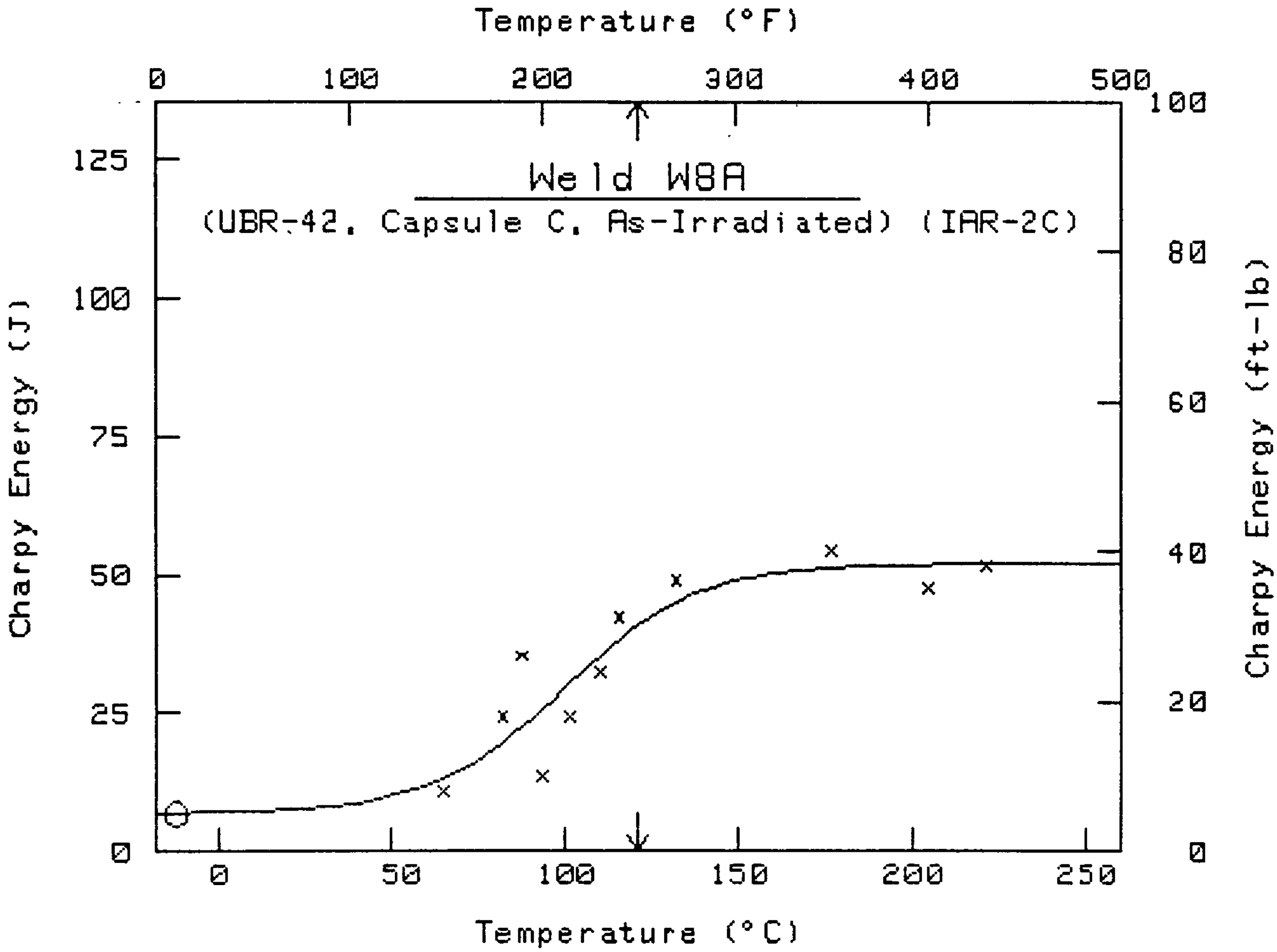

****

$$Cv = A + B \tanh[(T - To)/C]$$

	English	Metric
A =	21.72 ft-lb	29.45 J
B =	16.65 ft-lb	22.57 J
C =	68.79 °F	38.22 °C
To =	212.24 °F	100.13 °C

Cv = 30 ft-lb (41 J) at T =	249.8 °F	121.0 °C
Upper Shelf Energy =	38.4 ft-lb	52.0 J

****

PT #	Temp (°F)	Energy (ft-lb)
1	150	8.0
2	180	18.0
3	190	26.0
4	200	10.0
5	215	18.0
6	230	24.0
7	240	31.0
8	270	36.0
9	350	40.0
10	400	35.0
11	430	38.0
12 O	10	5.0
13 O	10	5.0
14 O	10	5.0
15 O	10	5.0

O = Fictitious Point Added * = Test Point Not Included

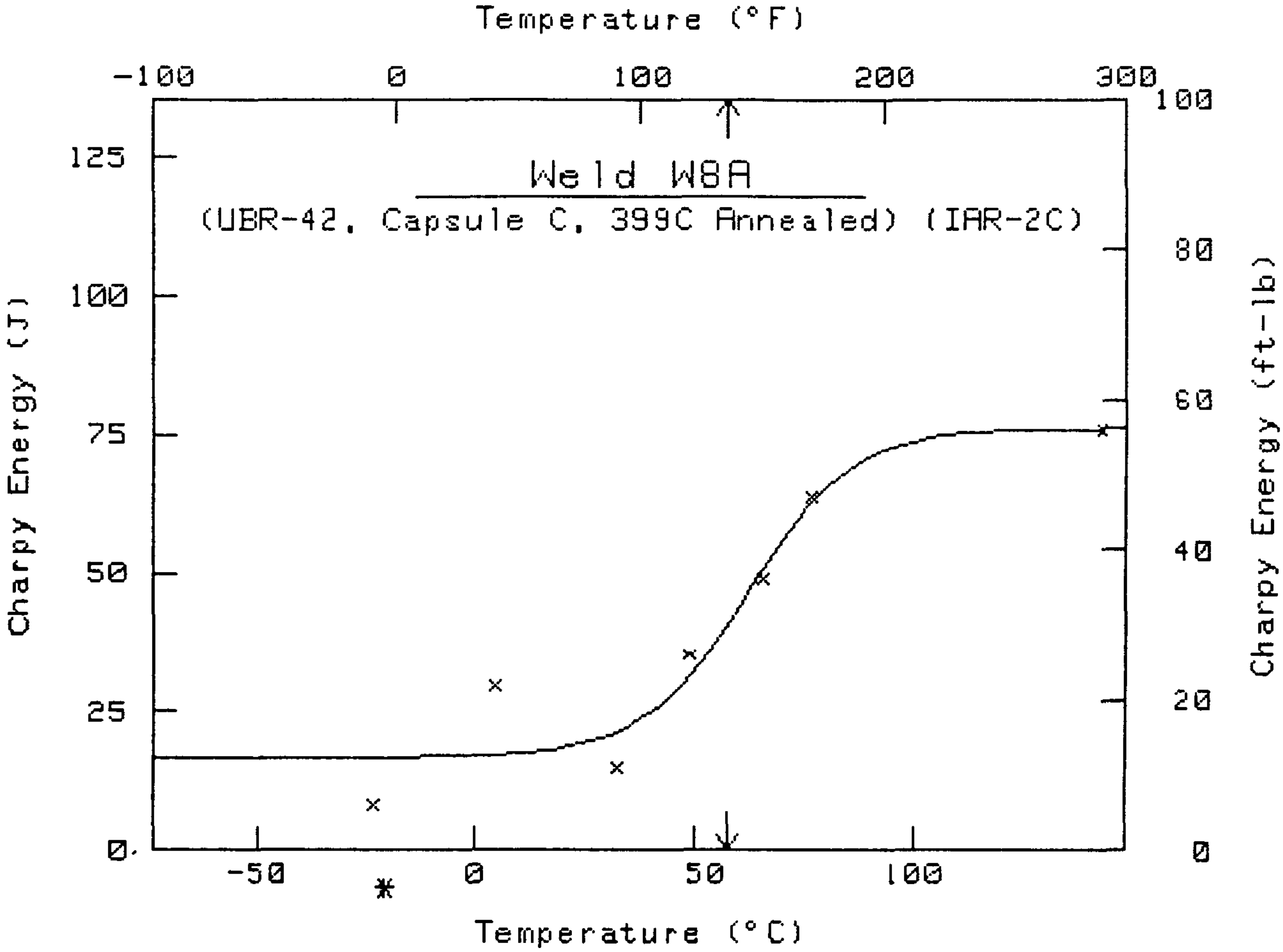

****

Cv = A + B tanh[(T - To)/C]

	English	Metric
A =	34.25 ft-lb	46.44 J
B =	21.88 ft-lb	29.66 J
C =	42.86 °F	23.81 °C
To =	143.55 °F	61.97 °C

Cv = 30 ft-lb (41 J) at T =	135.1 °F	57.3 °C
Upper Shelf Energy =	56.1 ft-lb	76.1 J

****

PT #		Temp (°F)	Energy (ft-lb)
1		-10	6.0
2	*	-5	-5.0
3		40	22.0
4		90	11.0
5		120	26.0
6		150	36.0
7		170	47.0
8		290	56.0

O = Fictitious Point Added   * = Test Point Not Included

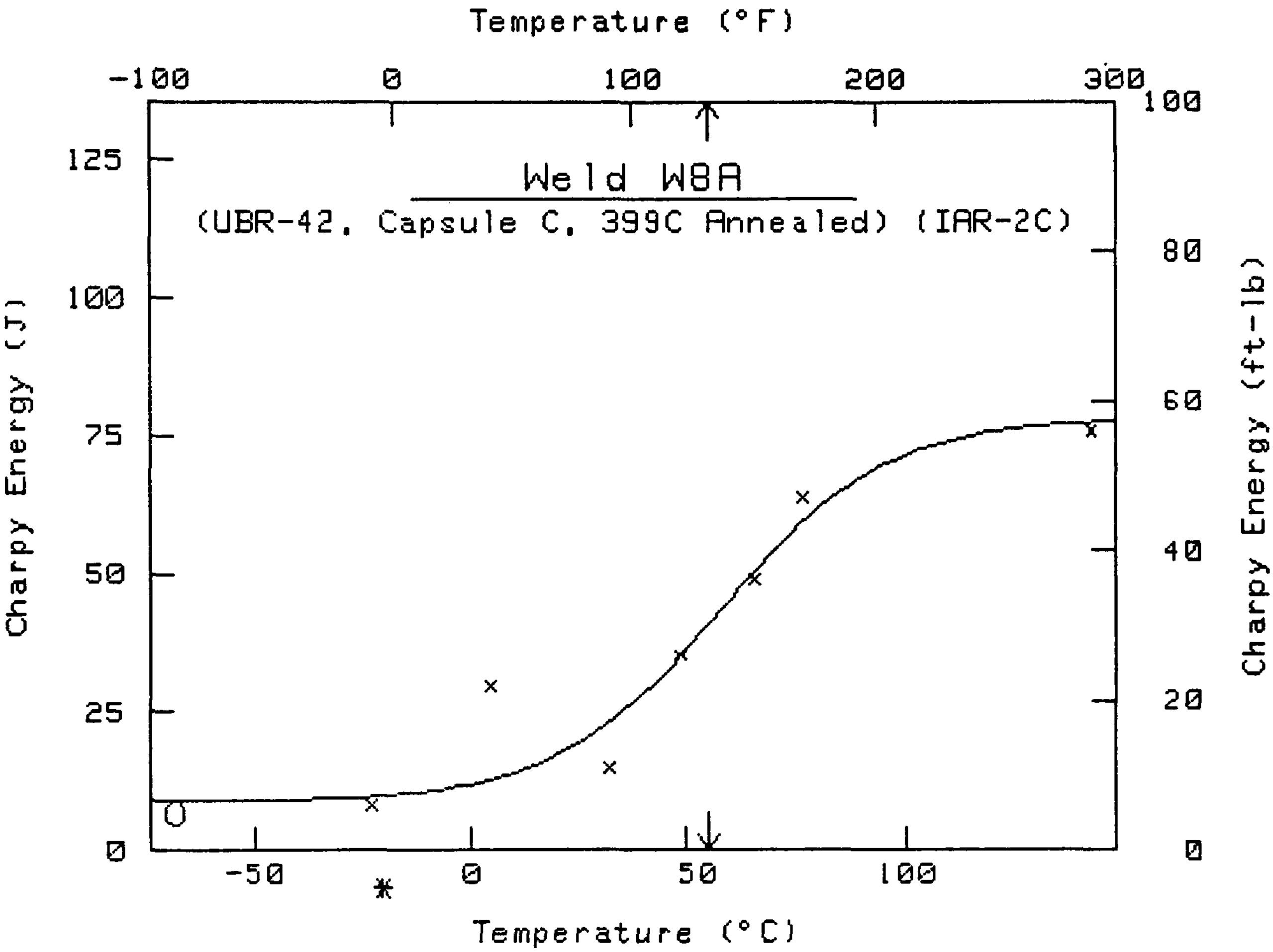

$$Cv = A + B \tanh[(T - To)/C]$$

		English	Metric
A	=	32.07 ft-lb	43.48 J
B	=	25.55 ft-lb	34.64 J
C	=	67.94 °F	37.74 °C
To	=	136.25 °F	57.92 °C

Cv = 30 ft-lb (41 J) at T	=	130.7 °F	54.9 °C
Upper Shelf Energy	=	57.6 ft-lb	78.1 J

PT #		Temp (°F)	Energy (ft-lb)
1		-10	6.0
2	*	-5	-5.0
3		40	22.0
4		90	11.0
5		120	26.0
6		150	36.0
7		170	47.0
8		290	56.0
9	O	-90	5.0
10	O	-90	5.0
11	O	-90	5.0
12	O	-90	5.0

O = Fictitious Point Added　　　　* = Test Point Not Included

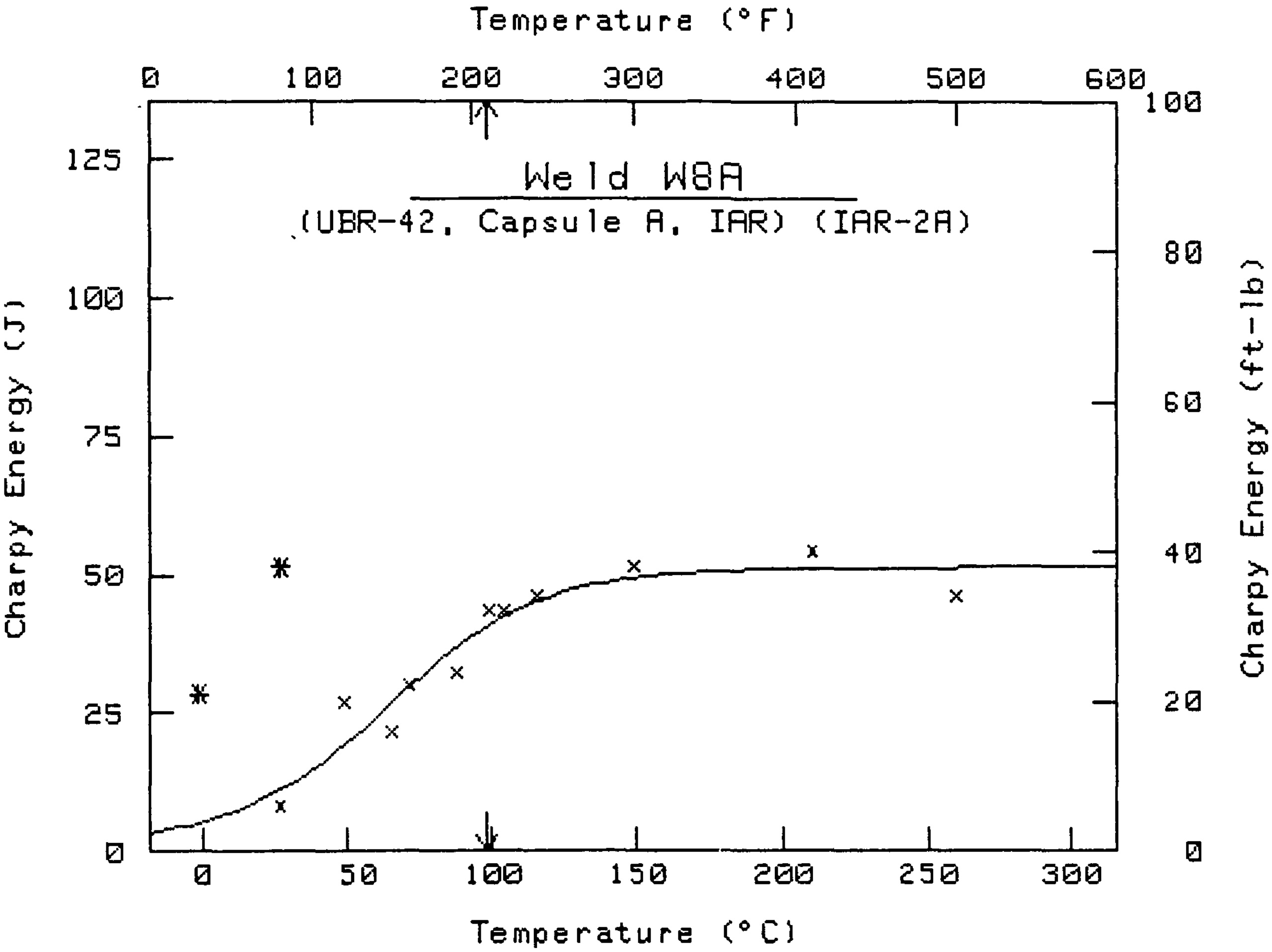

****

$$Cv = A + B \tanh[(T - To)/C]$$

		English	Metric
A	=	19.45 ft-lb	26.37 J
B	=	18.48 ft-lb	25.05 J
C	=	94.81 °F	52.67 °C
To	=	147.74 °F	64.30 °C

Cv = 30 ft-lb (41 J) at T = 209.3 °F 98.5 °C

Upper Shelf Energy = 37.9 ft-lb 51.4 J

****

PT #		Temp (°F)	Energy (ft-lb)
1	*	30	21.0
2		80	6.0
3	*	80	38.0
4		120	20.0
5		150	16.0
6		160	22.1
7		190	24.0
8		210	32.0
9		220	32.0
10		240	34.0
11		300	38.0
12		410	40.0
13		500	34.0

0 = Fictitious Point Added * = Test Point Not Included

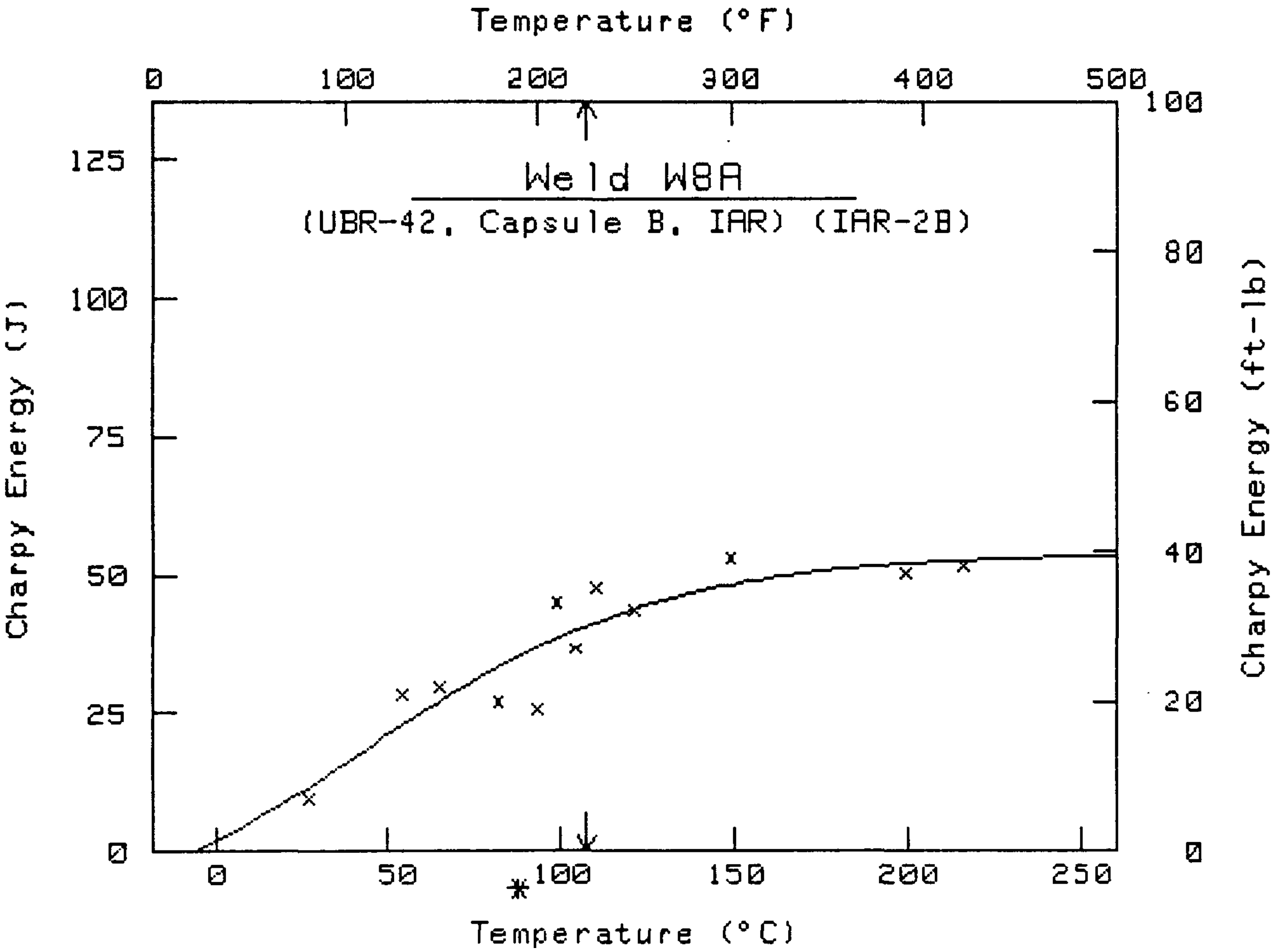

****

Cv = A + B tanh[(T - To)/C]

		English	Metric
A	=	13.76 ft-lb	18.66 J
B	=	26.02 ft-lb	35.28 J
C	=	155.46 °F	86.37 °C
To	=	111.91 °F	44.39 °C

Cv = 30 ft-lb (41 J) at T	=	225.6 °F	107.6 °C
Upper Shelf Energy	=	39.8 ft-lb	53.9 J

****

PT #	Temp (°F)	Energy (ft-lb)
1	80	7.0
2	130	21.0
3	150	22.0
4	180	20.0
5 *	190	-5.0
6	200	19.0
7	210	33.0
8	220	27.0
9	230	35.0
10	250	32.0
11	300	39.0
12	390	37.0
13	420	38.0

O = Fictitious Point Added   * = Test Point Not Included

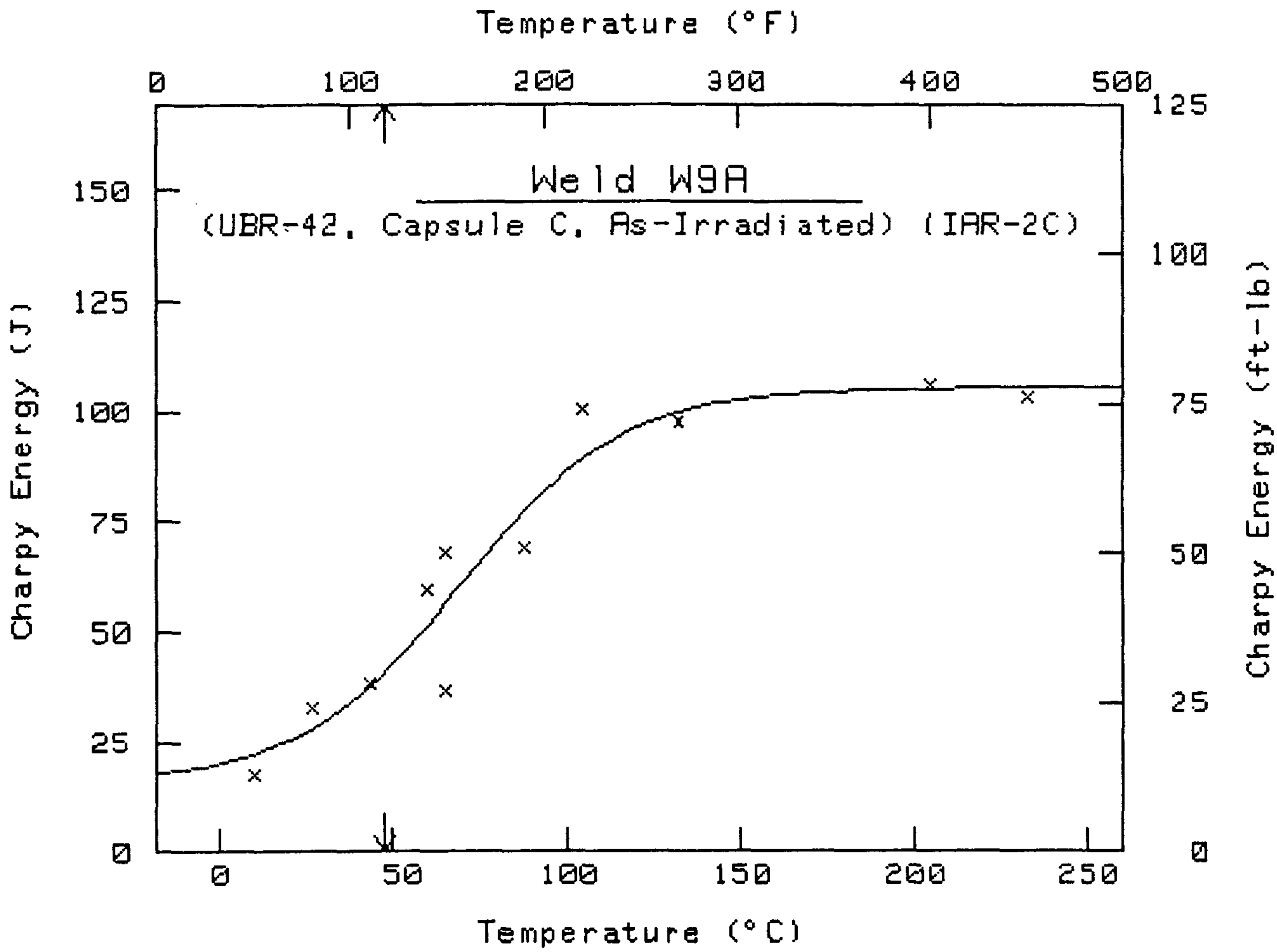

****

Cv = A + B tanh[(T - To)/C]

		English	Metric
A	=	44.70 ft-lb	60.61 J
B	=	32.97 ft-lb	44.71 J
C	=	82.97 °F	46.10 °C
To	=	157.59 °F	69.77 °C

	English	Metric
Cv = 30 ft-lb (41 J) at T =	117.8 °F	47.7 °C
Upper Shelf Energy =	77.7 ft-lb	105.3 J

****

PT #	Temp (°F)	Energy (ft-lb)
1	50	13.0
2	80	24.0
3	110	28.0
4	140	44.0
5	150	50.0
6	150	27.0
7	190	51.0
8	220	74.0
9	270	72.0
10	400	78.0
11	450	76.0

0 = Fictitious Point Added   * = Test Point Not Included

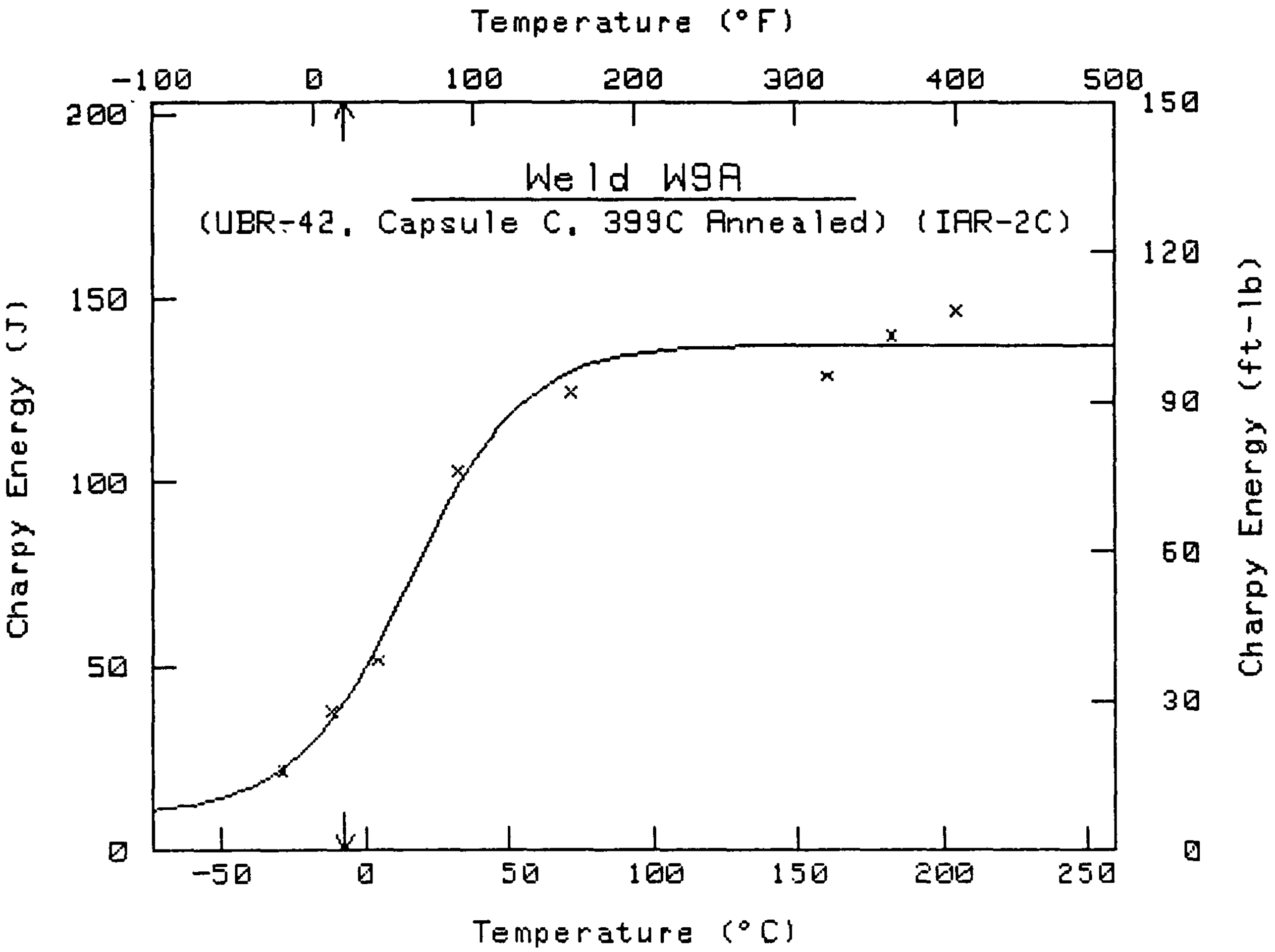

****

Cv = A + B tanh[(T - To)/C]

		English	Metric
A	=	54.20 ft-lb	73.48 J
B	=	47.14 ft-lb	63.91 J
C	=	72.21 °F	40.12 °C
To	=	60.08 °F	15.60 °C

	English	Metric
Cv = 30 ft-lb (41 J) at T =	19.1 °F	-7.2 °C
Upper Shelf Energy =	101.3 ft-lb	137.4 J

****

PT #	Temp (°F)	Energy (ft-lb)
1	-20	16.0
2	10	28.0
3	40	38.0
4	90	76.0
5	160	92.0
6	320	95.0
7	360	103.0
8	400	108.0

0 = Fictitious Point Added   * = Test Point Not Included

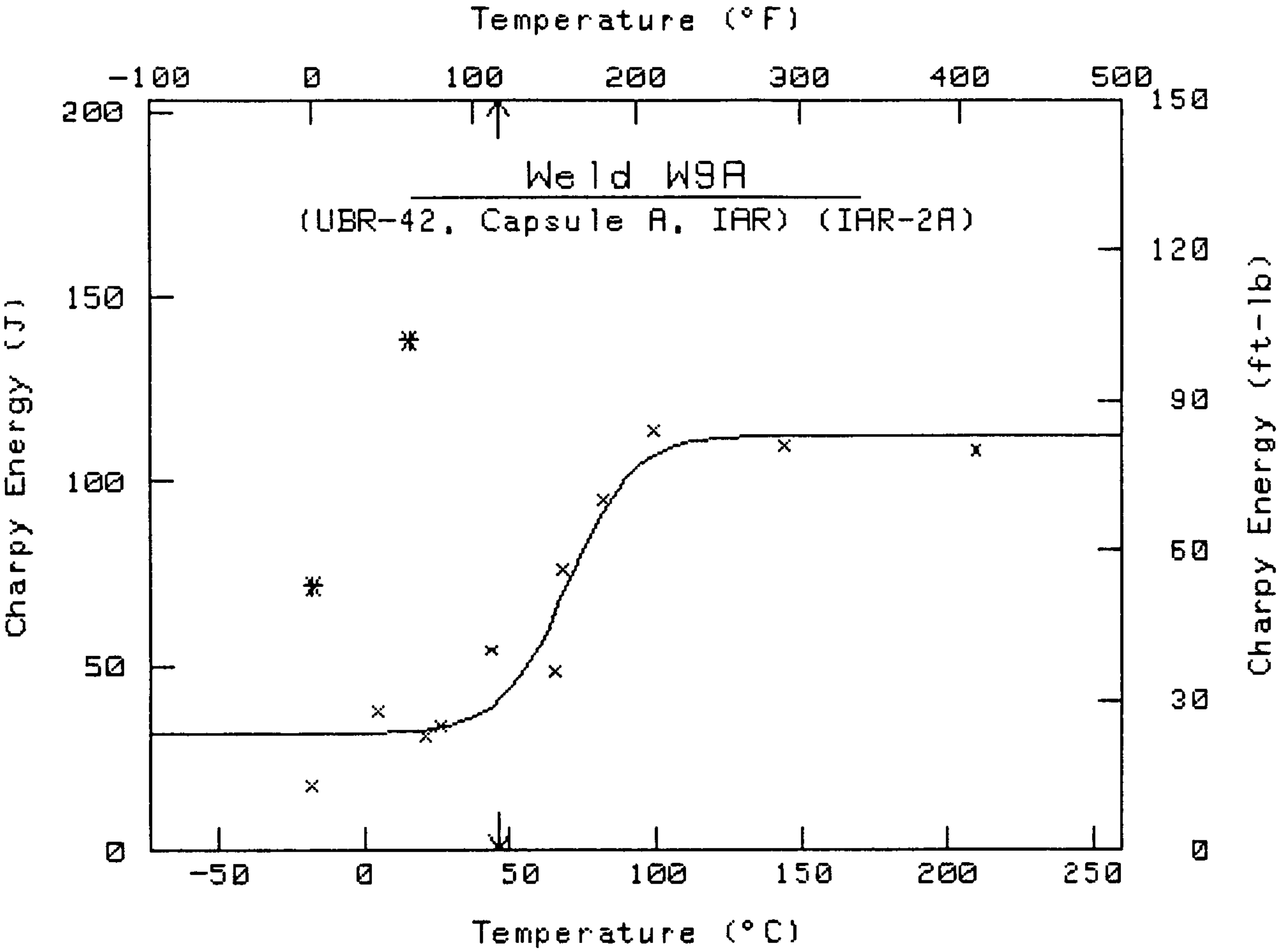

****

Cv = A + B tanh[(T - To)/C]

		English	Metric
A	=	53.18 ft-lb	72.10 J
B	=	29.76 ft-lb	40.35 J
C	=	40.51 °F	22.51 °C
To	=	157.65 °F	69.81 °C

Cv = 30 ft-lb (41 J) at T	=	115.4 °F	46.3 °C
Upper Shelf Energy	=	82.9 ft-lb	112.4 J

****

PT #		Temp (°F)	Energy (ft-lb)
1		0	13.0
2	*	0	53.0
3		40	28.0
4	*	60	102.0
5		70	23.0
6		80	25.0
7		110	40.0
8		150	36.0
9		155	56.0
10		180	70.0
11		210	84.0
12		290	81.0
13		410	80.0

O = Fictitious Point Added   * = Test Point Not Included

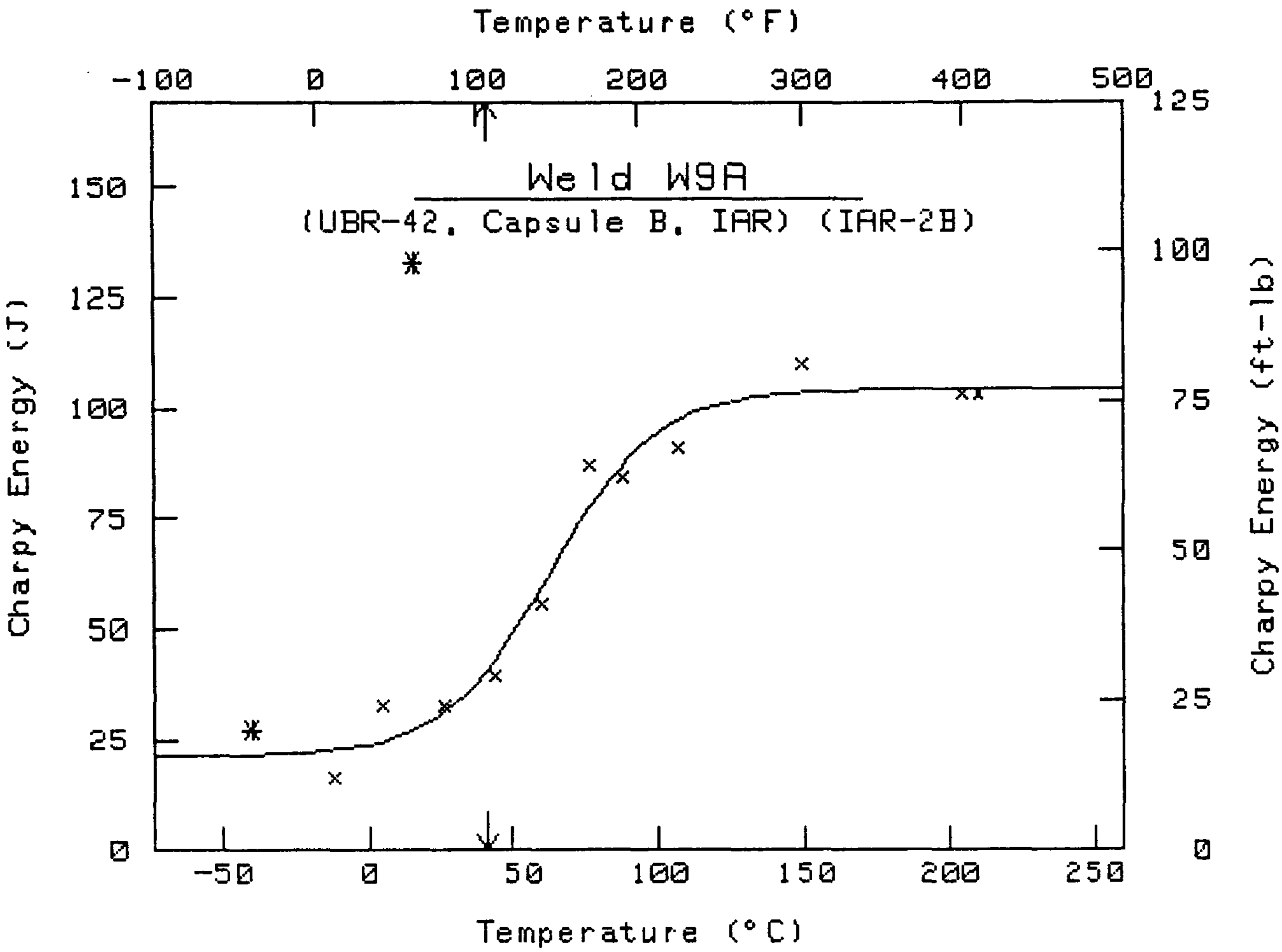

****

$$Cv = A + B \tanh[(T - To)/C]$$

		English	Metric
A	=	46.30 ft-lb	62.78 J
B	=	30.63 ft-lb	41.53 J
C	=	66.79 °F	37.11 °C
To	=	145.72 °F	63.18 °C

Cv = 30 ft-lb (41 J) at T = 106.1 °F 41.2 °C

Upper Shelf Energy = 76.9 ft-lb 104.3 J

****

PT #		Temp (°F)	Energy (ft-lb)
1	*	-40	20.0
2		10	12.0
3		40	24.0
4	*	60	98.0
5		80	24.0
6		110	29.0
7		140	41.0
8		170	64.0
9		190	62.0
10		225	67.0
11		300	81.0
12		400	76.0
13		410	76.0

0 = Fictitious Point Added * = Test Point Not Included

Computer Curve Fittings of Data from Irradiation Assembly UBR-43

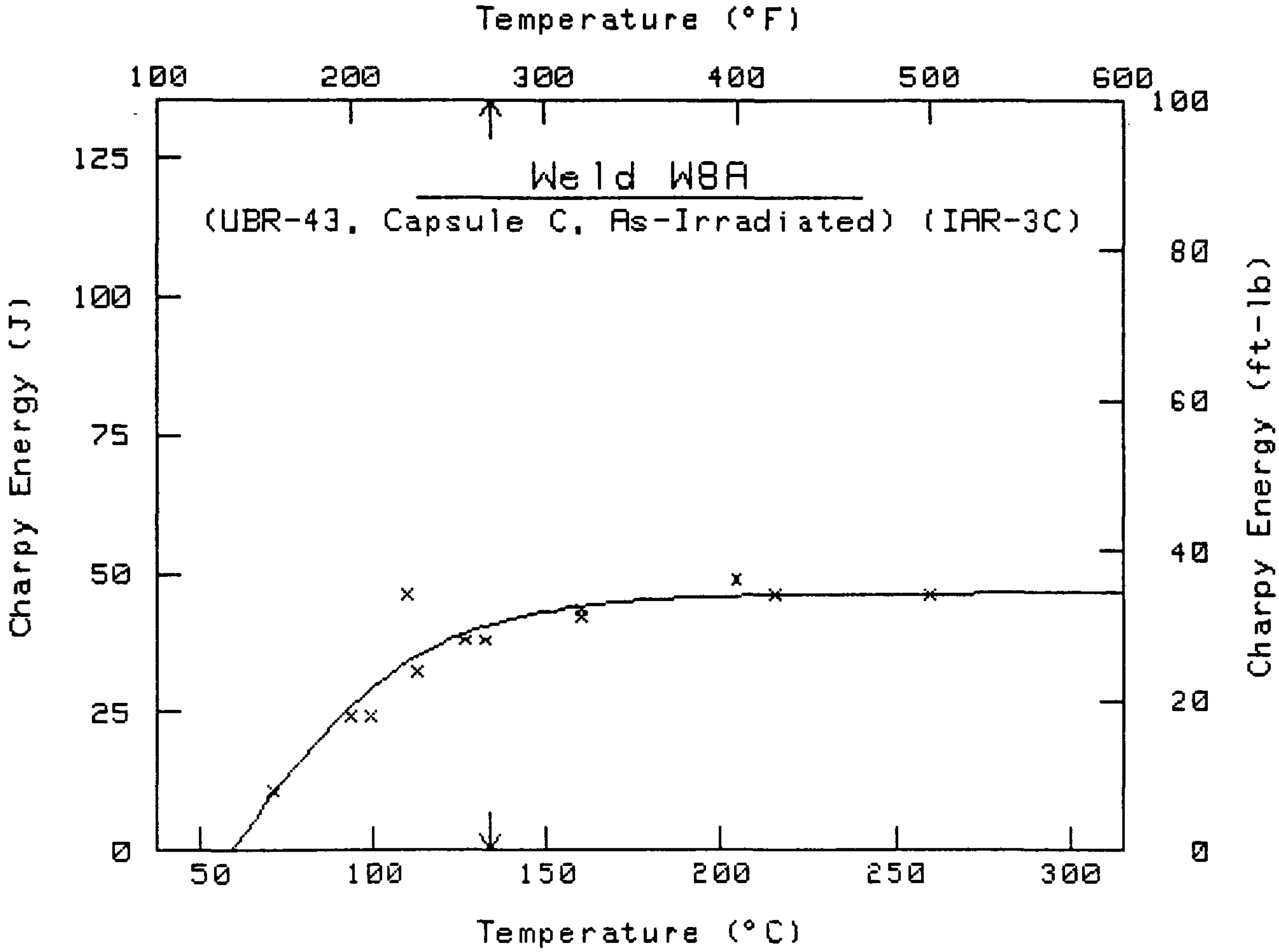

****

$$Cv = A + B \tanh[(T - To)/C]$$

		English	Metric
A	=	-3.38 ft-lb	-4.58 J
B	=	37.68 ft-lb	51.09 J
C	=	102.46 °F	56.92 °C
To	=	129.21 °F	54.00 °C

Cv = 30 ft-lb (41 J) at T = 272.8 °F 133.8 °C

Upper Shelf Energy = 34.3 ft-lb 46.5 J

****

PT #	Temp (°F)	Energy (ft-lb)
1	160	8.0
2	200	18.0
3	210	18.0
4	230	34.0
5	235	24.0
6	260	28.0
7	270	28.0
8	320	32.0
9	320	31.0
10	400	36.0
11	420	34.0
12	500	34.0

0 = Fictitious Point Added * = Test Point Not Included

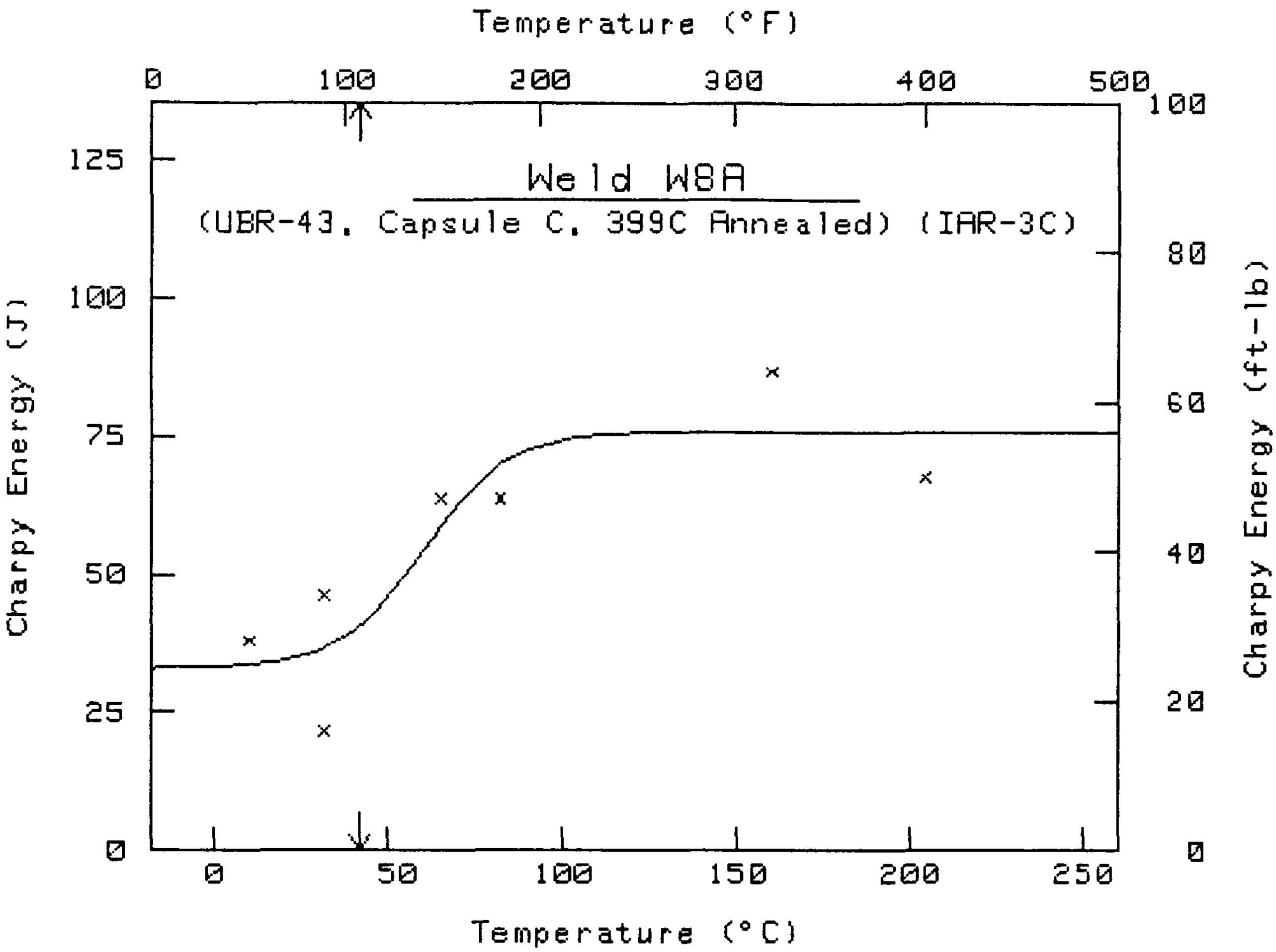

****

$Cv = A + B \tanh[(T - To)/C]$

	English	Metric
A =	40.15 ft-lb	54.43 J
B =	15.85 ft-lb	21.49 J
C =	43.90 °F	24.39 °C
To =	140.67 °F	60.37 °C

Cv = 30 ft-lb (41 J) at T =	107.4 °F	41.9 °C
Upper Shelf Energy =	56.0 ft-lb	75.9 J

****

PT #	Temp (°F)	Energy (ft-lb)
1	50	28.0
2	90	34.0
3	90	16.0
4	150	47.0
5	180	47.0
6	320	64.0
7	400	50.0

O = Fictitious Point Added   * = Test Point Not Included

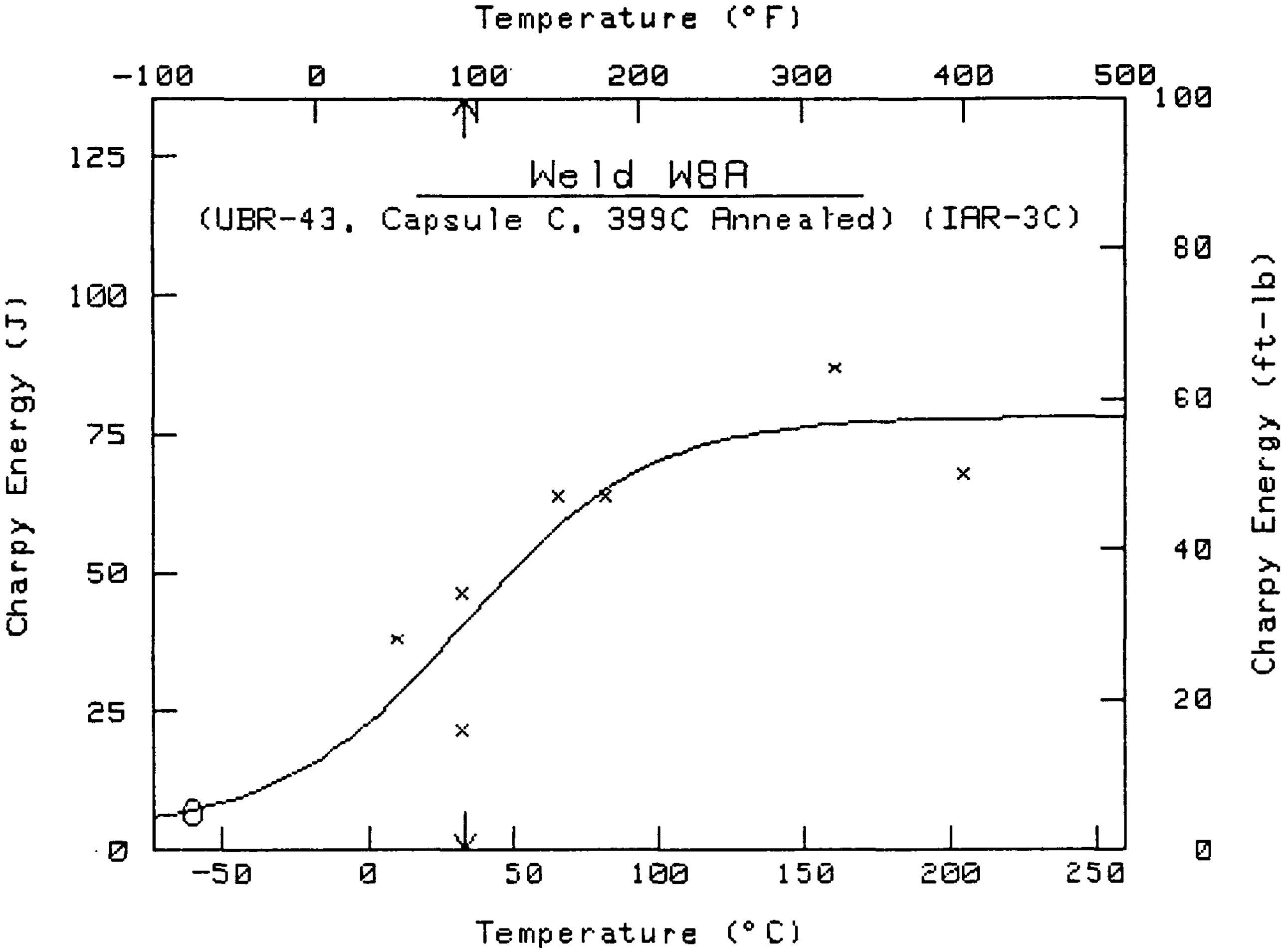

****

$$C_v = A + B \tanh[(T - T_o)/C]$$

		English	Metric
A	=	30.08 ft-lb	40.78 J
B	=	27.48 ft-lb	37.26 J
C	=	114.12 °F	63.40 °C
To	=	91.74 °F	33.19 °C

Cv = 30 ft-lb (41 J) at T	=	91.4 °F	33.0 °C
Upper Shelf Energy	=	57.6 ft-lb	78.0 J

****

PT #		Temp (°F)	Energy (ft-lb)
1		50	28.0
2		90	34.0
3		90	16.0
4		150	47.0
5		180	47.0
6		320	64.0
7		400	50.0
8	O	-76	5.0
9	O	-76	5.0
10	O	-76	5.0
11	O	-76	5.0

O = Fictitious Point Added   * = Test Point Not Included

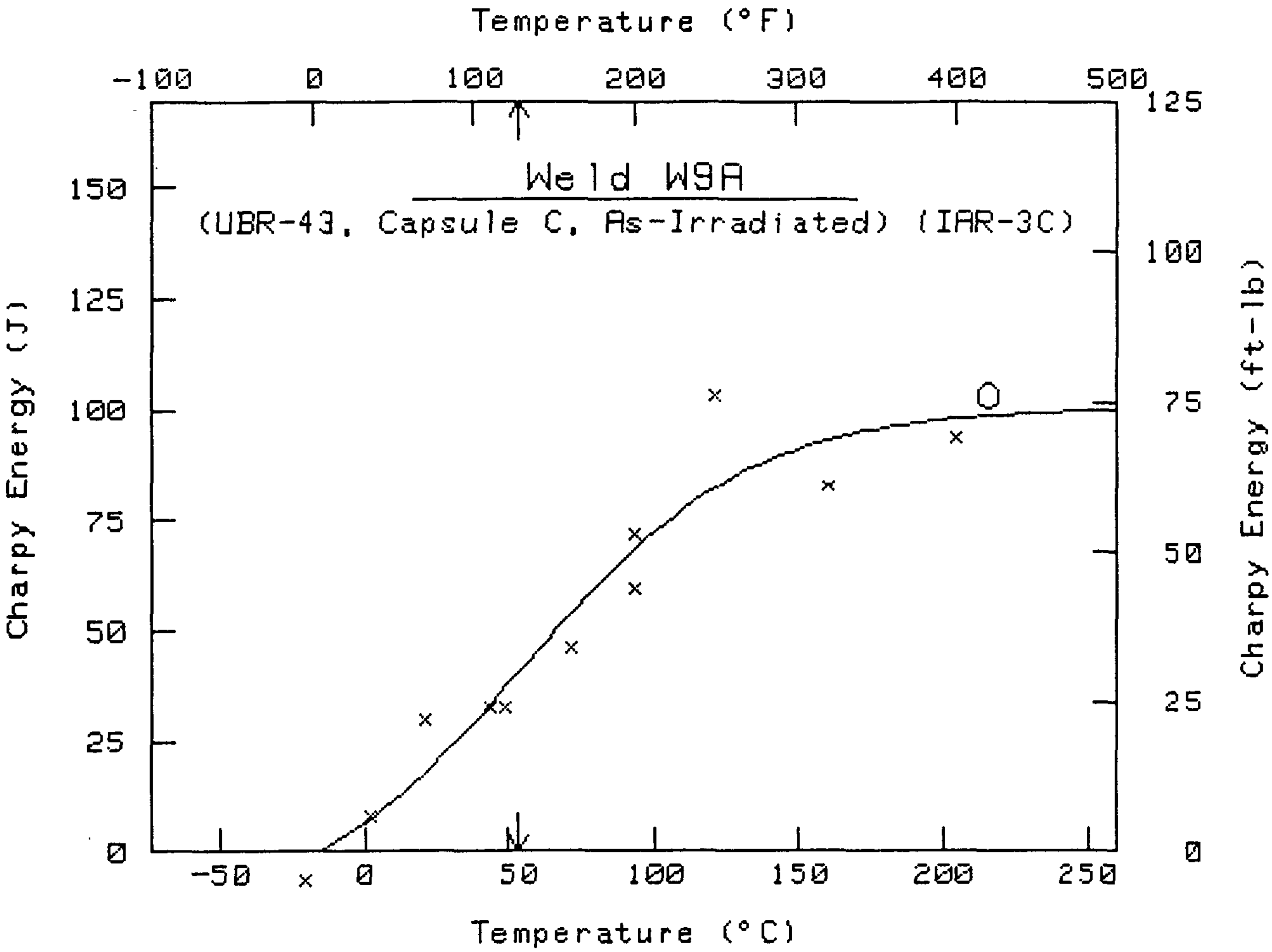

****

$$Cv = A + B \tanh[(T - To)/C]$$

	English	Metric
A =	31.24 ft-lb	42.35 J
B =	42.86 ft-lb	58.11 J
C =	139.16 °F	77.31 °C
To =	132.60 °F	55.89 °C

Cv = 30 ft-lb (41 J) at T =	128.6 °F	53.7 °C
Upper Shelf Energy =	74.1 ft-lb	100.5 J

****

PT #	Temp (°F)	Energy (ft-lb)
1	-5	-5.0
2	35	6.0
3	70	22.0
4	110	24.0
5	120	24.0
6	160	34.0
7	200	44.0
8	200	53.0
9	250	76.0
10	320	61.0
11	400	69.0
12 O	420	76.0

O = Fictitious Point Added   * = Test Point Not Included

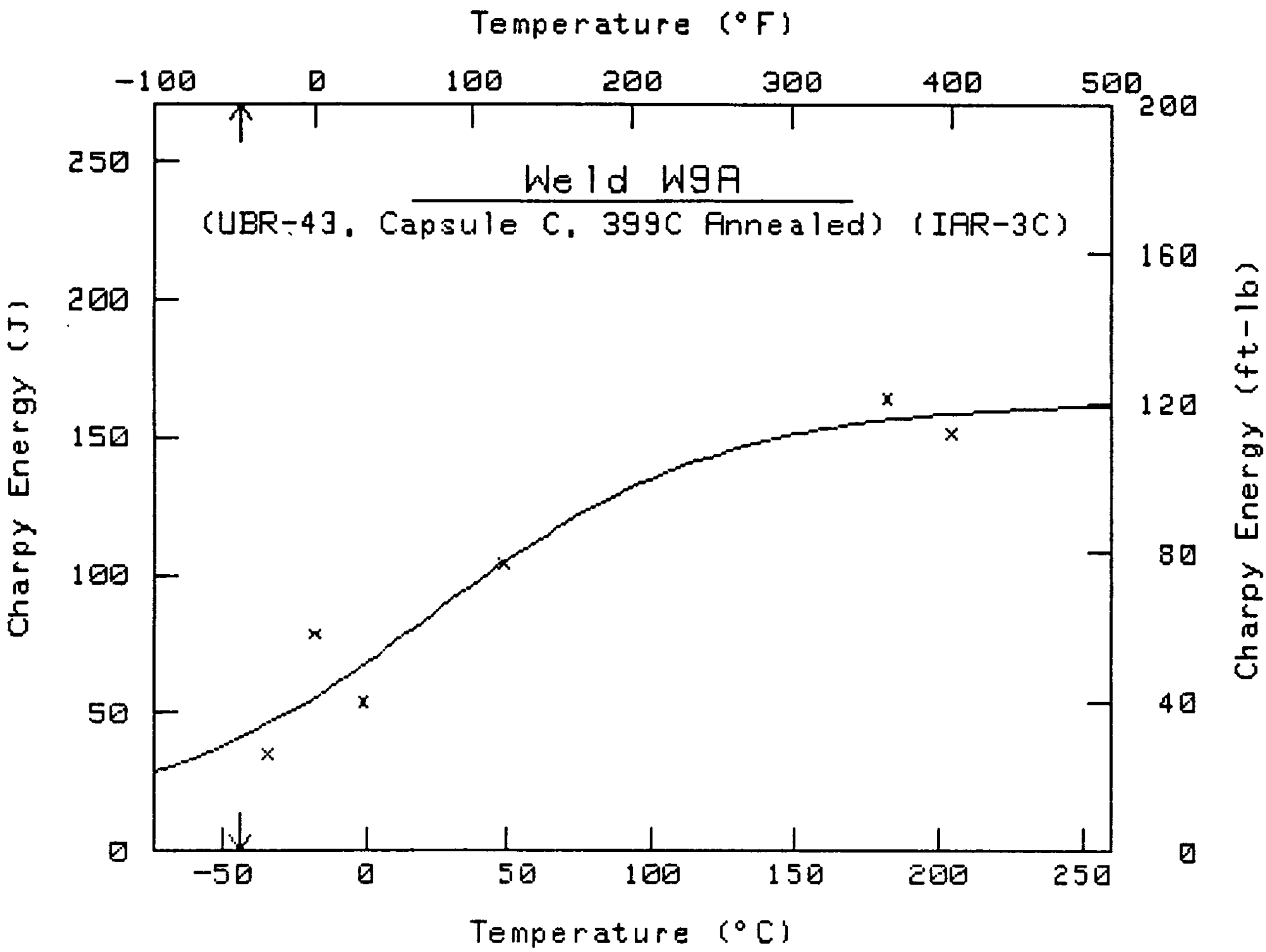

****

Cv = A + B tanh[(T - To)/C]

	English	Metric
A =	63.41 ft-lb	85.97 J
B =	56.85 ft-lb	77.08 J
C =	182.30 °F	101.28 °C
To =	75.45 °F	24.14 °C

Cv = 30 ft-lb (41 J) at T =	-47.4 °F	-44.1 °C
Upper Shelf Energy =	120.3 ft-lb	163.0 J

****

PT #	Temp (°F)	Energy (ft-lb)
1	-30	26.0
2	0	58.0
3	30	40.0
4	120	77.0
5	360	121.0
6	400	112.0

O = Fictitious Point Added   * = Test Point Not Included

Computer Curve Fittings of Data from Irradiation Assembly UBR-55

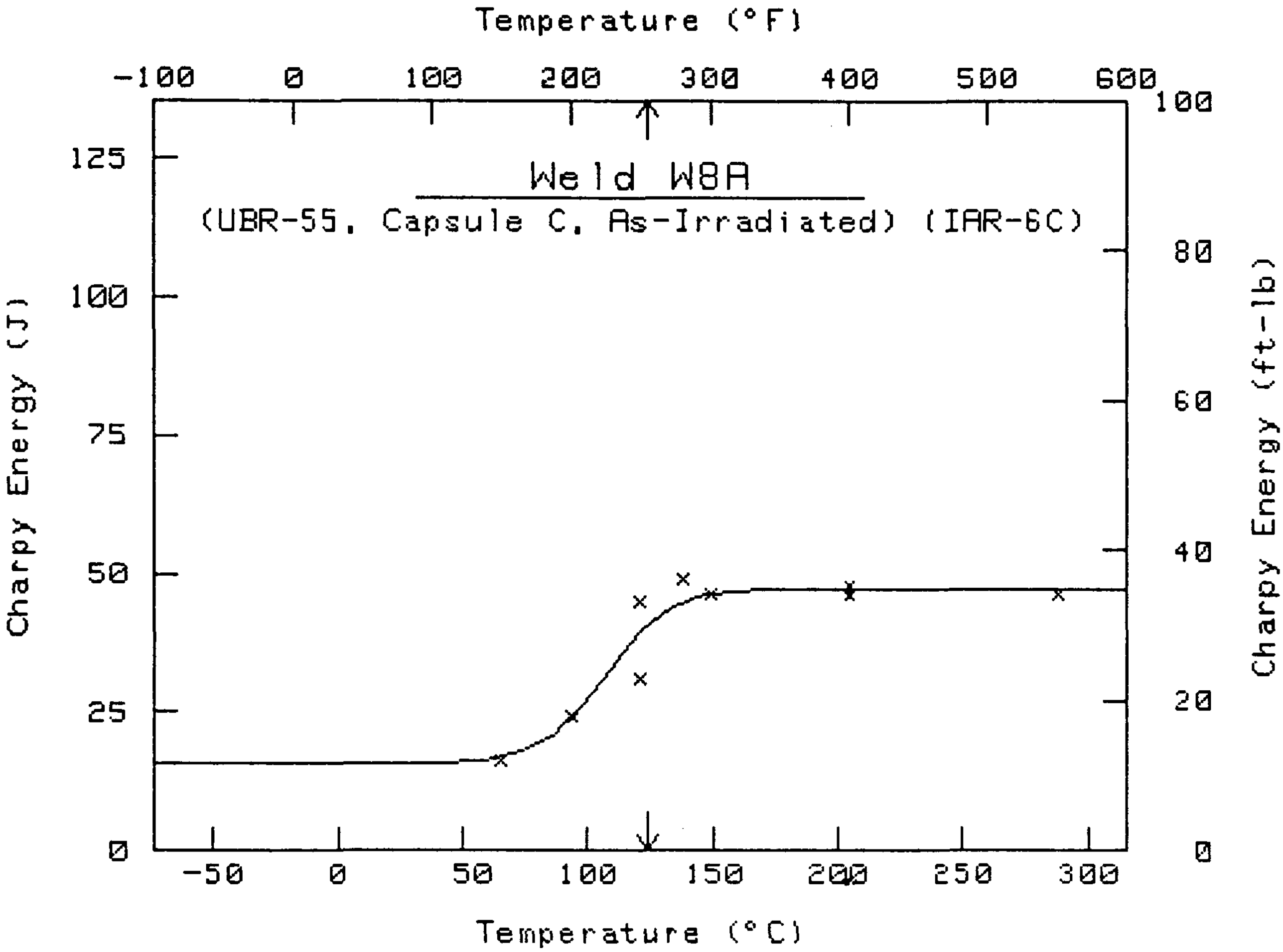

****

Cv = A + B tanh[(T - To)/C]

		English	Metric
A	=	23.18 ft-lb	31.42 J
B	=	11.66 ft-lb	15.81 J
C	=	46.27 °F	25.71 °C
To	=	224.34 °F	106.86 °C

Cv = 30 ft-lb (41 J) at T	=	255.4 °F	124.1 °C
Upper Shelf Energy	=	34.8 ft-lb	47.2 J

****

PT #	Temp (°F)	Energy (ft-lb)
1 *		
2	150	12.0
3	200	18.0
4	200	18.0
5	250	23.0
6	250	33.0
7	280	36.0
8	300	34.0
9	400	35.0
10 *		
11	400	34.0
12	550	34.0

O = Fictitious Point Added   * = Test Point Not Included

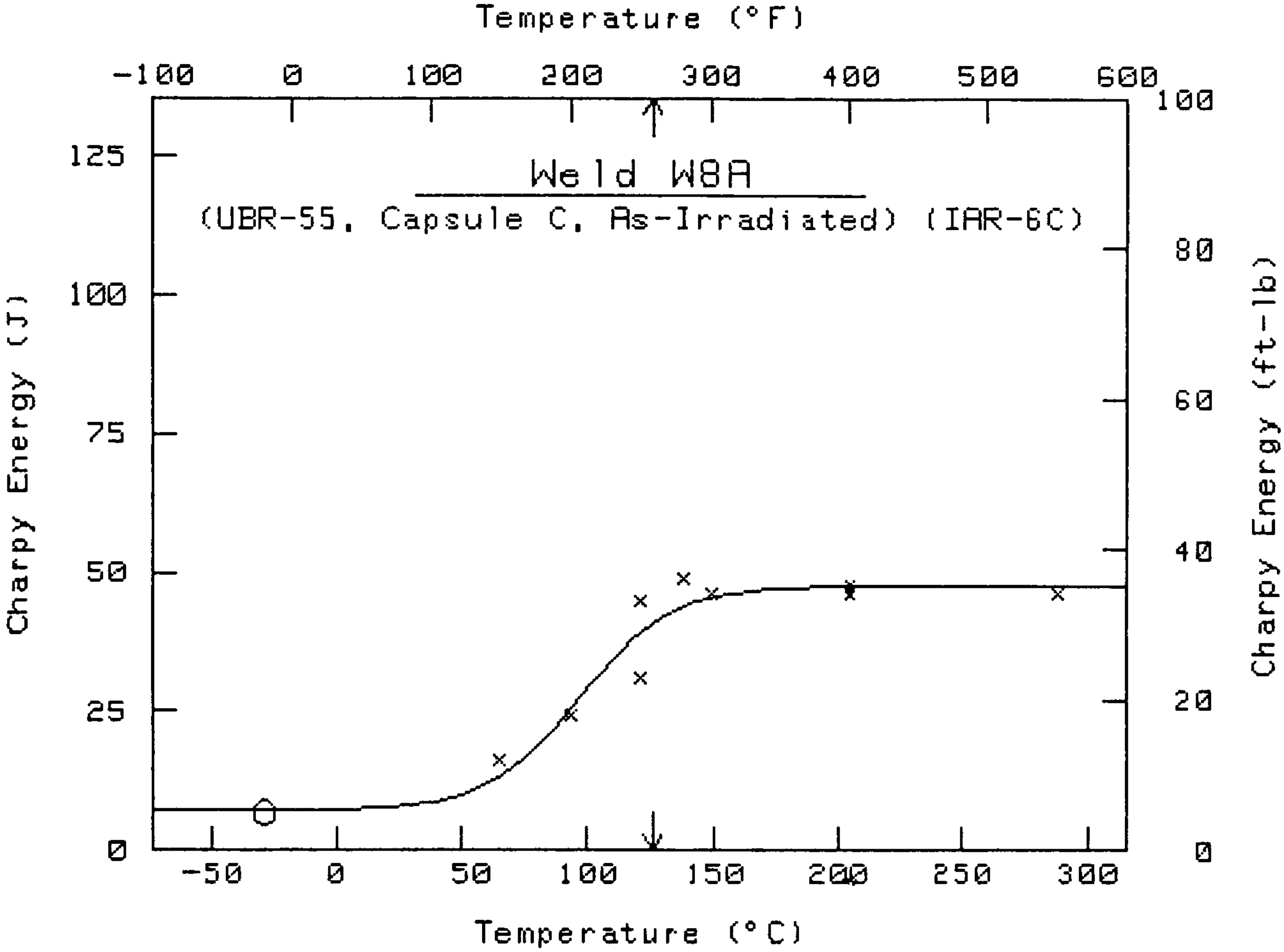

****

$$Cv = A + B \tanh[(T - To)/C]$$

	English	Metric
A =	20.19 ft-lb	27.37 J
B =	14.94 ft-lb	20.25 J
C =	65.59 °F	36.44 °C
To =	206.50 °F	96.95 °C

Cv = 30 ft-lb (41 J) at T =	258.1 °F	125.6 °C
Upper Shelf Energy =	35.1 ft-lb	47.6 J

****

PT #	Temp (°F)	Energy (ft-lb)	PT #	Temp (°F)	Energy (ft-lb)
1 *			9	400	35.0
2	150	12.0	10 *		
3	200	18.0	11	400	34.0
4	200	18.0	12	550	34.0
5	250	23.0	13 O	-20	5.0
6	250	33.0	14 O	-20	5.0
7	280	36.0	15 O	-20	5.0
8	300	34.0	16 O	-20	5.0

O = Fictitious Point Added   * = Test Point Not Included

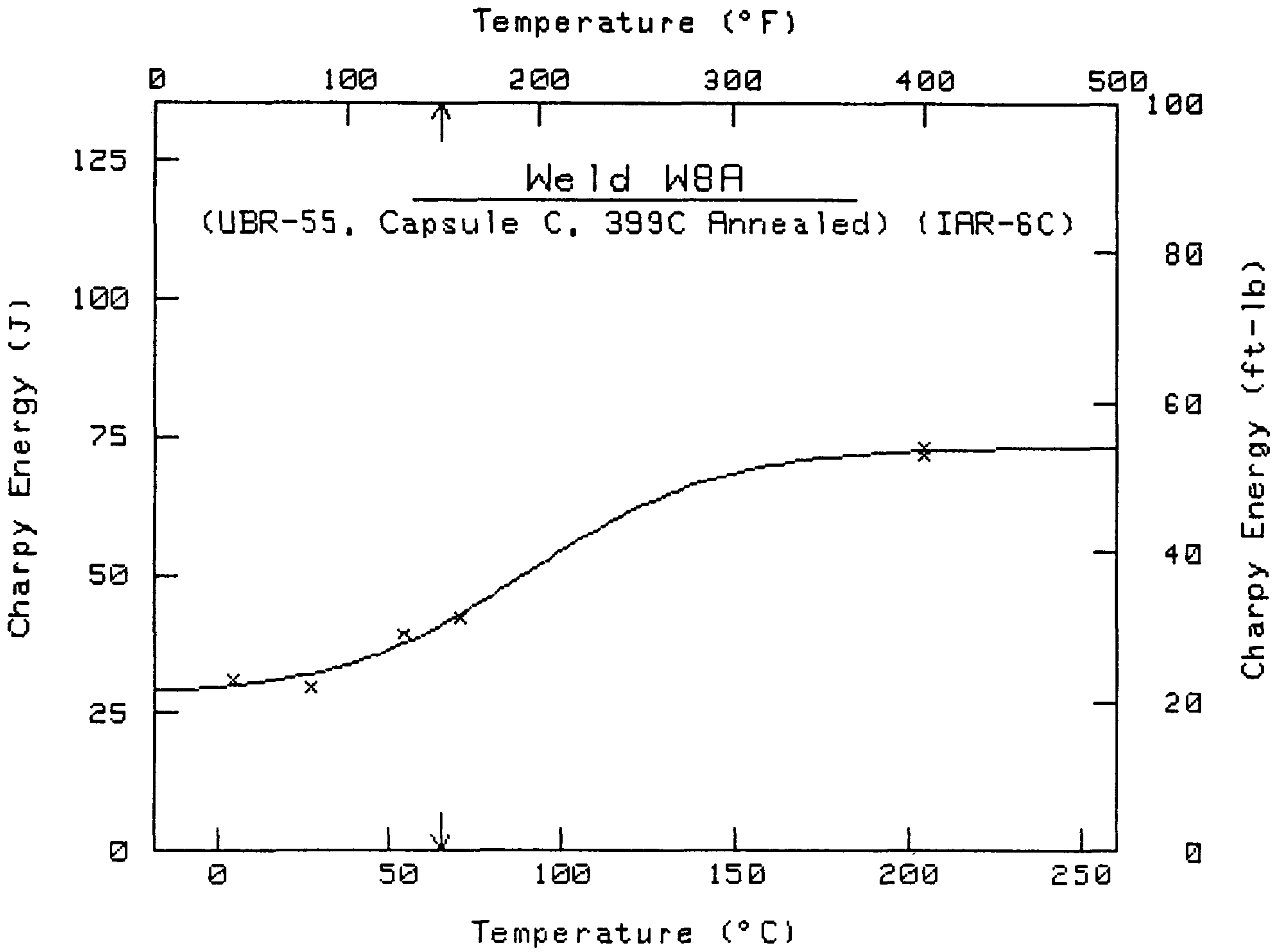

****

$$Cv = A + B \tanh[(T - To)/C]$$

		English	Metric
A	=	37.40 ft-lb	50.71 J
B	=	16.63 ft-lb	22.55 J
C	=	99.02 °F	55.01 °C
To	=	196.39 °F	91.33 °C

Cv = 30 ft-lb (41 J) at T	=	149.0 °F	65.0 °C
Upper Shelf Energy	=	54.0 ft-lb	73.3 J

****

PT #	Temp (°F)	Energy (ft-lb)
1	40	23.0
2	80	22.0
3	130	29.0
4	160	31.0
5 *		
6	400	53.0
7	400	54.0

0 = Fictitious Point Added * = Test Point Not Included

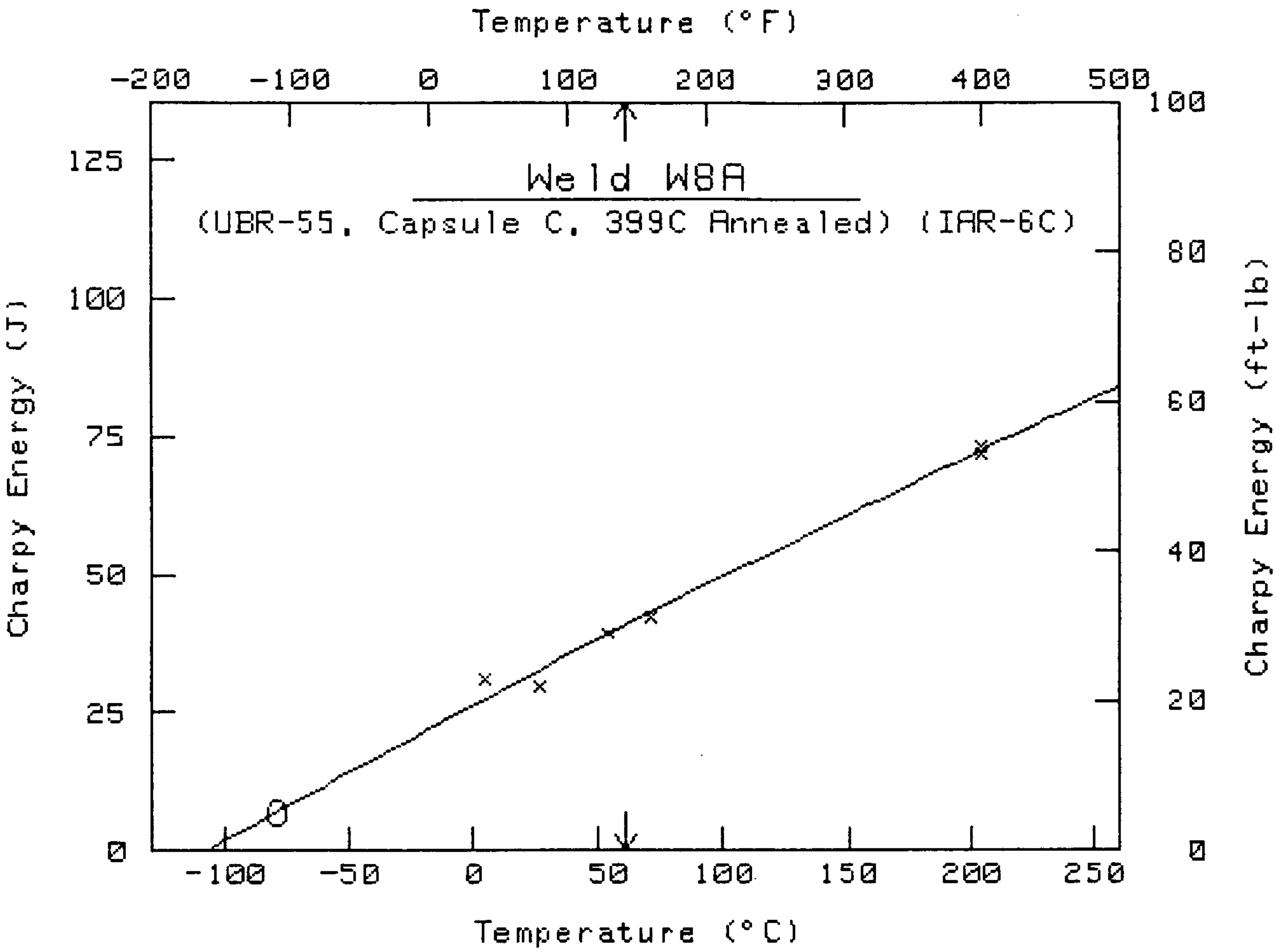

****

Cv = A + B tanh[(T - To)/C]

	English	Metric
A =	-113.10 ft-lb	-153.34 J
B =	325.20 ft-lb	440.91 J
C =	2764.74 °F	1535.97 °C
To =	-1163.31 °F	-664.06 °C

Cv = 30 ft-lb (41 J) at T =	142.4 °F	61.3 °C
Upper Shelf Energy =	212.1 ft-lb	287.6 J

****

PT #		Temp (°F)	Energy (ft-lb)
1		40	23.0
2		80	22.0
3		130	29.0
4		160	31.0
5	*		
6		400	53.0
7		400	54.0
8	O	-110	5.0
9	O	-110	5.0
10	O	-110	5.0
11	O	-110	5.0

O = Fictitious Point Added   * = Test Point Not Included

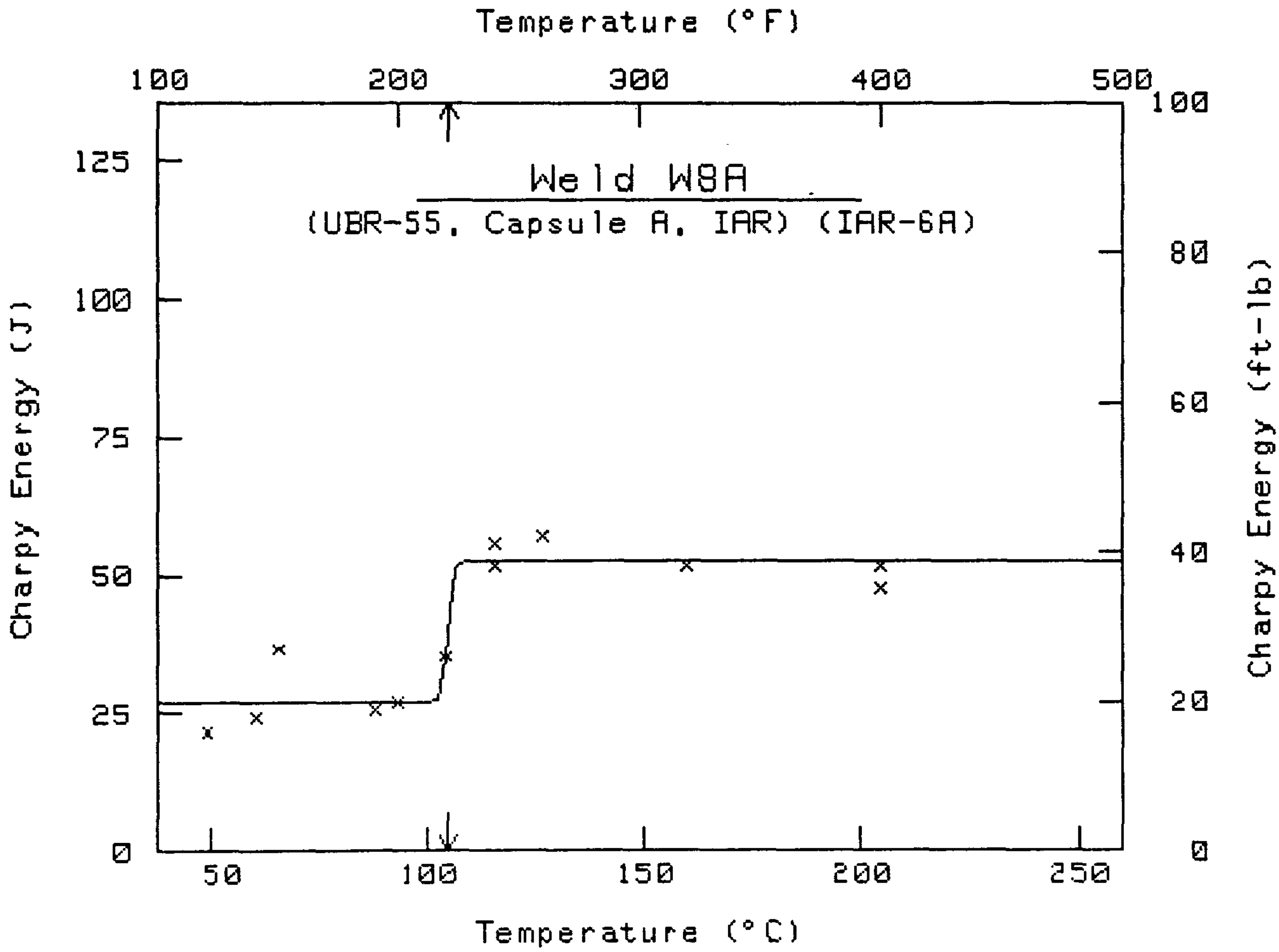

****

$$Cv = A + B \tanh[(T - To)/C]$$

		English	Metric
A	=	29.33 ft-lb	39.77 J
B	=	9.33 ft-lb	12.65 J
C	=	2.20 °F	1.22 °C
To	=	220.82 °F	104.90 °C

		English	Metric
Cv = 30 ft-lb (41 J) at T	=	221.0 °F	105.0 °C
Upper Shelf Energy	=	38.7 ft-lb	52.4 J

****

PT #	Temp (°F)	Energy (ft-lb)
1	120	16.0
2	140	18.0
3	150	27.0
4 *		
5	190	19.0
6	200	20.0
7	220	26.0
8	240	41.0
9	240	38.0
10	260	42.0
11	320	38.0
12	400	35.0
13	400	38.0

O = Fictitious Point Added   * = Test Point Not Included

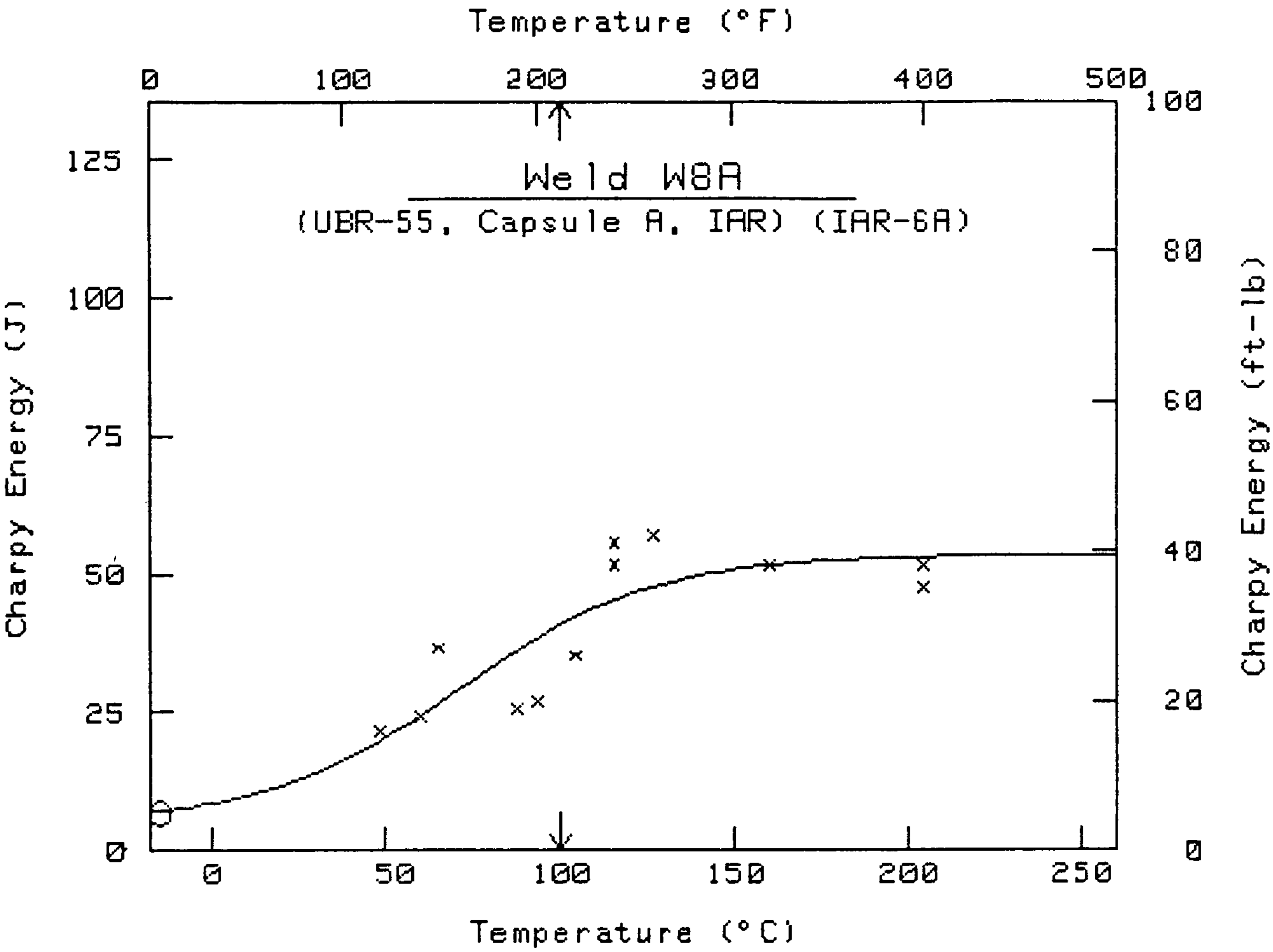

****

Cv = A + B tanh[(T - To)/C]

		English	Metric
A	=	21.67 ft-lb	29.38 J
B	=	17.80 ft-lb	24.13 J
C	=	99.75 °F	55.42 °C
To	=	161.31 °F	71.84 °C

Cv = 30 ft-lb (41 J) at T = 211.9 °F 100.0 °C

Upper Shelf Energy = 39.5 ft-lb 53.5 J

****

PT #	Temp (°F)	Energy (ft-lb)	PT #	Temp (°F)	Energy (ft-lb)
1	120	16.0	10	260	42.0
2	140	18.0	11	320	38.0
3	150	27.0	12	400	35.0
4 *			13	400	38.0
5	190	19.0	14 O	5	5.0
6	200	20.0	15 O	5	5.0
7	220	26.0	16 O	5	5.0
8	240	41.0	17 O	5	5.0
9	240	38.0			

O = Fictitious Point Added * = Test Point Not Included

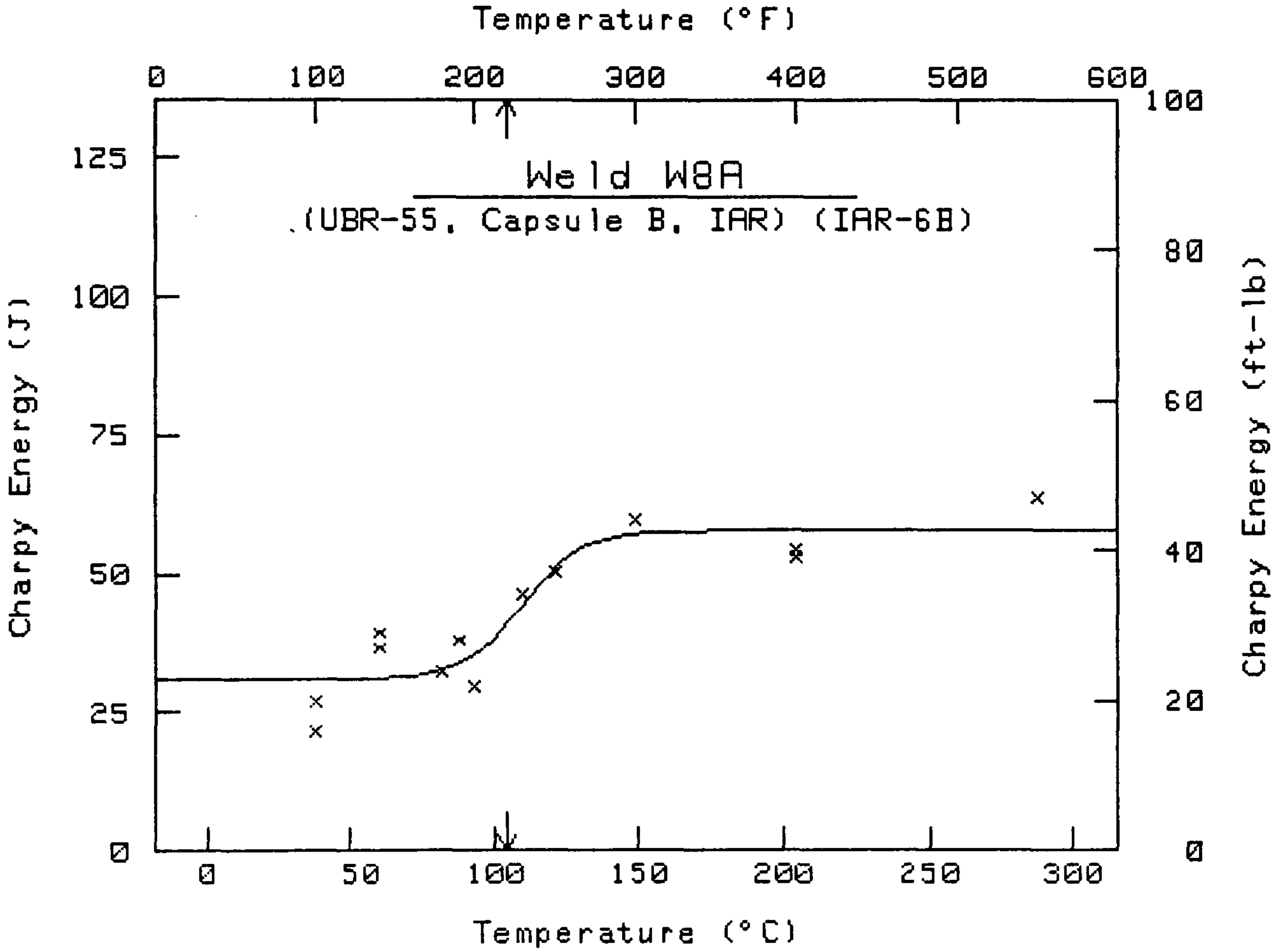

****

$$Cv = A + B \tanh[(T - To)/C]$$

		English	Metric
A	=	32.71 ft-lb	44.35 J
B	=	9.86 ft-lb	13.37 J
C	=	36.69 °F	20.38 °C
To	=	229.70 °F	109.83 °C

	English	Metric
Cv = 30 ft-lb (41 J) at T =	219.4 °F	104.1 °C
Upper Shelf Energy =	42.6 ft-lb	57.7 J

****

PT #	Temp (°F)	Energy (ft-lb)
1	100	16.0
2	100	20.0
3	140	29.0
4	140	27.0
5	180	24.0
6	190	28.0
7	200	22.0
8	230	34.0
9	250	37.0
10	300	44.0
11	400	39.0
12	400	40.1
13	550	47.0

O = Fictitious Point Added   * = Test Point Not Included

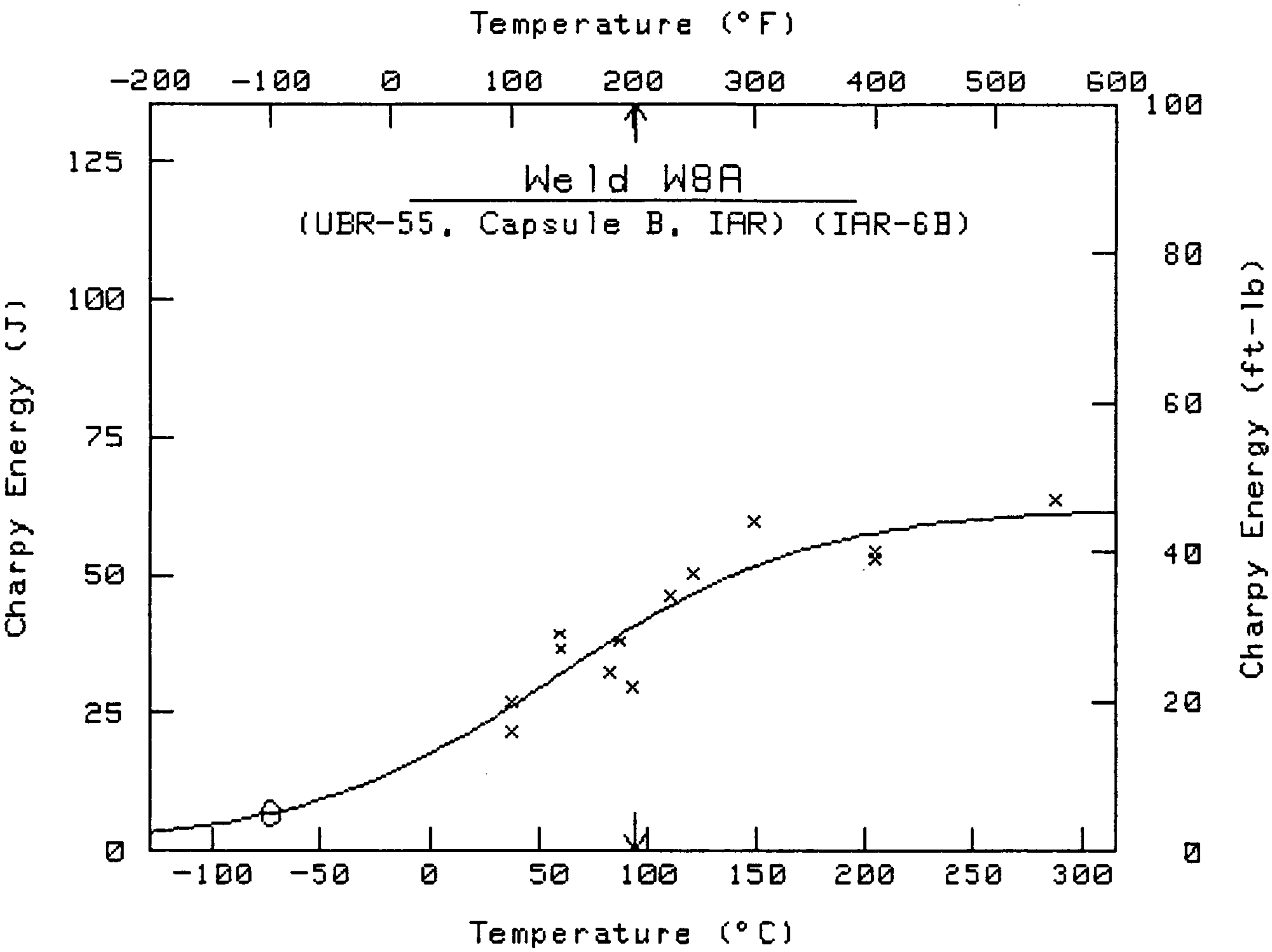

****

Cv = A + B tanh[(T - To)/C]

	English	Metric
A =	23.37 ft-lb	31.68 J
B =	22.57 ft-lb	30.61 J
C =	209.75 °F	116.53 °C
To =	138.43 °F	59.13 °C

Cv = 30 ft-lb (41 J) at T =	201.9 °F	94.4 °C
Upper Shelf Energy =	45.9 ft-lb	62.3 J

****

PT #	Temp (°F)	Energy (ft-lb)	PT #	Temp (°F)	Energy (ft-lb)
1	100	16.0	10	300	44.0
2	100	20.0	11	400	39.0
3	140	29.0	12	400	40.1
4	140	27.0	13	550	47.0
5	180	24.0	14 O	-100	5.0
6	190	28.0	15 O	-100	5.0
7	200	22.0	16 O	-100	5.0
8	230	34.0	17 O	-100	5.0
9	250	37.0			

O = Fictitious Point Added * = Test Point Not Included

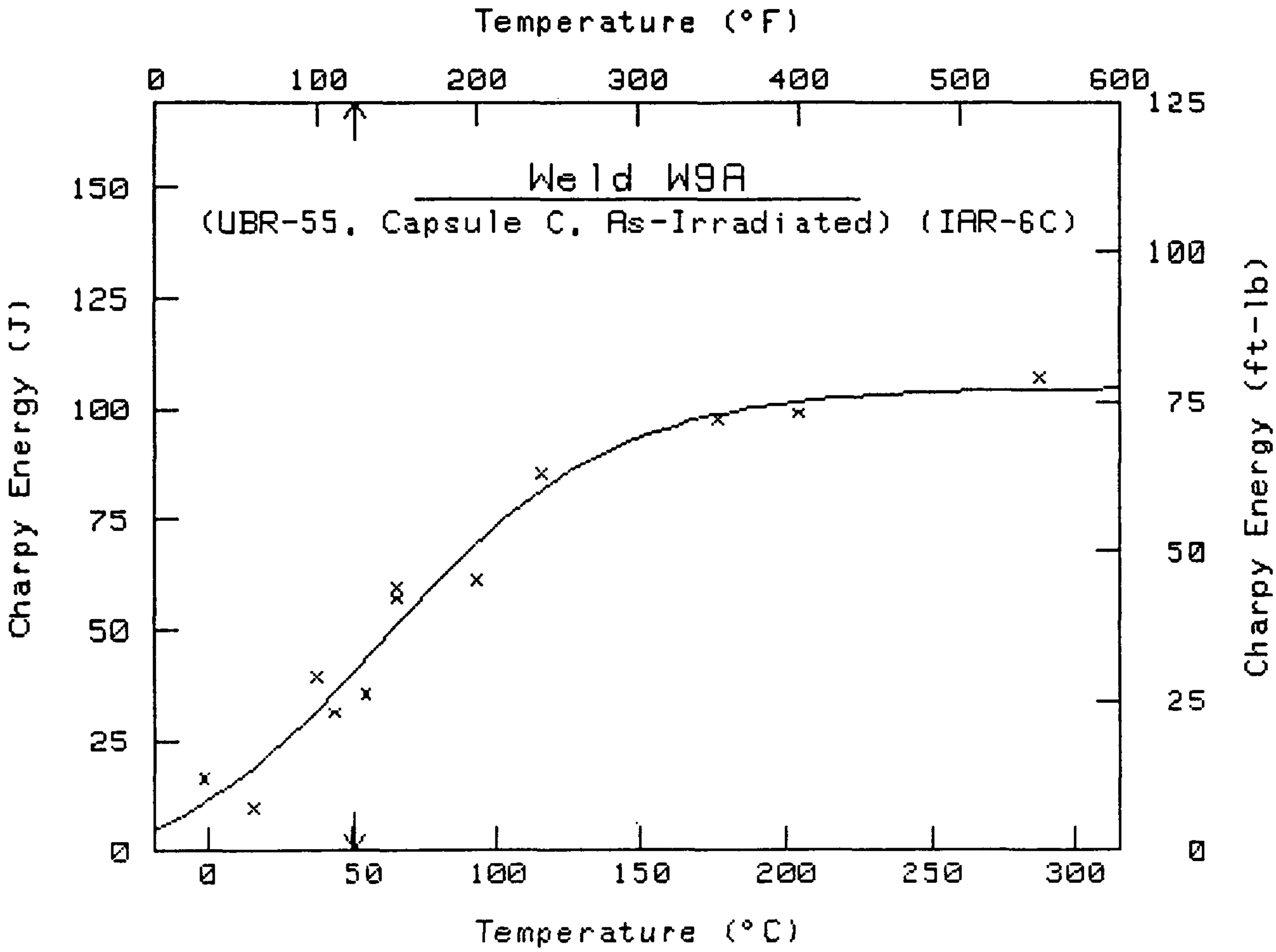

****

$$Cv = A + B \tanh[(T - To)/C]$$

	English	Metric
A =	34.95 ft-lb	47.38 J
B =	42.36 ft-lb	57.43 J
C =	146.49 °F	81.38 °C
To =	140.35 °F	60.20 °C

Cv = 30 ft-lb (41 J) at T = 123.2 °F 50.6 °C

Upper Shelf Energy = 77.3 ft-lb 104.8 J

****

PT #	Temp (°F)	Energy (ft-lb)
1	30	12.0
2	60	7.0
3	100	29.0
4	110	23.0
5	130	26.0
6	150	42.0
7	150	44.0
8	200	45.0
9	240	63.0
10	350	72.0
11	400	73.0
12	550	79.0

0 = Fictitious Point Added * = Test Point Not Included

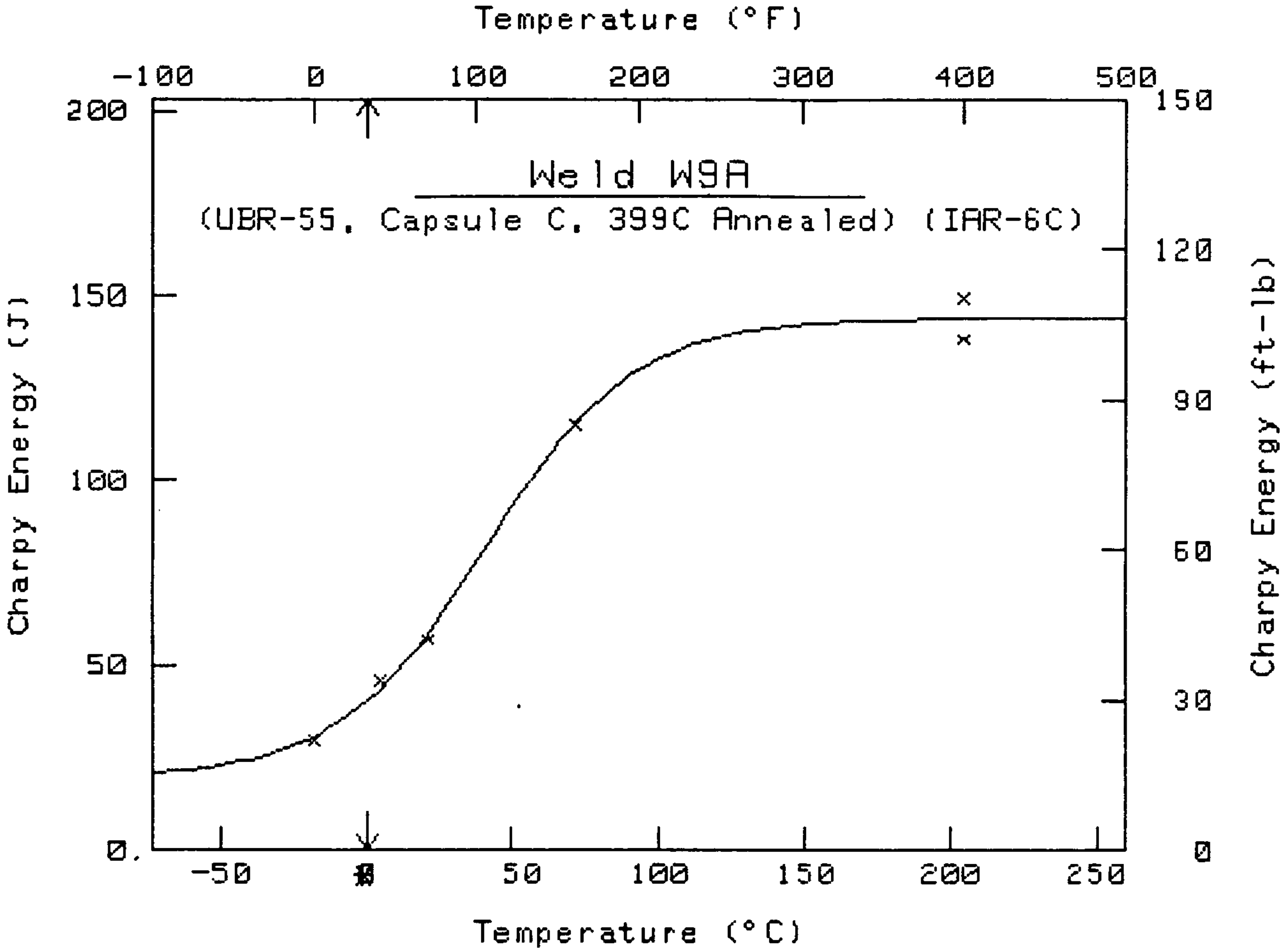

****

Cv = A + B tanh[(T - To)/C]

		English	Metric
A	=	60.35 ft-lb	81.83 J
B	=	45.84 ft-lb	62.16 J
C	=	91.52 °F	50.84 °C
To	=	105.77 °F	40.98 °C

Cv = 30 ft-lb (41 J) at T	=	32.9 °F	.5 °C
Upper Shelf Energy	=	106.2 ft-lb	144.0 J

****

PT #	Temp (°F)	Energy (ft-lb)
1	0	22.0
2 *		
3	40	34.0
4	70	42.0
5	160	85.0
6	400	110.0
7	400	102.0

O = Fictitious Point Added   * = Test Point Not Included

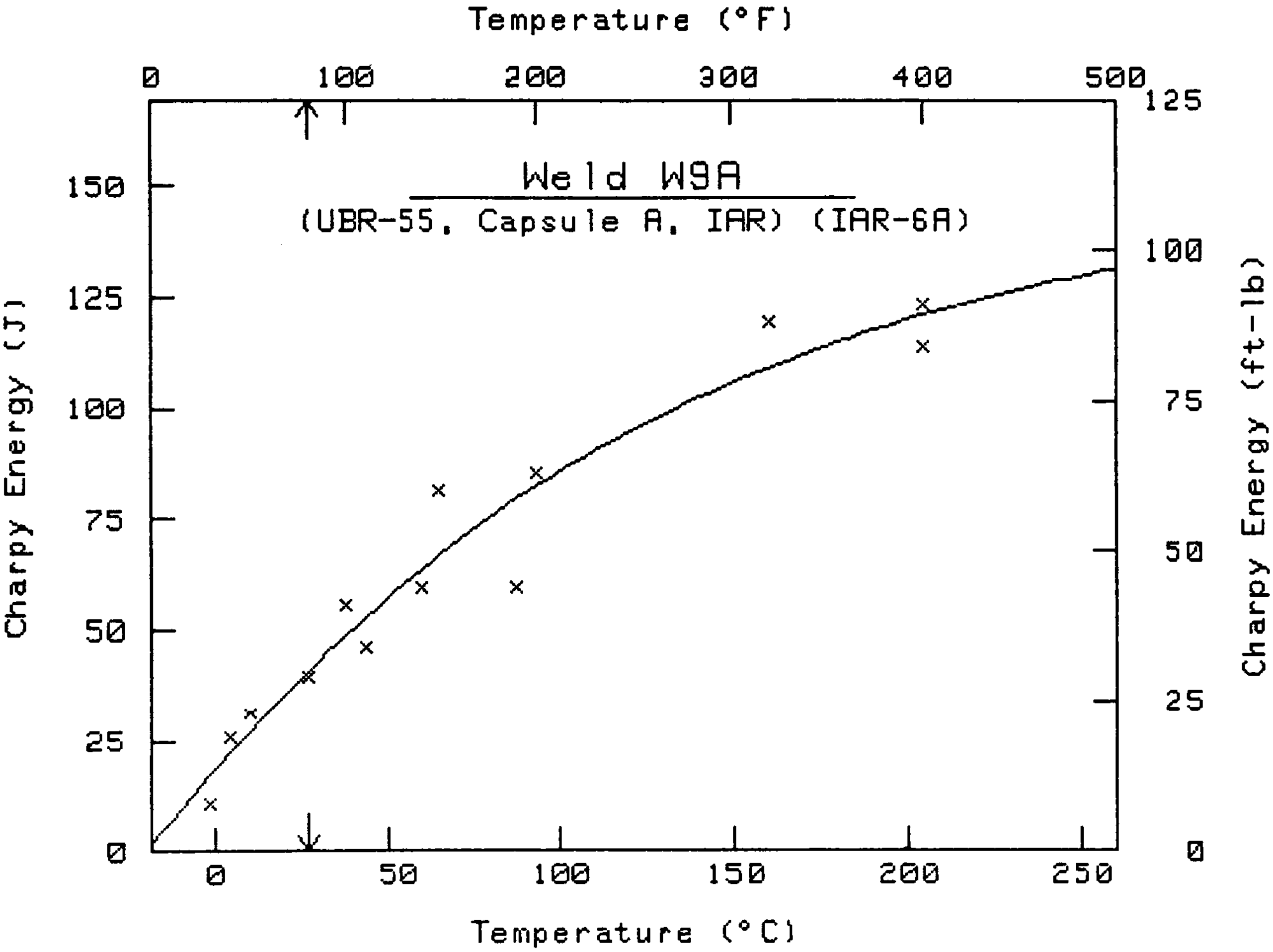

****

$$C_v = A + B \tanh[(T - T_o)/C]$$

		English	Metric
A	=	-229.60 ft-lb	-311.29 J
B	=	340.99 ft-lb	462.32 J
C	=	458.10 °F	254.50 °C
To	=	-377.28 °F	-227.38 °C

Cv = 30 ft-lb (41 J) at T = 80.5 °F 26.9 °C

Upper Shelf Energy = 111.4 ft-lb 151.0 J

****

PT #	Temp (°F)	Energy (ft-lb)
1	30	8.0
2	40	19.0
3	50	23.0
4	80	29.0
5	100	41.0
6	110	34.0
7	140	44.0
8	150	60.0
9	190	44.0
10	200	63.0
11	320	88.0
12	400	84.0
13	400	91.0

O = Fictitious Point Added * = Test Point Not Included

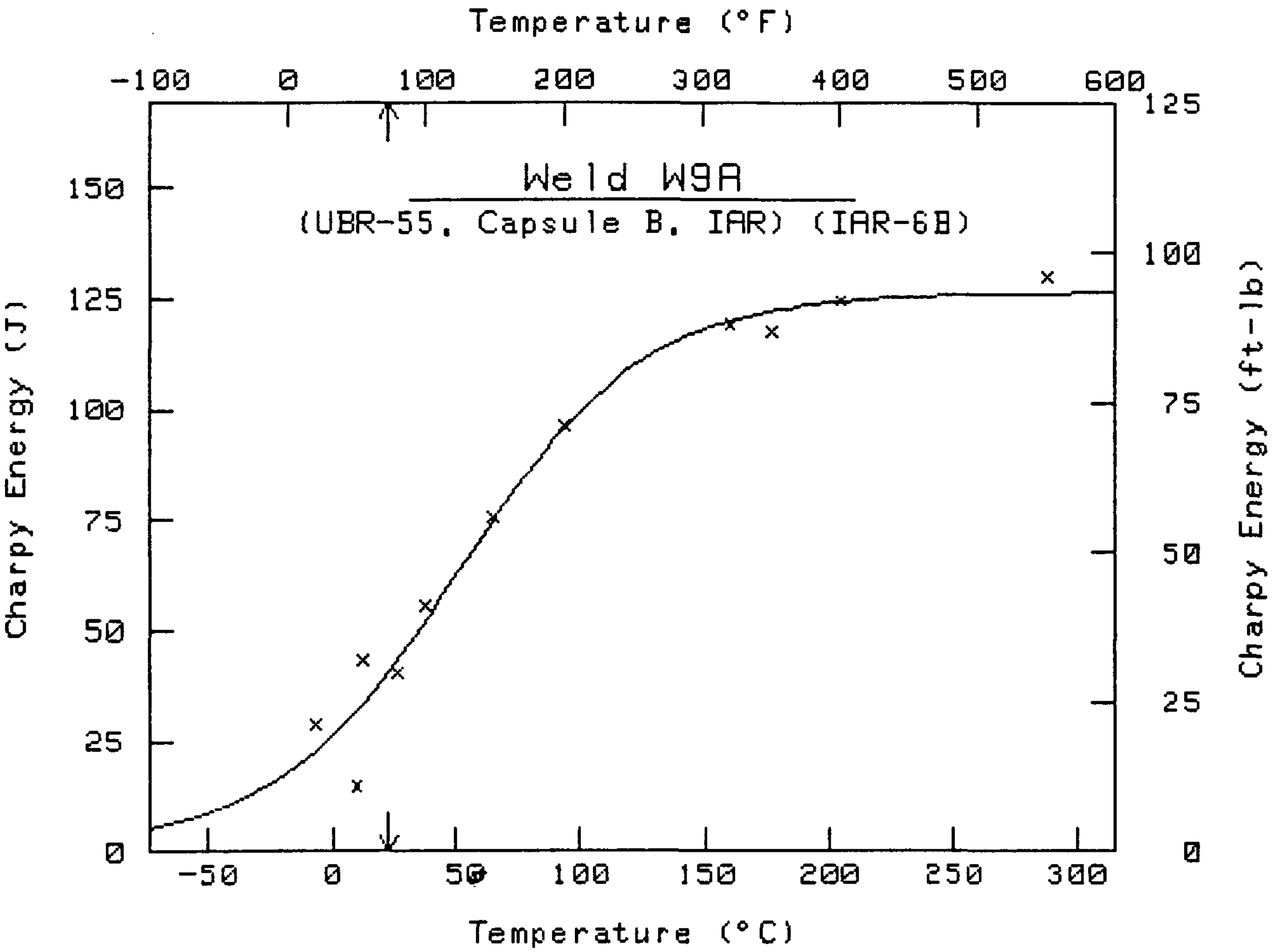

$$Cv = A + B \tanh[(T - To)/C]$$

	English	Metric
A =	47.11 ft-lb	63.88 J
B =	46.24 ft-lb	62.70 J
C =	133.88 °F	74.38 °C
To =	125.59 °F	51.99 °C

Cv = 30 ft-lb (41 J) at T = 73.6 °F 23.1 °C

Upper Shelf Energy = 93.4 ft-lb 126.6 J

PT #	Temp (°F)	Energy (ft-lb)
1 *		
2	20	21.0
3	50	11.0
4	55	32.0
5	80	30.0
6	100	41.0
7 *		
8	150	56.0
9	200	71.0
10	320	88.0
11	350	87.0
12	400	92.0
13	550	96.0

O = Fictitious Point Added * = Test Point Not Included

APPENDIX F

Results from Curvefitting of Transition Region Fracture Toughness Data

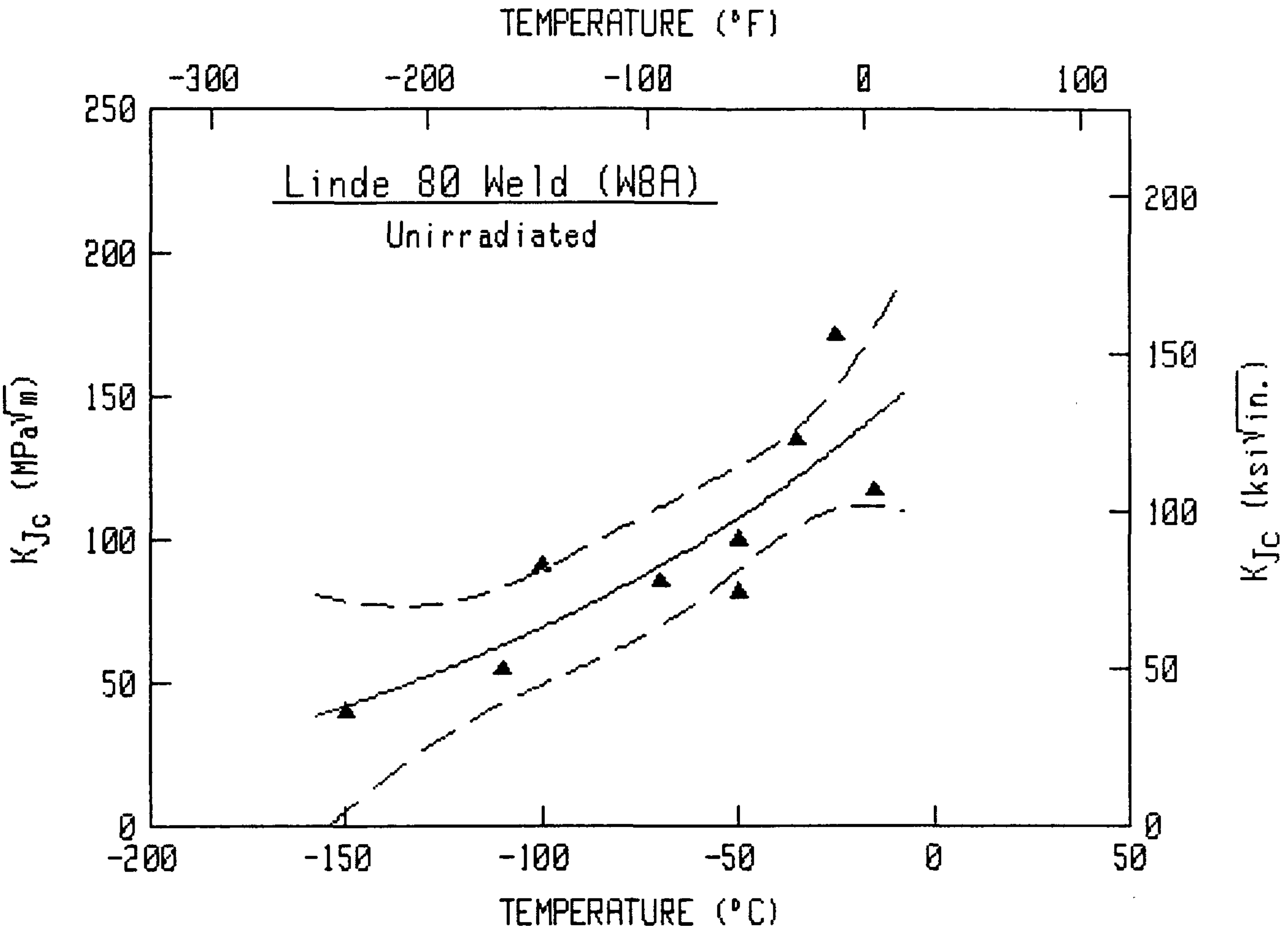

Kjc = A + B exp [(T-To)/C)]

	Metric	English
A =	-27.03 MPa√m	-24.60 ksi√in
B =	187.75 MPa√m	170.86 ksi√in
C =	149.72°C	269.50°F
To =	0.00°C	32.00°F

	Temperature at 100 MPa√m	
Upper Bound =	-85°C	-121°F
Mean Curve =	-58°C	-73°F
Lower Bound =	-39°C	-38°F

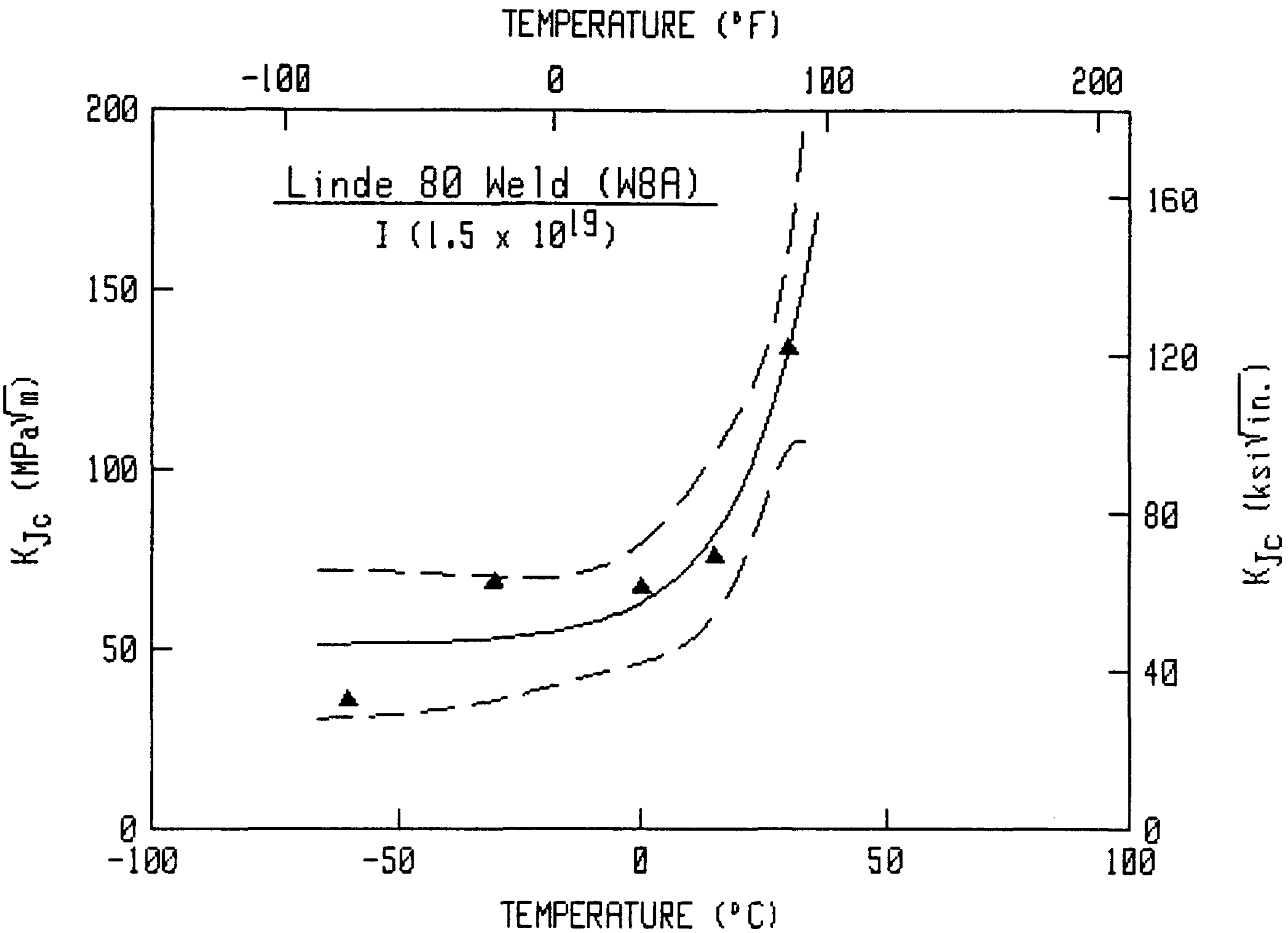

Kjc = A + B exp [(T-To)/C)]

		Metric	English
A	=	51.38 MPa√m	46.75 ksi√in
B	=	11.55 MPa√m	10.51 ksi√in
C	=	15.36°C	27.65°F
To	=	0.00°C	32.00°F

	Temperature at 100 MPa√m	
Upper Bound =	13°C	55°F
Mean Curve =	22°C	72°F
Lower Bound =	28°C	82°F

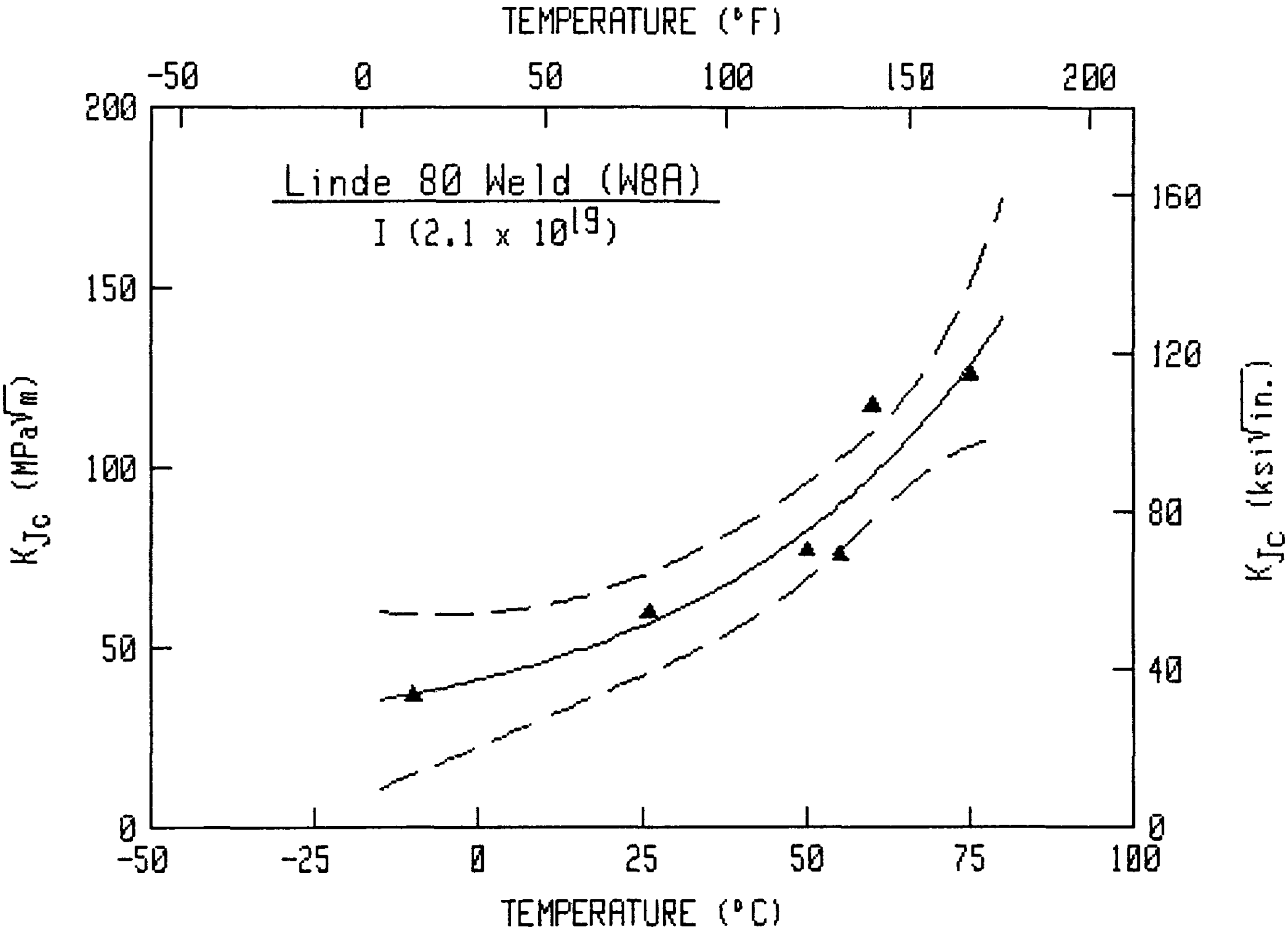

Kjc = A + B exp [(T-To)/C)]

	Metric	English
A =	21.16 MPa√m	19.26 ksi√in
B =	19.82 MPa√m	18.03 ksi√in
C =	44.29°C	79.71°F
To =	0.00°C	32.00°F

	Temperature at 100 MPa√m	
Upper Bound =	54°C	129°F
Mean Curve =	61°C	142°F
Lower Bound =	69°C	156°F

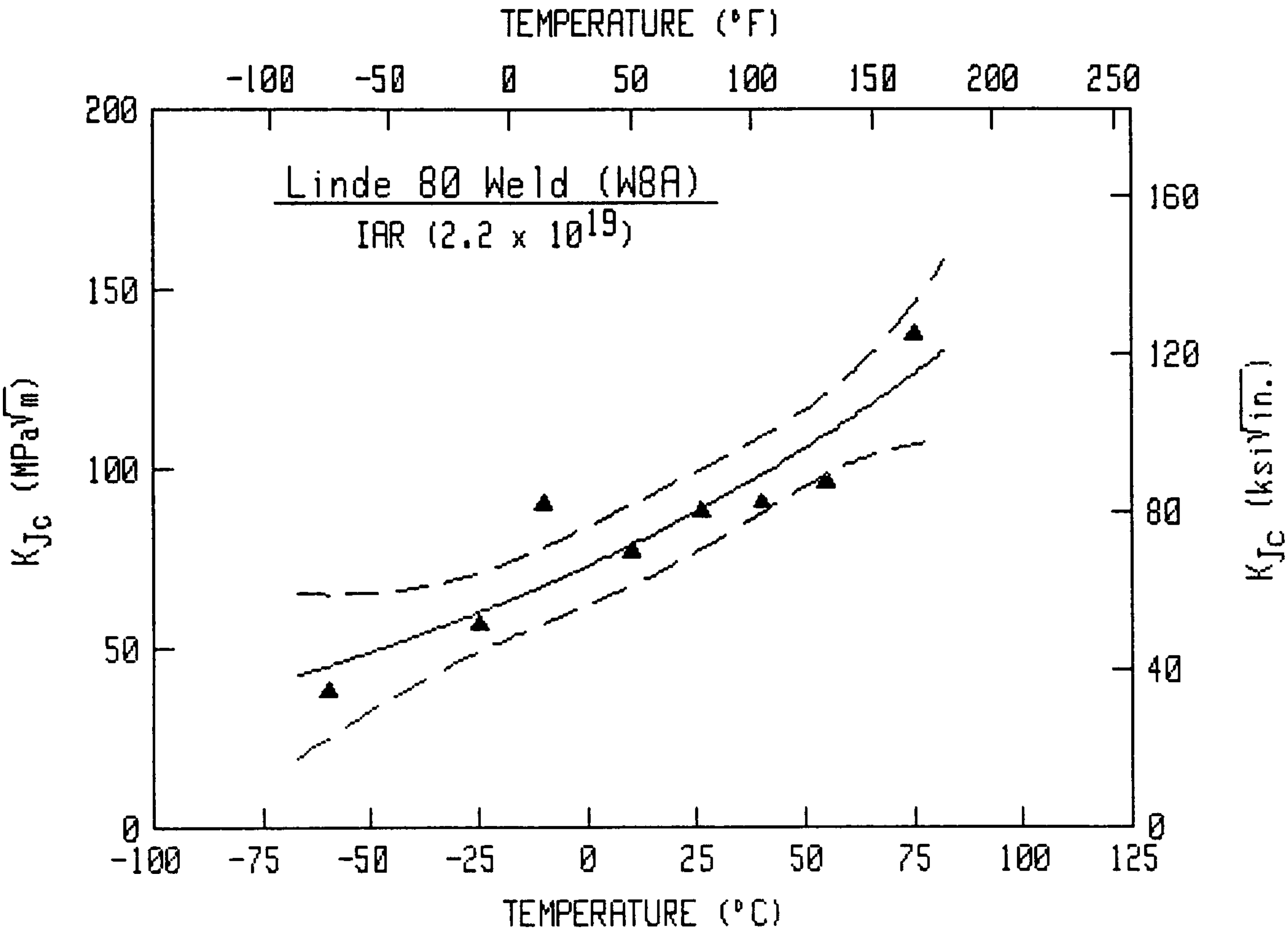

Kjc = A + B exp [(T-To)/C)]

		Metric	English
A	=	-14.89 MPa√m	-13.55 ksi√in
B	=	87.63 MPa√m	79.75 ksi√in
C	=	157.30°C	283.14°F
To	=	0.00°C	32.00°F

	Temperature at 100 MPa√m	
Upper Bound =	27°C	81°F
Mean Curve =	43°C	109°F
Lower Bound =	59°C	138°F

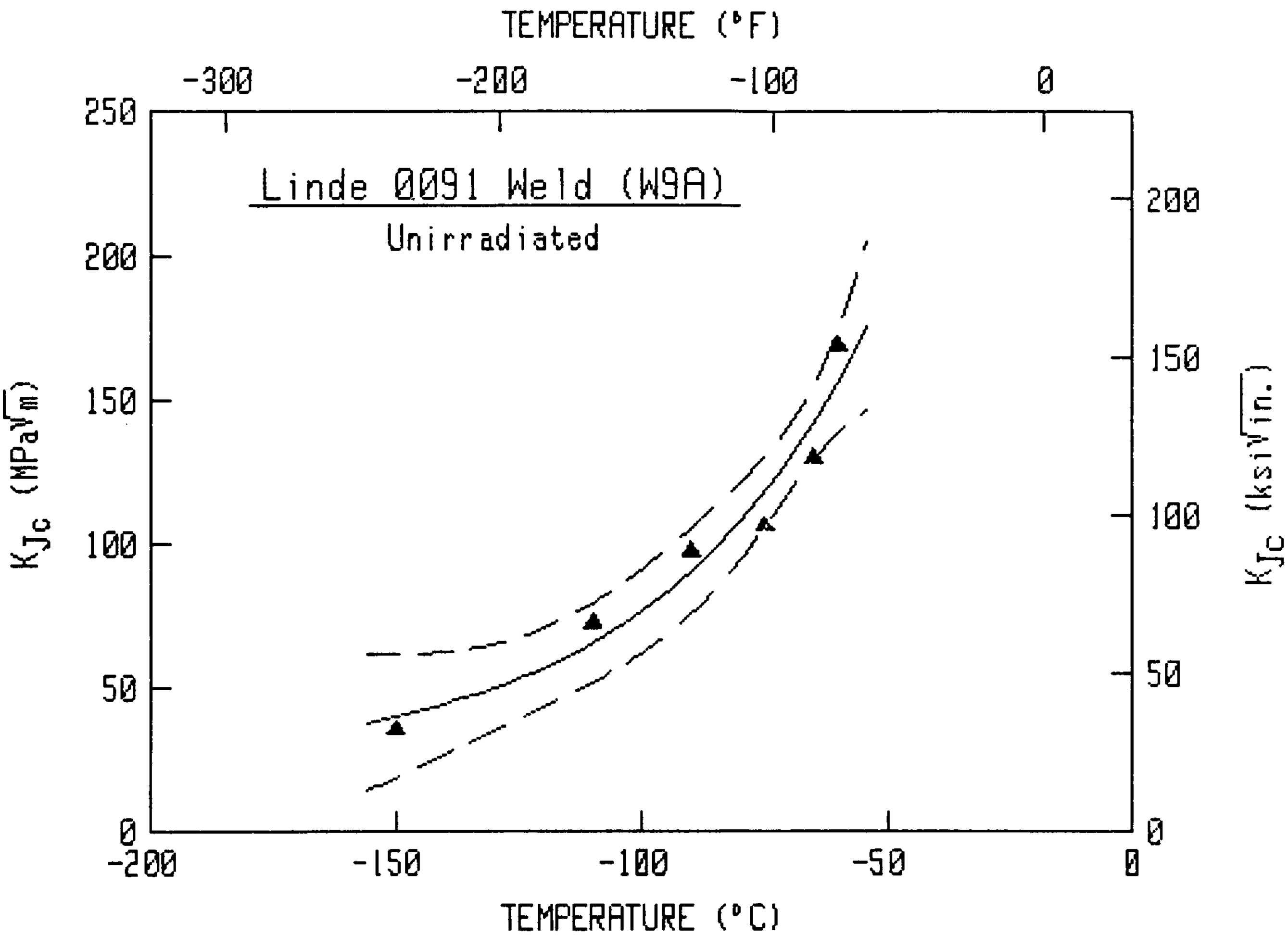

Kjc = A + B exp [(T-To)/C)]

	Metric	English
A =	22.40 MPa√m	20.38 ksi√in
B =	519.22 MPa√m	472.51 ksi√in
C =	44.24°C	79.63°F
To =	0.00°C	32.00°F

	Temperature at 100 MPa√m	
Upper Bound =	-93°C	-135°F
Mean Curve =	-84°C	-119°F
Lower Bound =	-77°C	-107°F

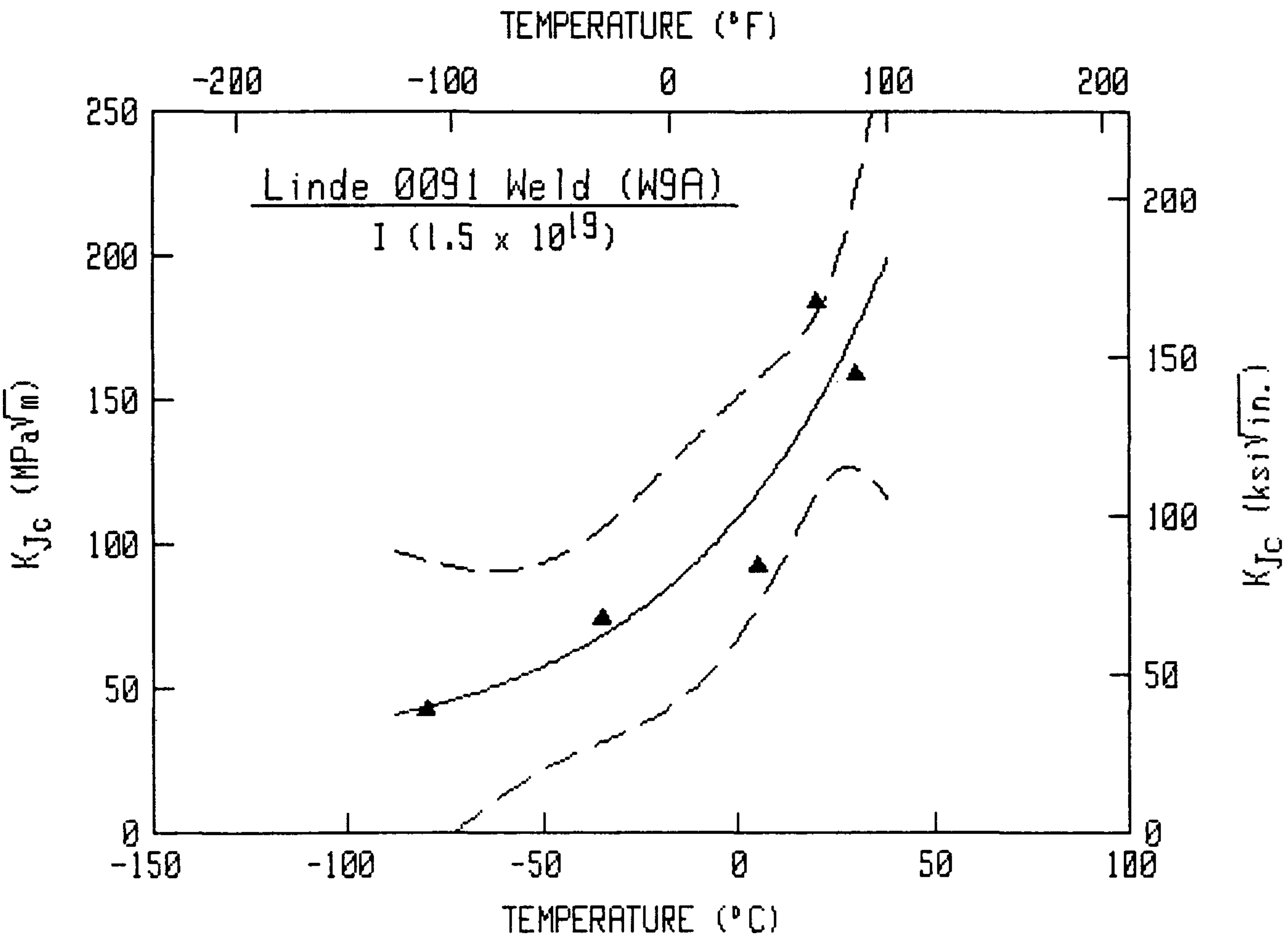

$K_{jc} = A + B \exp[(T-T_o)/C]$

	Metric	English
A =	24.97 MPa√m	22.72 ksi√in
B =	84.57 MPa√m	76.96 ksi√in
C =	52.46°C	94.43°F
To =	0.00°C	32.00°F

	Temperature at 100 MPa√m	
Upper Bound =	-40°C	-40°F
Mean Curve =	-6°C	21°F
Lower Bound =	14°C	57°F

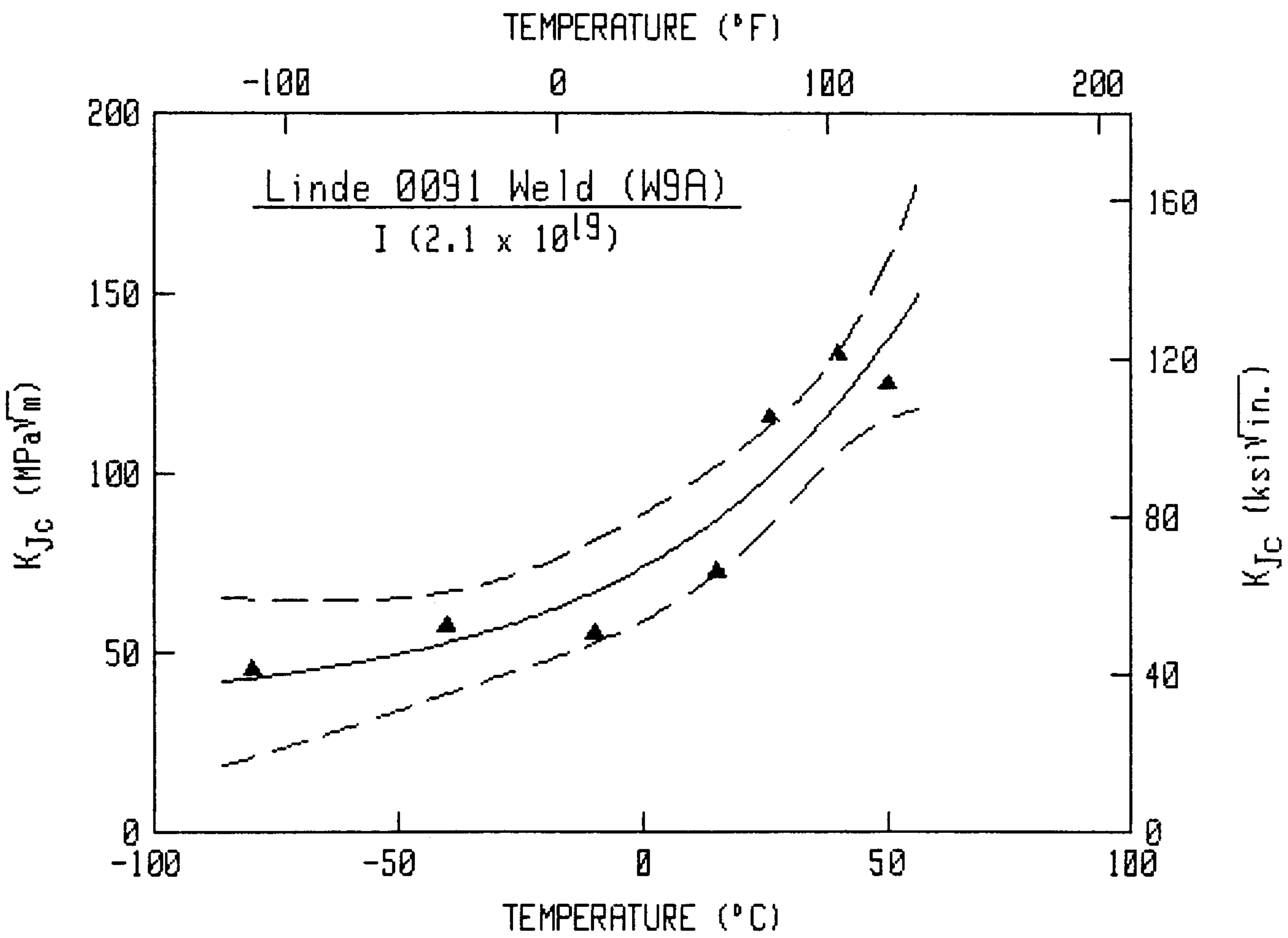

$$Kjc = A + B \exp[(T-To)/C)]$$

		Metric	English
A	=	34.24 MPa√m	31.16 ksi√in
B	=	39.55 MPa√m	35.99 ksi√in
C	=	52.19°C	93.94°F
To	=	0.00°C	32.00°F

	Temperature at 100 MPa√m	
Upper Bound =	13°C	55°F
Mean Curve =	27°C	80°F
Lower Bound =	37°C	99°F

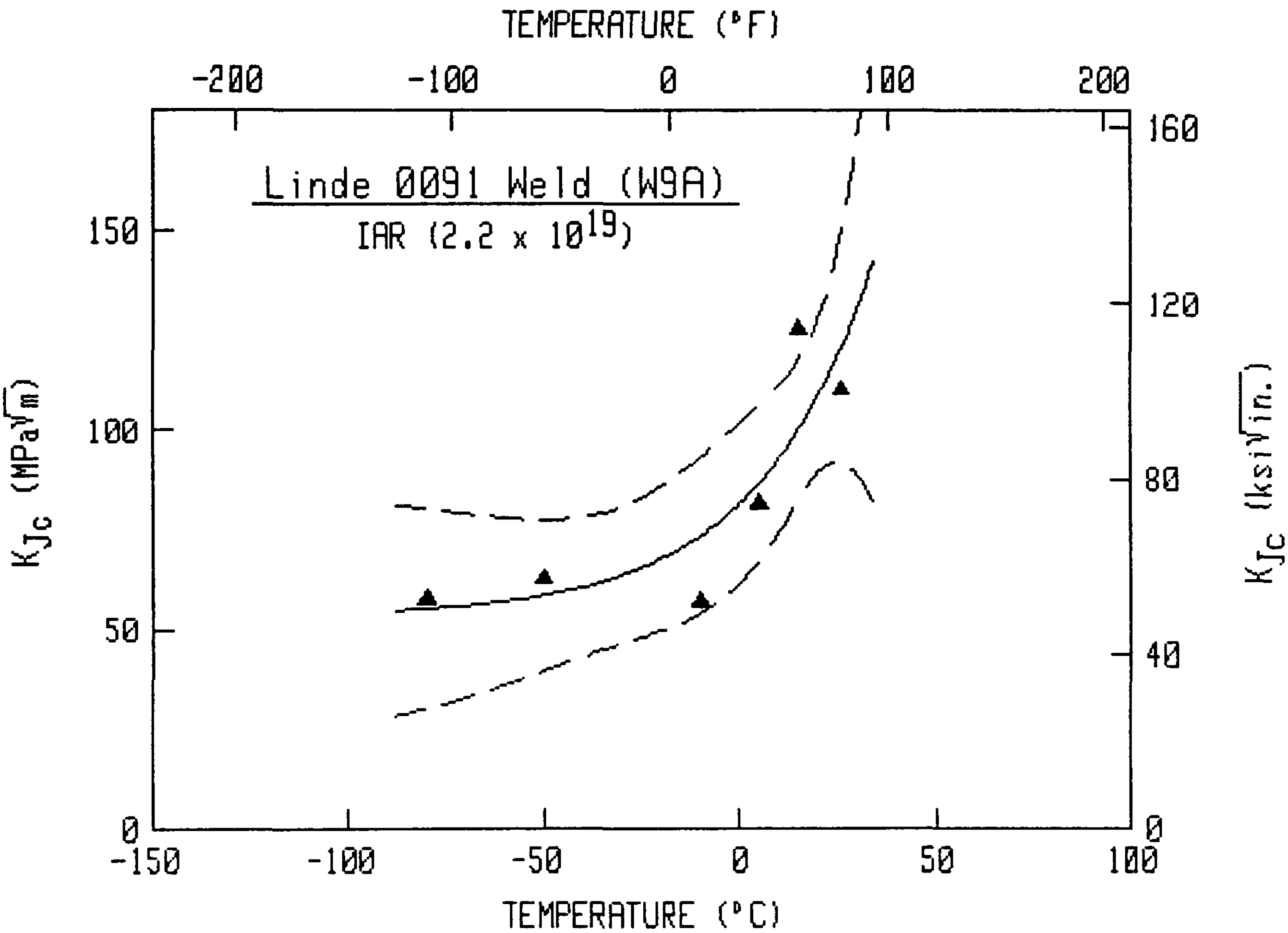

Kjc = A + B exp [(T-To)/C)]

	Metric	English
A =	53.32 MPa√m	48.52 ksi√in
B =	28.14 MPa√m	25.61 ksi√in
C =	29.63°C	53.33°F
To =	0.00°C	32.00°F

	Temperature at 100 MPa√m	
Upper Bound =	-1°C	30°F
Mean Curve =	15°C	59°F

NRC FORM 335
(2-89)
NRCM 1102,
3201, 3202

U.S. NUCLEAR REGULATORY COMMISSION

BIBLIOGRAPHIC DATA SHEET

(See instructions on the reverse)

1. REPORT NUMBER (Assigned by NRC. Add Vol., Supp., Rev., and Addendum Numbers, if any.)

NUREG/CR-5492
MEA-2088

2. TITLE AND SUBTITLE

Investigations of Irradiation-Anneal-Reirradiation (IAR) Properties Trends of RPV Welds

Phase 2 Final Report

3. DATE REPORT PUBLISHED

MONTH	YEAR
January	1990

4. FIN OR GRANT NUMBER

B8900

5. AUTHOR(S)

J. R. Hawthorne, A. L. Hiser

6. TYPE OF REPORT

7. PERIOD COVERED *(Inclusive Dates)*

8. PERFORMING ORGANIZATION — NAME AND ADDRESS *(If NRC, provide Division, Office or Region, U.S. Nuclear Regulatory Commission, and mailing address; if contractor, provide name and mailing address.)*

Materials Engineering Associates, Inc.
9700-B Martin Luther King, Jr. Highway
Lanham, Maryland 20706

9. SPONSORING ORGANIZATION — NAME AND ADDRESS *(If NRC, type "Same as above"; if contractor, provide NRC Division, Office or Region, U.S. Nuclear Regulatory Commission, and mailing address.)*

Division of Engineering Technology
Office of Nuclear Regulatory Research
U. S. Nuclear Regulatory Commission
Washington, D.C. 20555

10. SUPPLEMENTARY NOTES

11. ABSTRACT *(200 words or less)*

Notch ductility, fracture toughness and tensile property trends of two high copper content, submerged arc welds with 288°C irradiation (I), 399°C postirradiation annealing (IA) and 288°C reirradiation (IAR) were investigated. Primary objectives included the determination of weld metal reembrittlement rate with fluence following an anneal and the influence of first cycle fluence level (high or low) on reembrittlement susceptibility. The welds were commercially made using a single lot of filler wire and two welding fluxes (Linde 80 and Linde 0091).

A relatively-rapid reembrittlement of both weld types was observed with initial reirradiation; however, the reembrittlement rate decreased markedly after a reirradiation fluence of ~0.3 x 10^{19} n/cm^2, E > 1 MeV. In turn, the benefit of IA procedures toward reducing total properties change with fluence was retained. The reembrittlement trend was independent of first cycle fluence level for the range investigated. Residual embrittlement after 399°C - 168 hour annealing, indexed by the 41-J temperature, appears independent of the pre-anneal condition (I or IAR); however, wide variability among welds in percent recovery is indicated. Trends in IAR behavior from Charpy-V specimen tests were found to be reinforced by tensile specimen and fracture toughness (0.5T-CT specimen) test findings.

12. KEY WORDS/DESCRIPTORS *(List words or phrases that will assist researchers in locating the report.)*

irradiation, weld, fracture, temperature

13. AVAILABILITY STATEMENT

Unlimited

14. SECURITY CLASSIFICATION

(This Page) Unclassified

(This Report) Unclassified

15. NUMBER OF PAGES

16. PRICE